Prof. Morgenstern

THE UNIVERSITY OF ALBERTA

RELEASE FORM

NAME OF AUTHOR Luciano V. Medeiros

TITLE OF THESIS DEEP EXCAVATIONS IN STIFF SOILS

DEGREE FOR WHICH THESIS WAS PRESENTED DOCTOR OF PHILOSOPHY

YEAR THIS DEGREE GRANTED JUNE 1979

(SIGNED) ....

PERMANENT ADDRESS:

..Av. Copacabana...1298/504

..Rio de Janeiro.......

.....BRASIL...............

DATED..................19

THE UNIVERSITY OF ALBERTA

DEEP EXCAVATIONS IN STIFF SOILS

by

Luciano V. Medeiros

A THESIS

SUBMITTED TO THE FACULTY OF GRADUATE STUDIES AND RESEARCH

IN PARTIAL FULFILMENT OF THE REQUIREMENTS FOR THE DEGREE

OF DOCTOR OF PHILOSOPHY

IN

CIVIL ENGINEERING

DEPARTMENT OF CIVIL ENGINEERING

EDMONTON, ALBERTA

JUNE 1979

ABSTRACT

Investigations have been carried out regarding soil movement, lateral load and stress distribution in a deep excavation in stiff soil. The results presented are based on an integrated approach involving field observation, laboratory testing and analytical modeling. Special emphasis have been given to the influence of the stress path in the determination of the stress strain relationship.

A finite element program, using constant strain triangles, simulates the construction phases involved in the field was developed. Different stress strain relationship can be accomodated in the program to evaluate the most significant one.

The results indicated that the actual behaviour of the retaining structure can be successfully simulated if laboratory tests are performed following stress paths pertinent to the field conditions. The laboratory tests included the performance of active and passive tests in conventional triaxial and plane strain apparatus.

Use was made of an elastoplastic model to predict strains in the laboratory for active compression tests, based on conventional triaxial tests.

RESUME

Des recherches ont ete effectuees sur le mouvement des sols et la distribuition des tensions laterales d'une excavation profonde en sol dur. Les resultats presentes sont bases sur une approche integrale, induant des observations faites sur place, des essais de laboratoire et un modele analytique. Une attention speciale a ete portee sur l'influence de la ligne de tension sur la determination de la relation tension-deformation.

Un programme de elements finis utilisant des triangles de deformation constants simule les phases de construction du chantier. Differentes relations tension-deformation sont incluses dans le programme afin d'evaluer laquelle est la plus significative.

Les resultats indiquent que le comportement actuel de la structure de soutenement peut etre simule avec succes si les tests de labcratoire sont effectues suivant des lignes de tension pertinentes a l'etat du terrain. La performance de tests actifs et passifs de l'appareil triaxial et de deformation des plans conventionnel est incluse dans les tests de laboratoire

Un modele elasto-plastique a ete utilise pour predire les deformations en laboratoire pour les tests de compression actifs, base sur les tests triaxiaux conventionnels.

ACKNOWLEDGMENTS

So many people contributed to the completion of this work that I consider an act of selfishness to carry my name only as the author.

In the field I counted with the cooperation of I. Bruce, E. Evgin, F. El-Nahas, D. Hill, J.F. da Silva Filho, R. Tweedie, O. Wood and D. Fushtey. The difficult job of installing the load cells with the help of R. Tweedie became such an entertaining affair that we even made it to the Edmonton Journal. O. Wood besides being invaluable in the field, even risking his life to install the pressure cells, made the job much easier with his sharp sense of humour at the appropriate times. Without him I would still be working in the instrumentation. The field work was so heavy that I. Bruce slipped a disk. I owe him a straight spine.

The support received from A. Muir in the machine shop saved me in crucial times in many opportunities during the field and laboratory work.

During the construction of the plane strain apparatus I counted with the full time help of my very dear friend Roberto Azevedo.

For the laboratory testing the help of A. Gale and the advice of O. Wood. and D. Fushtey were of extreme value.

The long discussions about the theoretical aspects of the work with my friend and colleague E. Evgin helped me tremendously to clarify ideas.Thanks, Erman.

The exchange of ideas with my colleagues F. El-Nahas, S. Fontoura, P. Kaiser, J. Simmonds and J. Weaver gave me the opportunity to critically review my thoughts.

The support received from the administrative staff of the Department of Civil Engineering was a great help. The kindness and efficiency of E. Kangas are specially thanked.

The advice and sugestions of profs. N.R. Morgenstern and S. Thomson throughout the work are greatly appreciated.

I am thanked to Dr. P. Lade for illustrating some points in his model and to Dr. Y. Vaid for making available to me information regarding the plane strain apparatus.

To Dr. M. Dusseault I want to express my many thanks for his difficult task of editing the text which I initially thought was written in English.

Dr. Z. Eisenstein was omnipresent during all the phases of this project. He went out of his way in many opportunities to help me out. It was a very rewarding and pleasant experience to work with him all these years. Somehow I feel sorry the work is finished. Dr. Eisenstein, accept my sincere gratitude.

The financial support received from the Department of Civil Engineering of the University of Alberta, the Conselho Nacional de Pesquisas and the Pontificia Universidade Catolica do Rio de Janeiro is greatly appreciated.

The cooperation from the City of Edmonton, in the person of Mr. R. Yacyshyn, permiting me free access to the construction site, is acknowledged.

To my parents Zequinha and Carminha I owe a very special thank. Their effort to provide me a good education was absolutely amazing.

I am very grateful for the moral support and encouragement rendered by my wife Cica. Her love gave me strength to reach the end.

LIST OF FIGURES

FIGURE	TITLE	PAGE
1.1	WEDGE EQUILIBRIUM	6
1.2	MEEN'S HYPOTHESIS	10
1.3	TERZAGHI'S STRESS DISTRIBUTION IN BRACED CUTS	13
1.4	PECK'S STRESS DISTRIBUTION IN BRACED CUTS	15
1.5	TSCHEBOTARIOFF'S STRESS DISTRIBUTION IN BRACED CUTS	17
1.6	TERZAGHI AND PECK'S DISTRIBUTION OF EARTH PRESSURE IN BRACED CUTS IN CLAY (1967)	19
1.7	STRESS DISTRIBUTION IN BRACED CUTS IN OAKLAND (ARMENTO)	22
2.1	EDMONTON NORTHEAST RAPID TRANSIT SYSTEM	27
2.2	NORTH EAST OF CENTENNIAL STATION	28
2.3	TYPICAL CROSS SECTION	33
2.4	TANGENT PILE WALL	34
2.5	TANGENT PILE WALL	35
2.6	SHEET PILE CROSS SECTION	36
2.7	GIRDER'S CROSS SECTION	37
2.8	BOTTOM FLOOR'S CROSS SECTION	37
2.9	L SHAPED BEAM	38

2.10 MEZZANINE FLOOR....................................40

2.11 MEZZANINE FLOOR COMPLETED..........................41

2.12 EXCAVATION BELOW THE MEZZANINE.....................41

2.13 EXCAVATION NORTH OF CENTENNIAL STATION.............42

2.14 EXCAVATION BELOW THE GIRDERS.......................42

3.1 ONE STEP ANALYSIS OF EXCAVATIONS....................45

3.2 STRESS PATHS INVOLVED IN EXCAVATIONS................46

3.3 LAYOUT OF INSTRUMENTATION...........................49

3.4 SLOPE INDICATOR SI1 READINGS........................51

3.5 SLOPE INDICATOR (PLASTIC CASING) INSIDE A LONG PILE.53

3.6 SLOPE INDICATOR SI2 READINGS........................54

3.7 SLOPE INDICATOR SI3 READINGS........................55

3.8 SETTLEMENT POINTS READINGS..........................59

3.9 STRAIN GAUGES IN THE MEZZANINE......................61

3.10 NORMAL STRESS ALONG THE HEIGHT OF THE MEZZANINE....62

3.11 LOAD CELL FOR THE MEZZANINE........................64

3.12 LOAD CELLS MOUNTED IN PANEL........................65

3.13 LOAD CELL PANELS IN FRONT OF THE "L" SHAPED BEAM...66

3.14 LOWERING A GIRDER IN FRONT OF A LOAD CELL PANEL....67

3.15 GIRDER IN THE FINAL POSITION.......................67

4.1 EDMONTON TILL-GRAIN SIZE DISTRIBUTION...............74

4.2 LABORATORY STRESS PATHS......................77

4.3 PASSIVE COMPRESSION TEST EDMONTON TILL......................................79

4.4 PASSIVE COMPRESSION TEST EDMONTON TILL......................................80

4.5 PASSIVE COMPRESSION TEST EDMONTON TILL......................................81

4.6 PASSIVE COMPRESSION TEST EDMONTON TILL......................................82

4.7 PASSIVE COMPRESSION TEST EDMONTON TILL......................................83

4.8 PASSIVE COMPRESSION TEST EDMONTON TILL......................................84

4.9 PASSIVE COMPRESSION TEST EDMONTON TILL......................................85

4.10 PASSIVE COMPRESSION TEST EDMONTON TILL......................................86

4.11 PASSIVE COMPRESSION TEST EDMONTON TILL......................................87

4.12 ACTIVE COMPRESSION TEST EDMONTON TILL......................................89

4.13 ACTIVE COMPRESSION TEST EDMONTON TILL......................................90

4.14 ACTIVE COMPRESSION TEST EDMONTON TILL......................................91

4.15 ACTIVE COMPRESSION TEST EDMONTON TILL......................................92

4.16 ACTIVE COMPRESSION TEST EDMONTON TILL..93

4.17 UNLOADING RELOADING TEST EDMONTON TILL..94

4.18 UNLOADING RELOADING TEST EDMONTON TILL..95

4.19 UNLOADING RELOADING TEST EDMONTON TILL..96

4.20 UNLOADING RELOADING TEST EDMONTON TILL..97

4.21 PASSIVE COMPRESSION TEST IN PLANE STRAIN EDMONTON TILL..........................99

4.22 PASSIVE COMPRESSION TEST IN PLANE STRAIN EDMONTON TILL..........................100

4.23 PASSIVE COMPRESSION TEST IN PLANE STRAIN EDMONTON TILL..........................101

4.24 PASSIVE COMPRESSION TEST IN PLANE STRAIN EDMONTON TILL..........................102

4.25 PASSIVE COMPRESSION TEST IN PLANE STRAIN EDMONTON TILL..........................103

4.26 PASSIVE COMPRESSION TEST IN PLANE STRAIN EDMONTON TILL..........................104

4.27 COMPARISON BETWEEN MODULUS OF DEFORMATION FROM TRIAXIAL AND PLANE STRAIN IN PASSIVE COMPRESSION...............107

4.28 COMPARISON BETWEEN MODULUS OF DEFORMATION FROM PASSIVE AND ACTIVE

COMPRESSION TEST IN TRIAXIAL..................109

4.29 SHEAR STRENGTH ENVELOPE EDMONTON TILL..110

4.30 STRESS PATH IN LABORATORY AND FIELD TESTS.......................................114

4.31 SASKATCHEWAN SANDS GRAIN SIZE DISTRIBUTION.................................121

4.32 PASSIVE COMPRESSION TEST SASKATCHEWAN SANDS..........................123

4.33 PASSIVE COMPRESSION TEST SASKATCHEWAN SANDS..........................124

4.34 PASSIVE COMPRESSION TEST SASKATCHEWAN SANDS..........................125

4.35 PASSIVE COMPRESSION TEST SASKATCHEWAN SANDS..........................126

4.36 ACTIVE EXTENSION TEST SASKATCHEWAN SANDS..127

4.37 ACTIVE EXTENSION TEST SASKATCHEWAN SANDS..128

4.38 ACTIVE EXTENSION TEST SASKATCHEWAN SANDS..129

4.39 PROPORTIONAL-ACTIVE COMPRESSION SASKATCHEWAN SANDS..........................130

4.40 COMPARISON BETWEEN MODULUS OF DEFORMATION FROM PASSIVE COMPRESSION AND ACTIVE EXTENSION TESTS IN TRIAXIAL SASKATCHEWAN SANDS..................132

5.1 VARIATION OF K2 WITH STRESS LEVEL

EDMONTON TILL....................................145

5.2 RELATION BETWEEN PLASTIC WORK AND

STRESS LEVEL IN EDMONTON TILL.................146

5.3 REPRESENTATION OF THE YIELD SURFACES.........148

5.4 VARIATION OF PARAMETER a WITH

CONFINING STRESS EDMONTON TILL...............150

5.5 ELASTOPLASTIC MODEL PREDICTION...............151

5.6 ELASTOPLASTIC MODEL PREDICTION...............152

5.7 ELASTOPLASTIC MODEL PREDICTION...............153

5.8 ELASTOPLASTIC MODEL PREDICTION...............154

5.9 ELASTOPLASTIC MODEL PREDICTION...............155

5.10 STRESS WITH PREDOMINAT INCREASE IN

ISOTROPIC STRESS COMPONENT...................157

6.1 FLOWCHART....................................161

6.2 STRESS DISTRIBUTION BELOW THE BOTTOM

OF THE EXCAVATION............................165

6.3 DETERMINATION OF THE MODULUS OF

DEFORMATION..................................170

7.1 CROSS SECTION IDEALIZATION..................179

7.2 FINITE ELEMENT MESH..........................180

7.3 SIMULATION OF THE CONSTRUCTION

PHASES..183

7.4 COMPARISON OF FIELD MEASUREMENTS OF

SLOPE INDICATOR SI2 AND FINITE

ELEMENT PREDICTIONS...........................185

7.5 COMPARISON OF FIELD MEASUREMENTS OF

	SLOPE INDICATOR SI3 AND FINITE ELEMENT PREDICTIONS	187
7.6	COMPARISON OF GROUND MOVEMENT AND FINITE ELEMENT PREDICTIONS	188
7.7	LATERAL STRESS DISTRIBUTION ALONG THE WALL	190
7.8	COMPARISON OF LATERAL STRESS DISTRIBUTION BETWEEN CONCRETE TANGENT PILES AND SHEET PILE WALL ABOVE THE MEZZANINE	194
7.9	INFLUENCE OF THE WALL THICKNESS ON THE LATERAL STRESS DISTRIBUTION	195
7.10	INFLUENCE OF THE WALL THICKNESS ON THE LATERAL LOAD	196
7.11	INFLUENCE OF THE WALL THICKNESS ON THE GROUND MOVEMENT	198
A.1	LOAD TRANSFER	240
A.2	BLOW UP OF THE MESH CLOSE TO THE WALL	243
B.1	FRICTIONLESS END PLATE	294
B.2	LATERAL LOAD CELL	294
B.3	SEALING PLATE WITH MEMBRANE	295
B.4	LATERAL SUPPORT AND MEMBRANE SEALING PLATES	295
B.5	LOAD CELL AT THE BASE PEDESTAL	296
B.6	END PLATE	297
B.7	LATERAL MEMBRANE SEALING PLATE	298

B.8 LATERAL MEMBRANE SUPPORT PLATE....................299

B.9 LATERAL AND BOTTOM LOAD CELLS.....................300

B.10 LOADING FRAME..301

B.11 LOAD CAP AND PEDESTAL................................302

C.1 COMPOSITE CROSS SECTION OF THE MEZZANINE..304

LIST OF TABLES

TABLE	TITLE	PAGE
2.1	STRATIGRAPHY	31
4.1	HYPERECLAE PARAMETER FOR TRIAXIAL PASSIVE COMPRESSION TESTS	116
4.2	HYPERECLAE PARAMETERS FOR TRIAXIAL ACTIVE COMPRESSICN TESTS	117
4.3	HYPERECLAE PARAMETERS FOR PLANE STRAIN PASSIVE COMPRESSION TESTS	118
4.4	HYPREECLAE PARAMETERS FOR PLANE STRAIN ACTIVE COMPRESSION TESTS	118
7.1	NCRMAL STRESS IN THE MEZZANINE	182

Table of Contents

Chapter Page

1. INTRODUCTION..1

1.1 Nature of the problem..............................1

1.2 Mechanisms involved in excavations.................2

1.3 Earth pressure theories............................4

1.4 Semi-empirical rules...............................9

1.5 Proposed study....................................22

2. DESCRIPTION OF THE FIELD CASE......................26

2.1 Introduction......................................26

2.2 Geology...29

2.3 Local profile.....................................30

2.4 Structure and construction procedure..............32

3. FIELD INSTRUMENTATION..............................43

3.1 Preliminary study.................................43

3.2 Layout of the instrumentation.....................47

3.3 Ground movement...................................50

3.3.1 Inclinometer....................................50

3.3.2 Multipoint extensometer.........................56

3.3.3 Settlement points...............................57

3.4 Loads and stresses................................59

3.4.1 Pressure cells..................................59

3.4.2 Strain Gauges...................................60

3.4.3 Load cells......................................64

3.4.4 Summary...68

4. LABORATORY TESTING.................................69

4.1 Introduction..69

4.2 Till..72

4.2.1 Sampling..72

4.2.2 Characterization..................................73

4.2.3 Triaxial..74

4.2.3.1 Passive compression.............................78

4.2.3.2 Active compression..............................87

4.2.3.3 Unloading reloading.............................93

4.2.4 Plane strain......................................98

4.2.4.1 Passive compression.............................98

4.2.4.2 Active compression..............................102

4.2.5 Summary...104

4.3 Saskatchewan Sands..................................119

4.3.1 Sampling..119

4.3.2 Characterization..................................120

4.3.3 Triaxial tests....................................121

4.3.3.1 Passive compression.............................121

4.3.3.2 Active extension................................126

4.3.3.3 Proportional active compression.................129

4.3.4 Summary...130

5. CONSTITUTIVE MODEL..................................134

5.1 Introduction..134

5.2 Lade's stress strain theory.........................137

5.3 Determination of the elasto plastic parameters......144

5.4 Analysis..151

6. NUMERICAL SOLUTION..................................158

6.1 Introduction..158

6.2 General description of the solution..............158

6.3 Load determination....................................161

6.4 Stress strain relationship........................166

7. RESULTS OF ANALYSIS AND CONCLUSIONS.................175

7.1 Introduction..175

7.2 Pile movement...183

7.3 Vertical movement.....................................187

7.4 Lateral load and stress.............................189

7.5 Influence of the thickness of the wall..........193

7.6 Summary...198

7.7 Conclusions and suggestions for further research..199

BIBLIOGRAPHY...206

APPENDIX A. COMPUTER PROGRAM..........................230

APPENDIX B PLANE STRAIN APPARATUS......................293

APPENDIX C. CALCULATION OF MEZZANINE LOAD..............303

1. INTRODUCTION

1.1 Nature of the problem

The design of earth retaining structures involves the determination of the external forces imposed on the structure and the evaluation of the displacements in the surrounding ground. The structure has to be strong enough to carry the load safely and the ground movement should not cause excessive movement to existing buildings and utility ducts.

If the retaining wall replaces identically the excavated ground, the knowledge of the at rest coefficient of earth pressure would enable the soil engineer to predict the lateral load and no movement should be observed in the neighborhood. Under these circumstances no mobilization of the soil shear strength is permitted beyond the initial conditions. If, on the other hand, the construction procedure or the flexibility of the structure permits full mobilization of the shear strength of the soil, the determination of the lateral load can be easily obtained by conventional earth pressure theories. The wall, however, would have to move in a certain fashion to guarantee this condition. Most engineering situations, particularly braced cuts, do not fall into any of these two limiting conditions. As a result of the construction procedure the movement of the retaining structure does not produce the yielding necessary to allow the soil to fully mobilize its shear strength. The trend towards deeper excavations in congested areas is forcing the engineering profession to investigate the relationship between stress distribution and the magnitude and pattern of associated movement in connection with deep excavations.

1.2 Mechanisms involved in excavations

The disturbance of the original state of stress is produced in two ways. First, the removal of material adjacent to the wall causes a release of the horizontal normal stress. This released load is transmitted to the retaining wall and the struts whose deformation results in displacement in the adjacent soil which in turn mobilizes its shear strength. The load now is shared between the retaining structure and the surrounding material. Typically this situation is predominant when excavating narrow trenches. The soil movement is primarily due to bending of the wall and yielding of the struts. Second, the removal of the soil causes a release in vertical normal stress at the bottom of the excavation . As a consequence there is a reduction of the passive resistance of the soil inside the excavation. The soil movement this time occurs towards the bottom of the excavation. Again there is mobilization of the shear strength in response to the displacement. The width of the excavation and the depth to a firm base below the bottom will play an important role in this case. Bjerrum , Frimann and Duncan (1972) believe the reduction in vertical stress is almost the only factor responsible for values of horizontal stresses greater than Rankine's active value.

The deformed shape of the wall is influenced by the stiffness of the wall and the location of the struts. In the vicinity of the strut there will be much less horizontal movement than in the center of the wall. This uneven displacement will have a significant impact on the stress distribution. The mechanism of the phenomenon was explained by Terzaghi (1943) and it is referred to as the arching effect. In his own words :

> " If one part of the support of a mass of soil yields while the remaining stays in place , the soil adjoining the yielding part moves out of its original position between adjacent stationary masses of soil. The relative movement within the soil is opposed by shearing resistance within the zone of contact between the yielding and the stationary masses. Since the shearing resistance tends to keep the yielding part in its original position, it reduces the pressure on the yielding part of the support and increases the pressure on the adjoining stationary part. This transfer of pressure from a yielding mass of soil onto adjoining stationary parts is commonly called the arching effect, and the soil is said to arch over the yielding part of the support. Arching also takes place if one part of a yielding support moves out more than the adjoining

parts."

Arching will be a dominant feature in redistributing the normal stress to be carried by the retaining structure.

1.3 Earth pressure theories

Many advancements in engineering solutions have been generated in response to economic demands and material conditions of society. Such is the case of earth pressure theories where advancement was impelled by the construction of roads and canals in the eighteenth century.

The first comprehensive treatment of the problem was given by a French engineer , Charles Augustin Coulomb in 1776. In his memoirs he recorded various engineering problems including that of earth pressure. Coulomb isolated a wedge of soil and wrote two force equilibrium equations. The total value of the lateral pressure was calculated assuming a planar failure surface and shear resistance along this plane as fully motilized, although he stated there is no movement of the wall. He pointed out the possibility of different failure surfaces but experience with overturned walls led him to use this assumption. No reference was made about the state of stress inside the wedge. The greatest thrust for all possible wedges is the design load. Coulomb initially considered no friction being developed between the soil and the wall but in a later section the equations were modified to include it. The position of the resultant was clearly defined when he studied the equilibrium of the wall by writing a moment equilibrium equation around the toe. A triangular distribution of earth pressure was assumed. Although he recognized the influence of different types of soil, which was done for the first time, he concluded with a very practical recommendation: " I think that for all kinds of soil, retaining walls can be designed without danger with a batter of 1/6 and with the ridge one seventh of the height". In 1857 Rankine proposed basically a particular case of Coulomb's analysis in which there was no friction between the soil and the wall. Rankine, however , assumed a plastic state being developed behind the wall and, departing from Coulomb, a small movement of the wall being enough to reach that state of stress, although nothing was said with respect to the magnitude of this movement. In 1910 Resal extended Rankine's equation to determine the lateral load in cohesive materials.

The assumption of hydrostatic stress distribution both along the back of wall and the surface of sliding when applied to situations where there is friction between the wall and backfill material leads to a failure of the forces to concur at one point as shown in figure 1.1.a. , where W is the wedge's weight, R the soil reaction and Pa the lateral load.This violation of equilibrium can be explained by the fact the actual slip surface is curved as in figure 1.1.b. Similar to the Coulomb's asumptions, the general wedge theory became a very popular tool to design retaining structures. Instead of planar surfaces, circular and

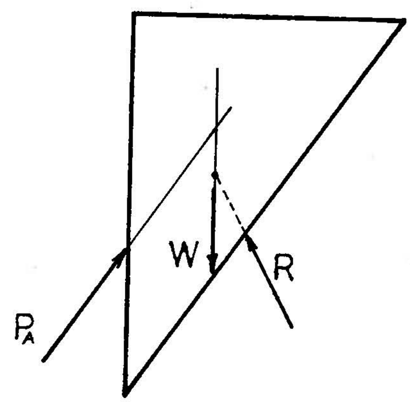

1.1.a

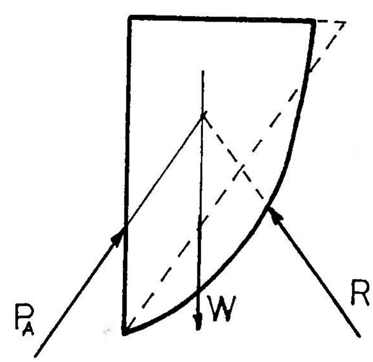

1.1.b

FIGURE 1.1 WEDGE EQUILIBRIUM

logarithmic spirals were extensively used. There is no requirement with respect to the location of the resultant of lateral stresses and consequently stress distribution. This very attractive theory just laid down induced designers to believe the problem was almost solved. Terzaghi (1936,b) expressed his concern about the limitations of the theory: "Hence the fundamental misconception associated with the traditional earth pressure computations does not reside in the theories as such. It lies in the failure of the designers to consider the limitations on the validity of the theory". Terzaghi's concerns were not very much about the shape of the failure surface, friction offered by the wall or the position of the resultant, although he was aware of their importance. His apprehension was related to the complete mobilization of the shear resistance of the soil along the failure plane. Coulomb simply assumed no movement and Rankine presumed little movement would be enough to reach a minimum value for the lateral stress. In 1936 Terzaghi reported large scale model tests results in sand to investigate the influence of the lateral displacement. He ran tests in loose and dense sands allowing the wall to displace in the horizontal direction and to rotate around the toe. Terzaghi concluded for dense sands a triangular stress distribution to be representative as long as the displacement was large enough to induce slip. The yielding necessary to reach Coulomb's total load was significantly smaller. Initial displacements change the initial state of stress (at rest) very rapidily to Coulomb's value but not with a hydrostatic distribution , and further yield causes a gradual redistribution of stress without changing the value of the resultant of the lateral stress. When testing loose sands , the resultant remained in the same position throughout the test and a much larger displacement of the wall was necessary to reach Coulomb's value. The stress distribution was of triangular shape during the entire duration of the test. It was evident the arching effect was a predominant factor in the redistribution of the stresses in dense sands.

The most striking difference between Terzaghi's tests and the actual behaviour of strutted excavations is in the type of deformation. As soon as the first level of struts is placed, the horizontal movement at the top is greatly obstructed, and further excavation causes movement of points below the strut until a new level of struts is installed. The final displacement shape is closer to a wall rotation around the top, although a simple rotation around the toe is far from the behaviour of actual engineering structures , since the wall bends and the struts contract as the excavation proceeds, not to mention details related to the construction procedure being used. Coulomb's earth pressure theories suit best to rigid retaining walls, where no bending of the structure is permitted.

From the above it seems that a proposition in the form of a comprehensive theoretical solution for strutted walls would be considered unattainable. The most efficacy can be obtained by gradually gaining experience from instrumented field cases to evaluate the shortcomings of the analytical solutions.

1.4 Semi-empirical rules

This section presents some case histories which illustrate the development of semi-empirical design rules for braced excavations. It is not the aspiration of the writer to present a complete collection of field measurements in the area. Some investigations which deserve to be mentioned may well have been overlooked.

One of the first engineers to direct his attention to the actual behaviour of braced excavations was Meen (1908) who noticed in strutted excavations in sands that the upper struts were working at very high stresses compared to the lower struts. It was a purely visual observation at that time. The upper struts in some cases even bent a little while the lower level ones were not so tight. This observation contracicted Coulcmb's hypothesis of a hydrostatic lateral pressure distribution. Meen attributed this anomalous behaviour at that time to arching effects. He then proposed a cifferent approach to the design of such structures. The resultant was to be applied at a distance of 2/3 of the height from the bottom of the excavation. He assumed a wedge cf soil (figure 1.2) ABC sliding freely along BC which makes a angle <u>a</u> (angle of repose) with the

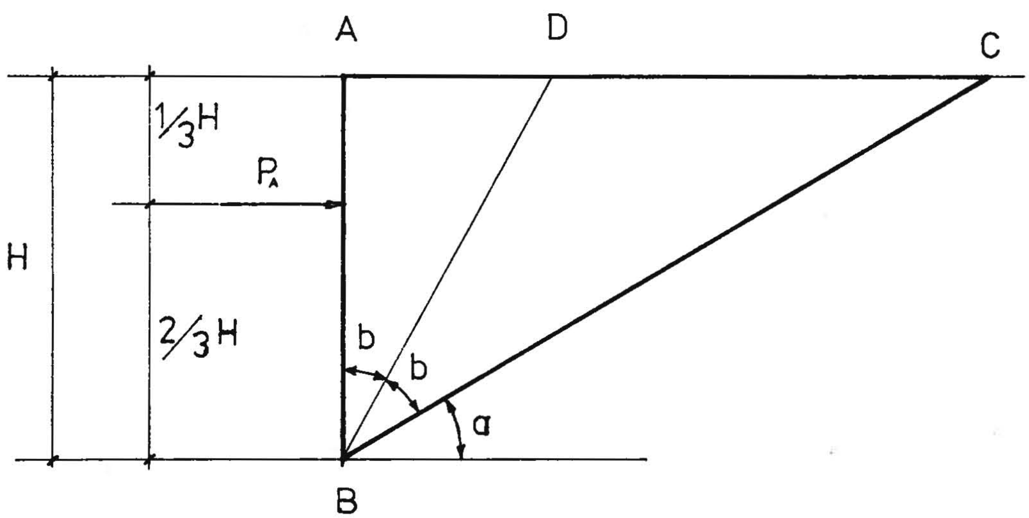

a = angle of repose

FIGURE 1.2 MEEN'S HYPOTHESIS

horizontal direction. The angle ABC is bisected by BD. The total horizontal thrust is calculated by :

$$Pa = W(ABD)/\tan a \quad (1.1)$$

This design procedure was widely used by the engineering profession on some of the most important constructions in that decade ; for example the retaining structure for the Brooklyn Subway in New York.

Moulton (1920) also recognized the influence of the arching effect and noticed that the maximum earth pressure was either at or slightly above the midheight. He argued the failure surface was not a function of the angle of repose but it would be , regardless of the type of soil , in a plane reaching the surface at a distance of half the depth from the wall.

Terzaghi (1936,a) assumed the ratio between the horizontal and vertical stresses to be of the form :

$$K = Kc (1 + Ci*Z/H) \quad (1.2)$$

where :

- Kc = minimum value of the ratio (Ka)

- Ci = coefficient which express the relation between K and the sheeting deflection. For example , for Rankine state (active) Ci = 0.
- H = depth of the excavation
- Z = vertical distance between the bottom of the excavation and the point in question.

He obtained a trapezoidal earth pressure distribution for sands. These results had still to be confirmed . Field measurement in sands was done in a braced excavation for the Subway in Berlin (Terzaghi, 1941) which confirmed Terzaghi's prediction. He then proposed the earth pressure distribution of figure 1.3 . He believed the reaction of the soil below the bottom of the excavation had little influence on the stress distribution, therefore it was ignored. The arching effect hypothesis was then substantiated by field measurements in sands.

Peck (1941,1943), during the construction of the Chicago Subway , took the opportunity to investigate the behaviour of cohesive soils. Peck's concern, besides the determination of the strut loads, was the validity of the implicit hypothesis in Coulomb, Rankine and the general wedge theory about full mobilization of the shear strength of the soil. It was clear to him that this had to be obtained at the expense of some lateral displacement. If

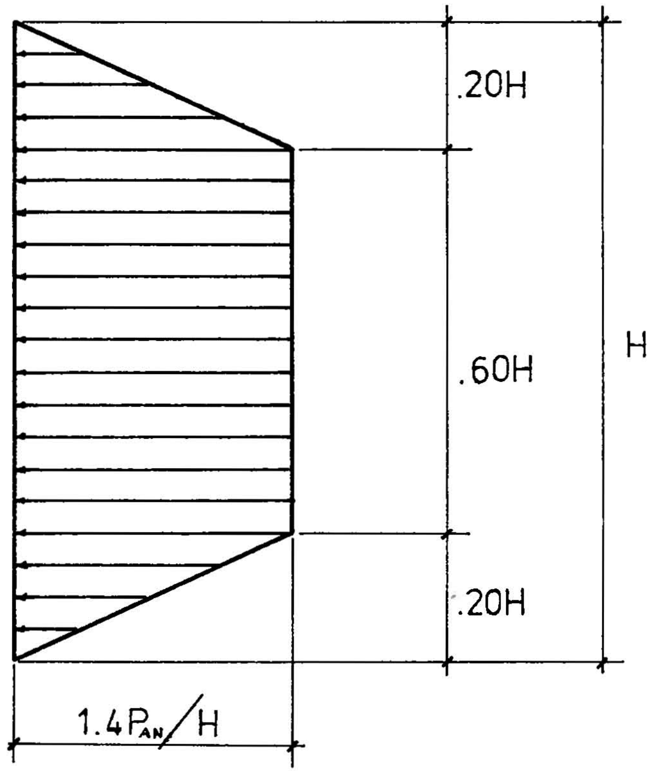

$P_{an} = 1/2 \gamma H^2 K_a$

$K_a \rightarrow$ Coulomb

FIGURE 1.3 TERZAGHI'S STRESS DISTRIBUTION IN

BRACED CUTS

insufficient expansion would explain loads larger than the earth pressure theories, he should obtain significant scattering between different contractors' section loads. Nevertheless, by monitoring loads in sections built by different contractors, he consistently obtained a ratio of 0.75 between the shear strength actually developed and the maximum available shear strength. The insufficient expansion hypothesis was very unlikely. It seemed the shear strength of the soil was being mobilized but the presence of the struts was inducing shear stress redistribution. The resultant of the lateral load was located at a distance of 0.43H from the bottom of the excavation. From Peck's measurements a new insight was brought with respect to the amount of yielding necessary to mobilize the soil's shear strength. The designers believed lateral displacement in the order of 5% of the depth of the excavation was necessary, but Peck observed 0.25% would be enough. In the conclusion to his work, Peck suggested the stress distribution of figure 1.4 . The factor of 1.2 was to compensate for the scattering of the results. These design recommendations emerged from field measurements in medium stiff clays. Peck's determination of Ka can be reproduced by computing the total lateral load Ea from Rankine's expression for active stresses where PHI = 0. (equation 1.2) and dividing by the total fluid pressure γH**2/2.

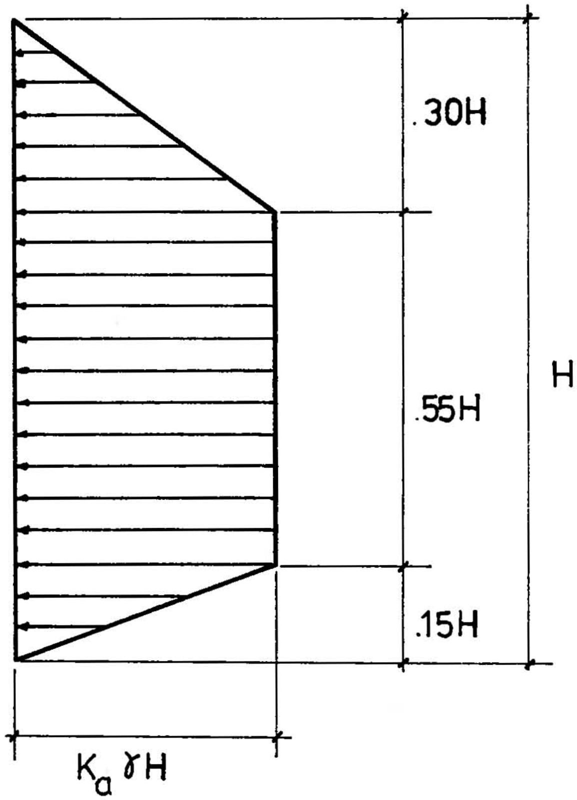

$$K_a = 1.2\left(1 - \frac{4\,Cu}{\gamma H}\right)$$

FIGURE 1.4 PECK'S STRESS DISTRIBUTION IN BRACED CUTS

$$Pa = \gamma H - 4\ Cu \qquad (1.3)$$

$$Ea = \gamma H^{**}2/2 - 2\ Cu\ H \qquad (1.4)$$

$$Ka = \gamma H^{**}2/2/Ea \qquad (1.5)$$

$$Ka = 1 - 4\ Cu/(\gamma H) \qquad (1.6)$$

It is implicit in this derivation that tension will be developed up to the height 4 Cu/γ contributing to the stability of the wa Tschebotarioff (1951) questioned the validity of Peck's recommendation and proposed the stress distribution on figure 1.5 .

Golder(1948) took measurements in a trench excavated in stiff fissured clays and according to classical earth pressure theories or Peck's recommendations the wall would have been able to stand by itself, but the struts were observed to be carrying a substantial load.

DiBiaggio and Bjerrum (1957) confirmed the presence of load in braced excavations in stiff fissured clays for depths in which Peck's distribution indicated no load , but after a certain depth Peck's predictions were suitable. In view of data collected since Terzaghi and Peck (1948) they reviewed their recommendations in 1967 which were even more substantiated by further measurements (Peck, 1969). Peck maintained that the cuts primarily investigated did not

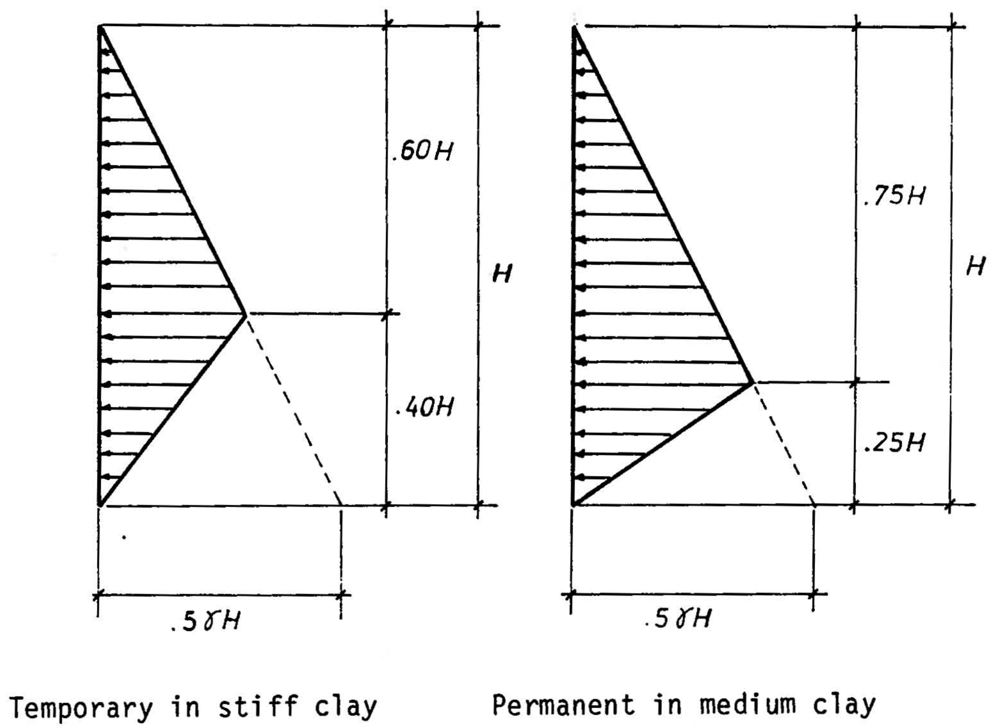

FIGURE 1.5 TSCHEBOTARIOFF'S STRESS DISTRIBUTION IN BRACED CUTS

allow development of failure below the bottom of the excavation due to the presence of much stiffer material . In this case the expression 1.6 would remain unaltered for medium and soft clays. The soil profile in Oslo(NGI, 1962) did not provide the same conditions. In this case the potential slip surface can extend well beyond the bottom of the cut therefore a new expression for Ka was proposed (equation 1.7) (figure 1.6a) .

$$Ka = 1 - m\ 4\ Cu/(\ H) \ldots\ldots\ldots\ldots\ldots\ldots\ldots\ldots\ldots\ldots (1.7)$$

in which m is an empirical reduction factor to be applied to the value of Cu. For the Oslo cuts the value of m was found to be 0.4 , which also applies to the measurements for the subway in Mexico City (Rodriguez and Flammand,1968). It is worth while to mention that in Chicago cuts the strut loads correspond to the value $m = 1.0$ even for intermediate depths, a situation in which the potential slip surface could develop beyond the bottom. Terzaghi and Peck (1967) attributed the variation of m to the stress strain characteristics of the clay, and not to the value of the stability number N (H/Cu), which is a factor indicative the excavation is approaching a complete base failure. They believed the basic difference between the Chicago and the Oslo clays was the preloading to which both have been

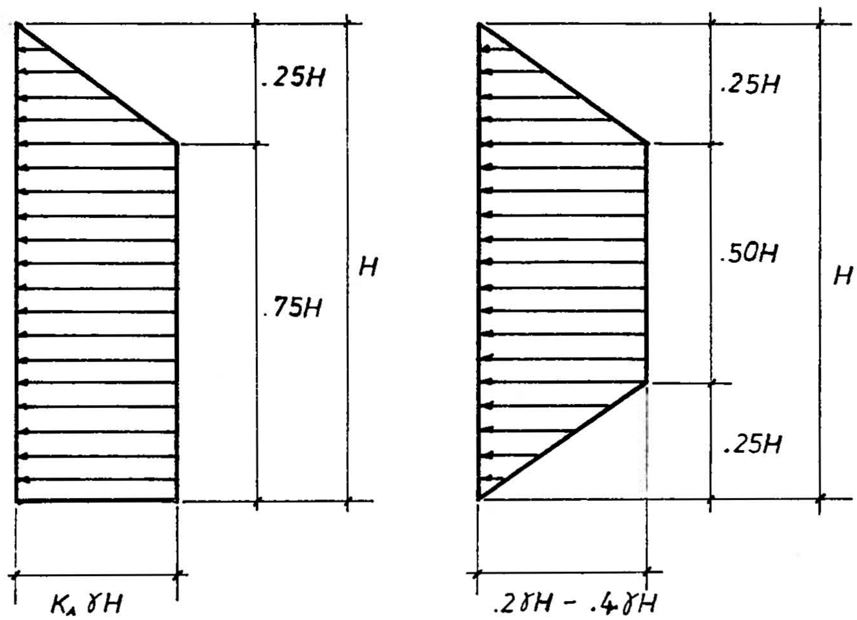

1.6.a 1.6.b

FIGURE 1.6 TERZAGHI AND PECK'S DISTRIBUTION OF EARTH PRESSURE IN BRACED CUTS IN CLAY (1967) subjected. The Oslo clays (as for Mexico City clays) are truly normally consolidated whereas the Chicago clays have been slightly preloaded. This preloading was not enough to alter the strength parameters but it was sufficient to modify the initial modulus of deformation. Based on a slip surface below the bottom of the excavation Henkel (1972) obtained values of lateral stress significantly higher than Rankine's value, and he therefore attributes the value of m to be associated with weak soil below the bottom of the excavation. With respect to stiff clays the value of Ka using equation 1.7 would still be negative. The expression for Ka was based on the assumption of the development of plastic zones, but for values of N<4 this would not be the case, therefore it should not be used for values of N<4. Terzaghi and Peck (1967) then proposed the stress distribution of figure 1.6.b. The lower va to retaining structures allowing reduced movement and for short construction time, and the upper value otherwise. This was an empirical recommendation still to be proved by field measurements. Special attention from now on will be devoted to excavation in stiff clays , an area in which there are more questions still to be answered.

Some more recent field instrumentations registered lateral loadon wall in stiff soils. Measurements of stress on a tied-back wall in stiff clays by Mensur and Alizadeh (1970) indicated a value of $0.10\gamma H$. Chapman, Cording and Schnabel (1972) instrumented several sections in the

Washington D.C. Subway . The soil profile is composed of stratified layers of stiff silty clay, sand and gravel. The results of their measurements suggested $0.15\gamma H$ for depths around 30 feet, $0.20\gamma H$ for depths of 40 to 50 feet and $0.23\gamma H$ for depths of 60 feet. Armento (1972) monitored the performance of a braced excavation in stiff sandy clay in Oakland, California. He proposed the stress distribution of figure 1.7 . Clough, Weber and Lamont(1972) obtained $0.4\gamma H$ as the best fit for their measurements on a tied-back wall in Seattle stiff fissured, varved lacustrine clay.

1.5 Proposed study

According to the type of structure designed to support lateral earth pressure and control settlements, different modes of behaviour are present , therefore requiring distinct treatments. The rigidity of the retaining structure has a direct impact on loads and displacements and here, for simplicity, they are divided into three categories:

1. rigid wall - the retaining structure is stiff enough to prevent any bending of the wall. It moves as a rigid block either by translation or rotation around the base. Traditional earth pressure theories estimate the total load and earth pressure distribution with satisfactory accuracy.
2. flexible wall - the stiffness of the retaining wall is such that significant bending is present. The embedment at the base provides a substantial contribution to

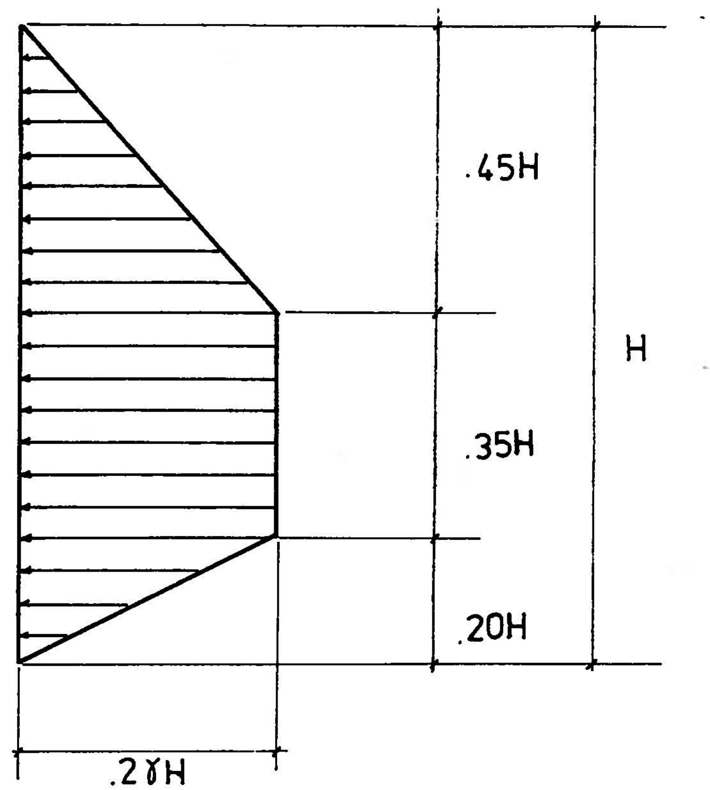

FIGURE 1.7 STRESS DISTRIBUTION IN BRACED CUTS IN OAKLAND

ARMENTO (1972)

resist the lateral load. Cantilever and anchored sheet piles fall into this category, as well as braced sheeting.

3. semirigid wall - a class of structure where bracing or anchors are present to avoid excessive settlement and the wall is not flexible as a sheet pile wall, but flexible enough to allow some bending, for example a diaphragm or tangent pile wall.

The problem being investigated here, relates to the behaviour of semirigid structure in stiff soil.

The objective of this research, besides documenting a field case of a deep excavation in stiff soil , is to improve the capability to predict earth pressure distribution and the pattern and magnitude of the displacement caused by the excavation.

The line of attack adopted here involves four different phases described as follows:

1. acquisition of field data

To evaluate the gap between theoretical methods and actual behaviour of engineering structures it is imperative to have field observation on full-size structures. An analytical method which is able to reproduce field data provides a sound basis for future design guidelines. The first phase involves the installation of field equipment necessary to monitor strut loads, soil movement and lateral stresses in a semirigid structure in stiff soil.

2. laboratory representation

Peck (1969) alleges the modulus of deformation of the ground to be the most important parameter governing displacement in deep excavations. Lambe (1970) and Henkel (1970) emphasized the importance of the stress path for excavation problems. The objective in this step lies in the determination of an adequate stress-strain relationship to represent the actual field conditions. Samples of "undisturbed" material will be extracted and submitted to laboratory tests under different stress paths.

3. analytical model

In situations where the stability factor is less than 4 there is no marked presence of a zone of plastification, therefore traditional earth pressure theories are not suitable. An adequate analytical solution for soft and medium clays under such circumstances is provided by the theory of elasticity, if there is no risk of base failure (Morgenstern and Eisenstein, 1970). The objective of this phase is an analytical solution for semirigid structures in stiff soils.

4. analysis of the case history

All the three previous steps will be brought together in this phase. With the stress strain relationship obtained from the laboratory representation, with the aid of the results generated by the analytical model , a critical analysis of the field data will be performed . It is hoped the field data can be reproduced by the analytical model, therefore allowing a reliable parametric study to evaluate the influence of some of the variables.

It is expected that a broader perspective can be obtained by this integrated approach. Field observation, laboratory investigation and the analytical solution will be all examined with the purpose to evaluate the relative importance of each one of them in the light of the overall behaviour.

2. DESCRIPTION OF THE FIELD CASE

2.1 Introduction

The rapid development of the City of Edmonton led the city planners to propose the construction of a light rail transit system to improve its public transportation facilities. The North East Rail Rapid Transit line (figure 2.1) was concluded to be the line of the highest priority. It joins the downtown area to zones which host public entertainment events, therefore requiring fast flow of people in short periods of time.

The dominant presence of stiff soil, in the form of a glacial till (figure 2.2) in the area of the underground portion of the line, offered a great opportunity to study the performance of retaining structures. The geotechnical properties and a brief summary of the local geology will be presented in subsequent sections. The underground part connecting Jasper and Centennial stations was constructed in two parallel tunnels and their performance has been described elsewhere (Eisenstein and Thomson , 1978). The Jasper station is located in the downtown core of the city surrounded by buildings. The Centennial station location, on the contrary , is free of interference from construction in the neighborhood, and is therefore a more appropriate case for an investigation.

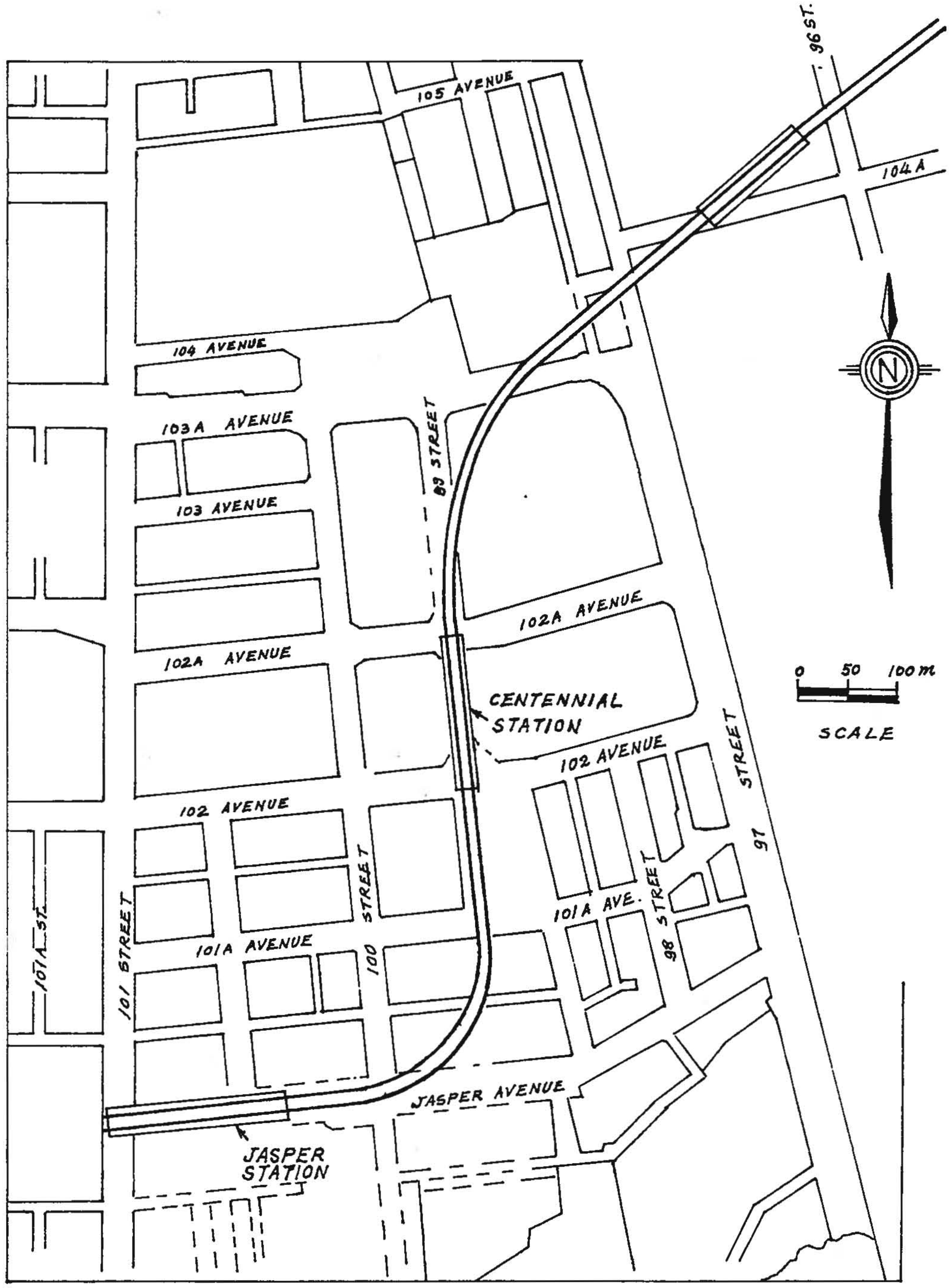

FIGURE 2.1 EDMONTON NORTHEAST RAPID TRANSIT SYSTEM

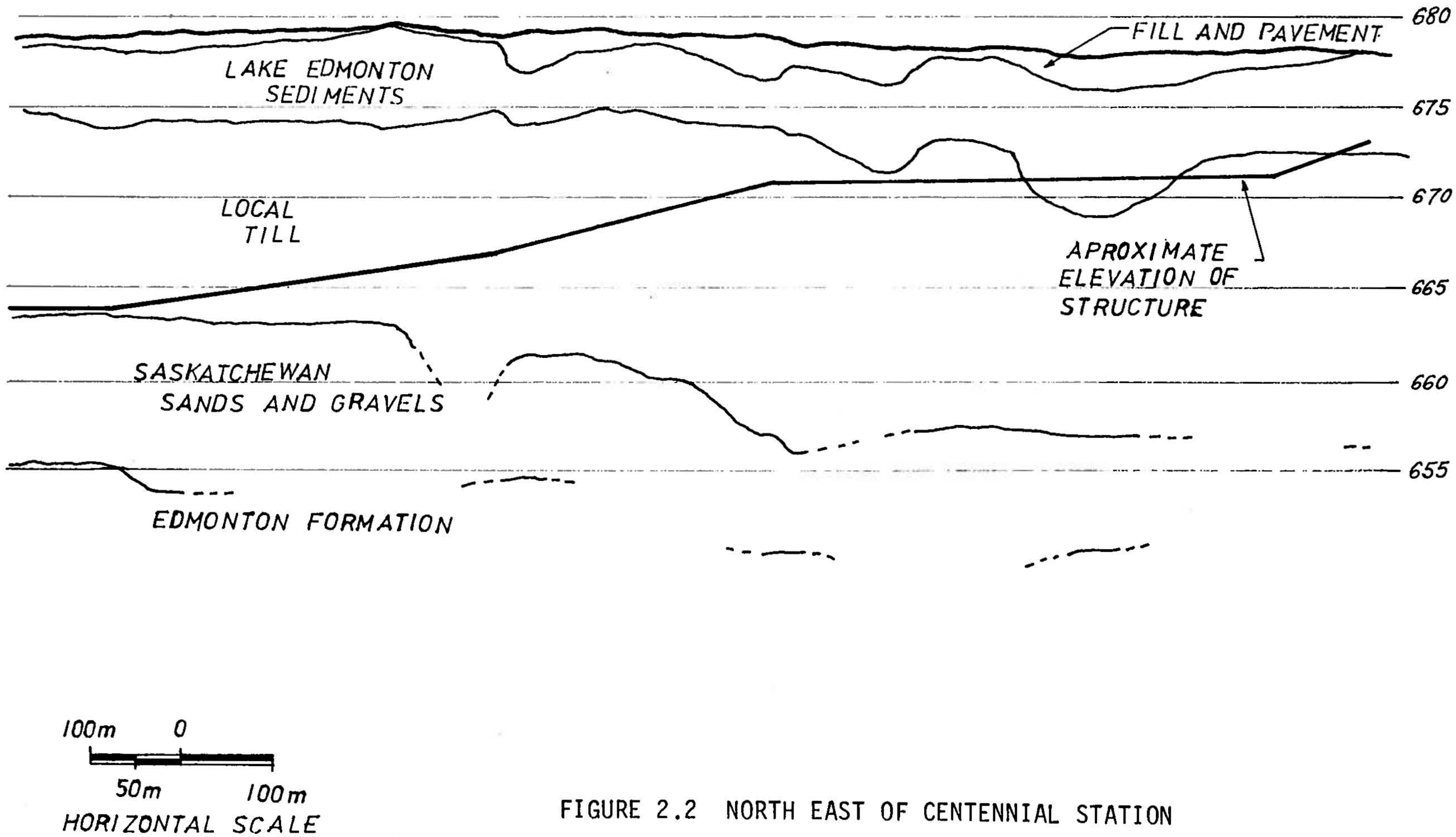

FIGURE 2.2 NORTH EAST OF CENTENNIAL STATION

2.2 Geology

The geology of the Edmonton area has been described by a large number of authors (Bayrock and Hughes , 1962 , Bayrock and Berg , 1966 , Westgate , 1969 , Ramsden and Westgate , 1971 and May and Thomson, 1978). A brief sumary will be presented here.

During late Cretaceous time (80,000,000 years B.P.) the Edmonton area was covered with a shallow continental sea. Clay, silt and sand were deposited. Some volcanic activicty in the west deposited blankets of volcanic ash. As a result, fine-grained bentonitic sandstones, siltstone and clay shales (sedimentary rock formed by particles less than 0.06 mm. with laminated structure) were formed. During much of the Tertiary and early Pleistocene times, the area was subjected to erosion cycles. The last major erosion cycle before glaciation formed the preglacial channel of the North Saskatchewan River. Streams flowing from the west deposited different sizes of quartzite rock fragments known as Saskatchewan sands and gravels. A thick ice steet advancing from the northeast laid down a glacial deposit called lower till. A later advancement from the northeast gave origin to the upper till. The upper till is yellowish with columnar joints and the lower one greyish with a rectangular joint system. The presence of thin layers of sand represent minor washing of glacial debris by running water. The meltwater from the glacier resulted in the formation of proglacial lakes which gave origin to the surficial deposit known as

Lake Edmonton clay.

2.3 Local profile

In addition to the test hole data obtained for this research project, boreholes logs from nearby projects were utilized to aid the interpretation of the local profile. At the location of the section under investigation three boreholes for multiple-point magnetic extensometers and one for a slope indicator were drilled. Previous light construction activities in the area has removed part of the surficial materials, and assorted fill has been encountered in the initial 1.5 meters. Table 2.1 can be taken as the general profile for the section under study. The presence of water was observed at depths of 27 meters.

TABLE 2.1

material	description	depth(m)
fill	Light brown clay. Some gravel and sand. Pieces of concrete and clay bricks from old construction	0 to 1.5
Lake Edmonton clay	Brown and dark grey silty clay. Firm to stiff	1.5 to 4.5
upper till	Medium brown clay till. Clay, silt and sand. Traces of coal. Some gravel. Stiff	4.5 to 10
lower till	Dark grey clay till. Clay silt and sand. Traces of coal. Some gravel. Stiff	10 to 17.5
Saskatchewan sands	Medium sand with traces of coal.	17.5 to 23
Edmonton formation	Interbedded mudstones and siltstones	25 to ?

2.4 Structure and construction procedure

The retaining structure for the Centennial station consists of a vertical wall supported laterally by three levels of permanent struts.

A typical cross section can be seen in figure 2.3 . The vertical wall is composed of concrete tangent piles (figures 2.4 and 2.5) . Every fifth concrete pile starts at the ground level and the bottom is belled and embedded in the bedrock; their diameter is 106.7 cm. The four intermediate concrete piles are 91.4 cm. diameter . Their tops are at the mezzanine level and their bottoms are located 200 cm. below the bottom of the excavation (figure 2.4). The sheet pile is composed of sections of the type MZ 27 which dimensions are in figure 2.6. The girders , forming the street level surface structure, are precast concrete beams with the cross section of figure 2.7.

On top of the long piles there is an "L" shaped concrete beam which runs parallel to the axis of the excavation, providing a support for the girders(figure 2.9). The mezzanine floor structure is cast-in-place with the dimensions of figure 2.10. . The bottom floor is a continuous beam also cast in place with the dimensions of figure 2.8.

The first stage of the construction procedure consists of drilling holes for the long belled piles, followed by the placement of the reinforcement and the concrete. After all

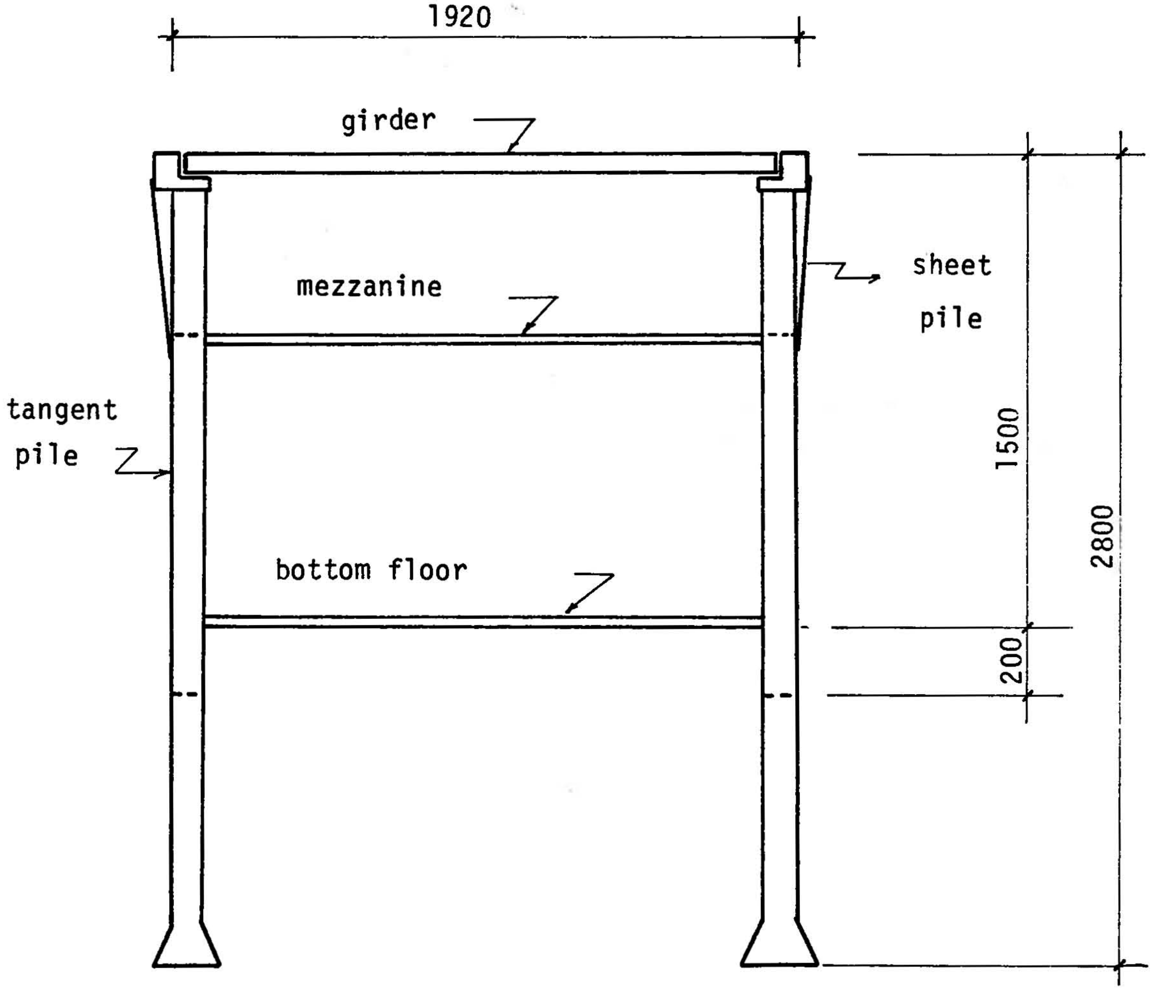

note: all dimensions in cm

FIGURE 2.3 TYPICAL CROSS SECTION

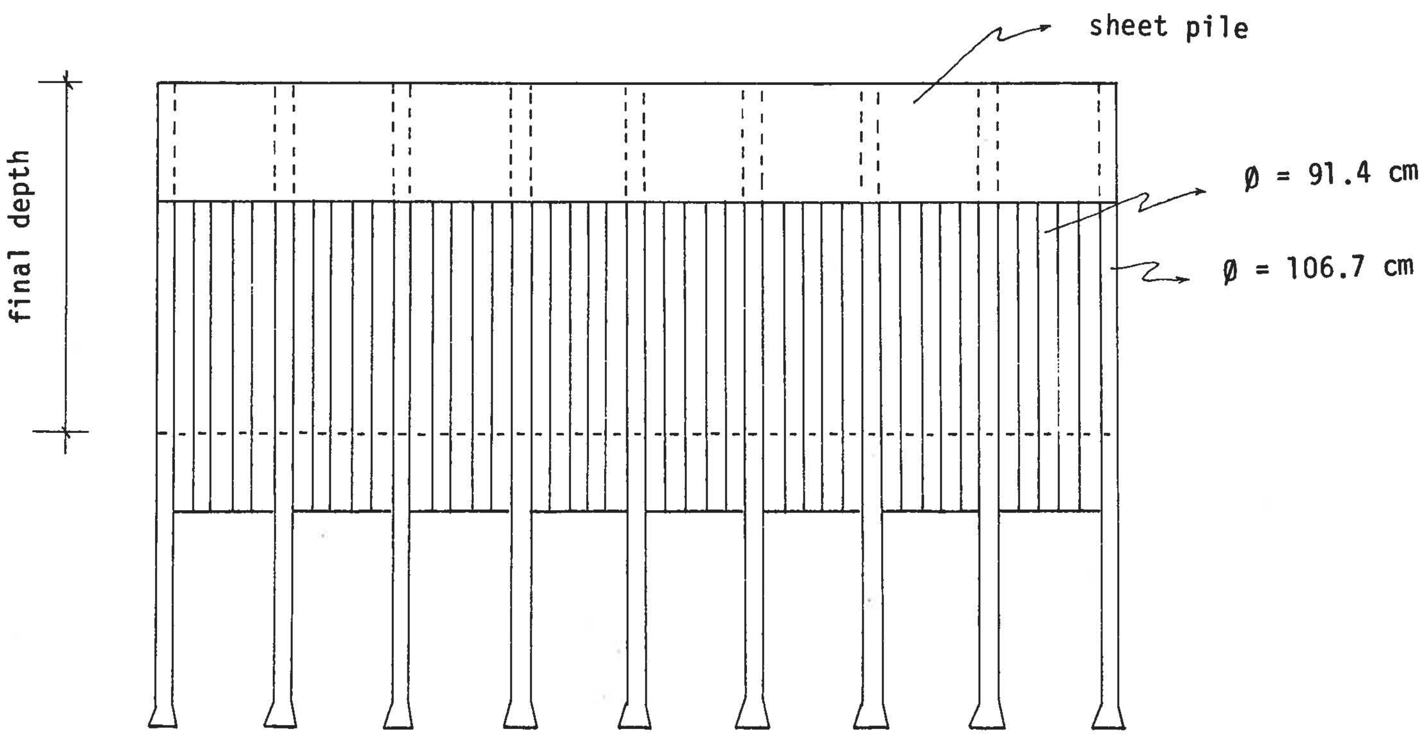

FIGURE 2.4 TANGENT PILE WALL

FIGURE 2.5 TANGENT PILE WALL

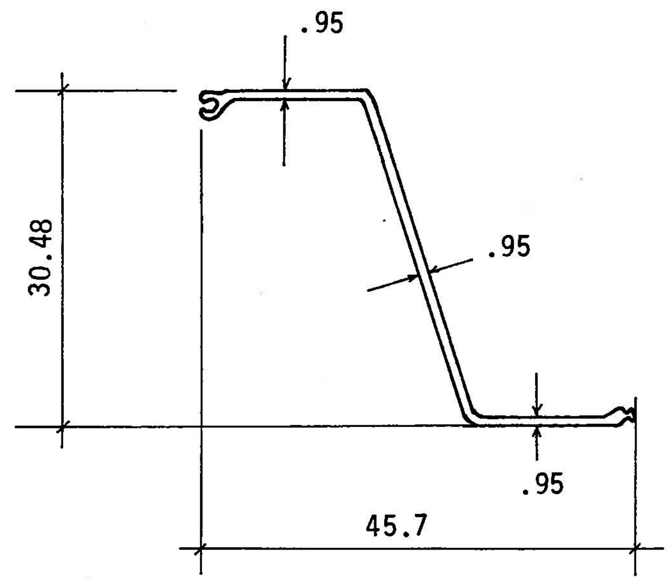

note: all dimensions in cm

FIGURE 2.6 SHEET PILE CROSS SECTION

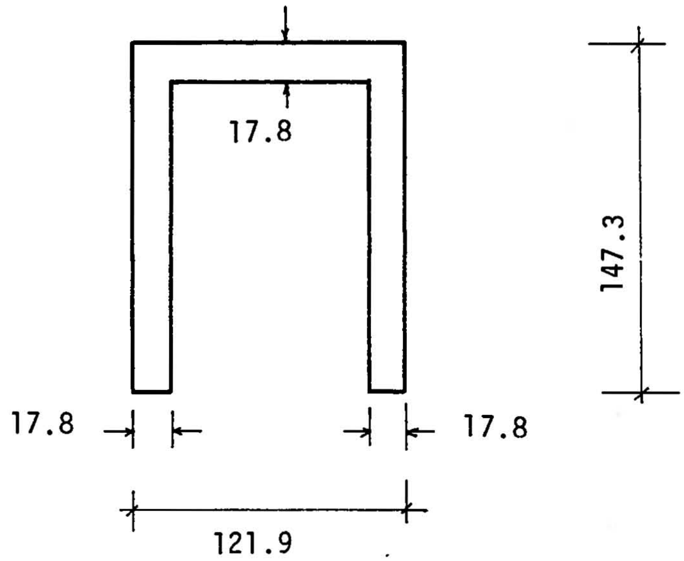

note: all dimensions in cm

FIGURE 2.7 GIRDER'S CROSS SECTION

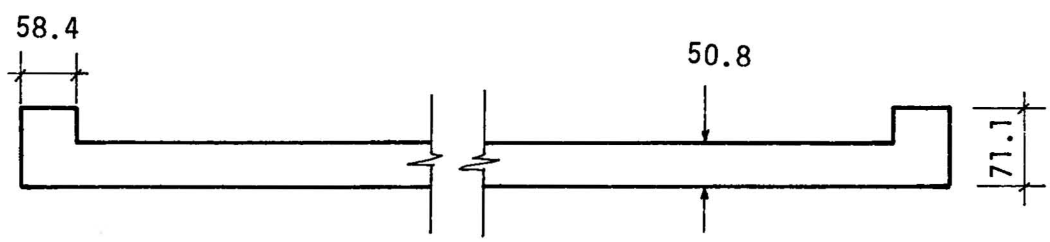

note: all dimensions in cm

FIGURE 2.8 BOTTOM FLOOR'S CROSS SECTION

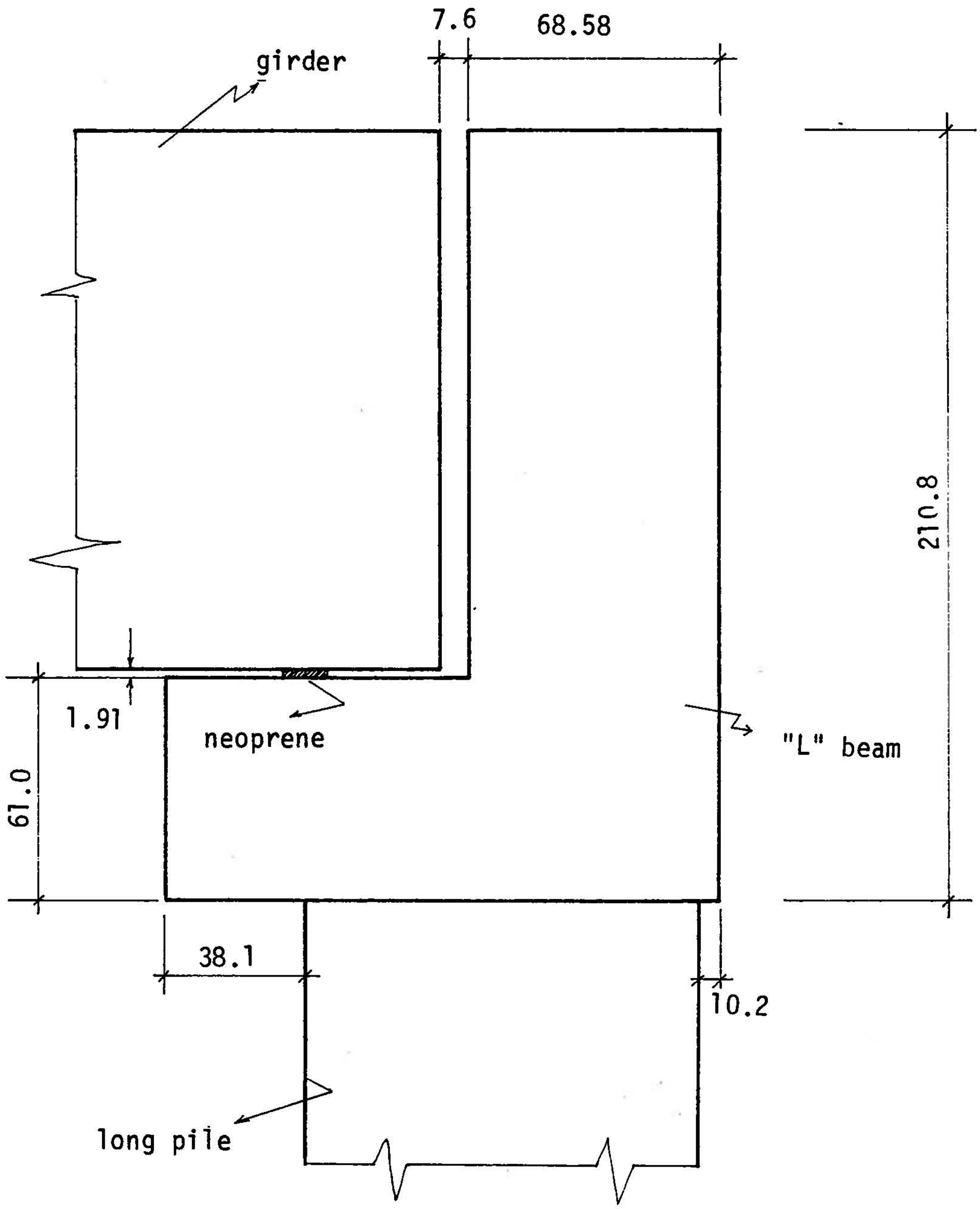

note: all dimensions in cm

FIGURE 2.9 L SHAPED BEAM

the long piles are in place, the same operation is repeated for the short ones alternatively . The upper part of the short piles is backfilled with soil and compacted. The next step consists of a small excavation for the "L" shaped beams, which rest on top of the long piles. The sheet pile wall is then driven to cover the space between the girders and the mezzanine. At this point the actual excavation procedure starts. When at a depth enough to provide room for the excavation equipment to work below them, the girders are placed on top of the "L" beams. The excavation proceeds to the second level of struts (Figure 2.14) when the mezzanine floor is poured. Figure 2.11 illustrates the end of this stage of construction. After the concrete is cured for 28 days the excavation resumes from the ends of the station (figure 2.12) approaching the section under investigation (figure 2.13) . When the excavation reaches the midheight of the second span, a temporary sliding system of struts is installed. When the final depth is reached the bottom floor is poured and the temporary struts are released. The total elapsed time for the construction of the Centennial station was 2 1/2 years.

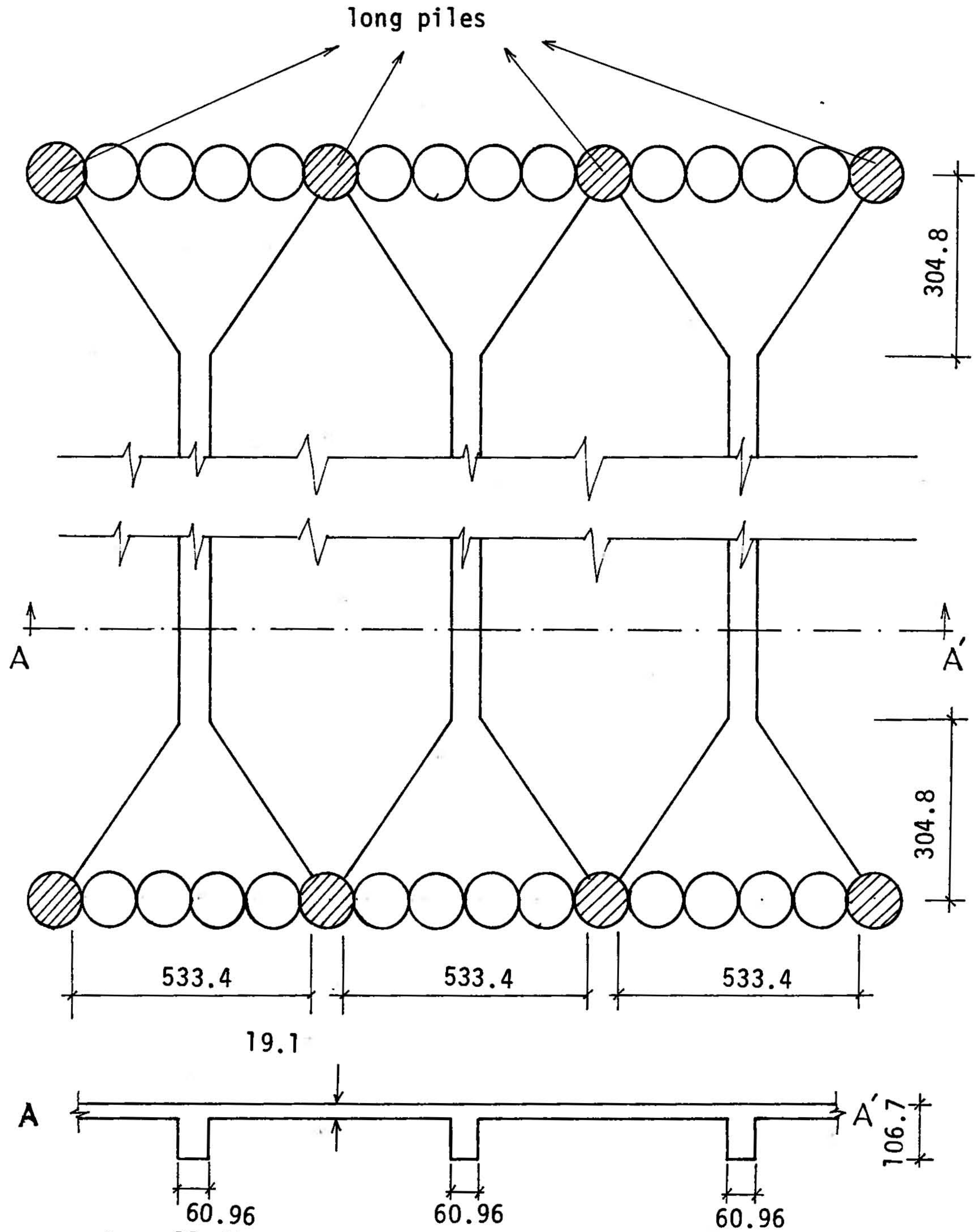

note: all dimensions in cm.

FIGURE 2.10 MEZZANINE FLOOR

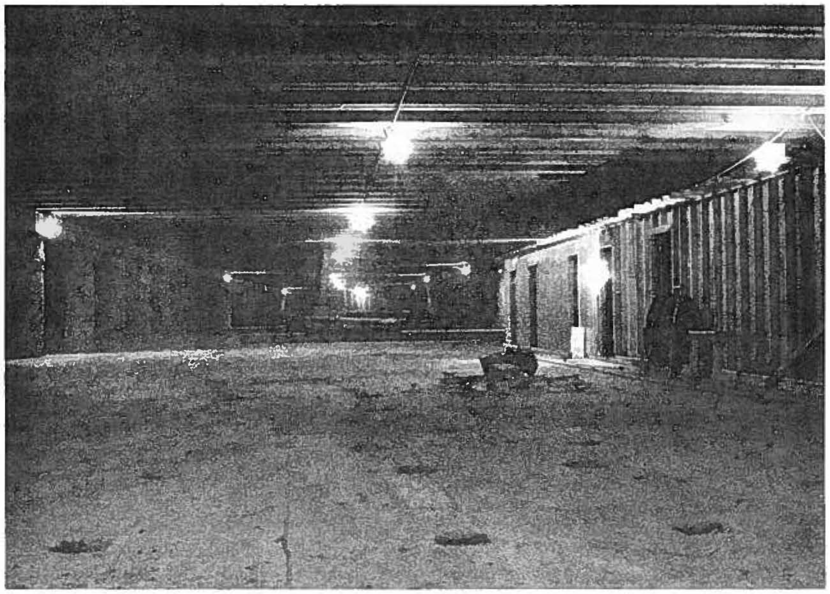

FIGURE 2.11 MEZZANINE FLOOR COMPLETED

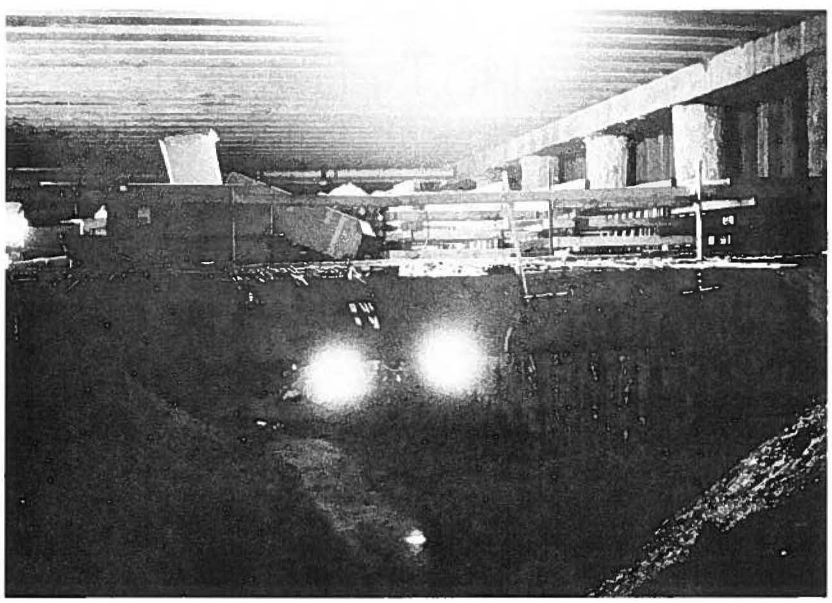

FIGURE 2.12 EXCAVATION BELOW THE MEZZANINE

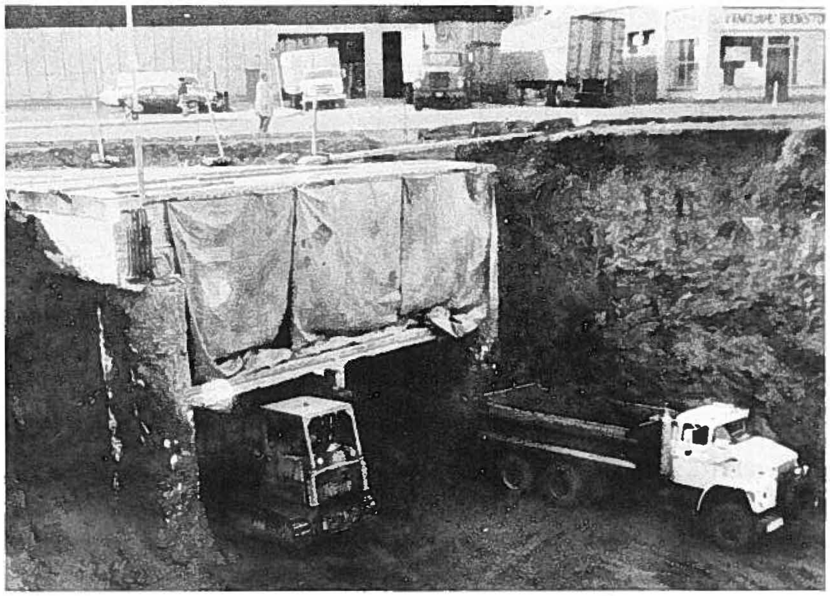

FIGURE 2.13 EXCAVATION NORTH OF CENTENNIAL STATION

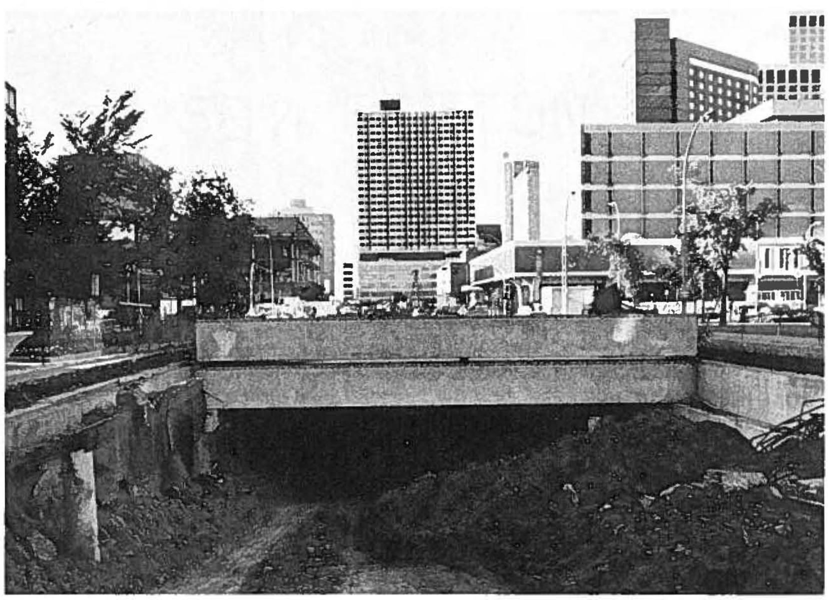

FIGURE 2.14 EXCAVATION BELOW THE GIRDERS

3. FIELD INSTRUMENTATION

3.1 Preliminary study

Previous to any field monitoring equipment installation a preliminary analysis was performed to guide the design of the field instrumentation.

The pertinent soil data were obtained from previous work in the area. As the behaviour of the construction is determined predominantly by the presence of the glacial till, the preliminary analysis concentrated on this material.

Morgenstern and Thomson (1970) presented results from unconsolidated undrained tests tc compare tests on specimens from blocks and from the Pitcher sampler. They indicated shear strength results smaller for block samples and the compressibility was independent of the mode of sampling. The compressive strength for samples taken from depths varying from 20 to 28 meters varied between 3.5 and 8.0 kg/cm2. De Jong (1971) and De Jong and Morgenstern (1973) considered the values obtained for the modulus of deformation inadequate when determined from triaxial tests results. Values as low as 80 kg/cm2 were obtained from unconsolidated undrained tests. Back analysing deformation measurements led to the conclusion that these results were far below the actual values. Eisenstein and Morrison (1973) predicted foundation deformation using results from pressuremeter tests which agreed remarkably well with field observations.

A value of 1400 kg/cm2 for the modulus of deformation in the area transpired from their work, therefore it was used throughout the preliminary analysis. The geologic history indicates this material to be lightly overconsolidated, therefore K0 was estimated based on values of the plasticity index, overconsolidation ratio and angle of shearing resistance (Brooker and Ireland, 1965 and Wroth, 1975)to be in the neighbourhood of 0.85.

A simple finite element analysis was performed assuming the material to behave in a linearly elastic manner. The excavation simulation is achieved by applying boundary forces equal and with opposite sign to the initial state of stress along the excavation (figure 3.1) . The results then obtained represent the change in stress due to the excavation which, when added to the initial state of stress, yield the final state of stress. The analysis performed was done incrementally until the final depth was reached.

Three distinct stress paths emerged from this analysis. The elements located beside the wall in region A (figure 3.2) exihibited no significant change in the vertical normal stress, while the horizontal normal stress was gradually being reduced as the excavation was taking place. The elements in zone B showed no change in the horizontal normal stress and a reduction in the normal vertical stress. The elements in zone B conferred a proportional reduction in both stresses at the early stages of the excavation followed by a reduction in horizontal stress with constant values for

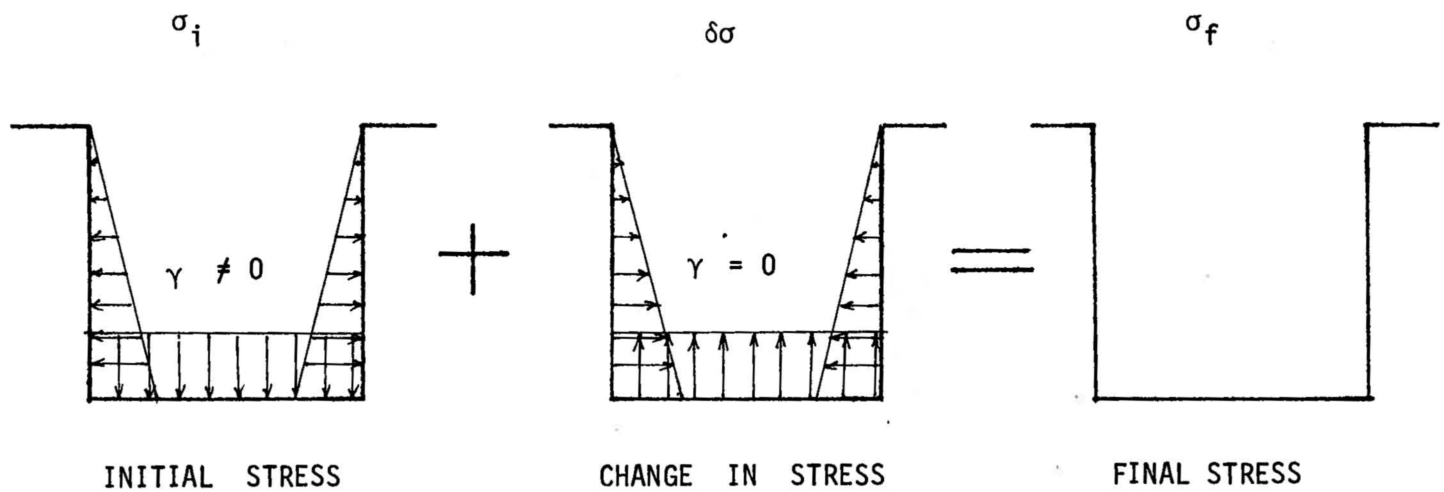

FIGURE 3.1 ONE STEP ANALYSIS OF EXCAVATIONS

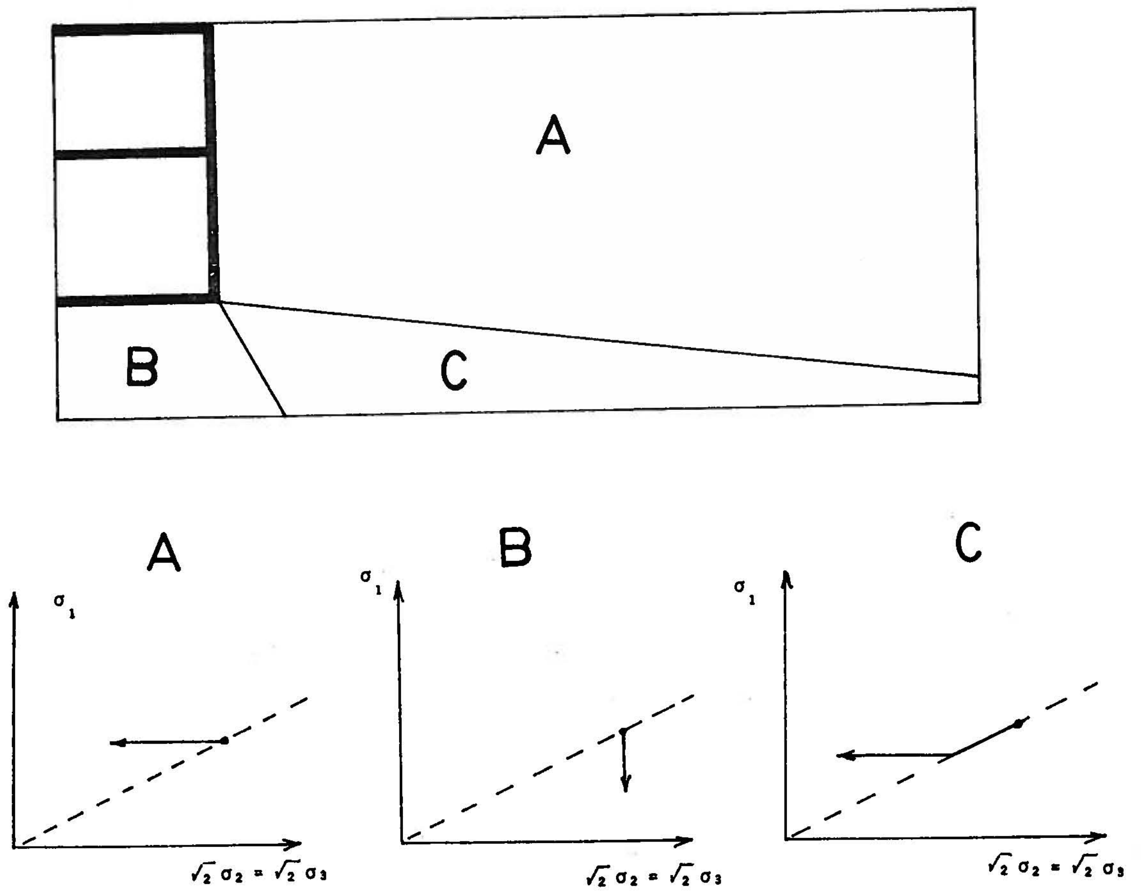

FIGURE 3.2 STRESS PATHS INVOLVED IN EXCAVATIONS

the vertical stress. The proportional loading (along K0 line) was observed until a reduction in 20% of the vertical stress took place. There was , of course, a gradual change from one stress path to another , therefore an arbitrary determination of the boundaries was established.

Based on this preliminary analysis the location of the displacements detectors was planned. Valuable information obtained was with respect to ground movements: it was initially planned to install slope indicators and surface monuments to distances as far as 20 meters from the wall, whereas the analysis suggested no significant movement would occur at those distances. It became clear that if the material behaviour is stress path dependent, laboratory testing would deserve some attention in that respect.

3.2 Layout of the instrumentation

The first question facing the investigation of an earth retaining structure is the measurement of the loads imposed on it by the surrounding ground. The overwhelming majority of the field work concerning the appraisal of lateral load on braced excavations involves the measurement of the strut load although it seems more useful to search for the lateral stress distribution along the wall. The low efficiency of measurements of lateral stresses directly compelled the researchers to look for an alternate approach which consists in monitoring strut loads. The efficacy of stress measurements is even lower when dealing with stiff soils.

During the course of this project an attempt to measure stress changes along the wall was done with the installation of two hydraulic pressure cells at the interface between the tangent pile wall and the surrounding ground (figure 3.3).

A direct measurement of the strut load on the girders was done with eighteen electrical load cells placed between the girders and the "L" shaped beam. It was necessary to measure lateral load covering the horizontal distance between 2 long piles to pick up changes due to the nonhomogeneity of the cross section along the axis of the excavation. It was decided to monitor the horizontal distance between 3 long piles to account for eventual faulty load cells. The same procedure was adopted for the other two level of struts.

The second level of struts was resting on top of the short piles , thereby preventing the measurements by load cells. Eight strain gauges were installed at this level (figure 3.3) . The bottom floor resting on the ground and cast in place allowed the installation of twelve load cells and eight strain gauges.

To evaluate the extent and magnitude of the ground movement, three slope indicators , eleven settlement points and three borehole extensometers were installed. Due to the nature of the soil and the dimensions of the structure,it was anticipated, based on experience collected by Peck (1969), that it would be necessary to monitor points as far as 3 times the depth of the excavation. After results

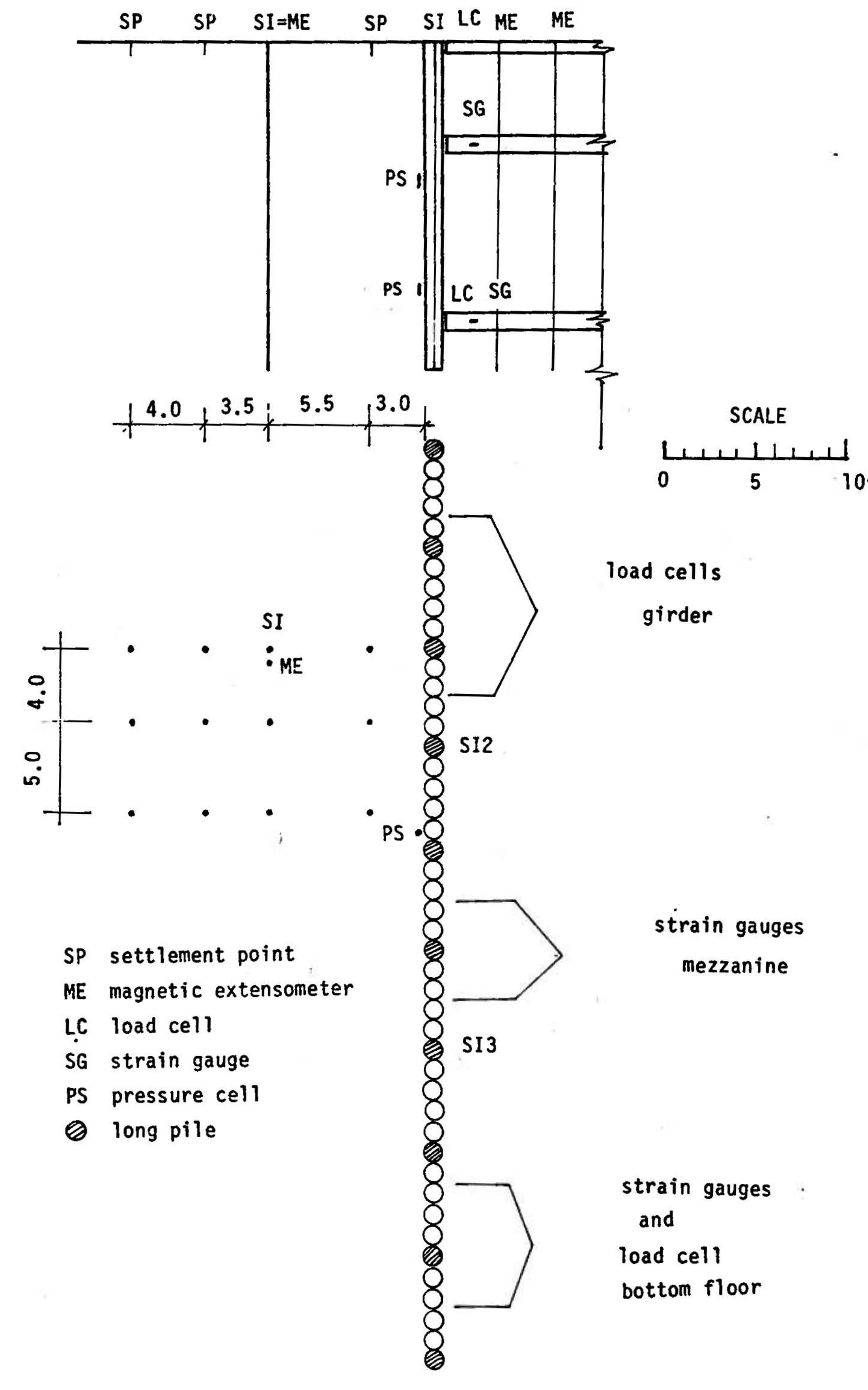

FIGURE 3.3 LAYOUT OF INSTRUMENTATION

obtained from the preliminary analysis it was concluded that the movement of points situated that far from the wall would be insignificant.It was decided therefore not to place any displacement measurement equipment further than the depth of the excavation.

The movement of the soil around the excavation can be caused by inward movement of the wall, volume change of the ground and flow of soil below the wall. The movement of the wall was being monitored by the slope indicators in the long piles. In order to detect the influence of the vertical stress release below the bottom of the excavation, which ultimately causes flow of soil, it was decided to install two borehole extensometers inside the excavation (figure 3.3)

3.3 Ground movement

3.3.1 Inclinometer

One slope indicator (SI1) with aluminum casing was placed at a distance of 8.5 meters from the retaining wall. Concrete sand was used as backfilling material, as dense as possible to provide good contact beteween the slope indicator and the surrounding ground. Very litte movement (figure 3.4) was observed due to the excavation. The preliminary analysis suggested that the zone affected by the excavation to be very reduced, and according to the results obtained from this slope indicator it proved to be even smaller than the analysis indicated. It transpires from this

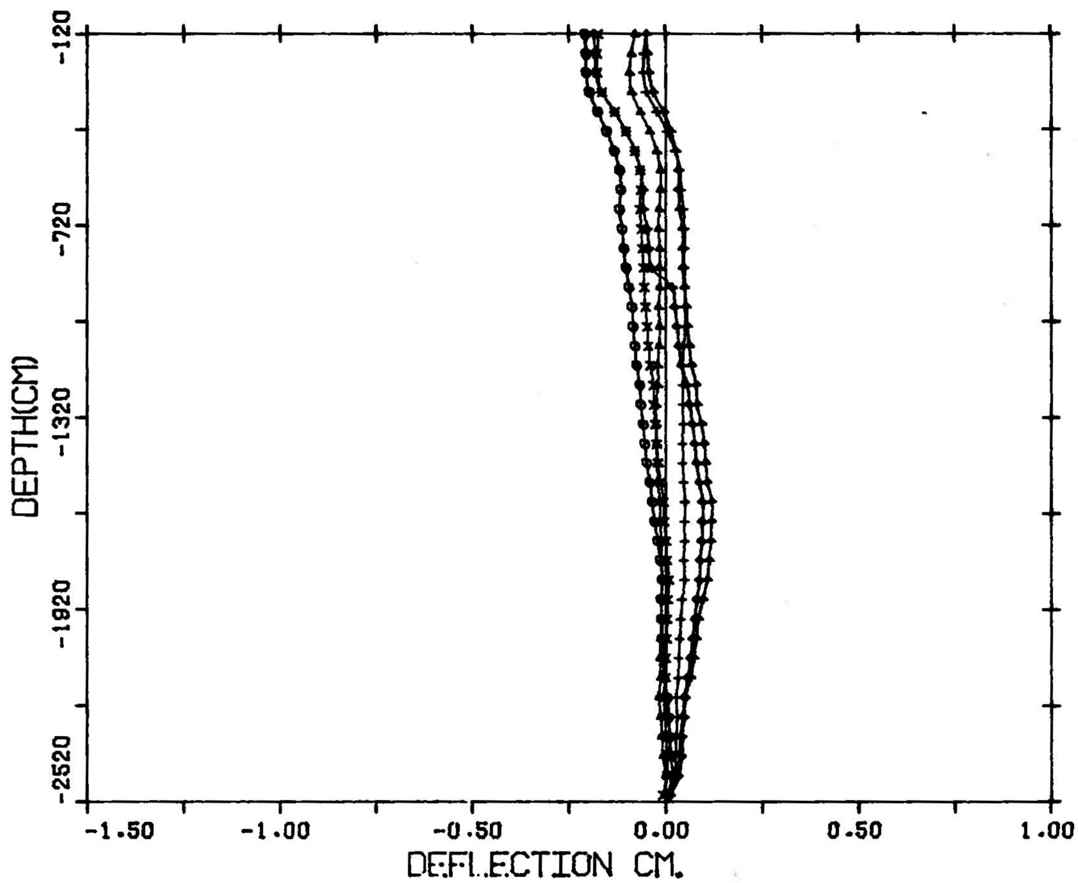

A DIRECTION DEFLECTION CURVE

Notation	Depth(m)	Date
◊	2.7	July 19,76
+	4.5	July 26,76
△	5.1	Sept 14,76
×	10.0	Nov 15,76
⬡	15.2	Feb 27,77

FIGURE 3.4 SLOPE INDICATOR SI1 READINGS

inclinometer readings there is a remarkably small zone of influence of the lateral displacement for the present case history. Lambe, Wolfskill and Jaworsky, 1972) reported for the subway in Washington D.C. (very stiff to stiff clays) movements of about 3 cm and 2.5 cm. for points 4 m. and 11 m. from the wall.

Two slope indicators were installed in the deep piles. The first one of them (SI2) had its aluminum casing attached to the reinforcement of the pile which was being mounted in the horizontal position. During the lifting operation excessive deflection caused the collapse of one of the joints. When it was being repaired a rotation of the casing caused misaligrement of the groove with the axis of the excavation. The angle of misalignment was measured and proper correction was done by the computer program. To avoid similar problems the next slope indicator (SI3) had plastic casing where no difficulties were encountered (figure 3.5). The reading for SI3 (figure 3.7) indicated a maximum deflection of 0.91 cm. at a point between the girder and the mezzanine level. SI2 (figure 3.6) recorded a much greater deformatior (1.4 cm.) registered at the ground surface. SI3 indicates the presence of a significant load being carried by the girders while SI2, where no bending is observed above the mezzanine level, exhibits the inverse situation. The lateral load in the upper part is carried by the sheet piles which transmit it to the "L" shaped beam and finally to the girders. There is a clearance of 7.6 cm. between the "L"

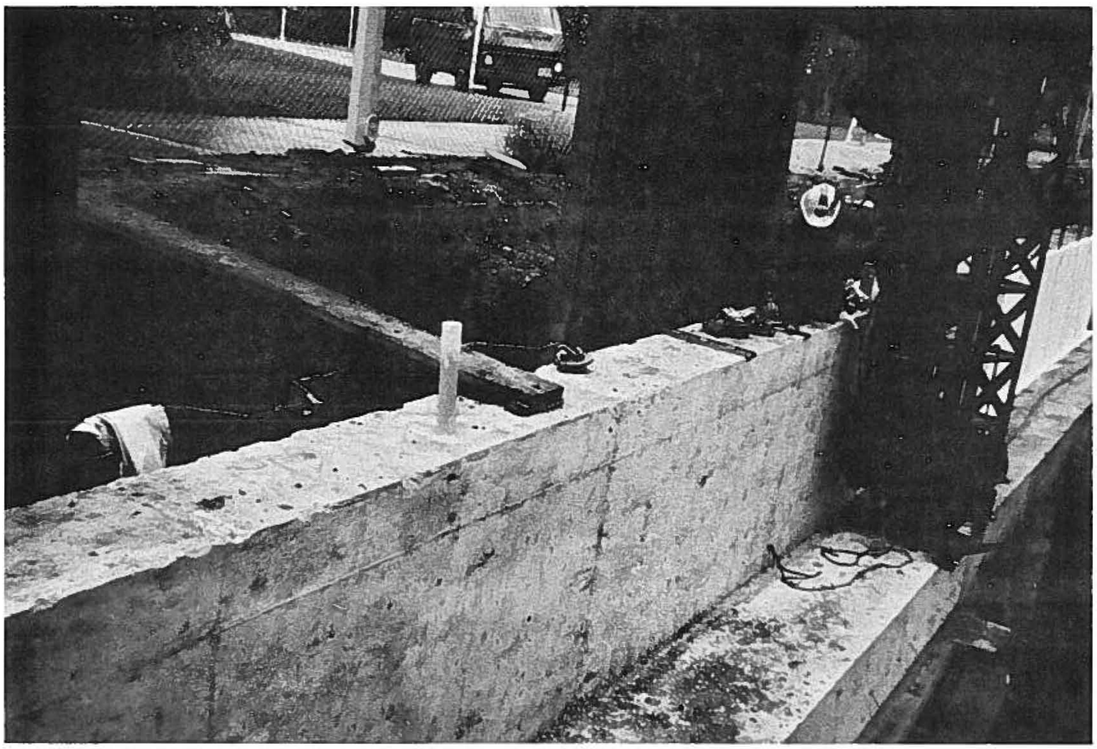

FIGURE 3.5 SLOPE INDICATOR (PLASTIC CASING) INSIDE A LONG PILE

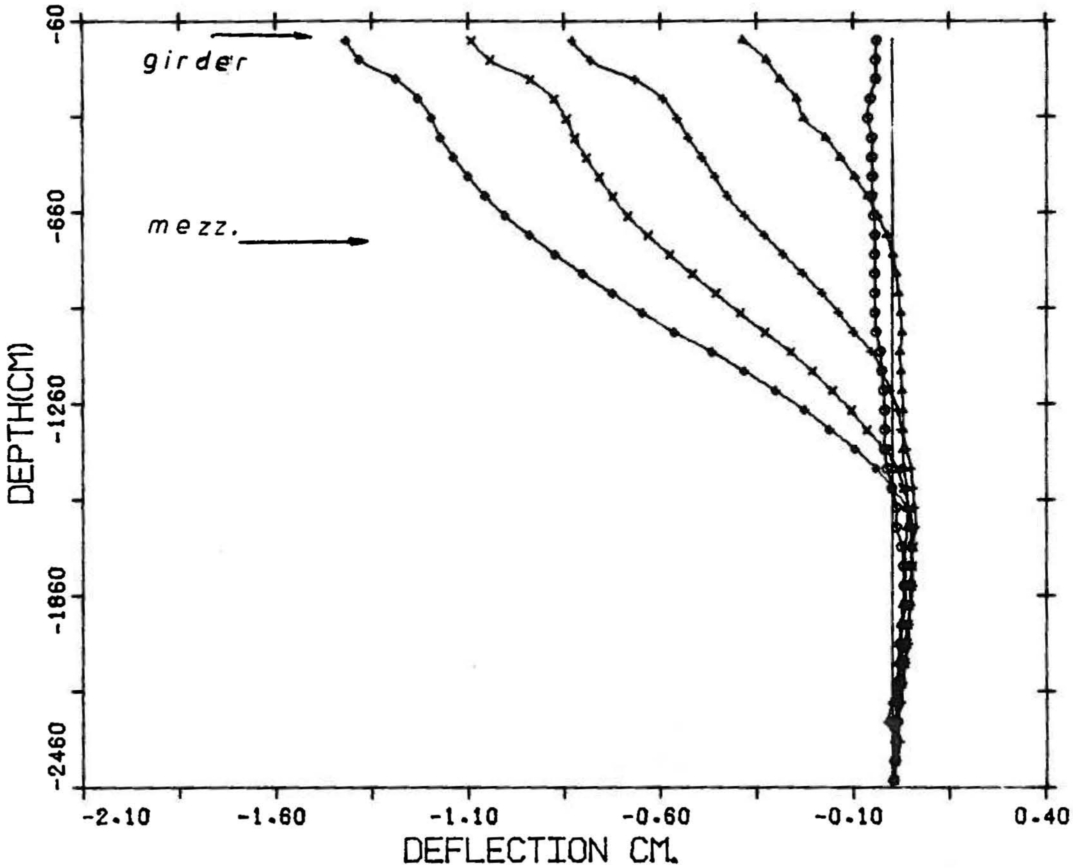

A DIRECTION DEFLECTION CURVE

Notation	Depth(m)	Date
○	2.7	July 19,76
△	4.5	July 26,76
+	5.1	Sept 14,76
×	10.0	Nov 15,76
◊	15.2	Feb 27,77

FIGURE 3.6 SLOPE INDICATOR SI2 READINGS

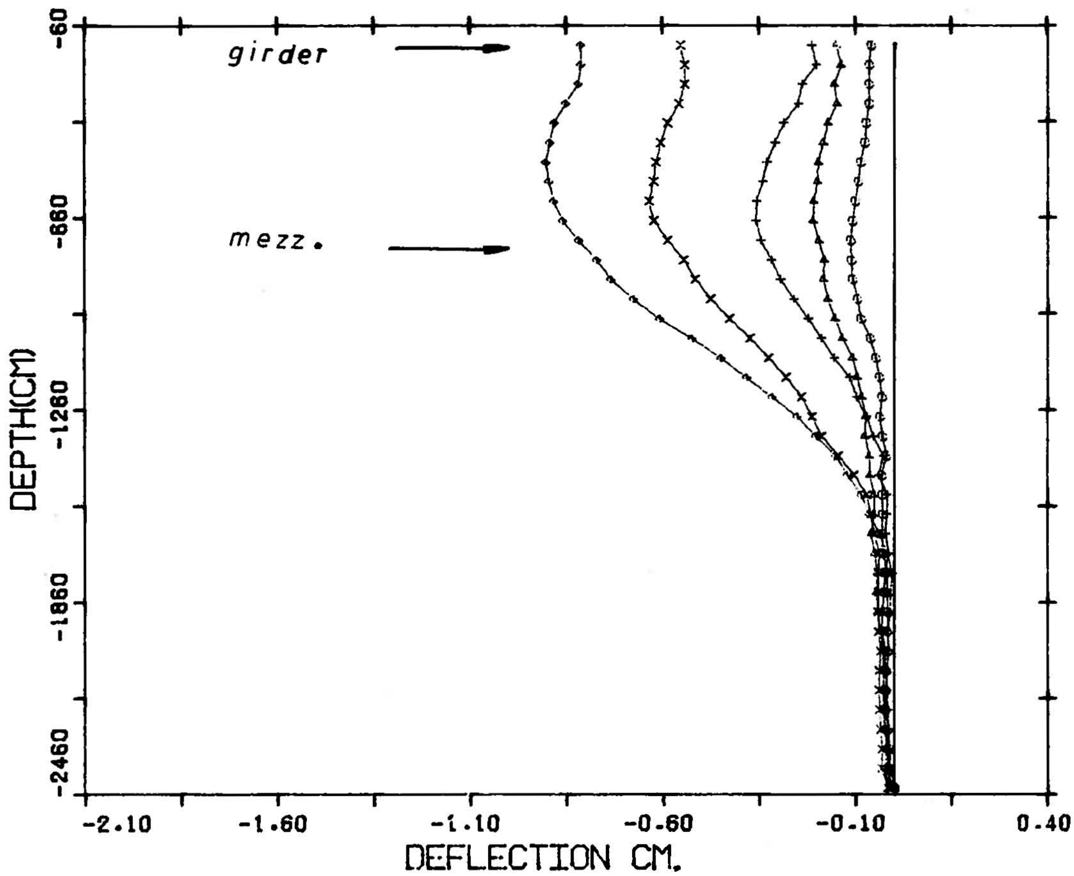

A DIRECTION

Notation	Depth(m)	Date
○	2.7	July 19,76
△	4.5	July 26,76
+	5.1	Sept 14,76
×	10.0	Nov 15,76
◊	15.2	Feb 27,77

FIGURE 3.7 SLOPE INDICATOR SI3 READINGS

shaped beam and the precast girders which is filled with cement grout. The grout in the cross section of slope indicator SI2acted as a soft material therefore not transmiting the lateral load to the girders.

3.3.2 Multipoint extensometer

The multipoint borehole extensometer developed by the Building Research Establishment (Burland ,Moore and Smith 1972, Ward and Burland 1973 and Smith and Burland 1976) consists basically of a magnetic ring housed in a PVC cylindrical unit which is spring loaded against the wall of the borehole. The depth of each magnetic ring is determined by lowering a probe containing reed switches which operate as they pass through the magnet.

For the first borehole a 7.62 cm. diameter hole was drilled until the Edmonton formation was reached and kept filled with drilling mud to prevent caving. The PVC pipe was introduced and the placing tool lowered to install the first magnet. Great difficulty was encountered at the depth of approximately 6 meters, indicating some caving took place. A 20 cm. diameter hollow auger was placed outside the PVC pipe to the depth of 6 meters. All the remaining magnets were installed and the same procedure was adopted for the other two boreholes. To prevent similar problems in the long run, after the installation of each magnet , the hole was backfilled with concrete sand to the depth of the next magnet to be lowered. Measurements during the early stages of the excavation indicated no movement of the magnets. This behaviour was attributed to the high degree of densification attained by the sand caused by the vibration of the construction equipment. The strength of the backfilling material became then comparable to the surrounding soil which effectively locks the magnets on the PVC pipe (Marsland and Quarterman , 1974). After the recognition of the problem an extra borehole was drilled inside the excavation when it reached the mezzanine level. No caving was to be expected considering the upper 6 meters had already been excavated. A 12.7 cm diameter hole was drilled, thereforethe springs had to be modified for the new diameter borehole. A bentonite slurry was used as backfill as opposed to concrete sand and special heavy protection around the top of the PVC pipe was made to prevent the dropping of small lumps of soil by the excavation equipment. Once more no movement was recorded. It appears the springs which had been lengthened could not provide enough spring load to overcome the small friction beteween the PVC pipe and the cylindrical unit. No records of bottom heave and deep-seated vertical movements could therefore be obtained.

3.3.3 Settlement points

To monitor the surface vertical movement of the ground, eleven surface monuments were established. The installation procedure consisted of augering a 20.3 cm. diameter hole 1.5 meters below the surface. A 1.8 meters long steel bar (diameter = 1.25 cm.) was placed inside and hammered down the remaining 30 cm and the hole was backfilled with concrete sand. A precision level was used to determine the change in vertical position with the excavation. Figure 3.8 represents the vertical movement when the excavation reached its final depth. The gradual reduction of vertical movement with the proximity of the wall indicates the angle of friction between the retaining wall and the surrounding ground was enough to prevent relative movement.

3.4 Loads and stresses

3.4.1 Pressure cells

Two Gloetzl hydraulic pressure cells were placed to detect the change in the lateral stress with excavation. The units were located at the interface between the concrete piles and the surrounding soil. After the hole for the pile was augered and the reinforcement cage already introduced, a vertical surface was excavated beside the pile at the required level, providing a flat surface to rest the pressure cell on. A metal frame braced the cell against the opposite side of the borehole to avoid displacement while the concrete was being poured. The concrete in this pile was dropped at a much slower rate. Visual inspection was done during this operation to insure the cell was kept in the proper position. Despite all the precautions the oil pressure during the early readings was already below the nominal values, indicating there was a leak somewhere in the

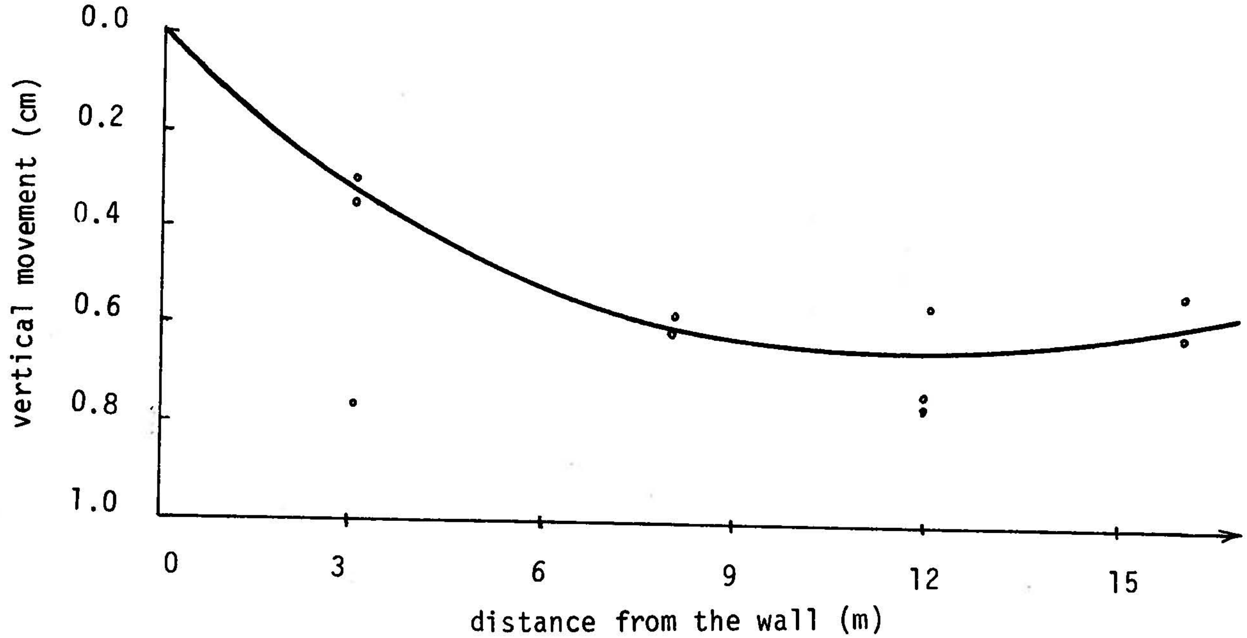

FIGURE 3.8 SETLEMENT POINTS READINGS

leads.

3.4.2 Strain Gauges

Each horizontal beam shaping the mezzanine provides lateral support for 5 consecutive tangent piles. Two of these beams were instrumented with 3 vibrating wire, 3 electrical strain gauges embedded in the concrete, and 2 weldable electrical strain gauges on the reinforcement. Their locations in the cross section can be seen in figure 3.9. When the excavation reached 10 meters deep a modification introduced in the original design was to be executed. An additional pedestrian exit adjacent to the wall required an excavation to the mezzanine floor outside the wall. As a result of this modification the lateral load was to be partially released. Therefore the results presented herein express the lateral load produced by 10 meters of excavation. The inferred stress distribution (figure 3.10) indicates a lateral load of 40,000 kg per linear meter along the axis of the excavation (Appendix C).

For the bottom floor 5 vibrating wire and 3 electrical strain gauges were installed to monitor the lateral load in this strut. All the strain gauges were embedded in the concrete. As was mentioned before, a set of temporary struts was placed half way between the mezzanine and the bottom floor. The temporary struts were released 14 days after the bottom floor was poured . The strain gauge readings were taken until a month after the temporary struts were released

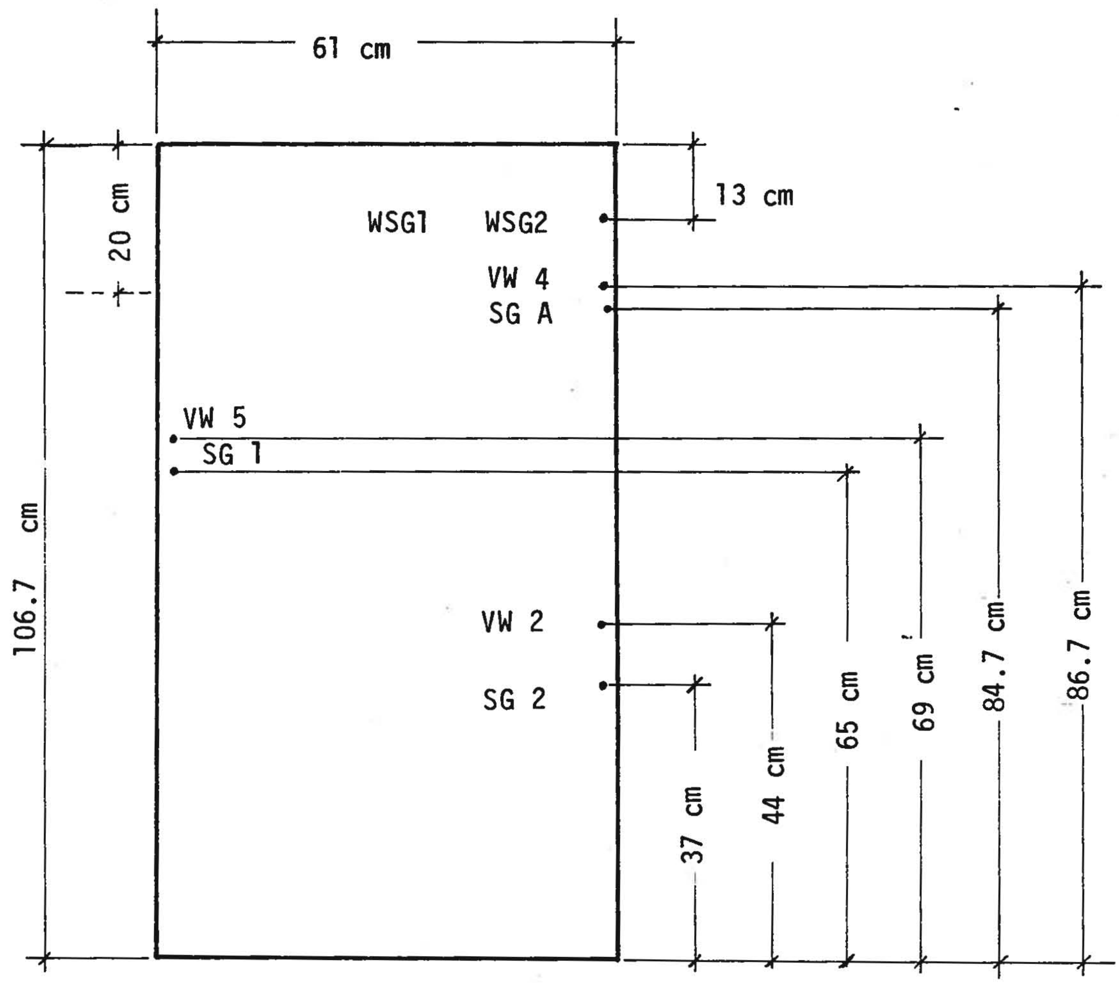

VW vibrating wire strain gauges

SG electrical strain gauges embeded in the concrete

WSG weldable strain gauges in the reinforcement

FIGURE 3.9 STRAIN GAUGES IN THE MEZZANINE

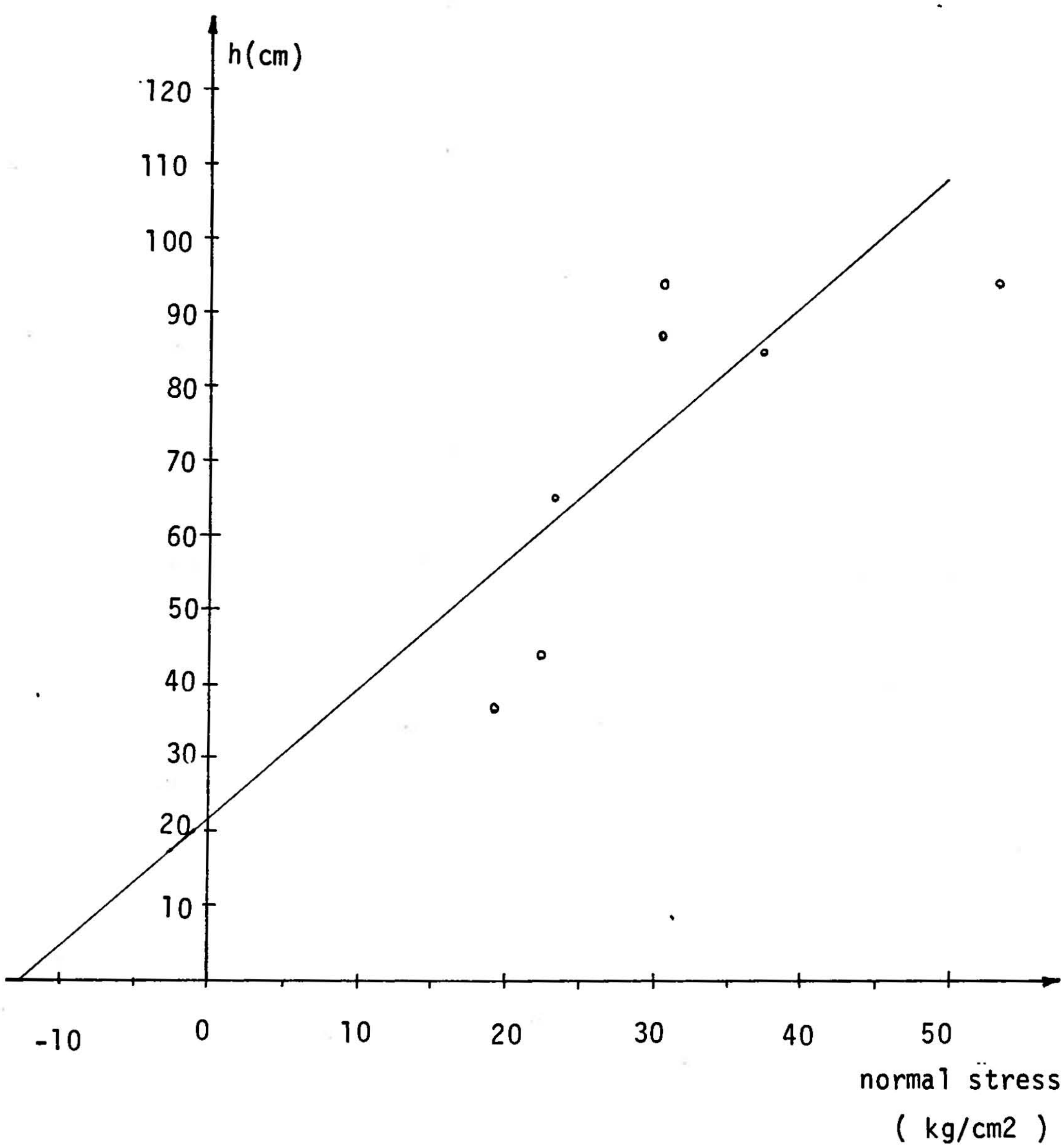

FIGURE 3.10 NORMAL STRESS ALONG THE HEIGHT OF THE MEZZANINE

and no load was recorded. It appears the load was carried solely by the mezzanine. This is confirmed by negligible movement of the wall at the level of the bottom floor compared with the movement at the mezzanine level (figure 3.7)

3.4.3 Load cells

The load cells for the girder and bottom floor consisted of a hollow cylinder having its ends resting on two circular grooved plates (figure 3.11) Each set of three load cells for the girders were assembled in a styrofoam panel (figure 3.12) isolating each girder load. A roller was placed under each girder to prevent transfer of the load by friction between the girder and the "L" shaped beam. The panels were then in contact with the vertical face of the "L" shaped beam (figure 3.13) and the girders finally lowered in front of each panel (figure 3.14 and 3.15). The load cells for the bottom floor were mounted in a very similar way.

The results of the load cells on the girders indicated the absence of load in all panels. This observation agrees with the readings of SI2 which is located in the same area (figure 3.3). Due to the small magnitude of the displacements in this case history the stress strain properties of the grout which a space of only 7.6 cm. assumes great importance in the lateral stress distribution and even more in its primary function which is to transmit

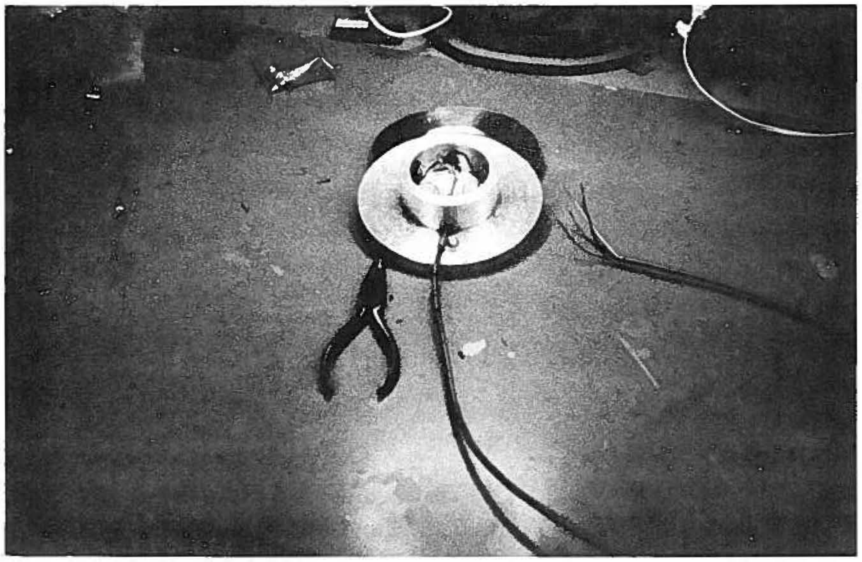

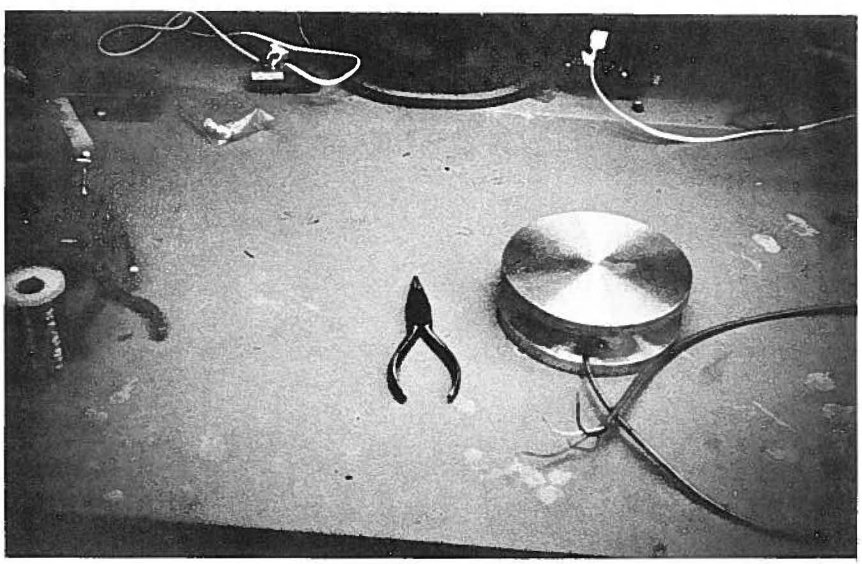

FIGURE 3.11 LOAD CELL FOR THE MEZZANINE

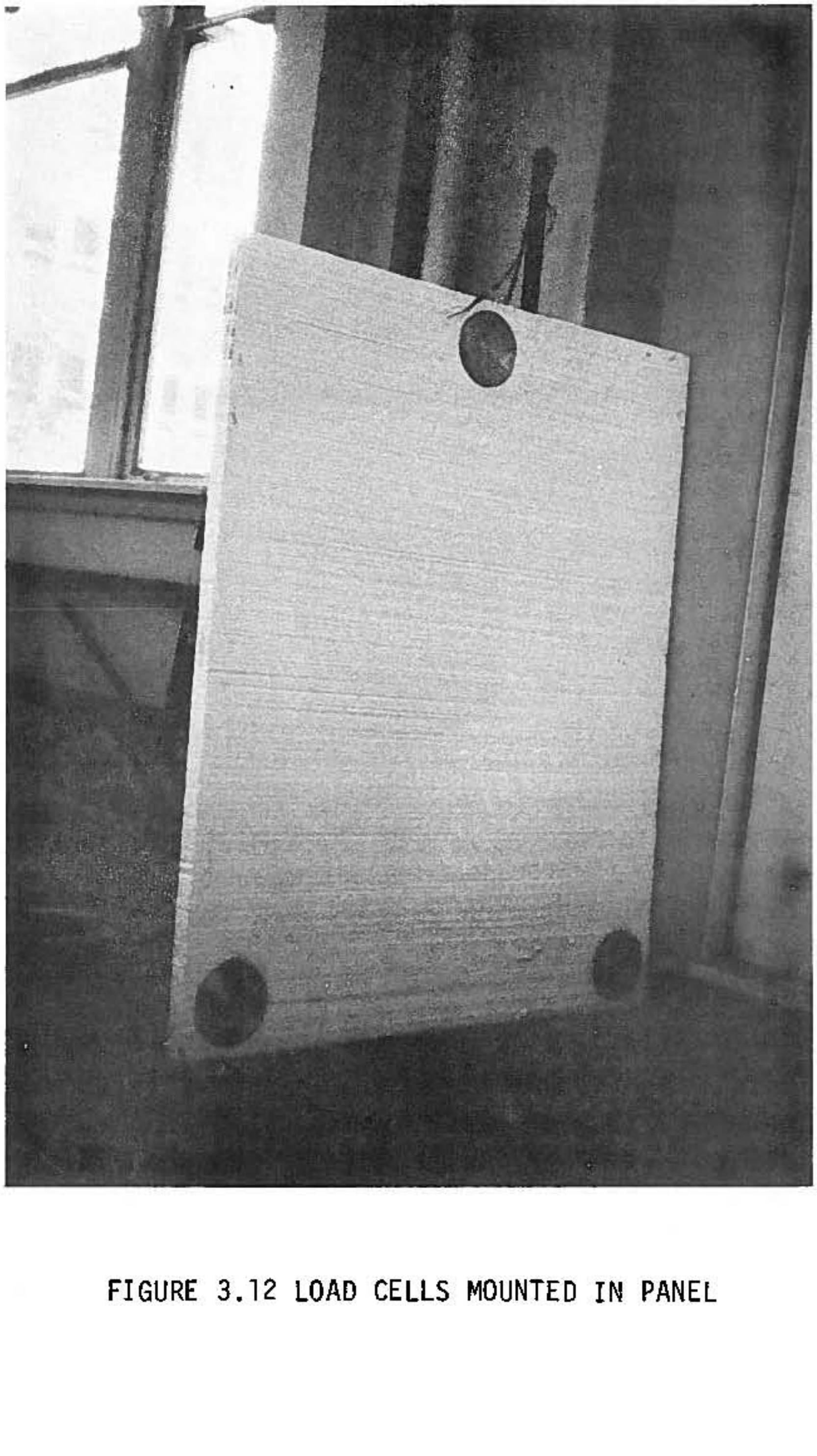

FIGURE 3.12 LOAD CELLS MOUNTED IN PANEL

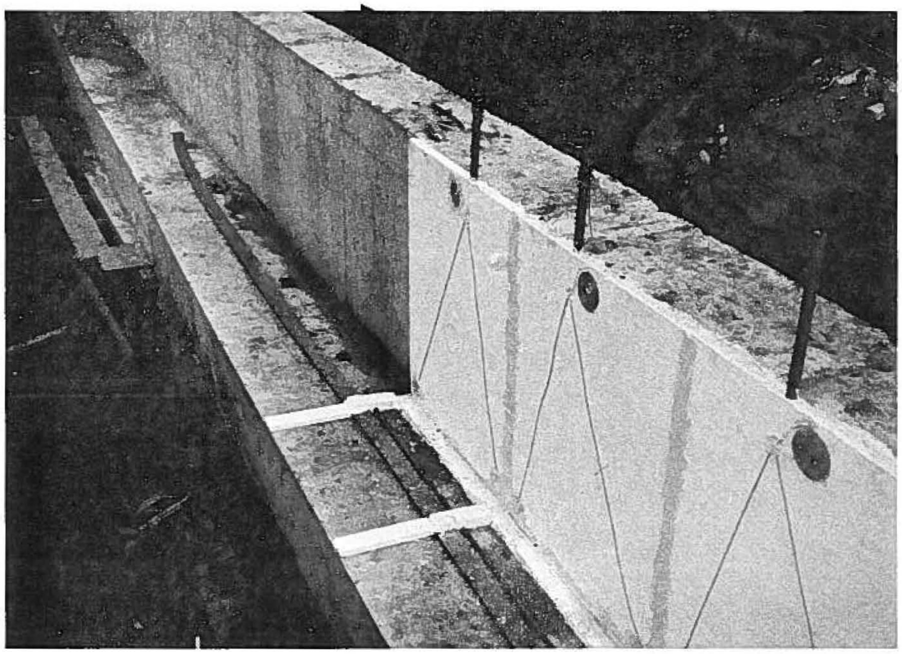

FIGURE 3.13 LOAD CELL PANELS IN FRONT OF

THE "L" SHAPED BEAM

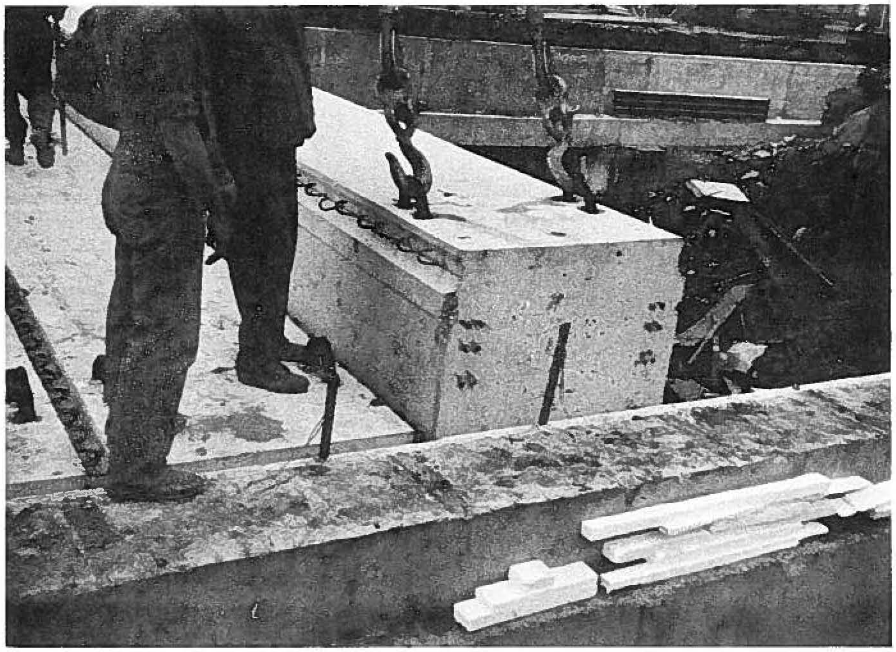

FIGURE 3.14 LOWERING A GIRDER IN FRONT OF A LOAD CELL PANEL

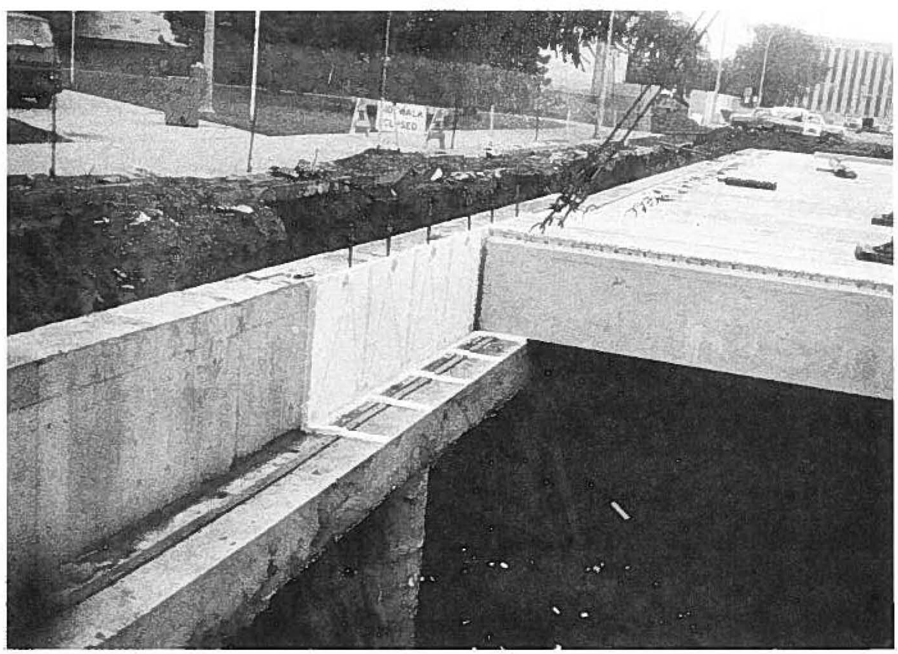

FIGURE 3.15 GIRDER IN THE FINAL POSITION

the load to the strut.

The readings for the bottom load cells confirm the results of the strain gauges where no load was present along the bottom floor.

3.4.4 Summary

A deep excavation in stiff clays was instrumented with the purposeto of registering lateral load and displacementsassociated with the excavation

Vertical ground movement was monitore by settlement points which indicated the zone affected by the excavation to be reduced to the points situated at a horizontal distance of approximately the depth of the excavation from the wall. The maximum displacement occurred at points situated 11 m from the wall, The pile movements indicated a maximum lateral displacement of 0.91 cm a firm contact is provided between the wall and the struts and 1.4 cm for a situation in which the girder is not activated.

Load cells and strain gauges were installed in the struts indicating a load of 40,000kg per linear meter along the axis of the excavation, at the mezzanine level.

4. LABORATORY TESTING

4.1 Introduction

Although much attention has been devoted lately to the importance of stress paths in soils, the assumption that stiff clays behave as linearly elastic materials (Burland 1977 and Wroth 1971) obscured the significance of the stress path for such materials. For predictions of settlement in London Clay, which is the classical example of stiff clay, Simons and Som (1969) concluded it is of the utmost importance to reestablish the existing in situ stresses and submit the specimen to stress paths similar to the field conditions.

During the preliminary analysis for this project it became clear the stress paths associated to excavation problems bear no resemblance with conventional laboratory testing. As the prediction of soil movement is considered one of the major goals of this work, the laboratory testing will concentrate on the effects of different stress paths on the stress strain parameters.

A typical feature in stiff clays is the presence of fissures which makes the job of determining in situ strength and stress strain parameters much more difficult. Small specimens are not representative of the field conditions and tend to overestimate the shear strength.

When these materials have their in situ stresses relieved, they tend to swell, causing a reduction of the modulus of deformation. Comparisons between different types of tests in London Clay indicated the moduli of deformation obtained from pressuremeter and laboratory tests to be substantially smaller than the ones obtained from large in situ tests (Marsland 1965). Moduli of deformation determined from large plate loading tests (865 mm) were compatible with ground movements for excavations and foundations, provided that, after the surface has been machine finished, the first 50 to 70 mm are removed by hand digging from the base of the borehole (Marsland 1971,a). One important factor to be considered during these tests is the length of time between the excavation and the performance of the test.

With respect to the undrained strength, the results from laboratory tests with samples large enough to contain sufficient fissures fell within the values obtained from large plate loading tests (Marsland 1977), while the values achieved by the pressuremeter tests were considerably higher (Marsland and Randolph 1977). Comparative studies between borehole and block samples (Ward, Samuels and Butler 1959 and Ward ,Marsland and Samuels 1965) indicated a reduction in undrained strength and the modulus of deformation for tube samples; the dominant reduction being observed on the modulus of deformation. When a block sample is taken from the ground, the fissures open due to the stress release and the material behaves like blocks of weakly bonded material. Shearing forces developed during tube sampling operation weakens these bonds to a much higher degree.

The influence on the undrained strength, when compared to the undrained modulus of deformation, is less predominant but still present. With respect to drained strength, a different behaviour is present. Results from large in situ shear box tests, were within the range of data from triaxial tests with 75 and 125 mm diameter specimens (Marsland 1971,a). The same conclusion can be drawn from results in Barton clay published by Marsland and Butler (1967). Christensen and Hansen (1959) also encountered the same trend for drained strength data obtained from large plate loading tests and small triaxial specimens in fissured clays. Drained strength parameters from laboratory tests in stiff fissured clays from Nanticoke, Ontario were consistent with results from field shear box tests(Lo, Adams and Seychuk 1969). There was no definite tendency of the modulus of deformation with the sample size for block samples, but a pronounced disturbance in borehole samples (Lo, Seychuk and Adams 1971) was observed. Experience with the local till revealed no significant difference between block samples and borehole samples (Morgenstern and Thomson 1970) with respect to compressibility which was not the case for the stiff clays mentioned above. The fissures were observed to be spaced 30 to 40 cm apart randomly oriented.

The predominant influence of the fissures in London Clay causes an extremely pronounced reduction in the undrained shear strength and modulus of deformation from borehole samples , when compared with block samples.

Favorable comparisons between laboratory and in situ testing are encountered for drained tests. In view of the drained analysis being performed here and the good comparisons between block and borehole samples in the area it was decided to embark on a laboratory testing program. In situ shear, plate loading and pressuremeter results would not enable an investigation of the stress paths observed in excavations. The results from pressuremeter tests obtained previously by Eisenstein and Morrison (1973) will also be used during the analysis in chapter 7.

4.2 Till

4.2.1 Sampling

Cubic block samples of 50 cm. edge were extracted from vertical walls as the excavation proceeded.They were collected by first removing the outside material of the face of the excavation and sawing a prism of soil from it. The vertical face was then marked and the blocks were immediately covered with sheets of polyethylene to prevent drying. The block was then wrapped with cloth and a layer of paraffin was applied. Upon the arrival in the laboratory an extra thick coating of paraffin wax was applied and the samples were stored in a moist room. Before testing, the blocks were sawn in smaller blocks and trimmed by hand into a cylindrical shape (diameter 38 mm) for triaxial testing or into a prism shape for plane strain testing. Some loss of material occurred due to presence of small pebbles. In these cases the sample was abandoned since the laboratory specimens were only of 3.81 cm diameter. The carving was completed usually after 30 to 45 minutes.

4.2.2 Characterization

Grain size analysis (figure 4.1) from 3 different blocks indicated the following result:

Sample #	% CLAY	% SILT	% SAND
1	26	33	41
2	27	35	38
3	24	32	44

The average Atterberg limits for this material was 35% for the liquid limit and 15.5% for the plastic limit. Extensive determination of moisture content before carving the laboratory specimens registered an average of 14%. The specific gravity of solids was 2.69.

4.2.3 Triaxial

The great majority of experience on stiff clays available in the laboratory is related to undrained tests. The determination of the coefficient of consolidation indicated an average value of 0.02 cm2/sec. Very little time therefore is necessary for consolidation. Field data

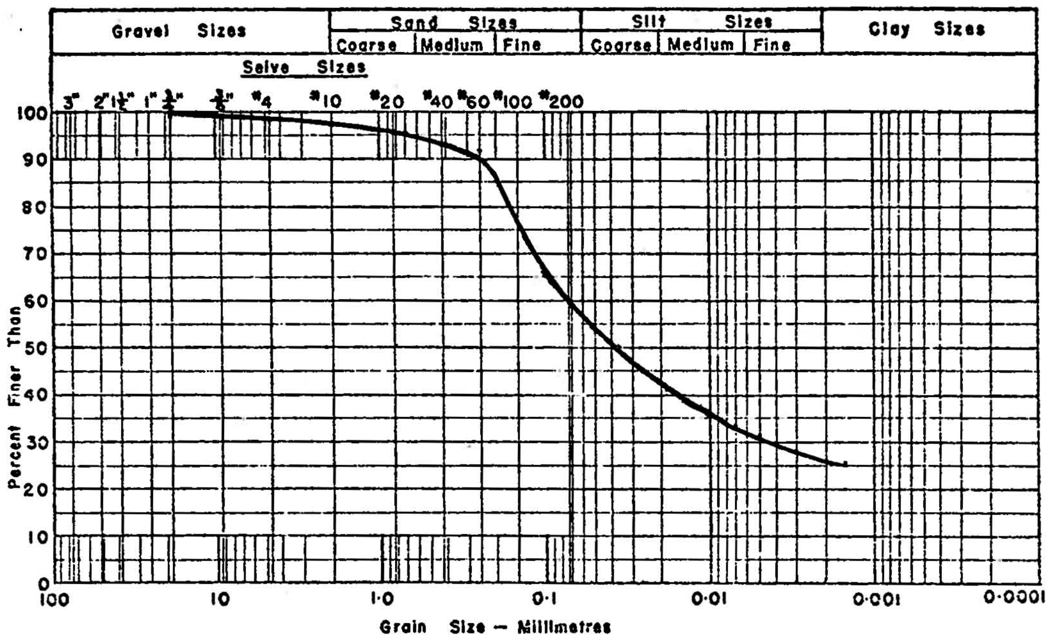

FIGURE 4.1 EDMONTON TILL GRAIN SIZE DISTRIBUTION

collected from slope indicator and settlement points showed an insignificant time dependent behaviour. Experience (Eisenstein and Thomson, 1978) from measurements in the tunnels joining Central and Centennial stations corroborated these readings. Based on these premises it was concluded that drained tests best suit the present field conditions. Rate of strains between 0.035 cm/h and 0.500 cm/h were tried without any significant difference being observed. The great majority of the strain controlled tests were performed at a rate of 0.200 cm/h.

For normally consolidated soils the widely used expression to determine the at rest earth pressure coefficient

$$KO = 1 - SIN(PHI) \qquad (4.1)$$

yields sufficiently accurate results for engineering purposes. In-situ measurements (Bjerrum and Andersen 1972) and laboratory determination (Poulos and Davis 1972) can be used in this type of soil.

With respect to overconsolidated soils Bishop (1958) doubts if KO can ever be measured for this type of material due to the disturbance the measuring device promotes. As KO is extremely sensitive to release of the in situ stresses, its determination in the laboratory leads to very erroneous results (Wroth 1975).

Correlations with other related properties like overconsolidation ratio and the plasticity index proposed by Brooker and Ireland (1965) and the angle of shear resistance as proposed by Wroth (1975) provide reasonable results. The upper till and the ice advance acted as a preconsolidation load on the lower till, while only the ice was responsible for the preconsolidation on the upper till. Estimative of the preconsolidation The assessment of K0 in the present study was based on these two correlations, yielding in both cases a value of 0.85.

The samples were subjected to different stress paths and figure 4.2 illustrates the stress paths being investigated in this project.

- <u>passive compression</u> conventional test in which the vertical stress is increased while the lateral stress is kept constant.
- <u>active compression</u> test in which the lateral stress is reduced while the vertical stress remains constant.
- <u>active extension</u> the lateral stress remains constant while the vertical stress is reduced.
- <u>proportional-active</u> the sample initially has horizontal and vertical stresses reduced along the K0 line and in the latter part the vertical stress remains constant while the horizontal stress is reduced.

With the exception of the passive compression tests, all of them were performed under stress controlled

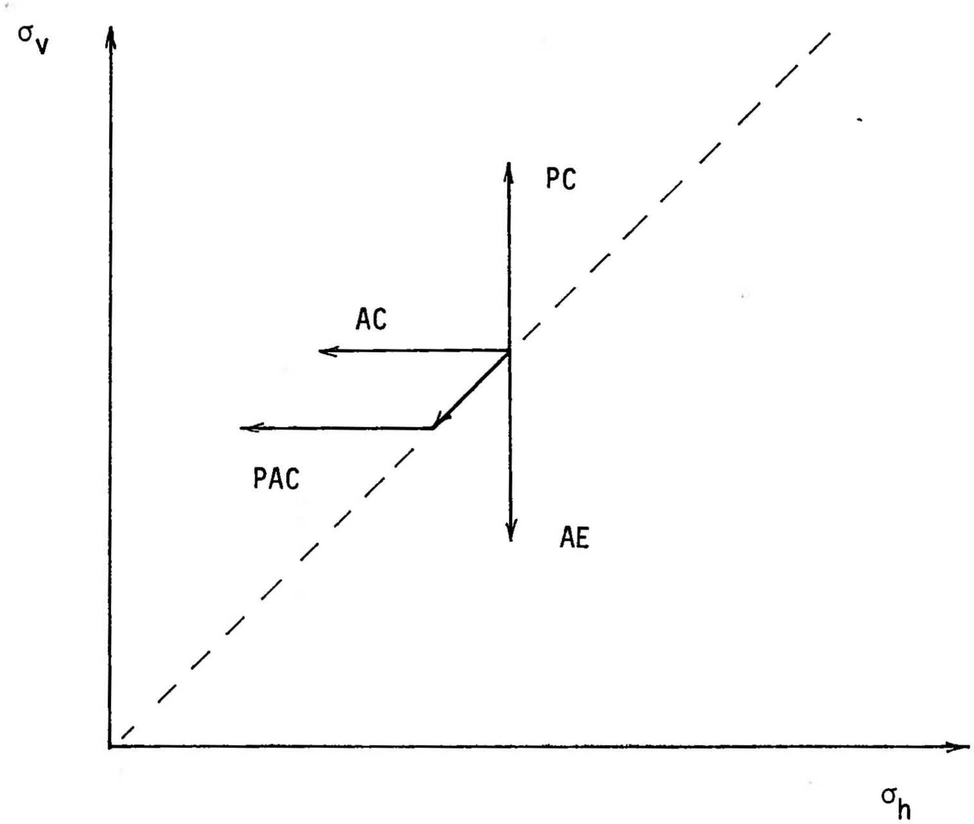

PC passive compression

AE active extension

AC active compression

PAC prop.-active compression

FIGURE 4.2 LABORATORY STRESS PATHS

conditions.

4.2.3.1 Passive compression

During these tests the samples were first submitted to an isotropic compression slightly higher (10%) than the overburden pressure. The vertical stress was gradually increased without any change in the lateral stress. This is the commonly used triaxial test. Its results will be used to compare it with the nonconventional stress paths encountered in the preliminary analysis. The points in the graphs represent laboratory measuring points, while the curve stands for hyperbolae fitted to the results. Some of the results are in figures 4.3 to 4.11.

The angle of shearing resistance observed was 40.1 and the strain to failure within the range from 3% to 4%. At the early stages of the stress strain curve a decrease in volume is observed , whereas at a later stage the sample increases in volume, a behaviour typical of dense sands and overconsolidated clays.

4.2.3.2 Active compression

This type of stress path is experienced by points situated beside the retaining wall. It was simulated in the laboratory by a reduction in the confining stress and a simultaneous increase in the axial load to compensate for the relief of the cell pressure. Because of the reduced value of the axial strain at failure, it was very difficult

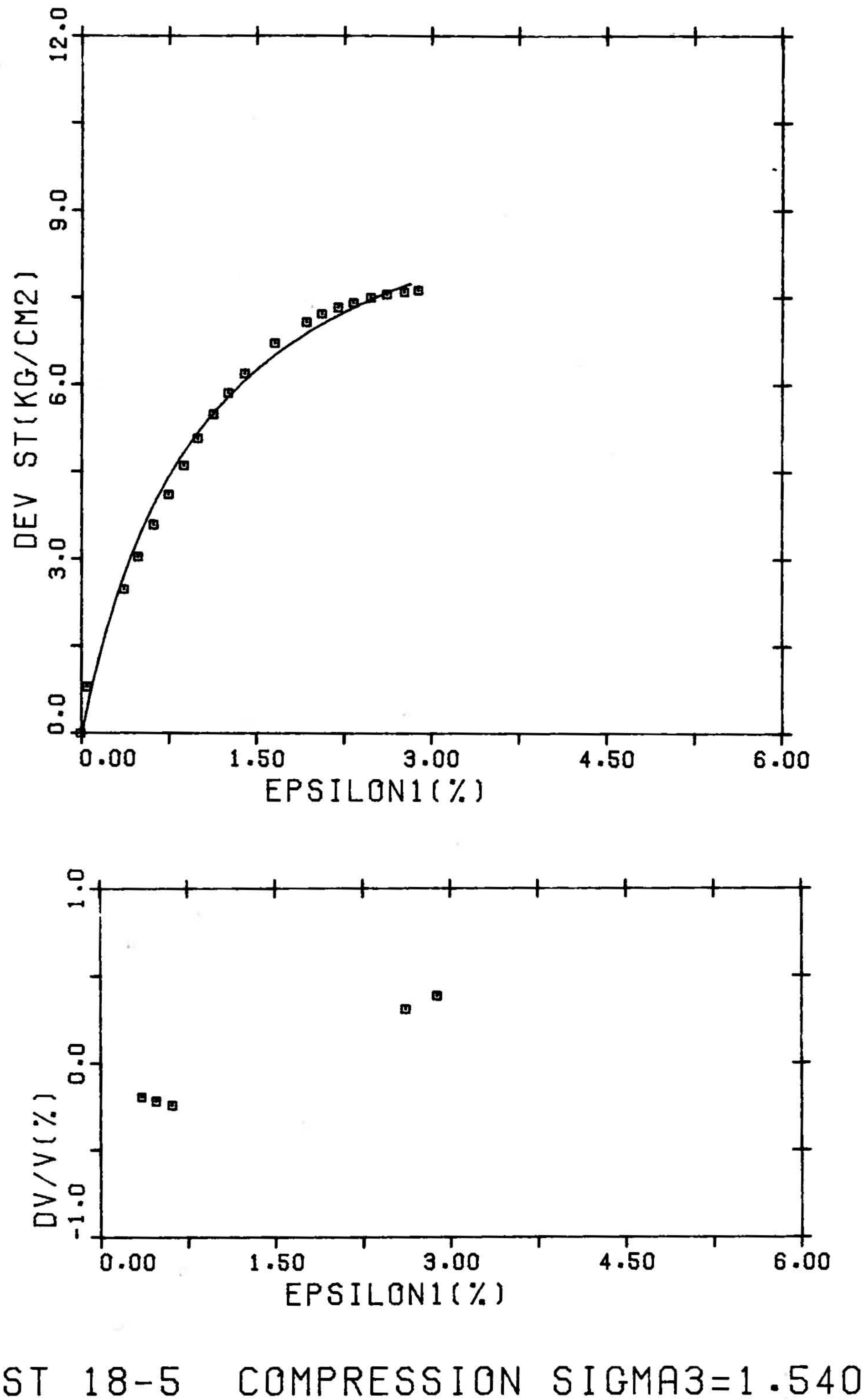

FIGURE 4.3 PASSIVE COMPRESSION TEST EDMONTON TILL

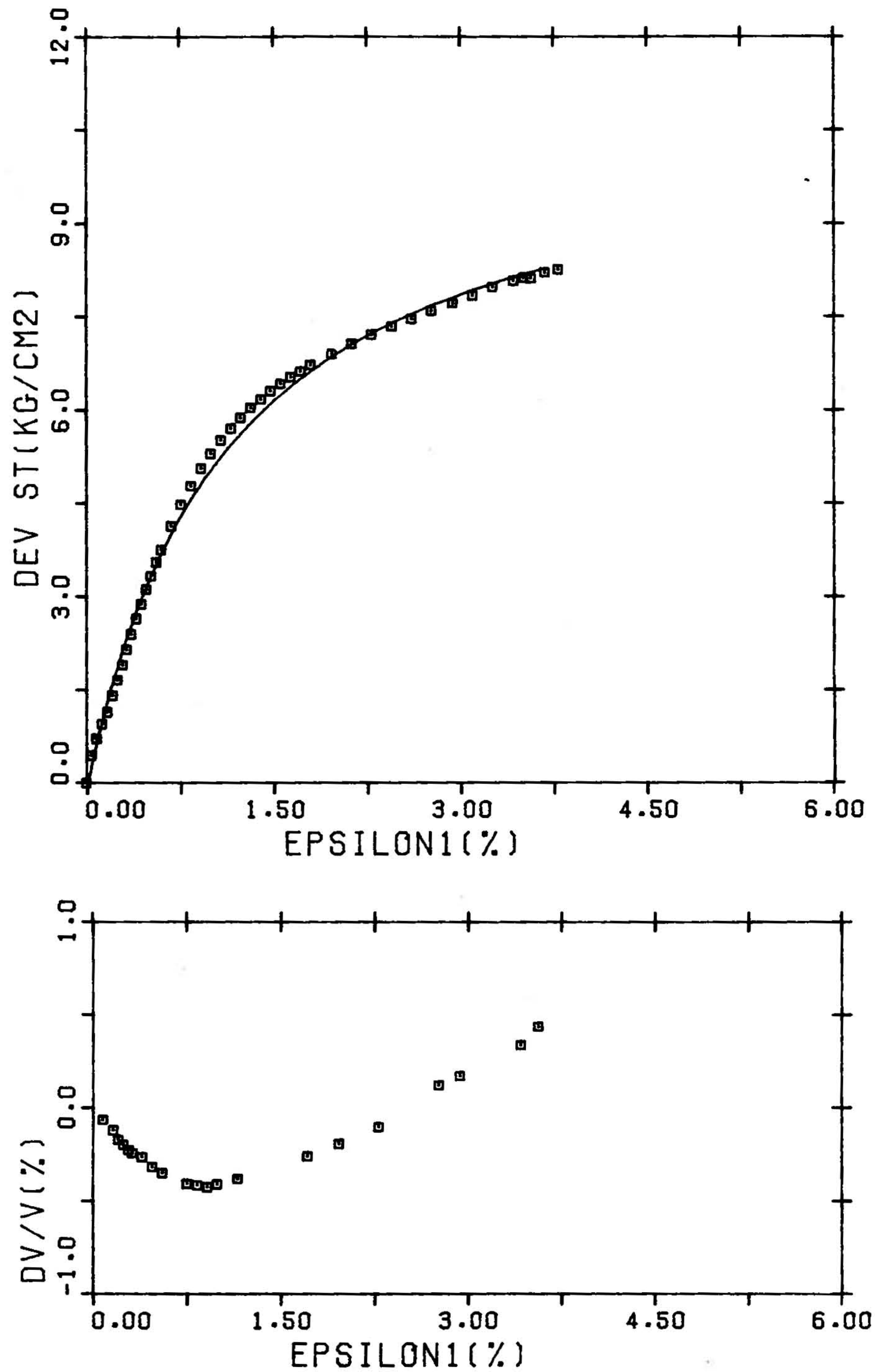

TEST 18-7 COMPRESSION SIGMA3=1.890

FIGURE 4.4 PASSIVE COMPRESSION TEST EDMONTON TILL

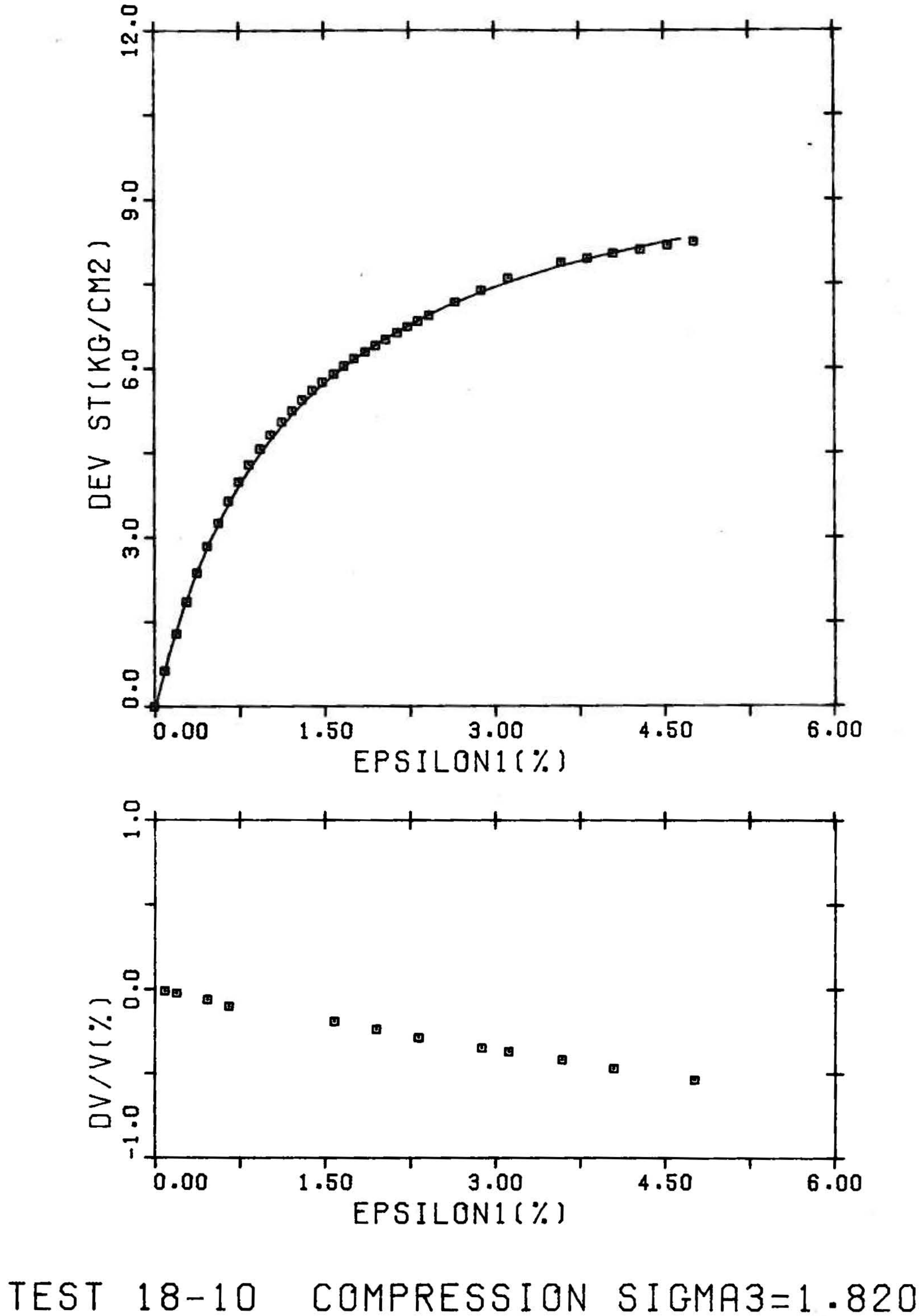

FIGURE 4.5 PASSIVE COMPRESSION TEST EDMONTON TILL

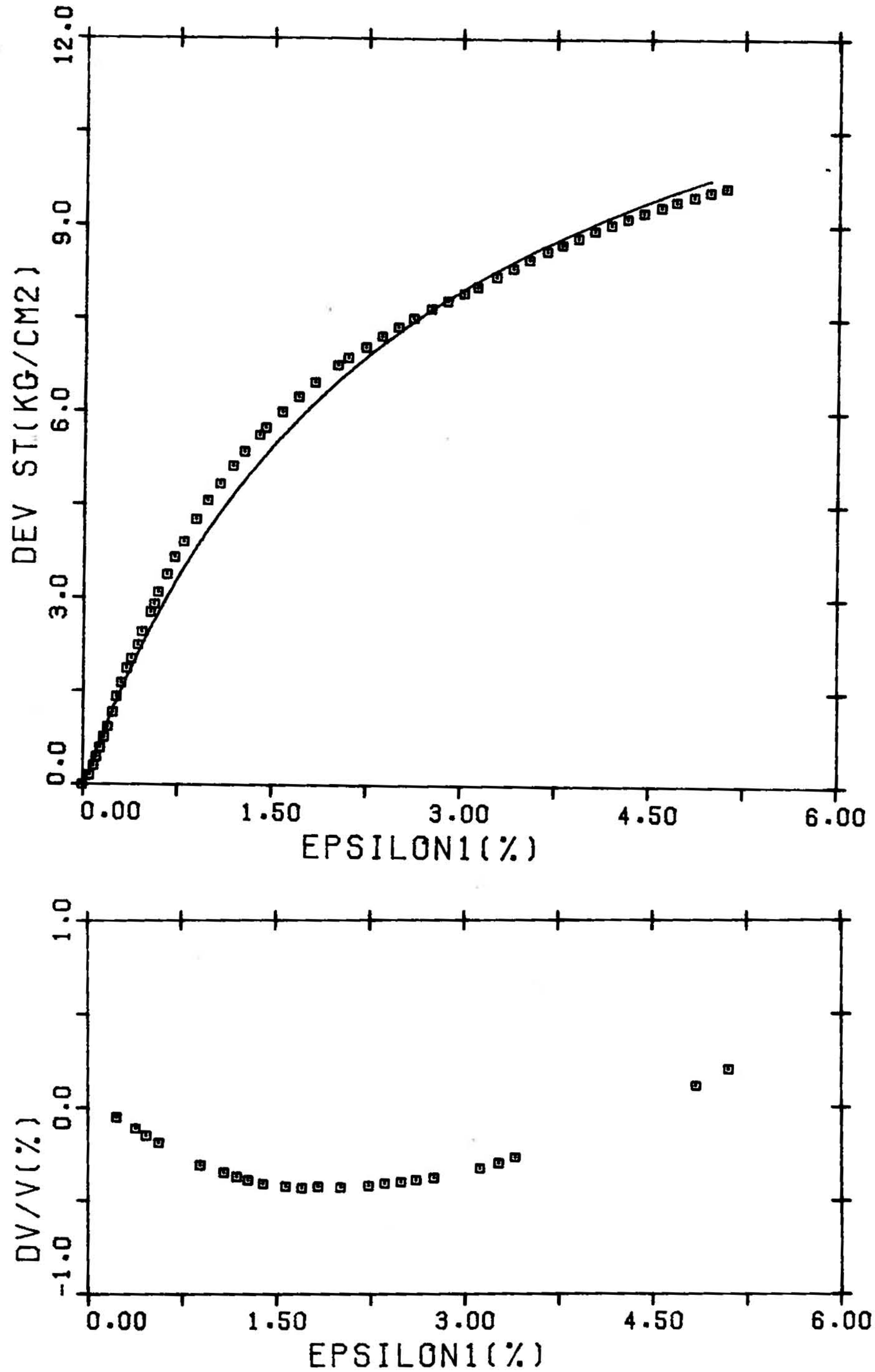

TEST 18-18 COMPRESSION SIGMA3=2.765

FIGURE 4.6 PASSIVE COMPRESSION TEST EDMONTON TILL

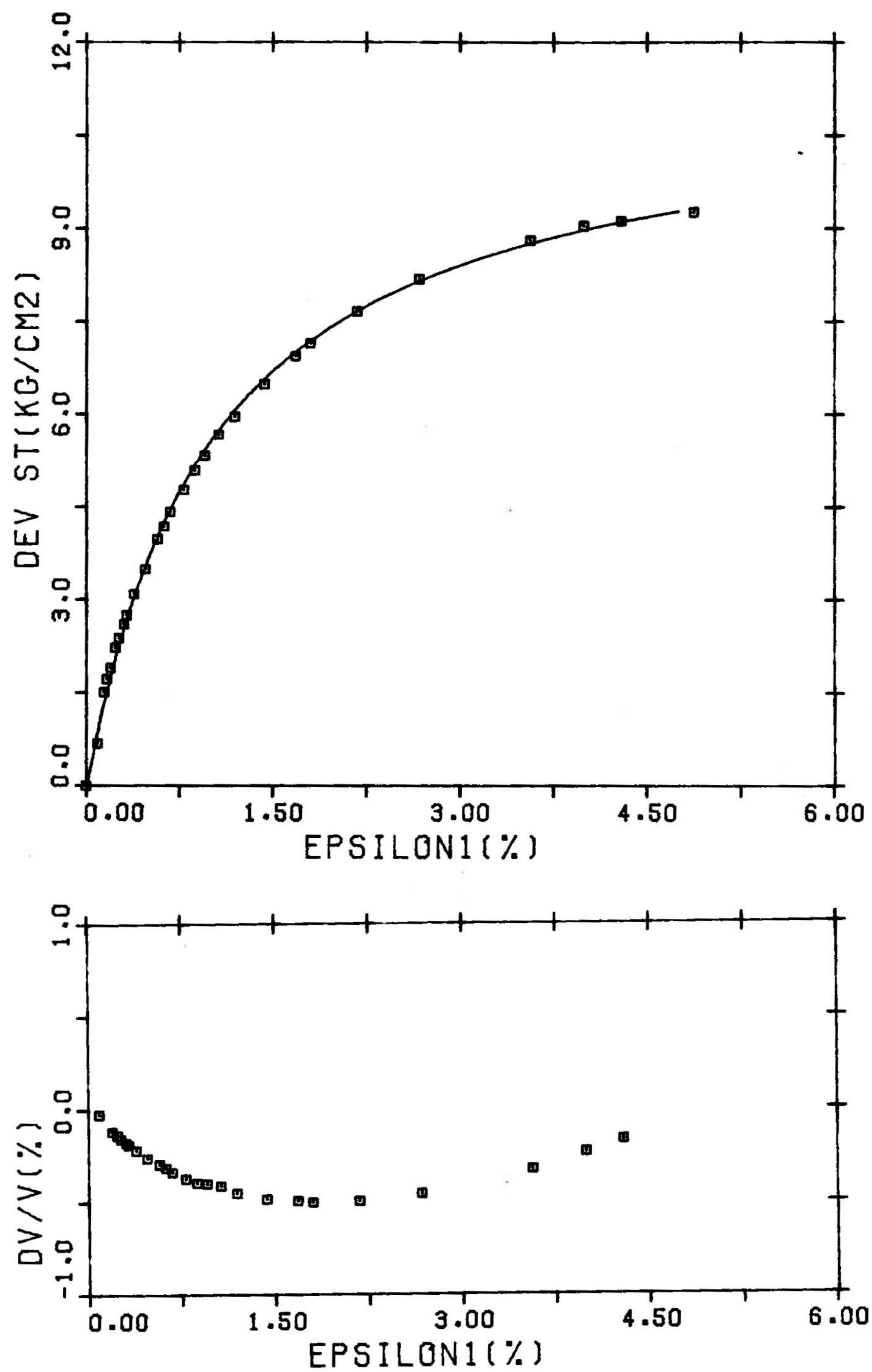

TEST 18-19 COMPRESSION SIGMA3=3.045

FIGURE 4.7 PASSIVE COMPRESSION TEST EDMONTON TILL

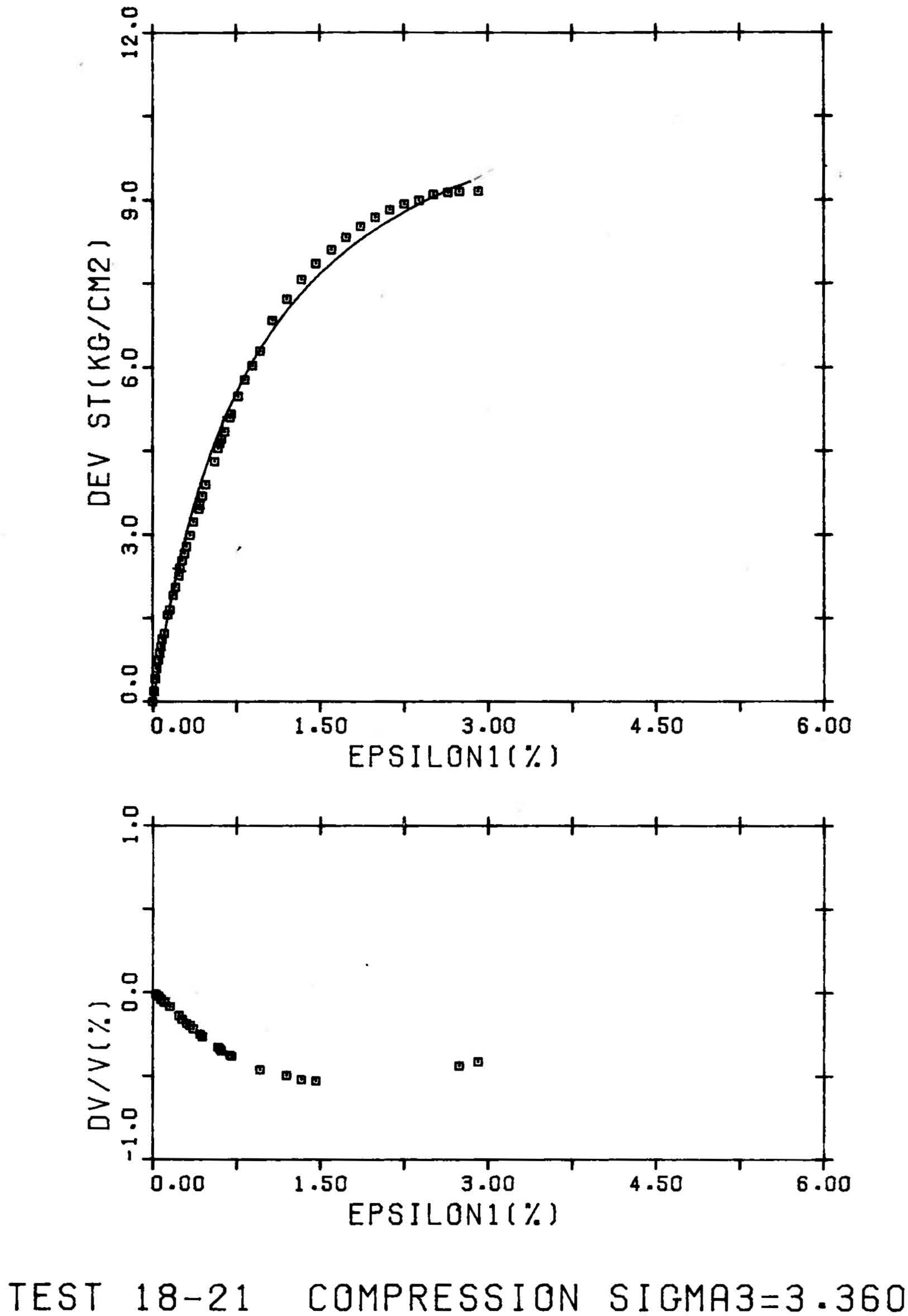

FIGURE 4.8 PASSIVE COMPRESSION TEST EDMONTON TILL

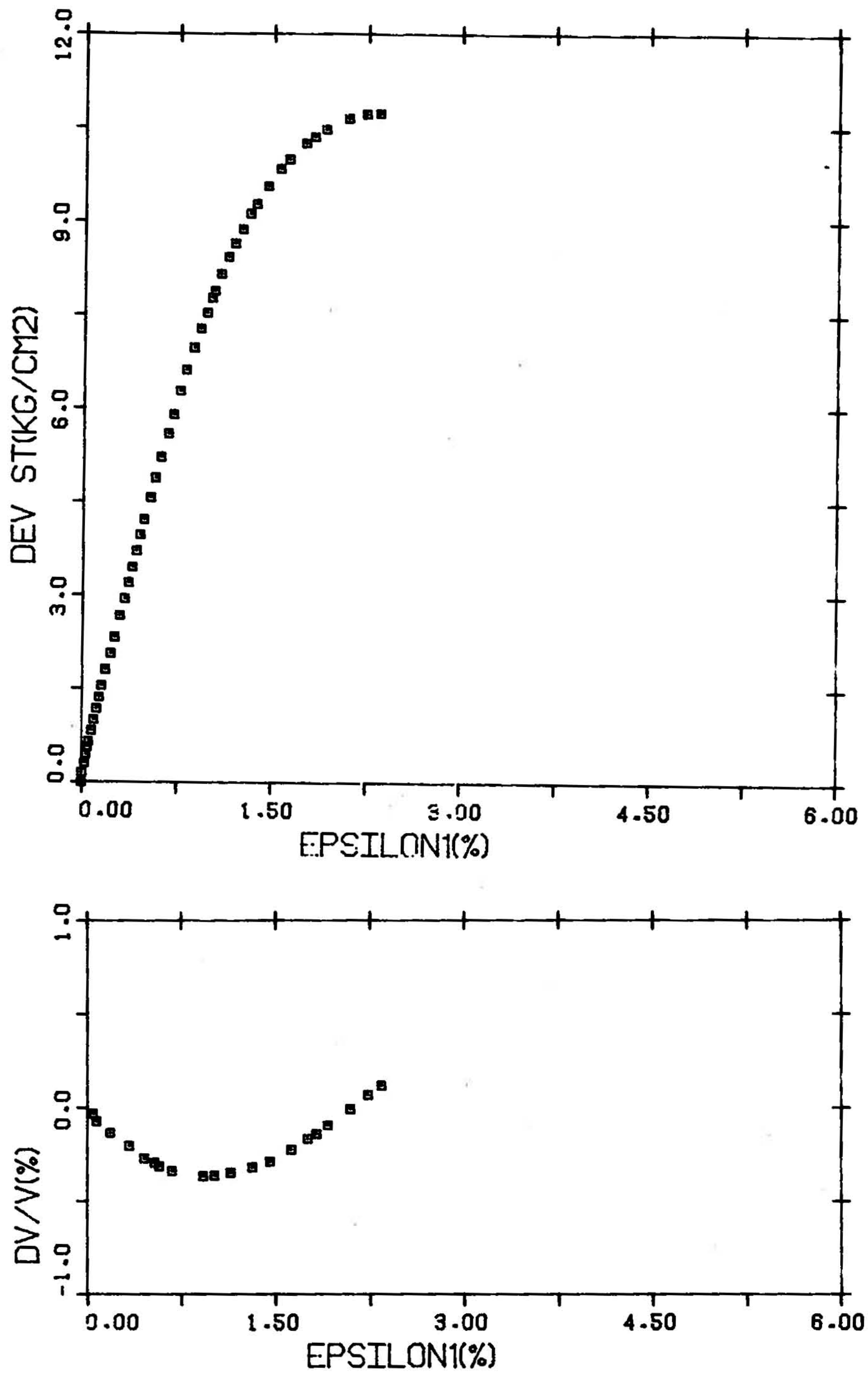

TEST 18-17 COMPRESSION SIGMA3=2.590

FIGURE 4.9 PASSIVE COMPRESSION TEST EDMONTON TILL

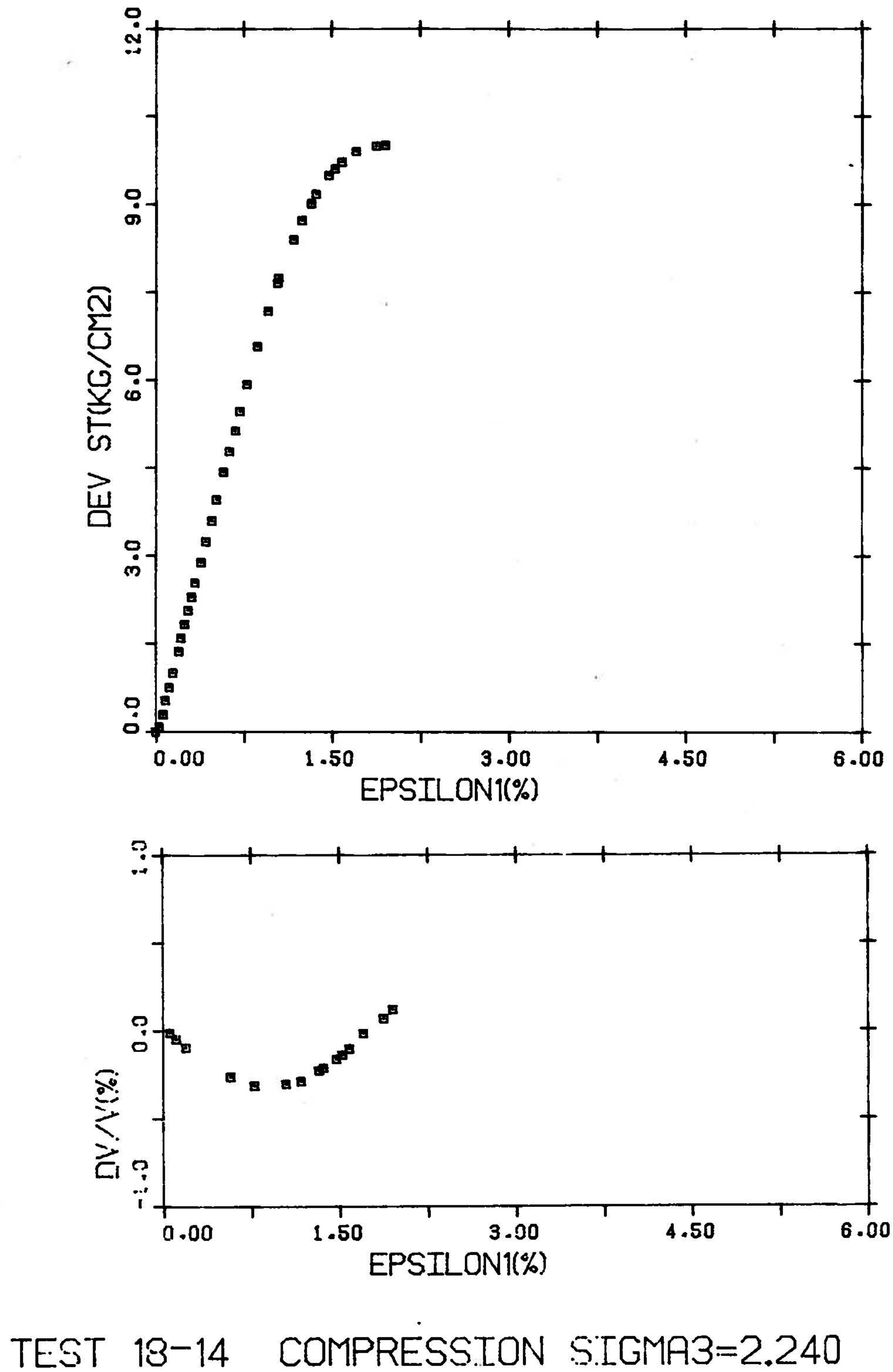

FIGURE 4.10 PASSIVE COMPRESSION TEST EDMONTON TILL

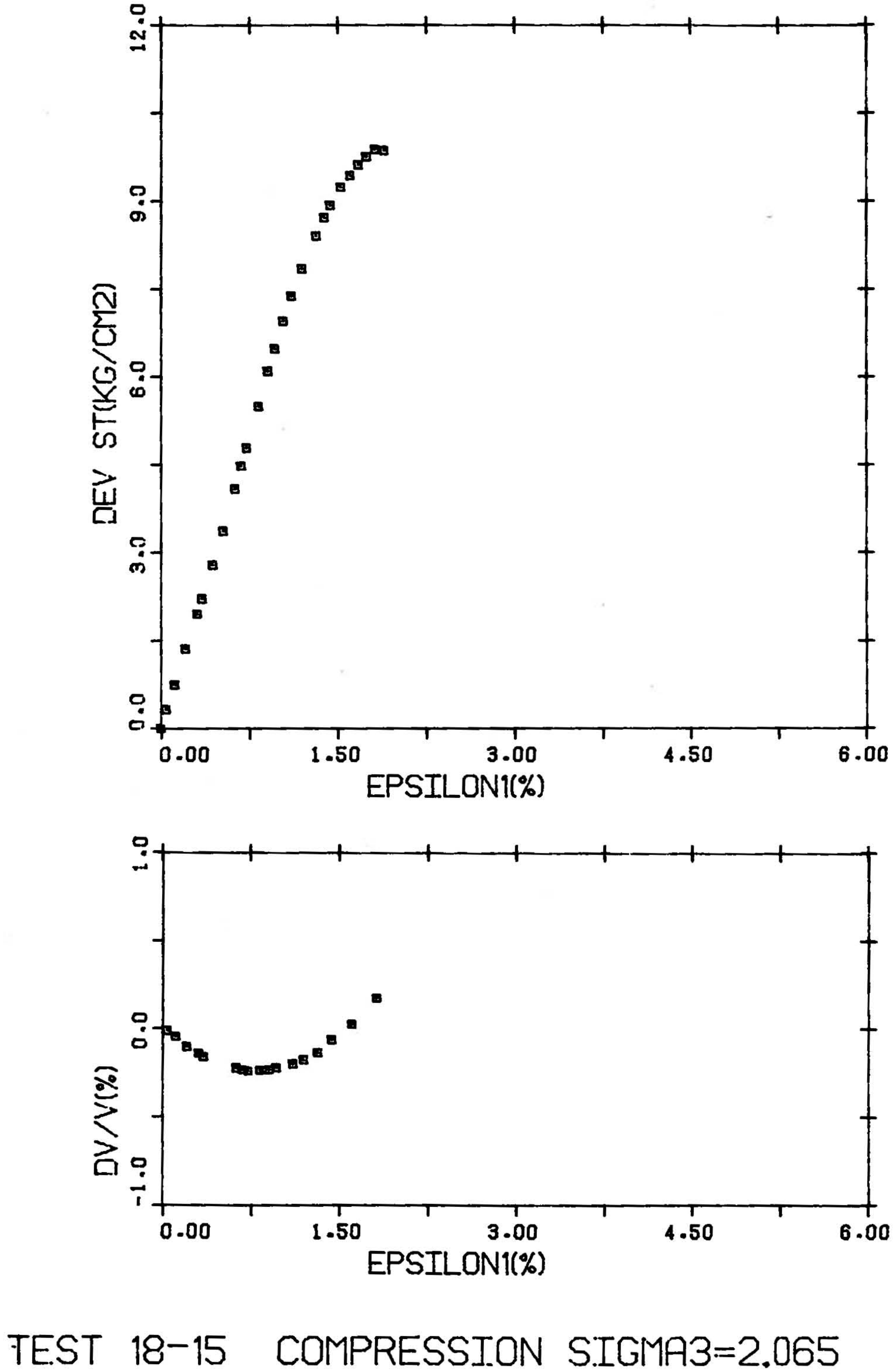

FIGURE 4.11 PASSIVE COMPRESSION TEST EDMONTON TILL

to depict the exact point of failure. As the material was not saturated the volume change had to be monitored by the amount of liquid flowing in or out of the cell. A calibration of the volume change of the cell with the confining stress was made, but the very reduced volume change of the specimen, especially in this type of stress path, made the correction for the expansion of the cell much greater than the volume change of the soil. In this series of tests the samples were consolidated isotropically. Stress strain curves in figure 4.12 to 4.16 indicate failure occurred at values of axial strain from 0.35% to 0.50%, which represents a significant reduction from the passive compression tests.Hyperbolae were also fiited to the stress strain curves.

4.2.3.3 Unloading reloading

These tests were performed with a dual purpose. First the use of the elastoplastic model to be explained in chapter 5 required the unloading-reloading modulus of deformation and second, moduli of elasticity determined from the reloading part in large plate loading tests, besides exhibiting a much lower scatter of values, are in very close agreement with the in situ values determined from field observation (Marland 1971). These results must be closer to the reloading part of large plate loading tests. The stress strain curves are in figures 4.17 and 4.18.

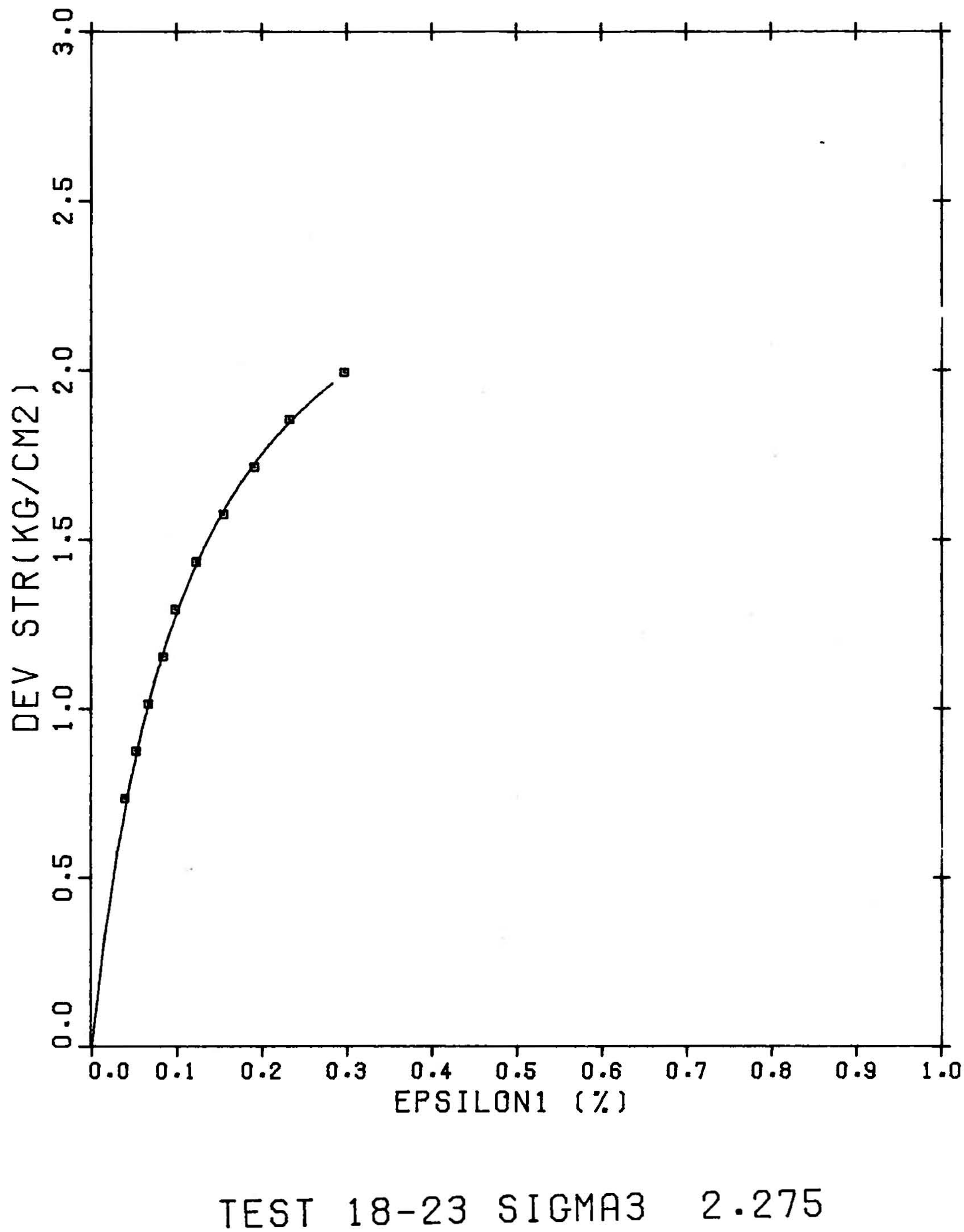

FIGURE 4.12 ACTIVE COMPRESSION TEST EDMONTON TILL

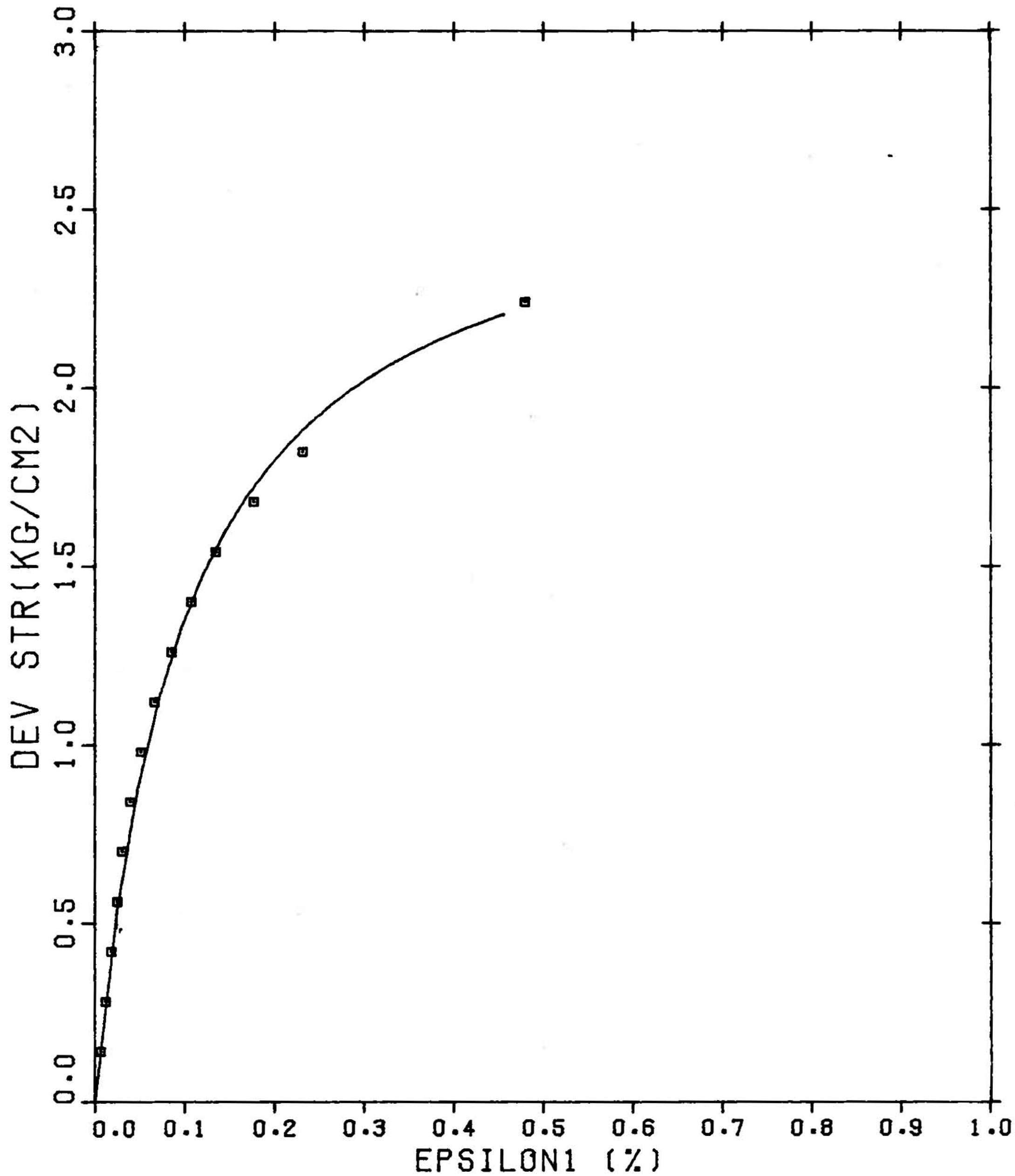

TEST 18-24 SIGMA3 2.80

FIGURE 4.13 ACTIVE COMPRESSION TEST EDMONTON TILL

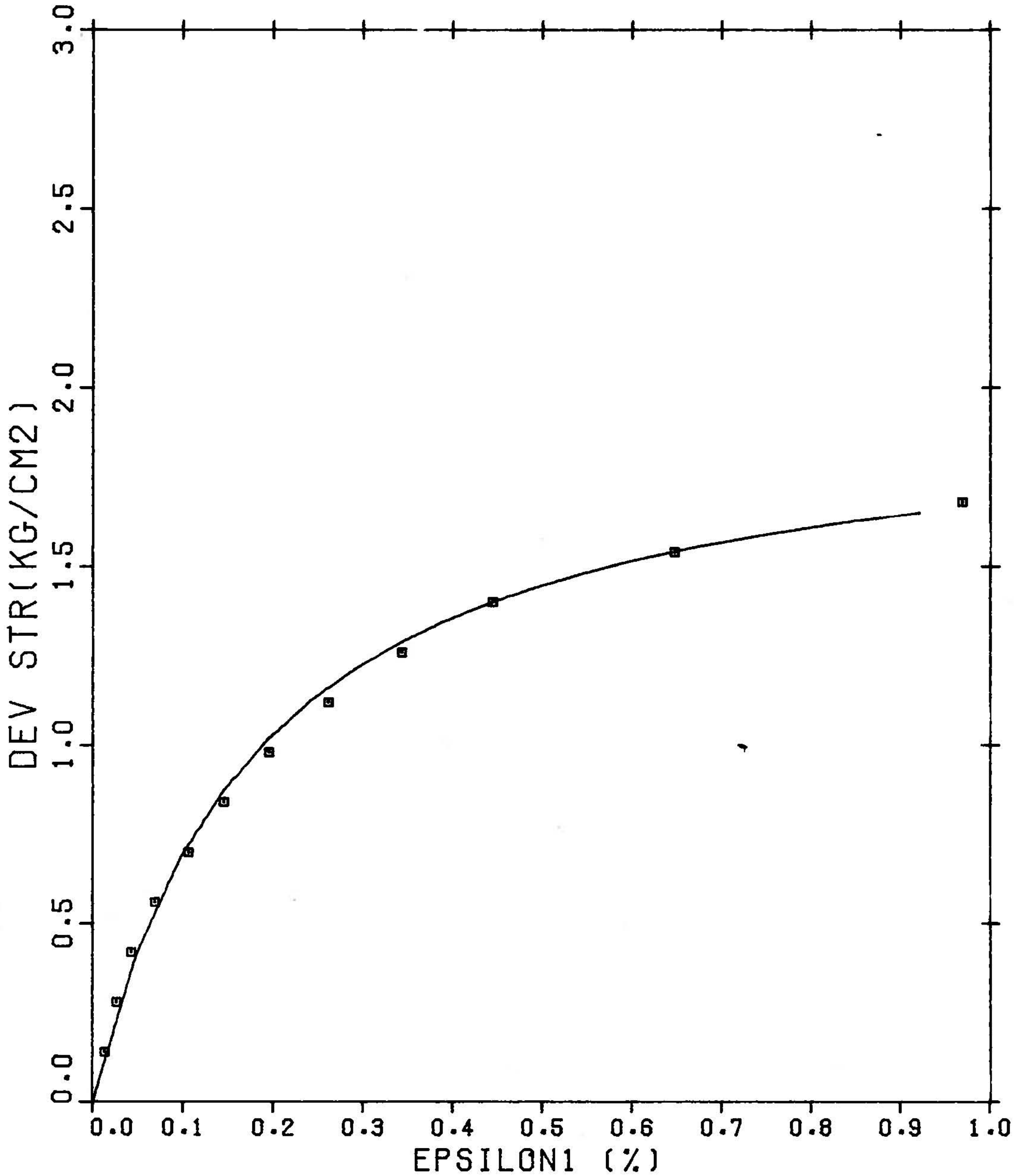

TEST 18-25 SIGMA3 2.10

FIGURE 4.14 ACTIVE COMPRESSION TEST EDMONTON TILL

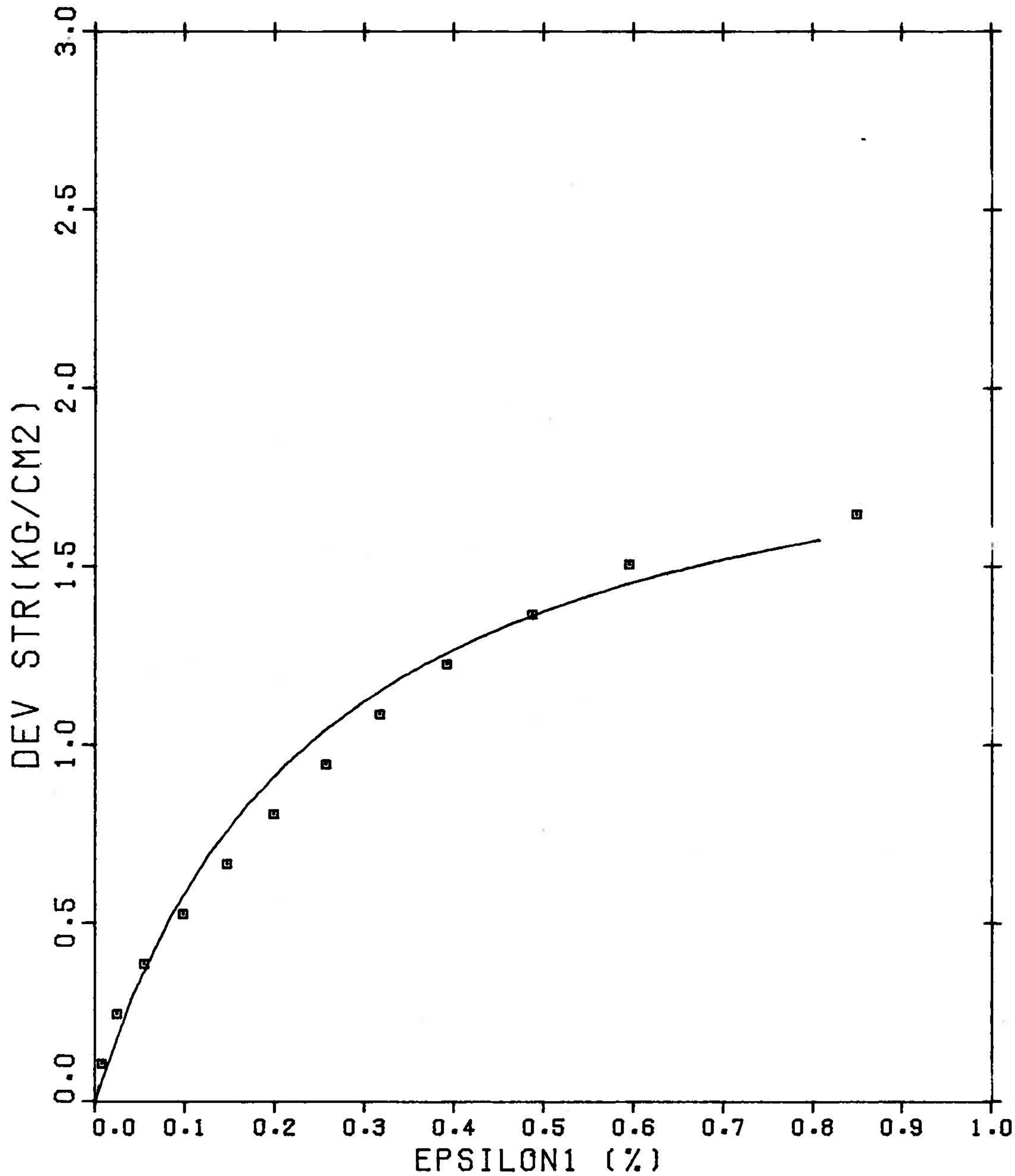

TEST 18-26 SIGMA3 1.925

FIGURE 4.15 ACTIVE COMPRESSION TEST EDMONTON TILL

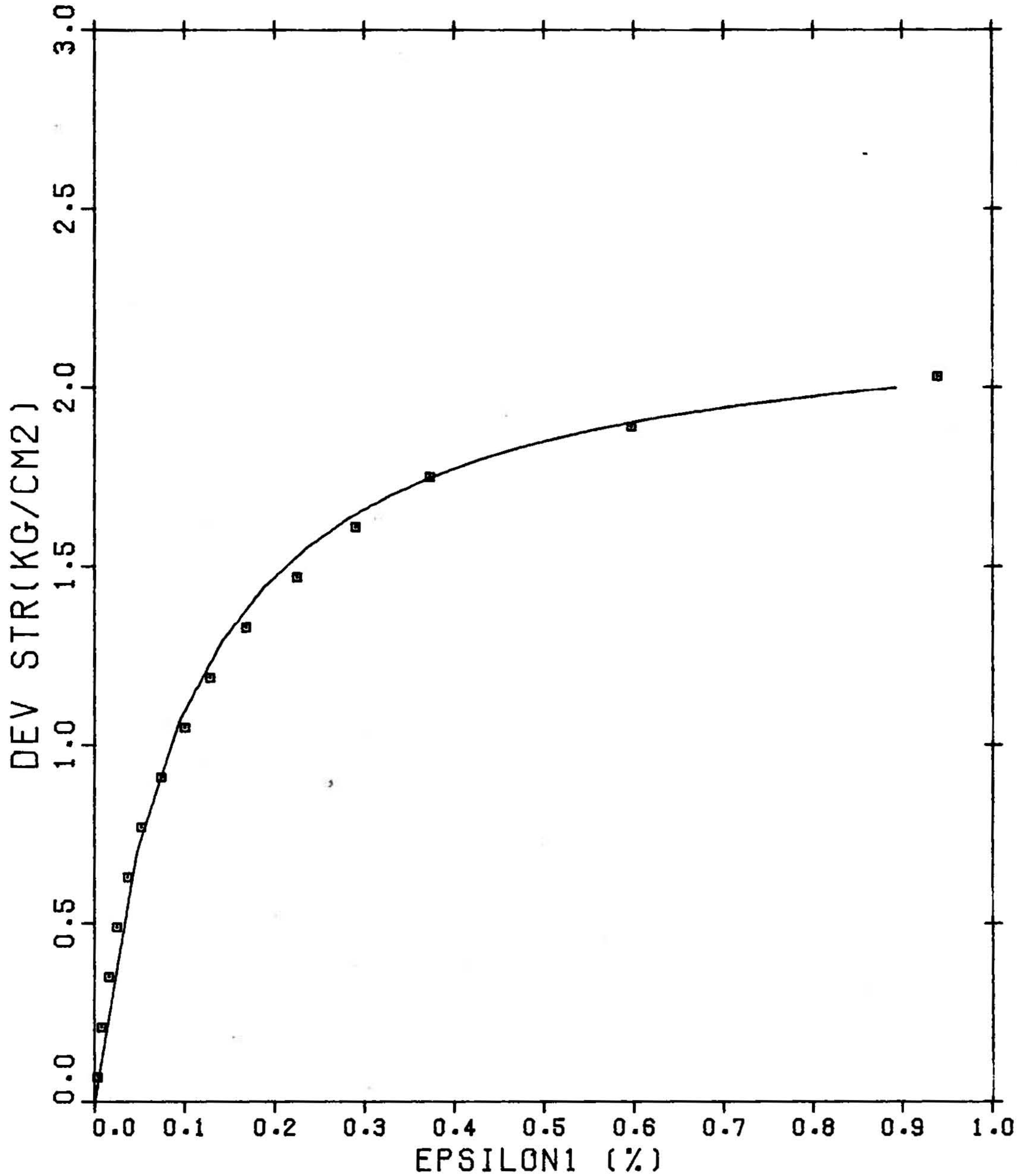

TEST 18-27 SIGMA3 2.45

FIGURE 4.16 ACTIVE COMPRESSION TEST EDMONTON TILL

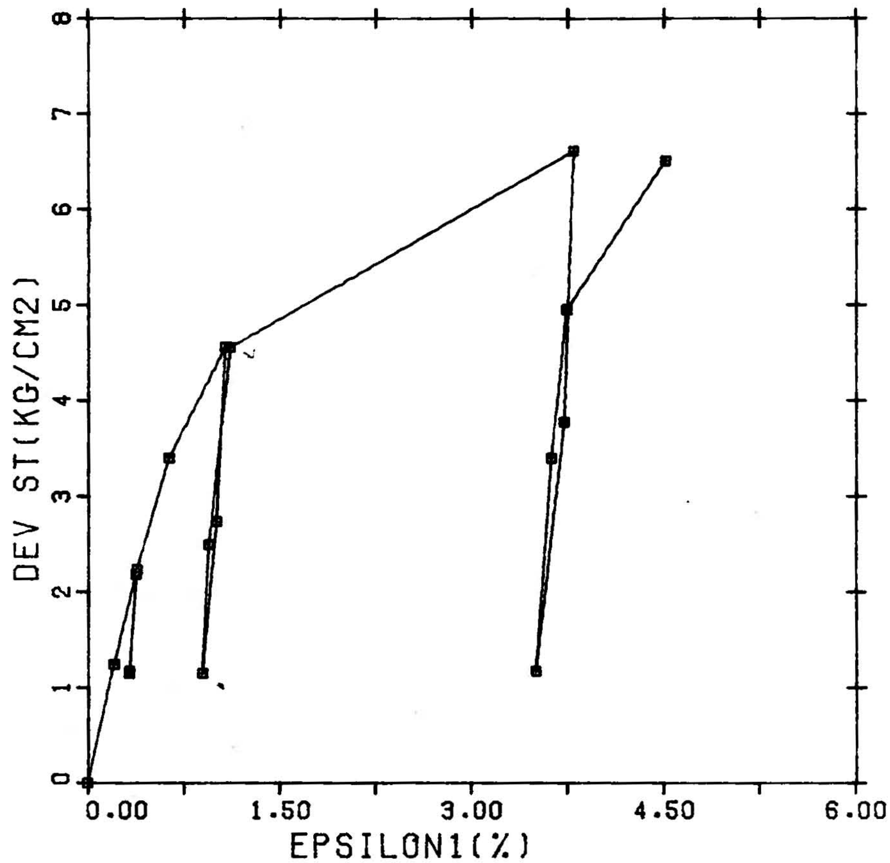

TEST 18-12 UNLOAD-RELOAD SIG3=1.89

FIGURE 4.17 UNLOADING RELOADING TEST EDMONTON TILL

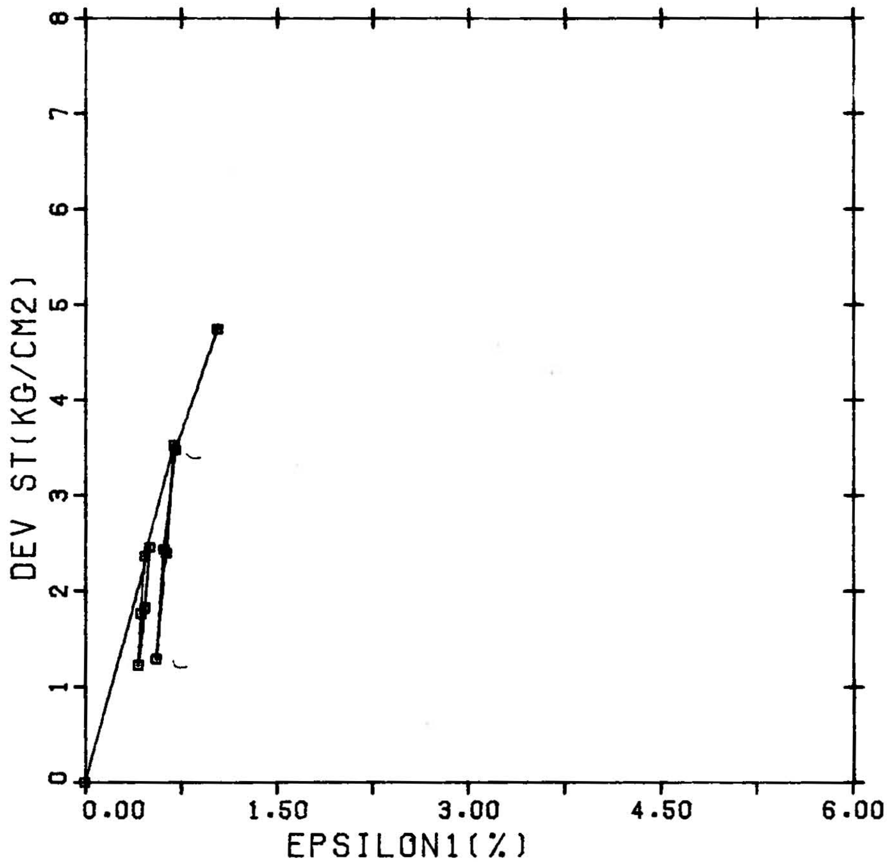

TEST 18-13 UNLOAD-RELOAD SIG3=2.24

FIGURE 4.18 UNLOADING RELOADING TEST EDMONTON TILL

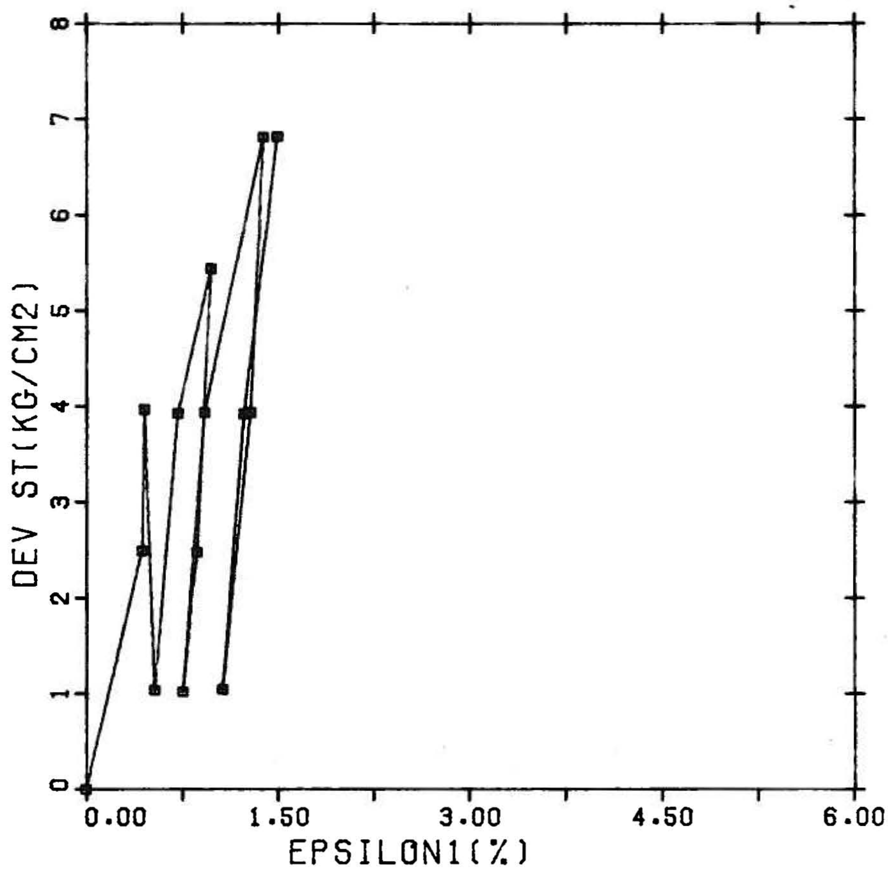

TEST 18-20 UNLOAD-RELOAD SIG3=2.59

FIGURE 4.19 UNLOADING RELOADING TEST EDMONTON TILL

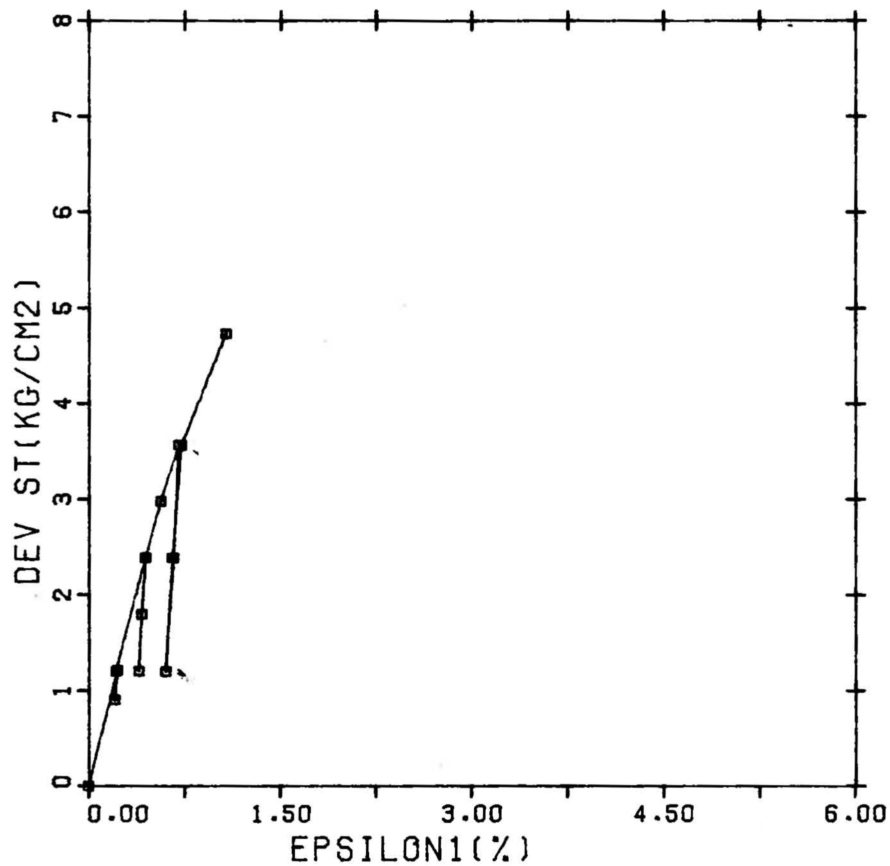

TEST 18-11 UNLOAD-RELOAD SIG3=1.54

FIGURE 4.20 UNLOADING RELOADING TEST EDMONTON TILL

4.2.4 Plane strain

In order to simulate as closely as possible the actual fieldstress conditions, a plane strain apparatus was designed and constructed for this project. Details of the equipment are in appendix B.

4.2.4.1 Passive compression

The samples were submited to vertical and lateral stresses slightly higher than the overburden pressure. The vertical stress was increased until failure, without change in the lateral stress. The results are in figure 4.21 to 4.24 . Specimen PS2 failed at the contact between the typical Edmonton till and an extremely silty material encountered where this block was taken. The results from the other 3 tests indicated an angle of shearing resistance of 46.5 degrees.

4.2.4.2 Active compression

The samples in this type of test are supposed to be as close as possible to the field conditions and therefore were consolidated anisotropically with the ratio between the principal stresses of 0.85. Figures 4.25 and 4.26 show the stress strain curves for these tests.

4.2.5 Summary

Plane strain tests performed by Lee (1970) on dense sand indicated an increase of 8 degrees in the angle of

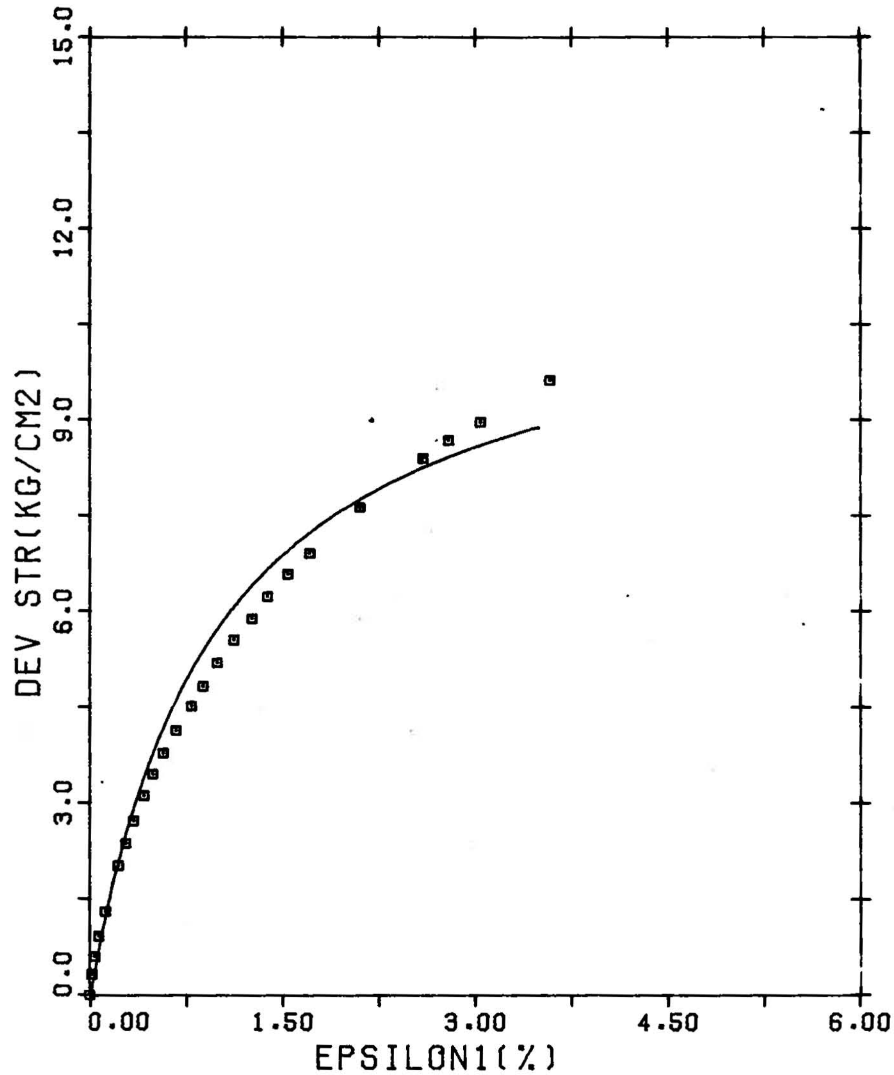

PS1 PL STRAIN SIG3=1.75

FIGURE 4.21 PASSIVE COMPRESSION TEST IN PLANE STRAIN EDMONTON TILL

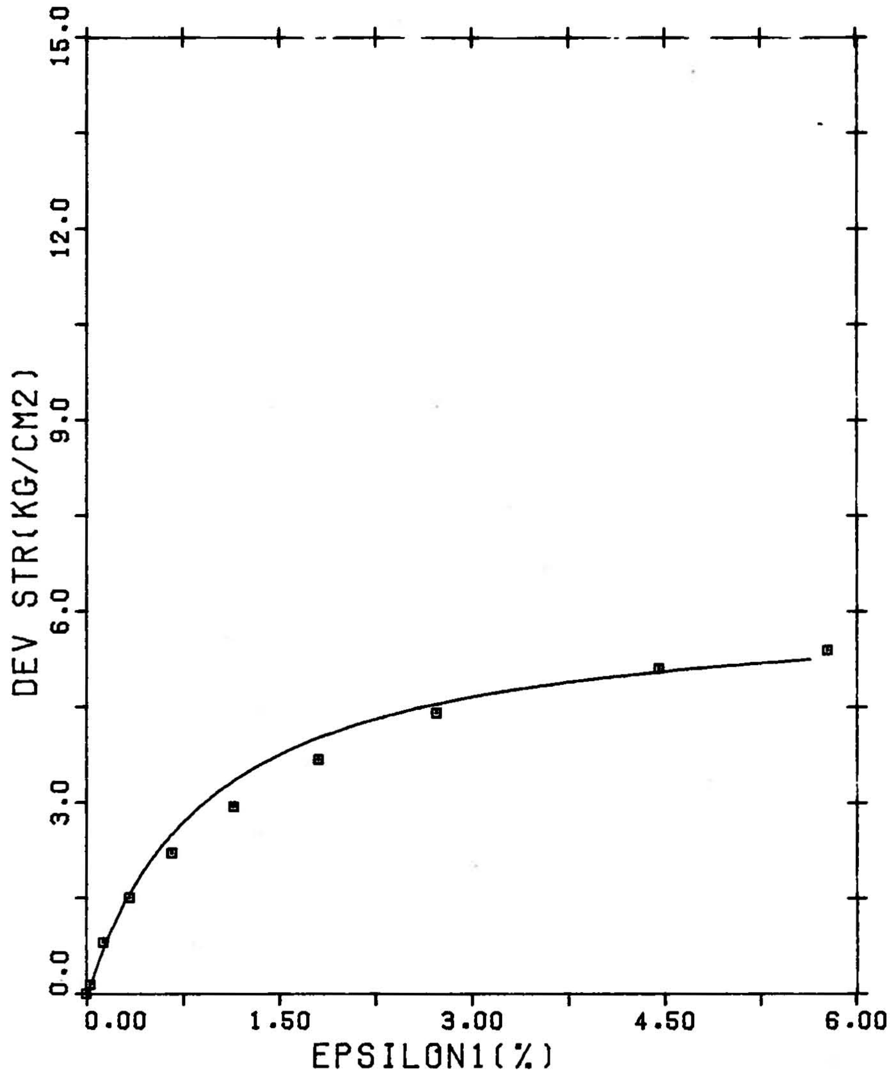

PS2 PL STRAIN SIG3=2.10

FIGURE 4.22 PASSIVE COMPRESSION TEST IN PLANE STRAIN EDMONTON TILL

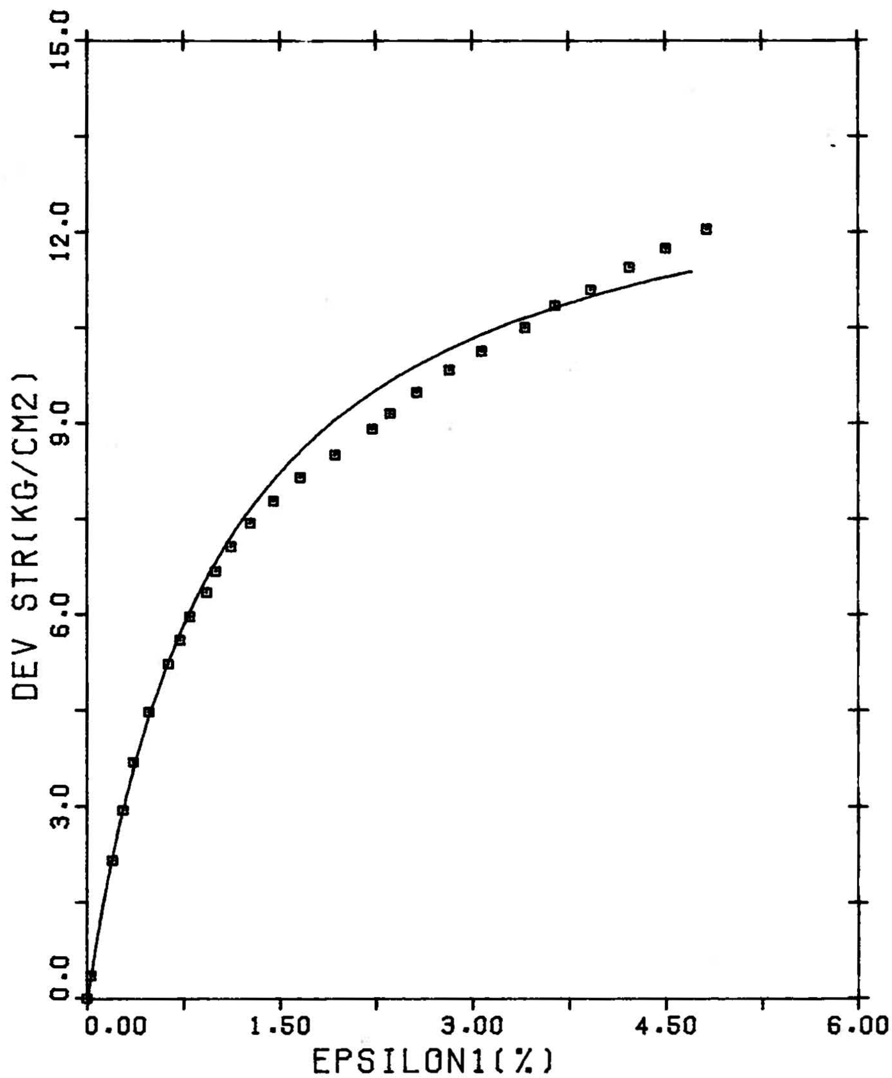

PS3 PL STRAIN SIG3=2.45

FIGURE 4.23 PASSIVE COMPRESSION TEST IN PLANE STRAIN EDMONTON TILL

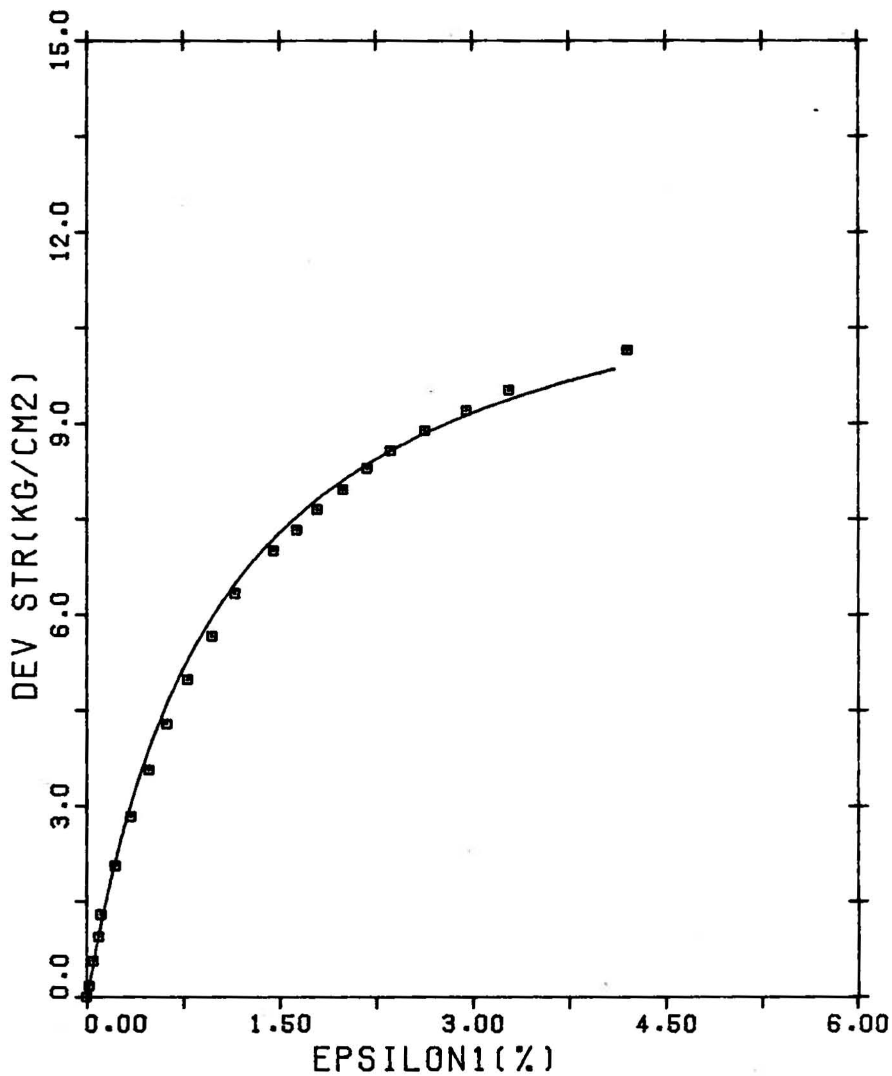

PS4 PL STRAIN SIG3=1.925

FIGURE 4.24 PASSIVE COMPRESSION TEST IN PLANE STRAIN EDMONTON TILL

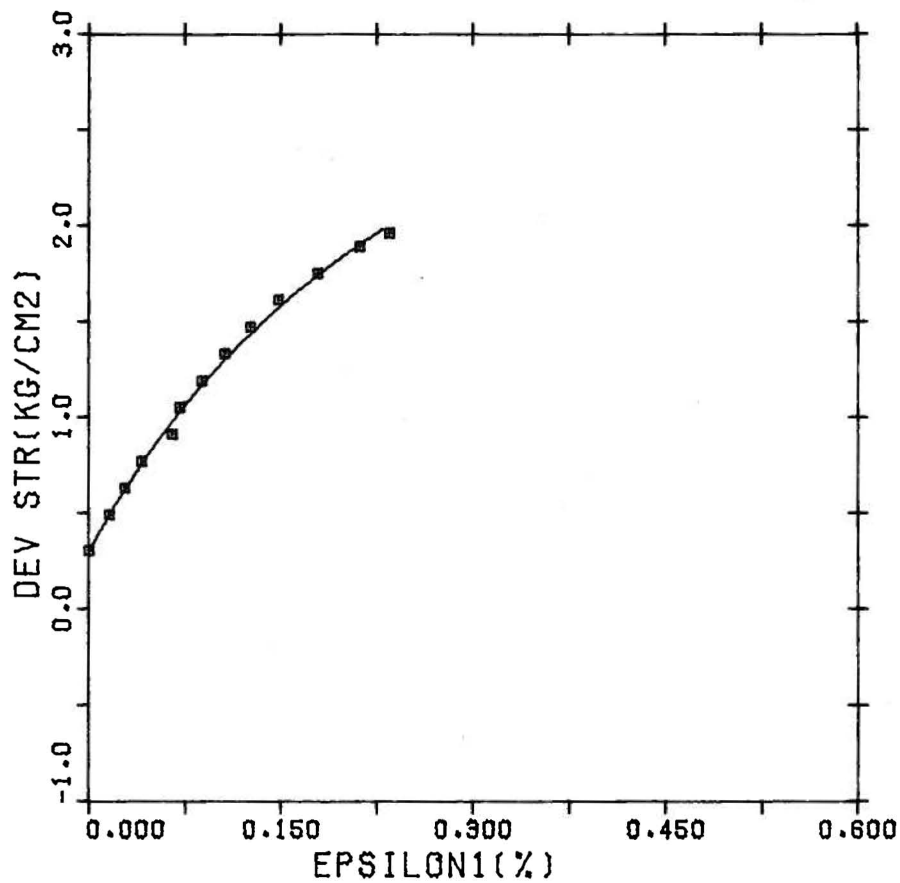

PS7 PL STRAIN SIG3=1.726

FIGURE 4.25 ACTIVE COMPRESSION TEST IN PLANE STRAIN EDMONTON TILL

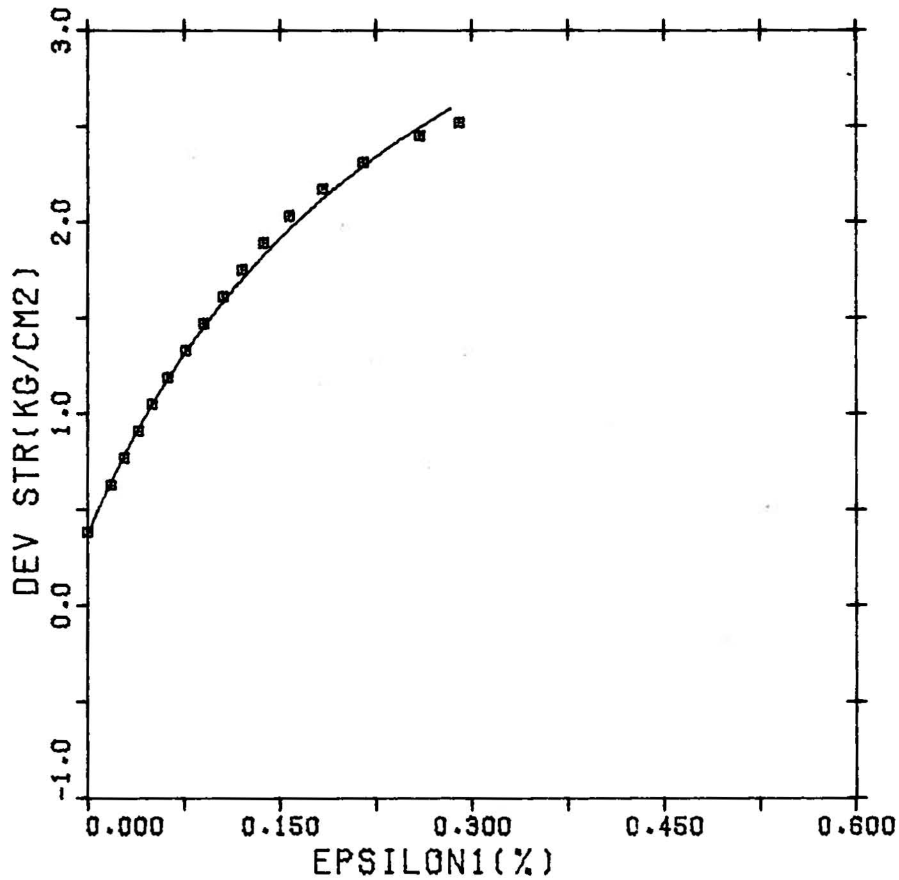

PS9 PL STRAIN SIG3=2.205

FIGURE 4.26 ACTIVE COMPRESSION TEST IN PLANE STRAIN EDMONTON TILL shearing resistance compared to triaxial tests, fcr low values of confining stress. For the Edmonton till an increase of 6.5 degrees was encountered, which still represents a significant difference in terms of shear strength.Figure 4.29 illustrates the shear strength results.

Comparing the stress strain behaviour one can write for linearly elastic material:

$$\Delta\epsilon_1 = \left(\Delta\sigma_1 - \mu\left(\Delta\sigma_2 + \Delta\sigma_3\right)\right)/E \qquad .....(4.2)$$

For triaxial passive compression tests the change in the intermediate and minor principal stresses is the same , therefore

$$\Delta\epsilon_1 = \frac{1}{E}\Delta\sigma_1 \qquad .....(4.3)$$

and for plane strain

$$\Delta\epsilon_{1ps} = \frac{1-\mu^2}{E}\left(\Delta\sigma_1 - \Delta\sigma_3\frac{\mu}{1-\mu}\right) \qquad .....(4.4)$$

For passive compression we can write

$$\Delta\epsilon_{1ps} = \frac{1-\mu^2}{E} \Delta\sigma_1 \qquad \text{.....(4.5)}$$

or

$$\Delta\epsilon_{1ps} = \frac{1}{E_{ps}} \Delta\sigma_1$$

where

$$E_{ps} = \frac{E}{1-\mu^2} \qquad (4.6)$$

Equation 4.6 relates the tangent of the stress strain curves in triaxial and plane strain tests. Figures 4.27 makes a comparison between the tangent moduli of deformation to evaluate the validity of equation 4.5. The curves drawn represent the values obtained from the hyperbolae fitted to the laboratory results. Lee (1970) encountered a ratio Ep/Et=1.4 while the theoretical expression indicated it to be 1.05. For the Edmonton till the theoretical expression indicates the ratio of 1.25 where the average value encountered was 1.55. Different values of Poisson ratio do not change significantly this conclusion. For a Poisson ratio of 0.5 the ratio would be 1.33 and a Poisson ratio of 0.3 reduces the ratio to 1.1 which still represents a a departure from the value of 1.55 obtained from the laboratory tests.

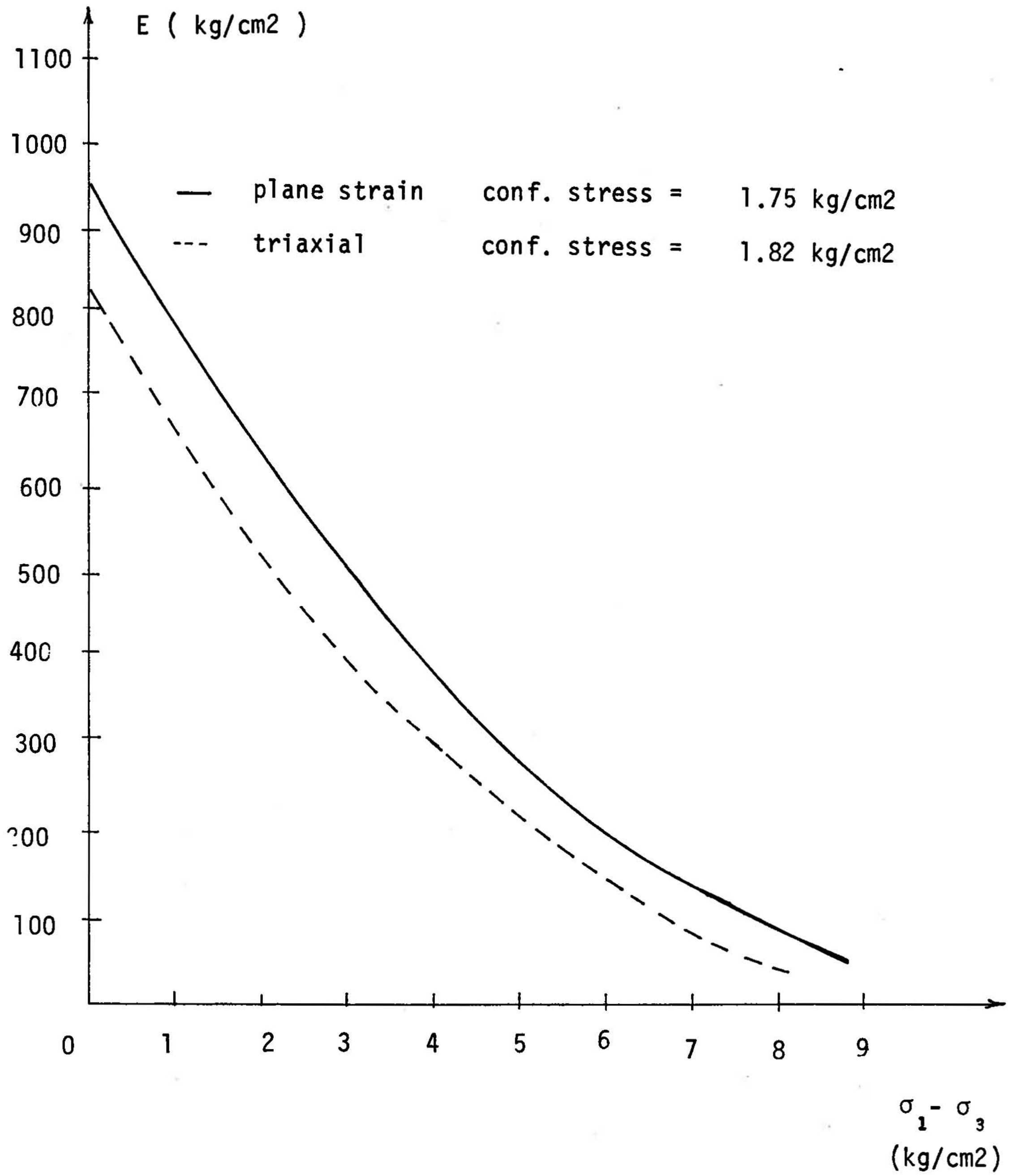

FIGURE 4.27 COMPARISON BETWEEN MODULUS OF DEFORMATION FROM TRIAXIAL AND PLANE STRAIN IN PASSIVE COMPRESSION

The modulus of deformation obtained from triaxial active compression exhibits a significant difference when compared with results from triaxial passive compression tests. (Figure 4.28) Vertical strain to failure is very much reduced in active compression tests. It is therefore reasonable to expect a reduction of the modulus of deformation when comparing conventional triaxial tests with field observation in excavations. A similar comparison was not possible with plane strain results since the active compression tests were consolidated anisotropically, therefore starting from a stress level much higher than isotropically consolidated tests.

A relationship of the type

$$E_i = K\,pa \left(\frac{\sigma_3}{pa}\right)^n \qquad .....(4.7)$$

- Ei is the initial modulus of deformation
- K and n are material constants
- σ_3 is the confining stress and
- pa is the atmospheric pressure

was not verified for this material.

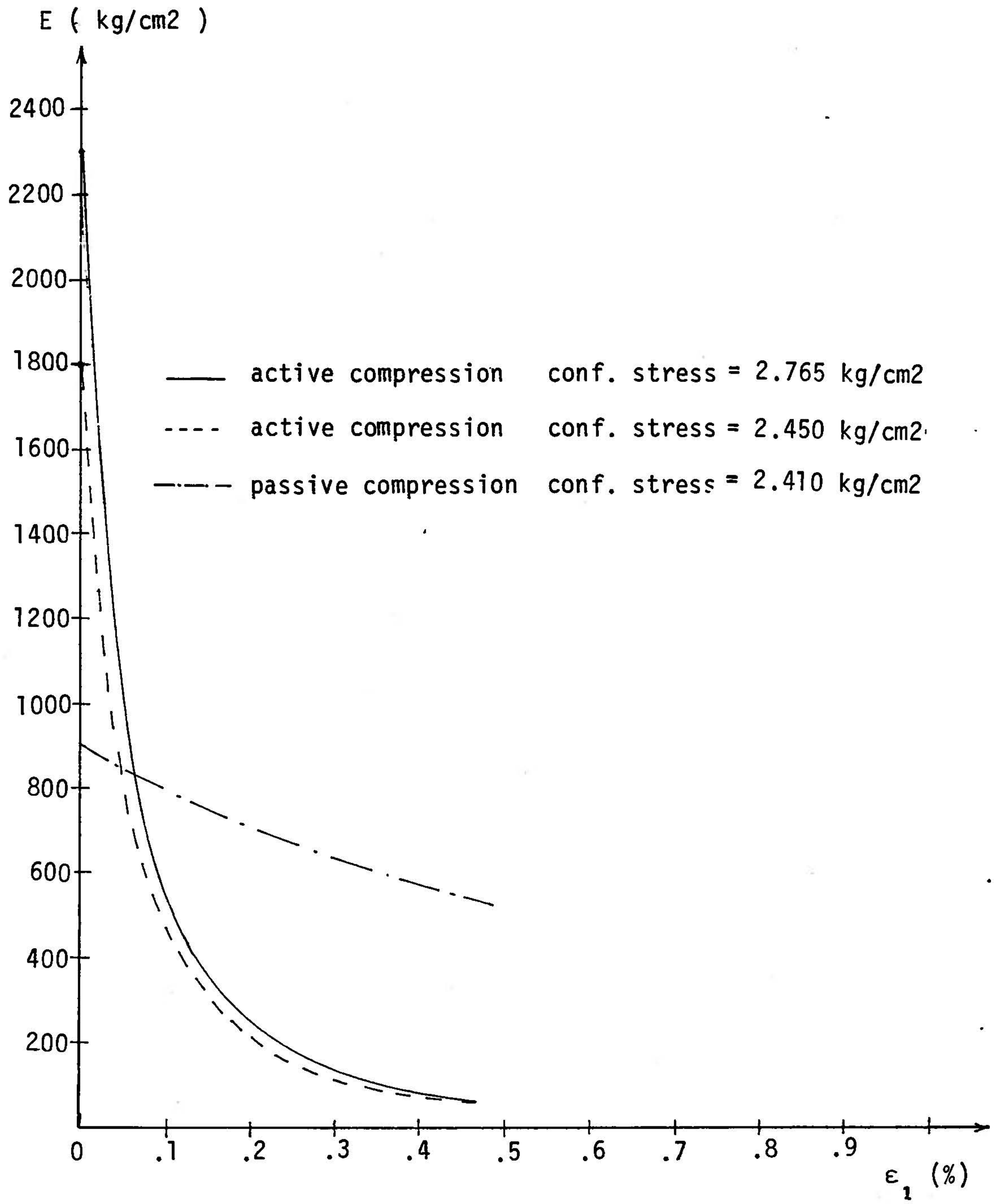

FIGURE 4.28 COMPARISON BETWEEN MODULUS OF DEFORMATION FROM PASSIVE AND ACTIVE COMPRESSION TESTS IN TRIAXIAL

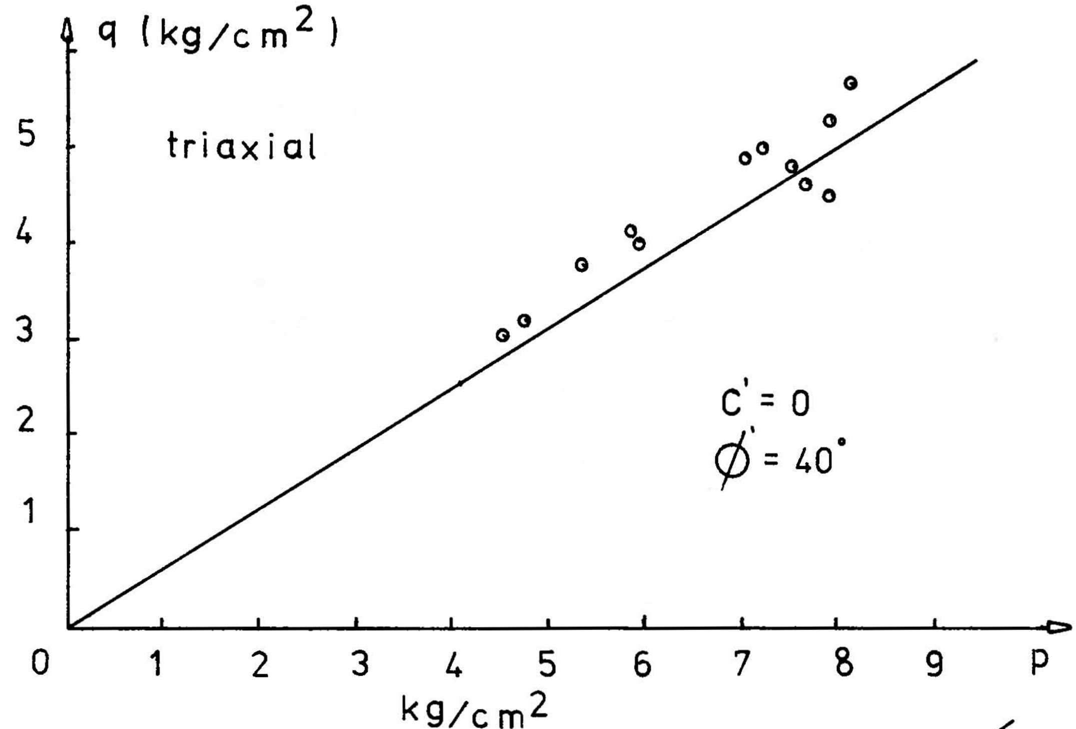

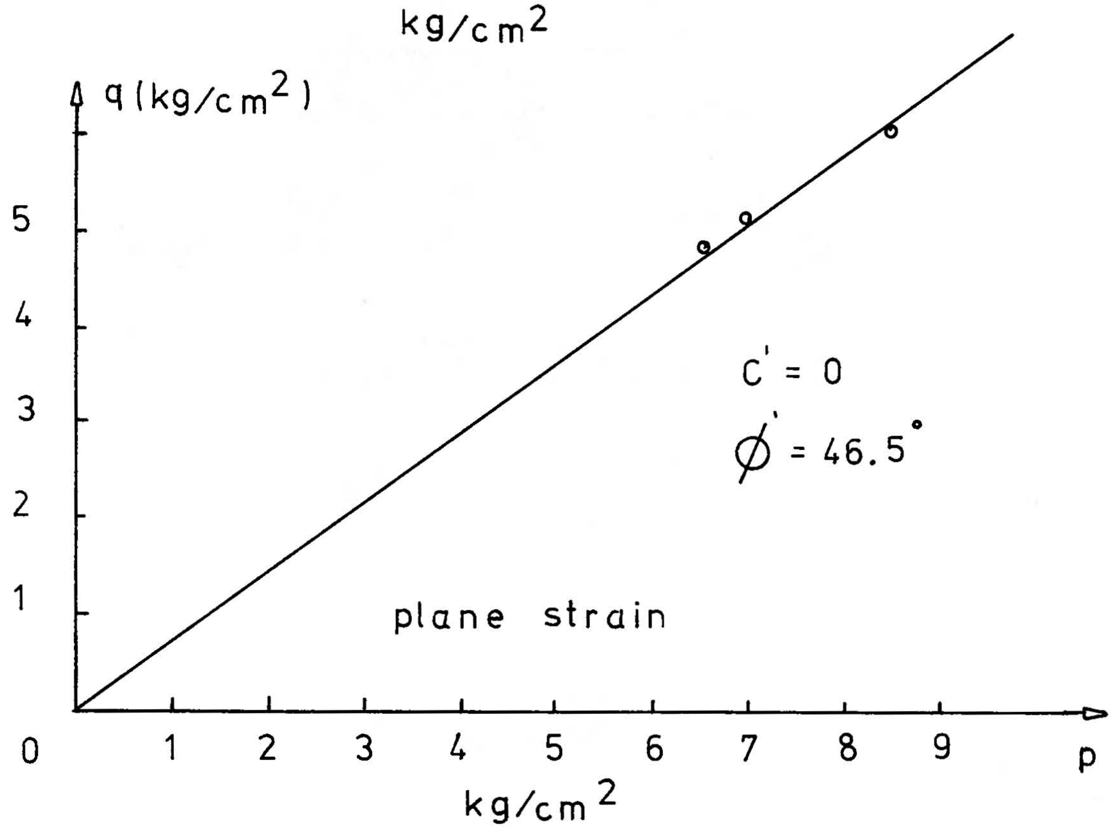

FIGURE 4.29 SHEAR STRENGTH ENVELOPE EDMONTON TILL

Although this material can not be assigned a single value for the modulus of deformation, as it is usually done for stiff clays, the active compression results were closer to the pressuremeter results from Eisenstein and Morrison (1973). For a hollow cylinder with internal and external pressure , the equilibrium equation in the radial direction for polar coordinates in terms of stress , assuming no body forces is:

$$\frac{\partial \sigma_r}{\partial r} + \frac{\sigma_r - \sigma_\theta}{r} = 0 \qquad .....(4.8)$$

where

- σ_r is the radial stress
- σ_θ is the tangential stress
- r is the radius.

The solution in plane strain for the following boundary condition

$$\sigma_r = p_1 \longrightarrow r = r_1$$
$$\sigma_r = p_2 \longrightarrow r = r_2$$

is

$$\sigma_r = \frac{p_2 r_2^2 - p_1 r_1^2}{\left(r_2^2 - r_1^2\right)} - \frac{\left(p_2 - p_1\right) r_1^2 r_2^2}{r^2\left(r_2^2 - r_1^2\right)} \qquad (4.9)$$

$$\sigma_\theta = \frac{p_2 r_2^2 - p_1 r_1^2}{\left(r_2^2 - r_1^2\right)} + \frac{\left(p_2 - p_1\right) r_1^2 r_2^2}{r^2\left(r_2^2 - r_1^2\right)} \qquad (4.10)$$

For an extremely large R2

$$\sigma_r = p_2\left(1 - \frac{r_1^2}{r^2}\right) + \frac{p_1 r_1^2}{r^2} \qquad \ldots.(4.11)$$

$$\sigma_\theta = p_2\left(1 + \frac{r_1^2}{r^2}\right) - \frac{p_1 r_1^2}{r^2} \qquad \ldots.(4.12)$$

For a point at a distance r from the center

$$K_1 = p_2\left(1 + \frac{r_1^2}{r^2}\right) = \sigma_h\left(1 + \frac{r_1^2}{r^2}\right)$$

$$\frac{r_1^2}{r^2}$$

$$K_2 = p_2\left(1 - \frac{r_1^2}{r^2}\right) = \sigma_h\left(1 - \frac{r_1^2}{r^2}\right)$$

are constants, therefore it can be written

$$\sigma_r = K_2 + K_3 p_1$$

$$\sigma_\theta = K_1 - K_3 p_1$$

for an increment in the internal pressure corresponds increments

$$\Delta\sigma_r = K_3 \Delta p_1 \qquad \Delta\sigma_\theta = - K_3 \Delta p_1$$

which when plotted in principal stress space indicates a stress path of the type of figure 4.30 , which does not correspond to any of the laboratory tests performed.

For small stress levels one can separate the contribution from the isotropic stress component and one from the deviator stress component. In conventional triaxial tests (figure 4.30) both are increasing, therefore the total strain will have contributions from both stress components. In active compression teste there is an increase in the

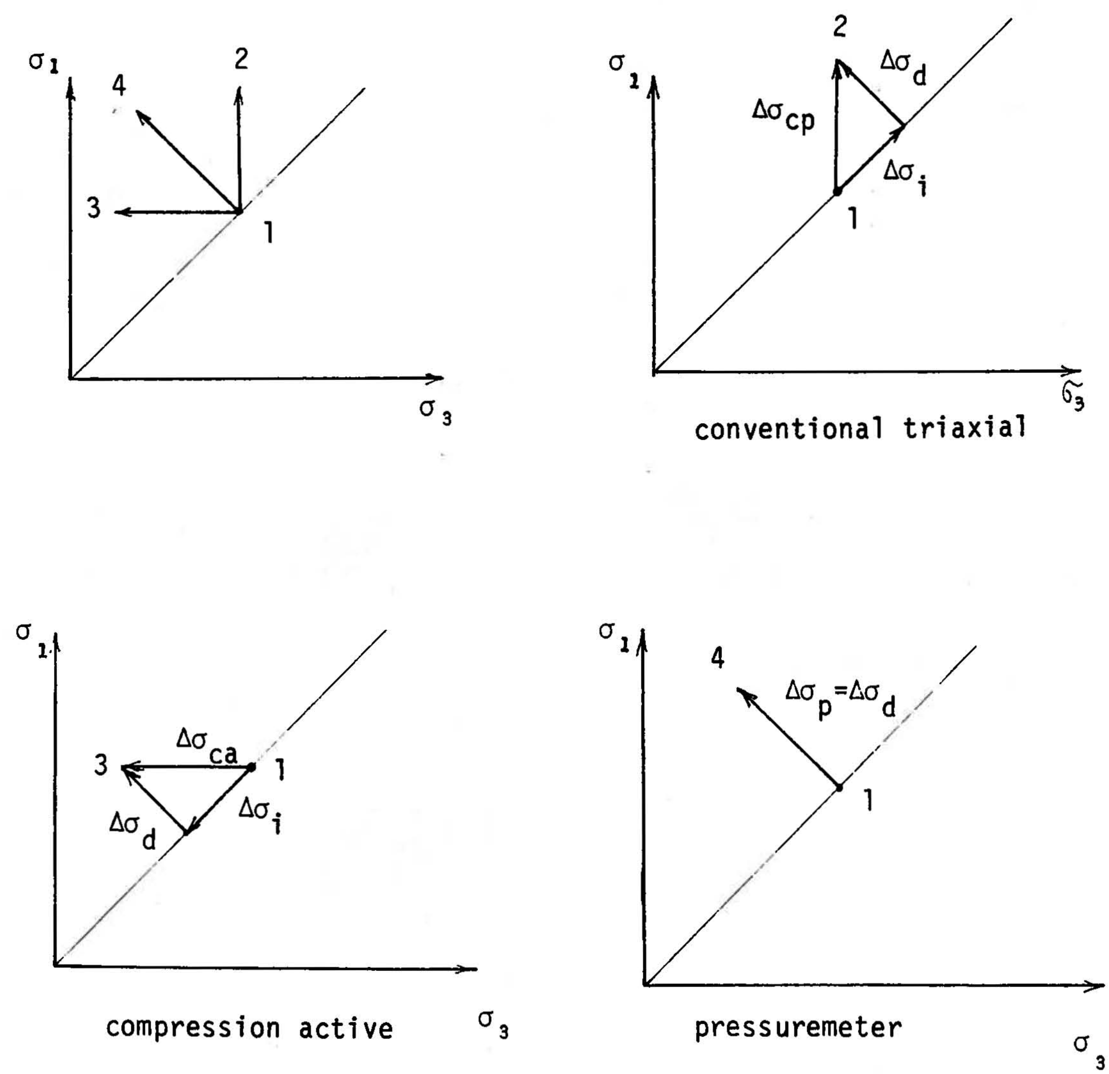

FIGURE 4.30 STRESS PATHS IN LABORATORY AND FIELD TESTS

deviator stress and a decrease in the isotropic stress component, therefore the vertical strain will represent the difference between them, which obviously will increase the modulus of deformation. During the pressuremeter test there is only the contribution from the deviator stress (figure 4.30). The modulus of deformation should then be greater than conventional triaxial and smaller than active compression.

Values of moduli of deformation from unloading reloading tests were not affected by the confining stress. For confining stresses of 1.89, 2.24 and 2.59 kg/cm2 they were found to be 1550.,1450. and 1680. kg/cm2 respectively.

To conclude this section , it is evident from the laboratory results the stress path dependency can not be neglected in the determination of moduli of deformation even for stiff soils, and an expressive non linearity of the stress strain relationship is present.

Tables 4.1 to 4.4 summarize the test results

TABLE 4.1

Hyperbolae parameters for triaxial passive compression tests

conf. stress (kg/cm2)	a	b
1.54	.229	.095
1.89	.106	.092
1.65	.206	.073
1.82	.118	.095
2.24	.148	.002
2.07	.137	.020
2.42	.113	.023
2.59	.079	.054
2.77	.173	.068
3.05	.090	.088
3.36	.074	.081

TABLE 4.2

Hyperbolae parameters for triaxial active compression tests

conf. stress (kg/cm2)	a	b
2.28	.041	.364
2.80	.037	.373
2.10	.093	.505
1.93	.122	.485
2.45	.046	.449

TABLE 4.3

Hyperbolae parameters for plane strain passive compression tests

conf. stress (kg/cm2)	a	b
1.75	.086	.088
2.10	.155	.163
2.45	.074	.072
1.93	.084	.081

TABLE 4.4

Hyperbolae parameters for plane strain active compression tests

conf. stress (kg/cm2)	a	b
1.73	.080	.248
2.21	.064	.229

4.3 Saskatchewan Sands

4.3.1 Sampling

As the bottom of the excavation is above the sand layer, a small excavation had to be made to allow the collection of some block samples. Sharp edged metal boxes were gently pushed in the ground by hand while the lower part was being carved. The samples were immediately wrapped in a polyethylene sheet and waxed. In the laboratory the metal boxes were opened up by removing the metal screws joining the sides. The samples were then covered with a thick coating of wax and stored in the moist room. At the time of testing the wax was removed and the blocks transported to a cold room with the temperature of -5 degrees Centigrade to be frozen. Due to the reduced degree of saturation the specimens were not successfully carved and most of them cracked during this operation. An alternate procedure consisted of carving the samples gently in a still unfrozen state and transporting them to the cold room. A small amount of water was then sprayed to provide a very thin outside crust of ice enabling the placement of the rubber membrane. The triaxial cell with the sample inside was removed from the cold room and immediately filled with water followed by the application of confining stress. Due to the very delicate nature of the sample it was not possible to carve specimens with the shape required by the plane strain apparatus. All the stress-strain relationships were obtained with the use of the triaxial equipment.

4.3.2 Characterization

Grain size analyses (figure 4.31) indicate the presence of 95% sand and 5% silt and clay. Most of the grains were under the medium-grained sand size range. The coefficient of uniformity of 2 resulting in a classification of soil type SP. Disturbed borehole samples taken from the lower part of the sand layer indicated the presence of some gravels. The average moisture content of the laboratory samples was 5% with a degree of saturation of 28%. Its unit weight was 1.87 g/cc and thespecific gravity of soils of was 2.67.

4.3.3 Triaxial tests

Due to the extreme difficulty in obtaining intact samples and because of some loss during laboratory preparation, a limited number of tests was performed. The scatter of the results was not as pronounced as the ones in the till and allowed the definition of the required properties with only 8 tests.

4.3.3.1 Passive compression

Four compression tests yielded an angle of shear resistance of 40.5 degrees. The strain at failure around 3% was observed. The fitting of an hyperbola was not satisfactory especially at stress levels approaching failure. The samples were consolidated isotropically to the

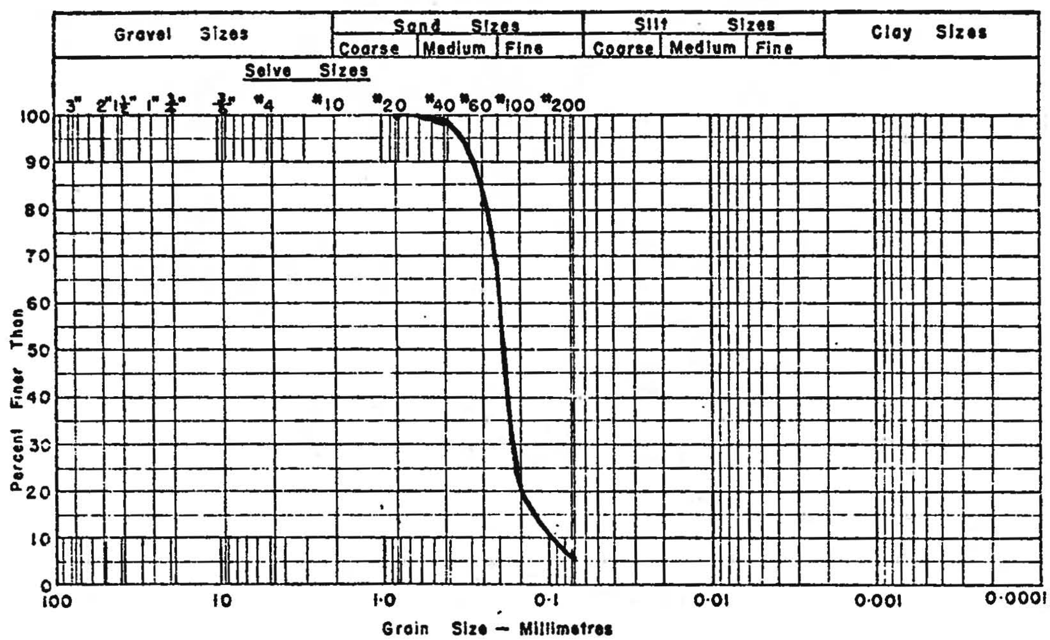

FIGURE 4.31 SASKATCHEWAN SANDS GRAIN SIZE DISTRIBUTION

overburden value. Figures 4.32 to 4.35 show the results of the tests in this phase.

4.3.3.2 Active extension

The samples were consolidated anisotropically with a ratio of 0.36 between the principal stresses, which was obtained using equation 4.1. An adaptation had to be done on the top cap to allow the application of tension in the rod. Strain to failure was observed at values of 0.9% which represents a major reduction from the compression passive results. Figures 4.36 to 4.38 shows the results of these tests.

4.3.3.3 Proportional active compression

Due to reduced number of elements submitted to this stress path only one test was performed in this phase. The sample was initially consolidated anisotropically followed by a simultaneous reduction in both principal stresses at a constant ratio and finally a reduction in the minor principal stress as in the compression active tests. Figure 4.39 illustrates the stress strain curve obtained.

4.3.4 Summary

A significant difference exists between the modulus of deformation in passive and active compression and extension tests. Although is it difficult to draw a parallel between the laboratory results, due to the fact that the passive

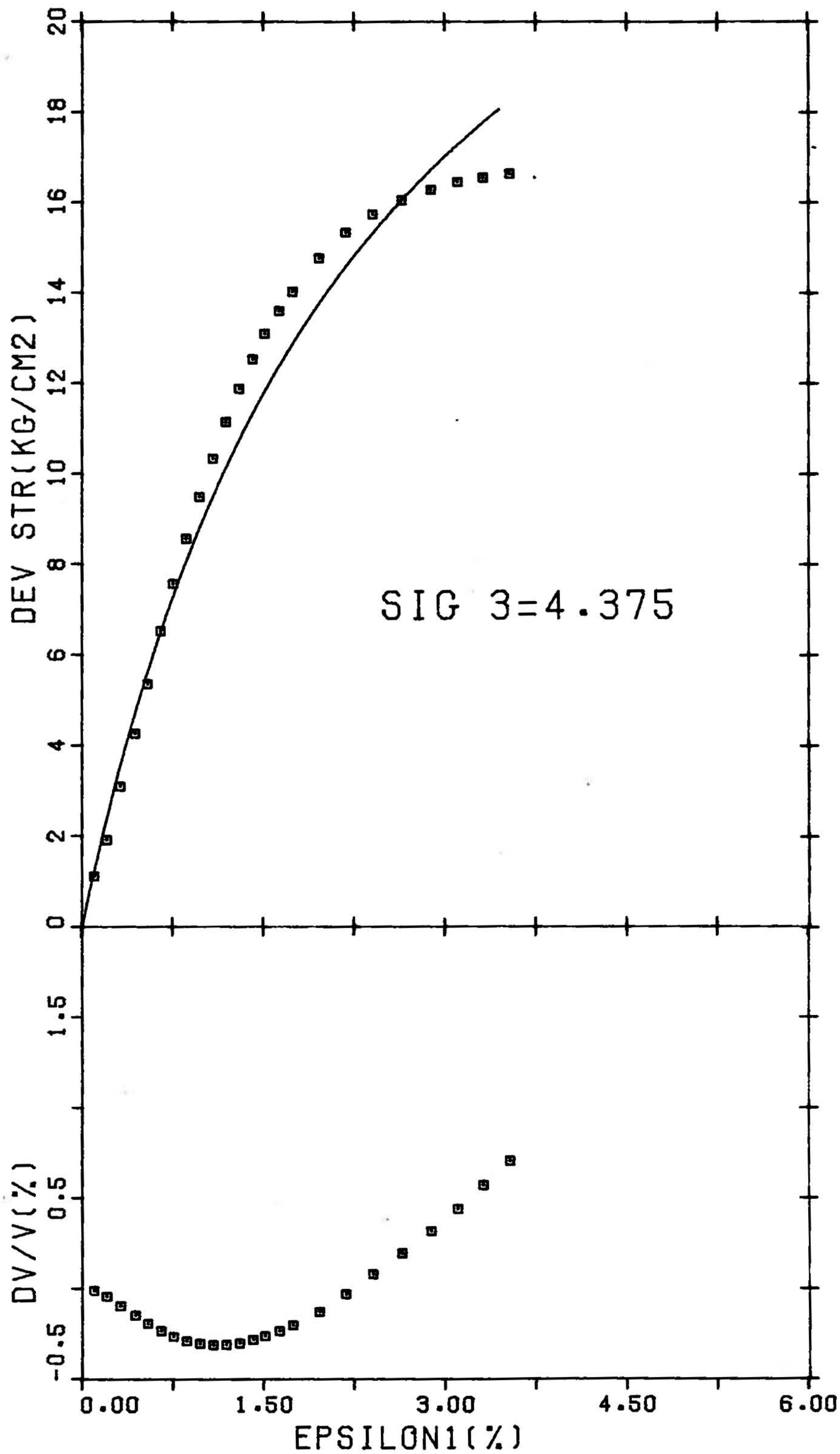

FIGURE 4.32 PASSIVE COMPRESSION TEST SASKATCHEWAN SANDS

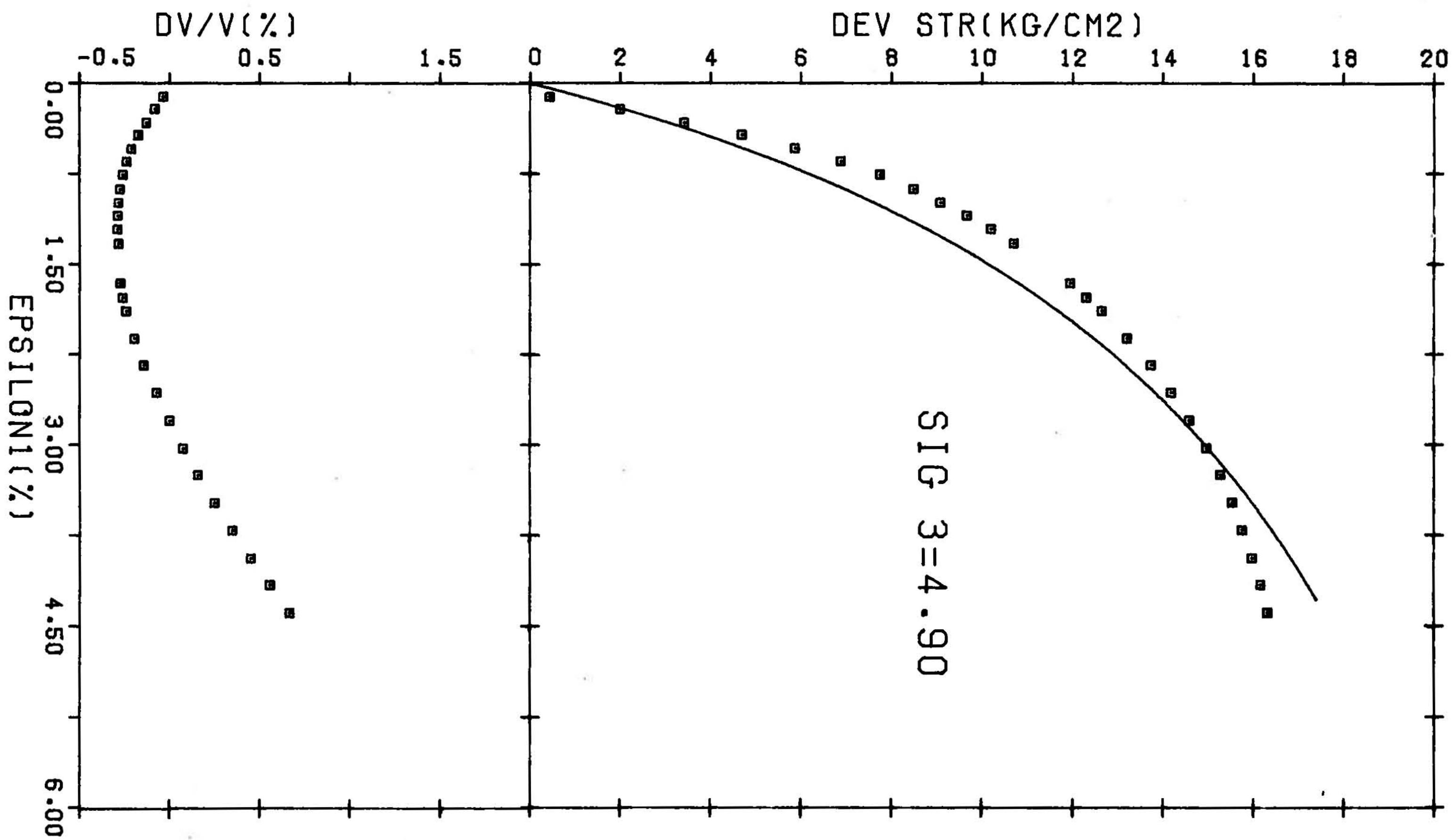

FIGURE 4.33 PASSIVE COMPRESSION TEST SASKATCHEWAN SANDS

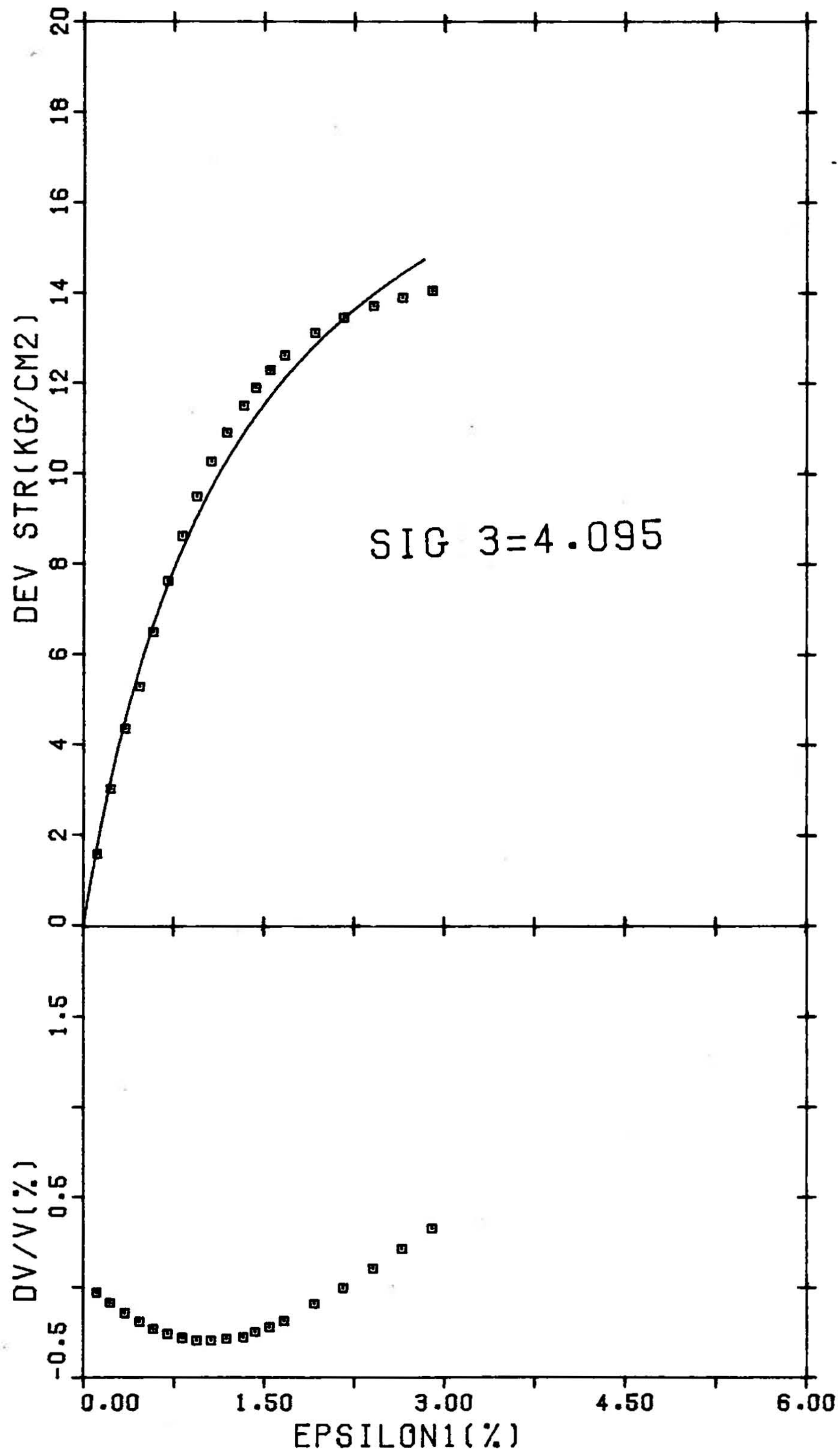

FIGURE 4.34 PASSIVE COMPRESSION TEST SASKATCHEWAN SANDS

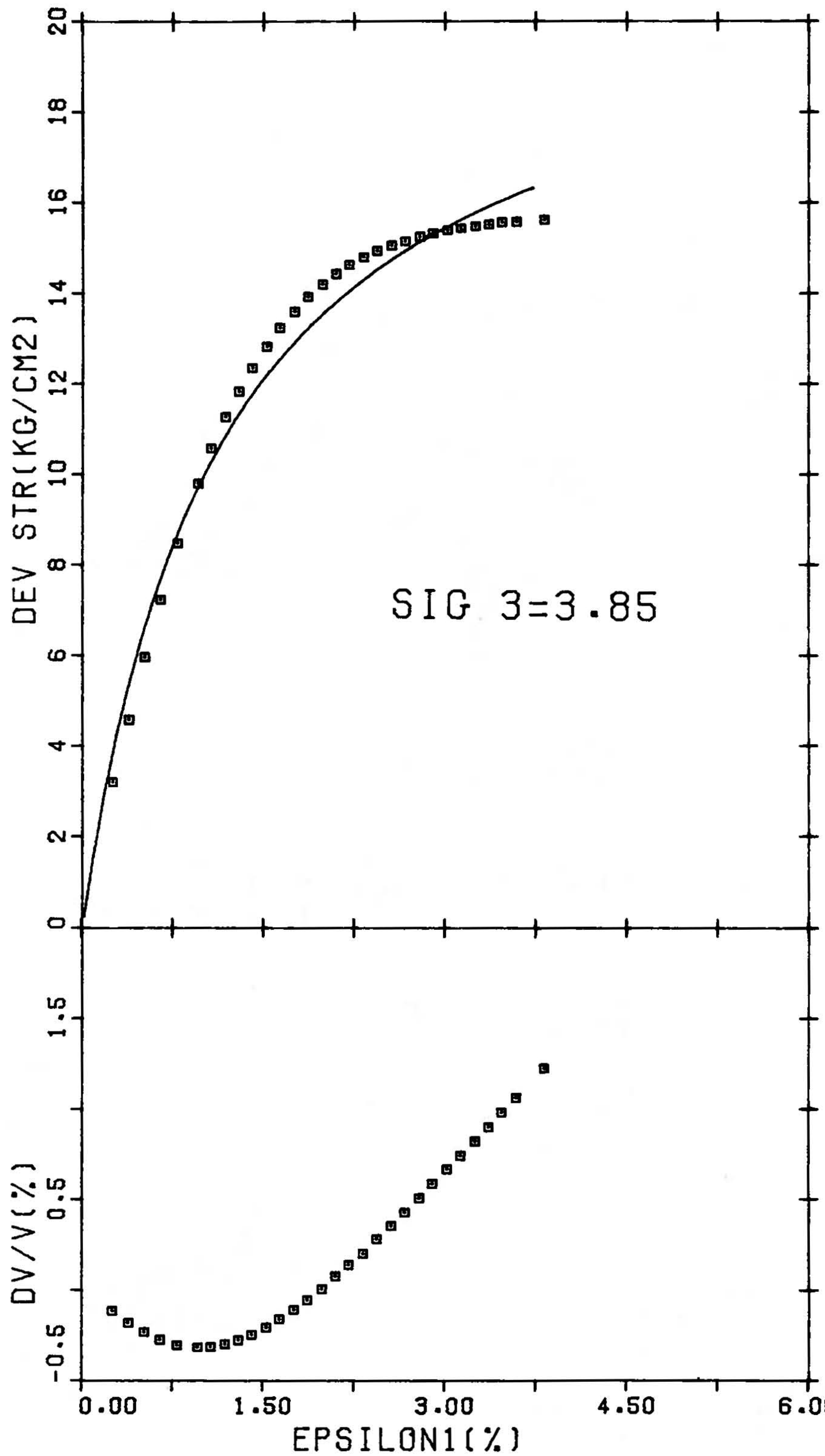

FIGURE 4.35 PASSIVE COMPRESSION TEST SASKATCHEWAN SANDS

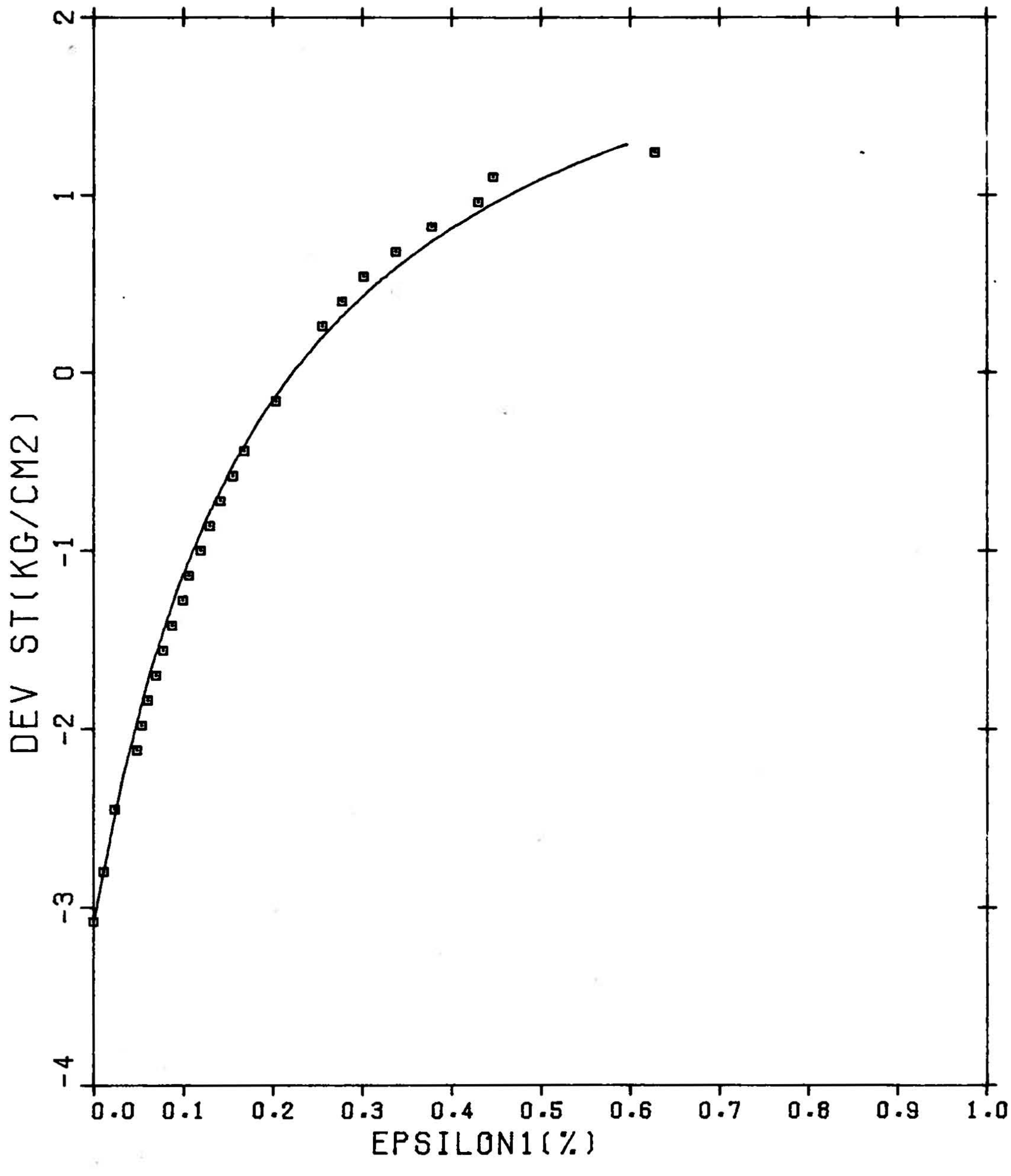

FIGURE 4.36 ACTIVE EXTENSION TEST SASKATCHEWAN SANDS

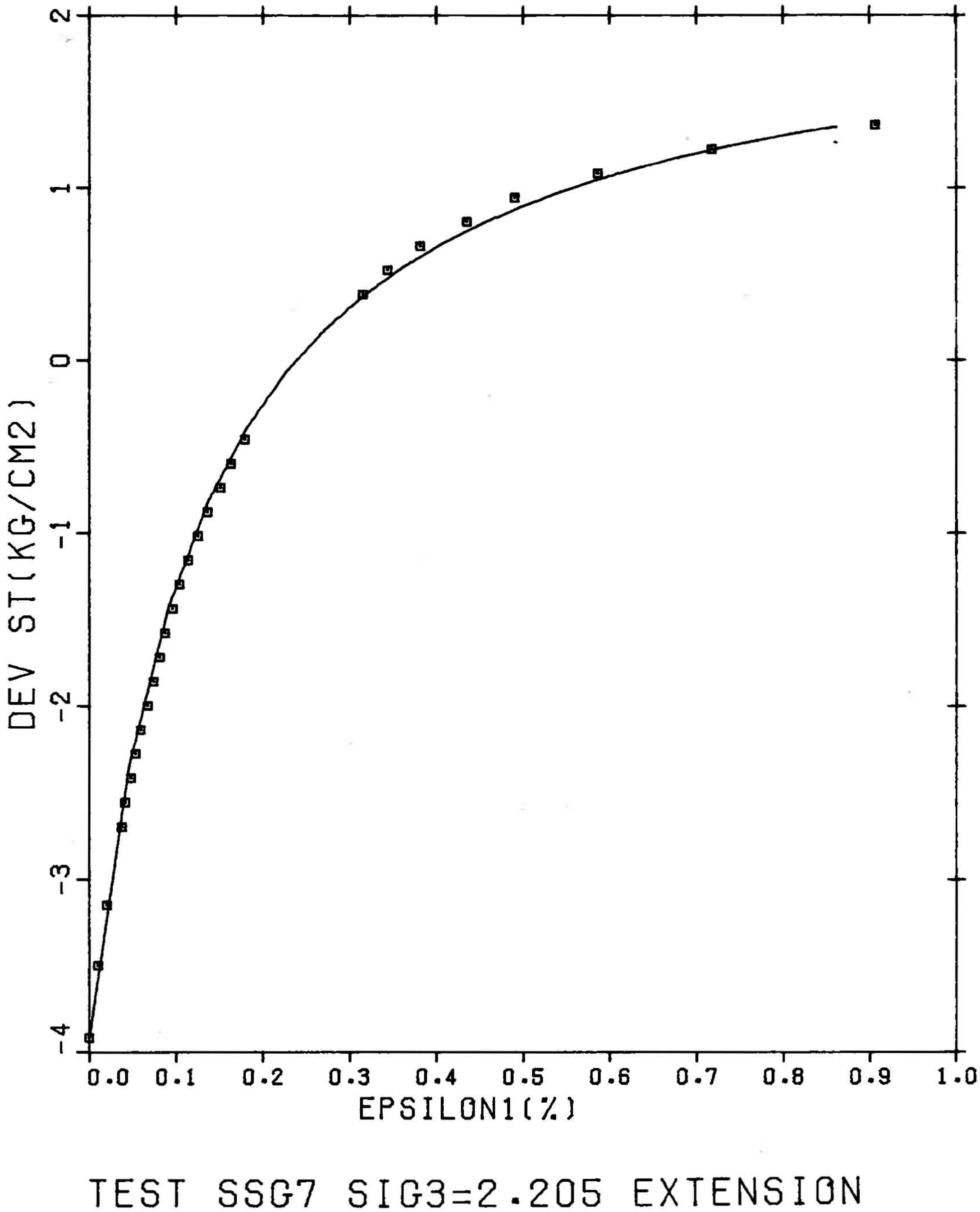

FIGURE 4.37 ACTIVE EXTENSION TEST SASKATCHEWAN SANDS

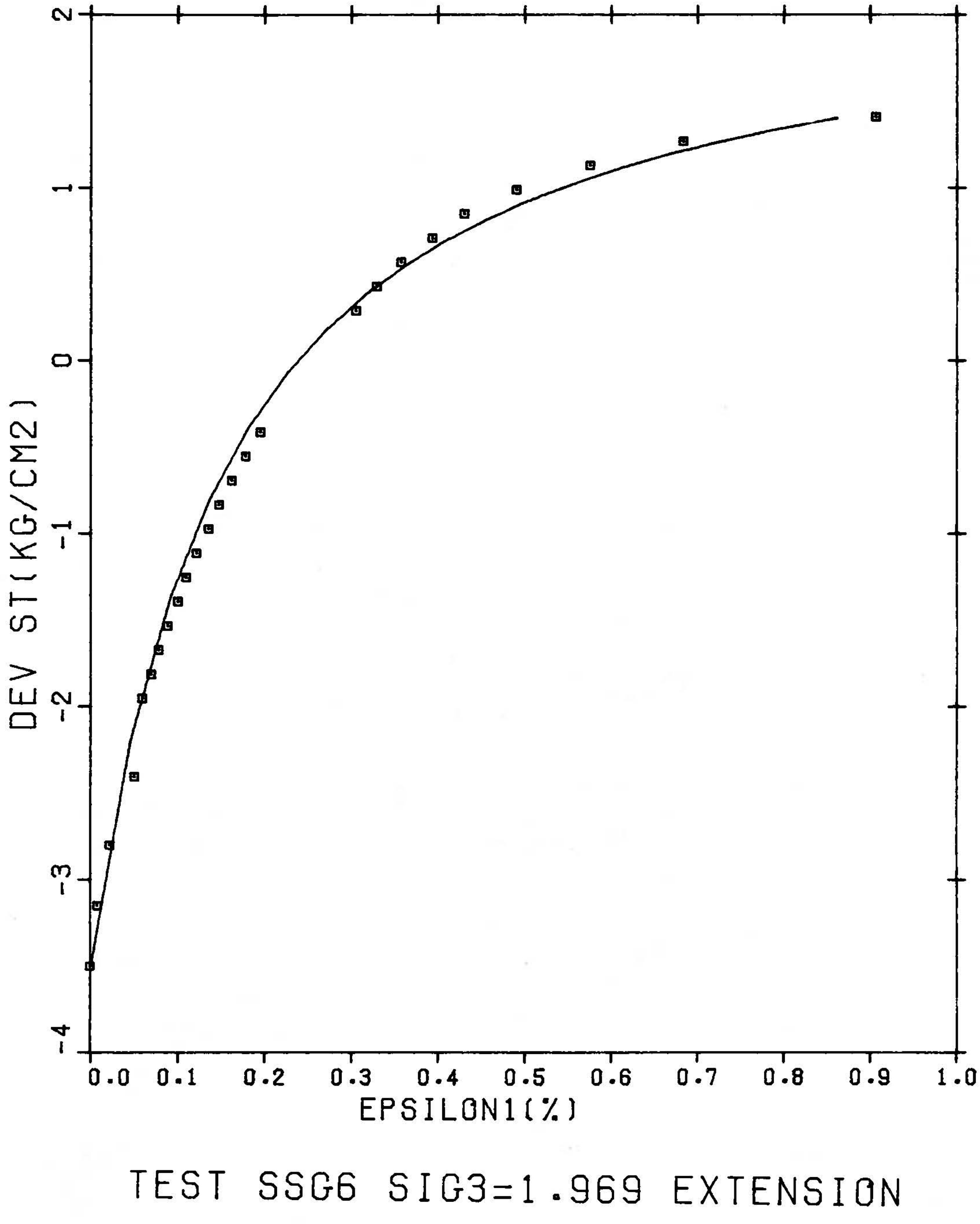

FIGURE 4.38 ACTIVE EXTENSION TEST SASKATCHEWAN SANDS

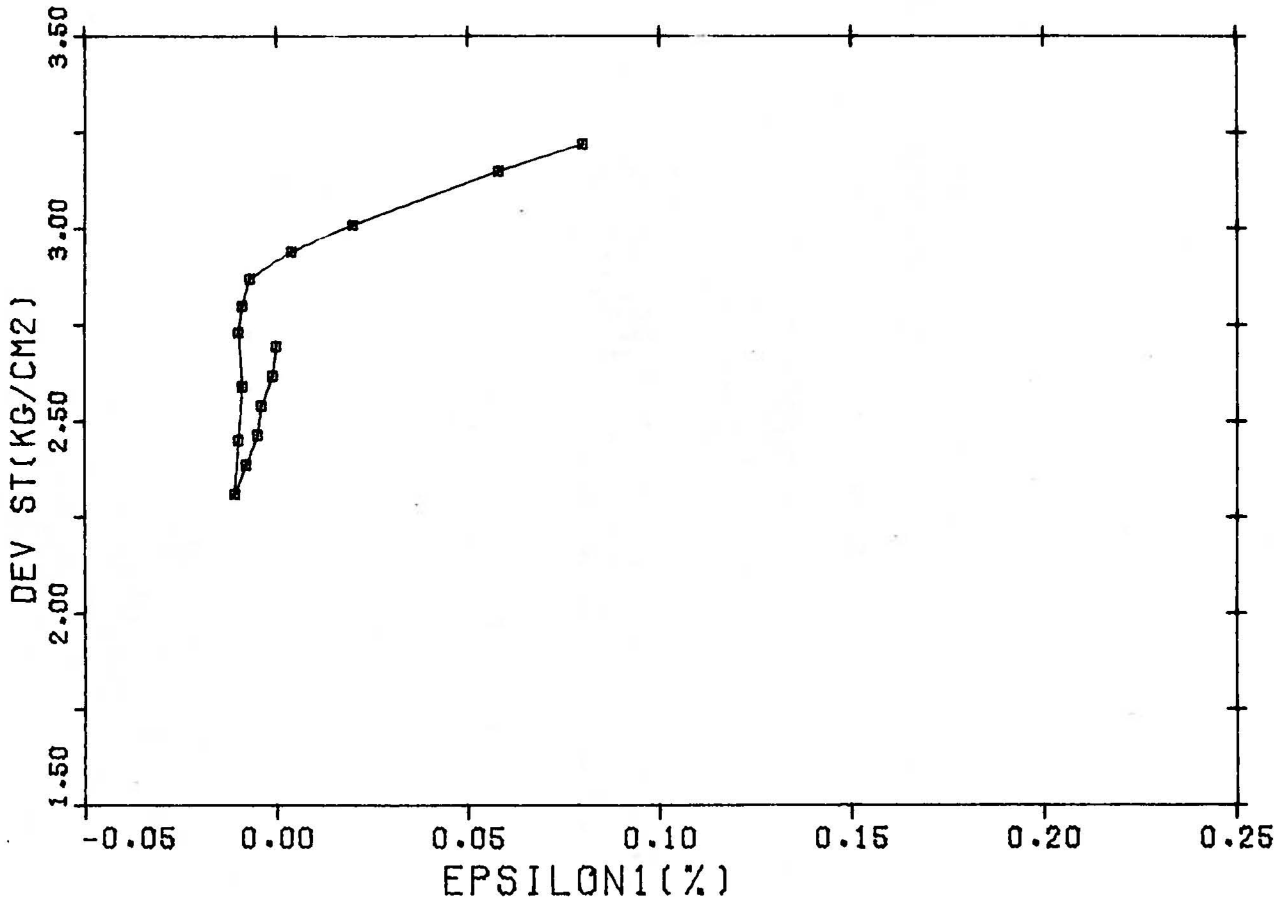

TEST SSG9 KO-ACTIVE SIGV= 4.9 SIGH= 2.21

FIGURE 4.39 PROPORTIONAL ACTIVE COMPRESSION SASKATCHWAN SANDS tests started with a ratio of 1 between the principal stresses and the extension tests started with 0.36, figure 4.40 the difference between the moduli of deformation. During a conventional triaxial test the sample is being loaded from the beginning of the test while in extension tests initially both isotropic and deviator stress components are reduced until the isotropic axes are reached, then the deviator component starts is increased. This condition stands for an expressive reduction in the prediction of deformation when compared with active extension results which predominantly occur at the bottom of the excavation.

The angle of shearing resistance remained the same for different stress paths, which was expected since this is a cohesionless soil.

A smaller strain to failure was observed for active extension tests indicating a much earlier mobilization of the shear strength compared to the results of the conventional triaxial test.

A complete evaluation of the influence of the stress path obtained here can only be appreciated by a comparison of the field measurements with the analysis supported by the stress strain representation observed here.

Due to the already expected limited movement around the excavation, the early portion of the stress strain curve should play a major role in this case history. The initial tangent modulus, either for sands or the Edmonton till,

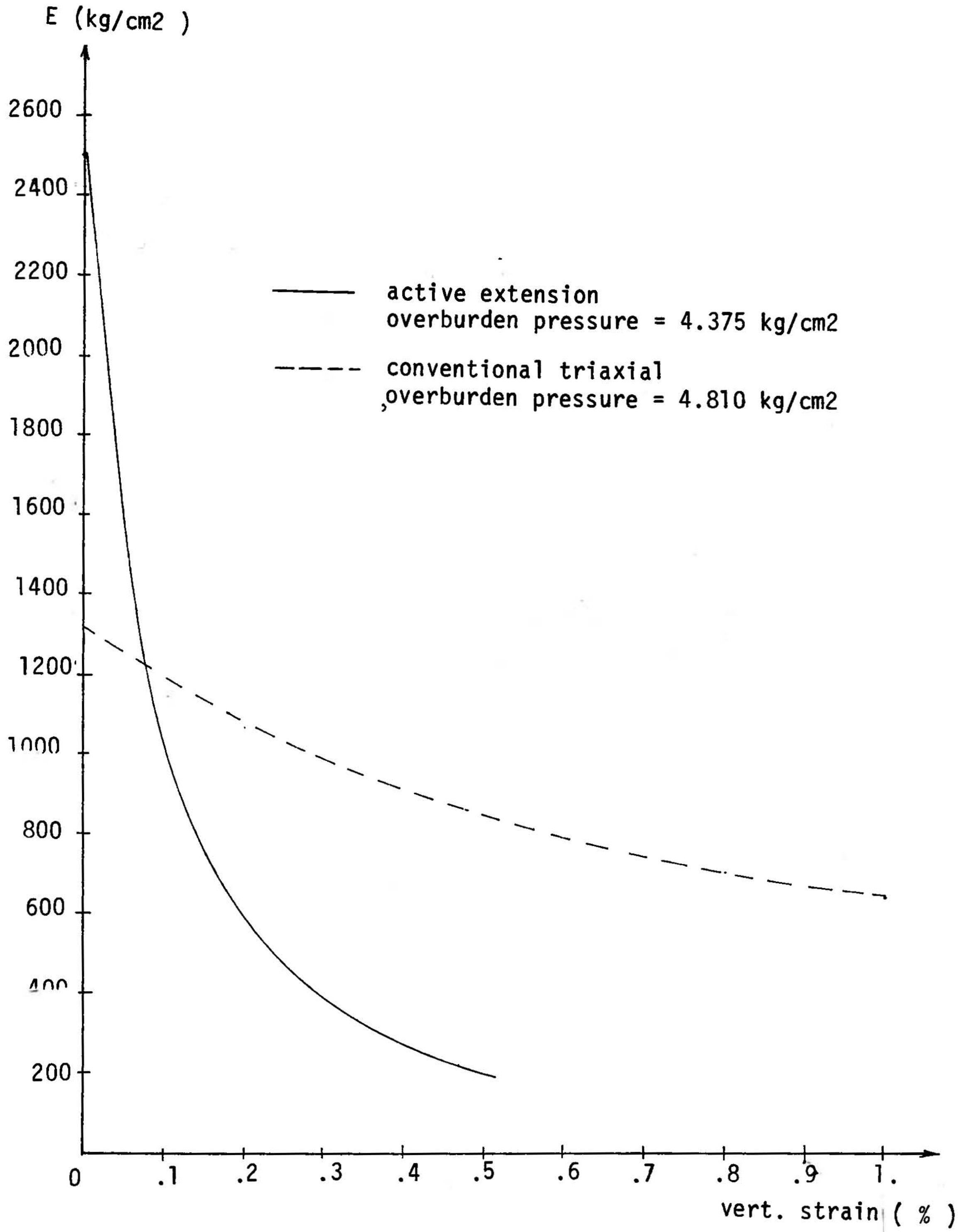

FIGURE 4.40 COMPARISON BETWEEN MODULUS OF DEFORMATION FROM PASSIVE COMPRESSION AND ACTIVE EXTENSION IN TRIAXIAL

being much higher when following the suggested stress path as compared to conventional tests, one should expect considerably less movement than analysis based on results from conventional triaxial tests. Expensive large plate loading tests or in situ shear may not represent field conditions if the stress path has such a dominant influence.

With respect to the lateral stress distribution, it seems the retaining structure can count on a much more significant contribution from the surrounding ground, therefore reducing the total load to be carried. Expensive large plate loading tests or in situ shear may not represent field conditions if the stress path has such a dominant influence.

5. CONSTITUTIVE MODEL

5.1 Introduction

The most usual type of analysis of stress and strains in Geotechnical Engineering consists of acquiring the stress-strain parameters from conventional triaxial tests where the deviator stress is increased up to failure, with the confining stress held constant. The continuum mechanics framework being pursued here so far consists of the use of the generalized Hooke's Law with the soil stress strain parameters obtained from laboratory tests under different stress paths. The stress paths followed in the laboratory aim to be representative of the field conditions and therefore the different behaviour exhibited by the soil under distinct stress paths should be depicted. Linked with this approach are the hypotheses associated with Hooke's Law. The most important of them is with respect to the principal axes of strain increments; principal axes of strain increment coincide with principal axes of stress increment which implies no volume change due to shear stress. Laboratory tests in cohesionless soil (Lade, 1972) exhibited coincidence of the axes of strain and stress increments at low level of stresses and coincidence of strain increments and total stresses at high level of stresses. It therefore can be concluded there is a predominancy of elastic strains at the early stages of the stress strain curve,with a gradual shift to a situation where the plastic strains become more important as failure is approached. In this chapter a constitutive model able to represent the behaviour of the soil for all stress levels and different stress paths for sands will have its application evaluated for the Edmonton till.

Ko and Scott (1967) and Frydman and Zeitlen (1969) separated the total strain into volumetric and shear strain components. The former is caused by the isotropic component of stress and the later by the deviatoric part. The total strain is determined by superposition. This approach proved to be rewarding whenever there was no slippage between the grains, which causes an irrecoverable deformation. Different stress paths can therefore be analysed using this procedure for situations involving unloading and reloading. During primary loading the grains slide one with respect to the other causing plastic strains. Perfect plastic idealization however, has been proved to be unsuitable for frictional materials (Drucker, 1952 ,1961 and 1964 and Drucker, Gibson and Henkel, 1957). The Cam Clay model (Roscoe, Schofield and Thurairajah 1963, Roscoe, Schofield and Wroth 1958 and Roscoe and Burland 1968) calculates separately elastic and plastic strains. The Cam Clay model predicts accurately results in normally consolidated clays for stress paths which do not include expansion (Roscoe and Poorooshasb 1963). During the development of Cam clay stress strain theory it is assumed a unique relationship between the moisture content and the stress parameters p (I1/3) and q

(SIG1-SIG3) which therefore excludes situations involving expansion which is the case of the Edmonton till (Chapter 4).

An elastoplastic model which accommodates volumetric expansion in shear has been developed by Lade(1972) to study loose and dense sands. This model has been substantiated by accurate predictions of strains under different stress paths (Lade and Duncan 1976). A further refinement in the model improved the results for strain softening cohesionless material (Lade 1975) and extended the study to normally consolidated clays (Lade and Musante 1976).

In this chapter an evaluation of the applicability of Lade's model in its initial form (1972) for the Edmonton till will be carried out. The required parameters will be obtained from conventional triaxial tests described in chapter 4. Based on them, the strains observed in triaxial active compression tests also described in chapter 4 will be compared with the ones predicted by the model. If this approach proves to be successful, there are two major advantages when compared to a stress path simulation. First, the fact that it considers both elastic and plastic strains with a predominancy of the elastic one at low level of stress and the plastic one close to failure permits a change of the strain increment direction with the same constitutive model. Second, it dismisses the necessity of performing tests with different stress paths to simulate field conditions.

5.2 Lade's stress strain theory

The total strain increment is divided into elastic and plastic components, each one being treated separately.

The elastic strain is calculated from Hooke's law using the unloading reloading modulus as suggested by Duncan and Chang (1970) with the use of the expression :

$$E_{ur} = K_{ur}\ pa\left(\frac{\sigma_3}{pa}\right)^n \qquad \text{.....(5.1)}$$

where

- K_{ur} and n are material constants
- pa is the atmospheric pressure
- σ_3 is the confining stress

For the plastic strain increment the measure of the stress level is defined as a function of the first and third invariants as :

$$f = \frac{I_1^3}{I_3} \qquad \text{.....(5.2)}$$

The yield surfaces are represented by :

$$F = I_1^3 - K\,I_3 \qquad \text{.....(5.3)}$$

where $\underline{K}$ is a work-hardening parameter which represents the maximum stress level ever experienced by the soil. Changes of stresses lying inside the yield surface will cause only elastic strains. If the change in stress crosses the yield surface the material will deform plastically and elastically and the yield surface will expand.

The plastic potential function incorporated in the theory is expressed as :

$$g = I_1^3 - K_2\,I_3 \qquad \text{.....(5.4)}$$

where K2 is a constant for any given value of $\underline{f}$. The use of an associated flow rule leads to values of volumetric expansion much higher than observed in laboratory experiments (Drucker 1964, Poorooshasb, Holubec and Sherborne 1966, Ko and Scott 1967 and Lade and Duncan 1973) , indicating the normality condition was not satisfied.

The plastic strain increment is derived from a non associated flow rule

$$\Delta \epsilon_{ij}^{p} = \Delta\lambda \frac{\partial g}{\partial \sigma_{ij}} \qquad .....(5.5)$$

where $\Delta\lambda$ is a factor of proportionality. It must be noted that g contains a parameter K2 (eq. 5.4) which is a function of the stress level, but the partial derivative is to indicate the value of K2 is to be considered constant. The use of equations 5.4 and 5.5 expresses the plastic strain increments as :

$$\Delta\epsilon_{x}^{p} = \Delta\lambda K_2 \left[\frac{3}{K_2} I_1^2 - \sigma_y \sigma_z + \tau_{yz}^2 \right]$$

$$\Delta\epsilon_{y}^{p} = \Delta\lambda K_2 \left[\frac{3}{K_2} I_1^2 - \sigma_x \sigma_z + \tau_{xz}^2 \right]$$

$$\Delta\epsilon_{z}^{p} = \Delta\lambda K_2 \left[\frac{3}{K_2} I_1^2 - \sigma_x \sigma_y + \tau_{xy}^2 \right]$$

$$\Delta\epsilon_{zx}^{p} = \left[\sigma_y \tau_{zx} - \tau_{xy} \tau_{yz} \right] \Delta\lambda K_2$$

$$\Delta\epsilon_{yz}^{p} = \left[\sigma_x \tau_{yz} - \tau_{xy} \tau_{zx} \right] \Delta\lambda K_2$$

$$\Delta\epsilon^p_{xy} = \left[\sigma_z \tau_{xy} - \tau_{yz}\tau_{zx}\right] \Delta\lambda \, K_2 \qquad \text{.....(5.6)}$$

K2 is determined by using the ratio :

$$-\nu^p = \frac{\Delta\epsilon^p_3}{\Delta\epsilon^p_1}$$

which, solving for K2 , yields

$$K_2 = \frac{3 I_1^2 \left(1 + \nu^p\right)}{\sigma_3\left(\sigma_1 + \nu^p \sigma_3\right)} \qquad \text{.....(5.7)}$$

Using equation 5.7 from triaxial compression tests Lade (1975) encountered a linear relationship between K2 and the stress level of the form :

$$K_2 = A_1 f + A_2 \qquad \text{.....(5.8)}$$

where A1 and A2 are material constants. The plastic work increment is calculated from:

$$dW^p = \left\{\sigma_{ij}\right\}^T \left\{d\epsilon^p_{ij}\right\} \qquad .....(5.9)$$

or

$$\Delta W^p = \left\{\sigma_{ij}\right\}^T \Delta\lambda \left\{\frac{\partial g}{\partial \sigma_{ij}}\right\} \qquad ....(5.10)$$

where

$$\left\{\frac{\partial g}{\partial \sigma_{ij}}\right\} = \frac{\partial g}{\partial I_1}\left\{\frac{\partial I_1}{\partial \sigma_{ij}}\right\} + \frac{\partial g}{\partial I_3}\left\{\frac{\partial I_3}{\partial \sigma_{ij}}\right\}$$

$$\frac{\partial g}{\partial I_1} = 3 I_1^2 \qquad\qquad \frac{\partial g}{\partial I_3} = - K_2$$

which, substituting into 5.10 , gives

$$dW_p = \Delta\lambda \; 3[I_1^3 - K_2 I_3]$$

$$\Delta\lambda = \frac{dW_p}{3g} \qquad \text{....(5.11)}$$

where dWp is the increment in plastic work due to an increase in stress level df .

Results from conventional laboratory testing indicated the relationship between the plastic work

$$W_p = \int \{\sigma_{ij}\}^T \{d\epsilon_{ij}^p\}$$

can be approximated by an hyperbola.

$$f - f_t = \frac{W_p}{a + b W_p}$$

....(5.12)

where

- ft is a value of the stress level up to which plastic work does not occur; the strains up to this point are purely of elastic nature. This was called the threshold stress level.
- a and b are the parameters which define the hyperbola.

The inverse of a represents the initial slope of the curve Wp versus f and its variation is expressed as :

$$a = M\ pa \left(\frac{\sigma_3}{pa} \right)^{l} \qquad \text{....(5.13)}$$

where

- M and l are the material constants
- pa is the atmospheric pressure
- σ_3 is the confining stress.

The inverse of b represents the value f-ft approaches at large magnitudes of the plastic work. From the defferential of 5.12

$$\Delta W_p = \frac{a \Delta f}{\left(1 - b(f - f_t)\right)^2} \qquad \text{....(5.14)}$$

where

- f is the average value of the stress level during the increment
- df is the increment on the value of the stress value . If df<0 , only elastic strains will occur.

5.3 Determination of the elasto plastic parameters

For the elastic portion of the strain, unloading reloading tests described in chapter 4 were performed. They have indicated a very narrow variation of the modulus of deformation (Eur) for the range of confining stresses between 1.54 kg/cm2 and 2.60 kg/cm2. A constant value of 1500 kg/cm2 for Eur was consequentely assumed.

Calculation of the total plastic work during the determination of the parameters for the plastic portion, require information with respect to the lateral strain. Tests 18-14 , 18-15 and 18-17 (chapter 4) were selected to determine the plastic parameters. Values of K2 obtained from the expression 5.7, were plotted against the stress level *f* (figure 5.1) indicating the values 0.485 for A1 and 13.63 for A2 (equation 5.8). Figure 5.2 illustrates the relationship between the total plastic work and the stress level. The threshold stress level *ft* (equation 5.12) value encountered was very close to 27 which corresponds to points on the hydrostatic axes. This indicates the existence of plastic strains at the early portion of the stress strain curve. All the curves should be asymptotic to a single value, regardless of the curve to be fitted, which did not

Measurement of Soil Properties Specialty Conference ASCE ,1975, North Carolina State University Raleigh, pp.181-230.

Wu ,T.H. and Berman ,S. "Earth pressure measurements in open cut: contract D-8 ,Chicago Subway" Geotechnique vol.3, 1953, pp.248-258

Yamada ,Y. and Yoshimura ,N. "Plastic stress strain matrix and its application for the solution of elastic plastic problems by the finite element method " International Journal of Mech. Sci. vol.10 , 1968 , pp.343-354

Zienkiewicz ,C.C. ,Valliappan ,S. and King ,I.P. " Elastoplastic solution of Engineering problems "initial stress" ,finite element approach" International International Journal of Numerical Methods in Engineering" vol.1, 1969 , pp.75-100

APPENDIX A. COMPUTER PROGRAM

A.1 Introduction

This computer program was developed to analyse stress changes and displacements caused by excavations in soil or rock, with the aid of the finite element method.

The analysis is divided in a number of distinct phases which consist of excavation of different layers and installation of permanent struts. Each phase is subdivided in increments to allow updating of the elastic parameters in each element. The program at the beginning of each phase calculates the new load vector which will be applied. It performs the calculations for different types of stress strain relationships according to the stress path which has been prescribed for the element.

A.2 Organization of the program

The main program obtains the initial nodal and element stresses prior to the excavation by calling the subroutine INIT. By means of the the subroutine NLOAD the elements excavated are assigned extremely low values of the modulus of deformation. The elements representing the strut level to be installed are assigned the correspondent values of the elastic parameters (concrete or steel) and the nodal loads caused by the excavation in this phase are determined. At this point the load is divided in 4 increments. The number of increments can be easily changed by altering lines 81 to

84 if required by the user. The subroutine DETE is then called to calculate the value of the modulus of deformation. The program has the capability of analysing 6 different types of stress strain relationship which are described in detail in chapter 6. A sub routine CST is called to perform the finite element analysis using constant strain triangles to obtain the stress change due to the increment just performed. An option to plot the displacement is available at the end of the program.

A.3 Input data

1. GEOMETRY

   a. output options..................................(4I5)

      1) IPRINT If equals to 1 it prints all the geometric information at the begining of each phase for every increment

      2) NIPRINT If equals to 1 it prints the nodal load for each phase of construction

      3) IPLOT If equals to 1 it generates a plot with the displacements of some selected nodes.

      4) NIPRIE If equals to 1 it prints the modulus of deformation of all the elements at the begining of each phase for every increment.

   b. title..(20A4)

   c. size of the problem............................(3I6)

1) NUMNP number of nodal points

2) NUMEL number of elements

3) NUMAT number of materials

d. node cards........................(2I6,4F12.0,I5)

1) N node number

2) KODE(N) two digit number indicating whether a displacement or a force is applied at the node

a) 00 x force y force

b) 11 x displacement y displacement

c) 10 x displacement y force

d) 01 x force y displacement

3) X xcoordinate

4) Y ycoordinate

5) U x force or displacement at node N

6) V y force or displacement at node N

7) KODE1(N) it defines the material type to determine initial nodal stress. If KODE1(N)=4 the initial stresses are zero.

Obs. Nodal points must be in numerical order.If nodes are omitted the program generates coordinates for the intermediate points linearly displaced between the two points. For the generated nodes the program assigns KODE=0 , U and V=0 and KODE1 equals to the previous node

e. element cards..........................(5I6,F6.0)

1) M element number

2) NP(I,M) nodal points at the three corners of the element in counterclockwise order

3) MAT(M) element material number

4) TH(M) thickness of the element. If not defined the program assigns a unit thickness.

Obs. Element cards must be in numerical order. If element numbers are omitted the program generates element data in modules of two elements from the previous two.

2. PLOTTING DATA

a. general information..........................(2I5)

1) NNTP number of nodes to be plotted

2) NPH total number of phases

b. nodes.......................................(10I5)

1) NTP(I) node number which displacements will be plotted

c. title of the plotting (20A4)

1) TITLE(I)

a) col 1 to 48 headline for the plotting

b) column 49 to 64 abscissa label

c) column 65 to 80 ordinate label

d. contour.......................................(I5)

1) NNG number of nodes which will form the contour to define the excavation, retaining structure,

boundaries and subsoil.A line will be drawn joining all the NNG points without interruption.

e. contour definition..........................(10I5)

1) NTP(I) nodes defining the contour.If it is not required to use the plotting facility 5 blank lines have to be supplied to inform nothing is to be plotted.

3. MATERIAL PROPERTIES

This program was developed for 10 different materials to suit the needs of various analyses of the Rapid Transit in Edmonton. The nonlinear elastic stress strain relationship is fitted to a hyperbolae :

SIG1 - SIG3 = EPS1/(A+B*EPS1)

where

SIG1 and SIG3 are principal stresses

EPS1 is the major principal strain

A and B are the material parameters required.

a. Material number 1

This material corresponds to a stress path of the type compression active in conventional triaxial equipment. Three stress strain curves are to be supplied.

1) MM number 1..................................(I5)

2) a) PR(1) Poisson ratio

b) KO(1) at rest earth pressure coefficient....
(2F10.5)

3) Three lines , each one containing :

a) SIGC(1,J) initial confining stress

b) AA(1,J) Hyperbolae parameter

c) BB(1,J) Hyperbolae parameter........(3F10.6)

b. Material number 2

This material corresponds to a stress path of the type extension active in conventional triaxial equipment. Three stress strain curves are to be supplied.

1) MM number 2..................................(I5)

2) a) PR(2) Poisson ratio

b) KO(2) at rest earth pressure coefficient....
2F10.5

3) Three lines , each one containing :

a) SIGC(2,J) confining stress

b) AA(2,J) hyperbolae parameter

c) BB(2,J) hyperbolae parameter........(3F10.6)

c. Material number 3

This material corresponds to a stress path of proportional loading-compresion active test in triaxial equipment. One stress strain curve is to be supplied. For the proportional loading part linear elasticity is used and for the compression active part a hyperbolic relationship.

1) MM number 3................................(I5)

2) a) E(3) Modulus of deformation for the proportional loading.

b) AA(3,1) Hyperbolae parameter

c) BB(3,1) Hyperbolae definition.......(3F10.6)

d. Material number 4

This material behaves linearly elastic. It was used for the retaining structure.

1) MM number 4................................(I5)

2) a) PR(4) Poisson ratio

b) K0(4) at rest earth pressure coefficient.... (2F10.5)

3) E(4) modulus of deformation.............(F10.6)

e. Material number 5

This material corresponds to a stress path of the type compression active in plane strain apparatus. Two stress strain curves are to be supplied.

1) MM number 5................................(I5)

2) a) PR(5) Poisson ratio

b) K0(5) at rest earth pressure coefficient.... 2F10.5

3) Two lines each one containing

a) SIGC(5,1) initial confining stress

b) AA(5,J) Hyperbolae parameter

c) BB(5,J) Hyperbolae parameter........(3F10.6)

f. Material number 6

Similar to material number 4

g. Material number 7

This material corresponds to a stress path of the type compression passive in conventional triaxial equipment. Three stress strain curves are to be supplied.

1) MM number 7...................................(I5)

2) a) PR(7) Poisson ratio

b) KO(7) at rest earth pressure coefficient....

(2F10.5)

3) Three lines each one containing

a) SIGC(7,J) confining stress

b) AA(7,J) hyperbolae definition

c) BB(7,J) hyperbolae definition.......(3F10.6)

h. Material number 8

Similar to material number 4. It was used to define the properties of the material after it has been excavated

i. Material number 9

Similar to material number 7 with only one stress strain curve definition.

j. Material number 10

Similar to material number 4. It was used to define the different material which was used for grouting the struts and the vertical wall.

4. INITIAL STRESS

These data will be used by subroutine INIT. If the material definition is of the type 4 the initial element stress is set to zero.

a. Gama specific weight

b. ZSFC ordinate of the ground surface.........(2F10.3)

5. DESCRIPTION OF THE PHASES OF CONSTRUCTION

This set of data is required by subroutine NLOAD. The elements which will be excavated and the omes which will be concreted or grouted and the nodes which will be loaded have to be specified. The nodal load is determined from the elements to be excavated adjacent to the node.

a. 1) NPHASE phase number ,if zero it indicates the final phase was defined in the previous call to NLOAD.

   2) NYL number of nodes vertically loaded.

   3) NXL number of nodes horizontally loaded....(3I5)

b. nodal load definition

   1) vertical load definition NYL sets of two lines

      a) NELI number of elements excavated adjacent to this node

      b) NNYL(I) node number..................(2I5)

      c) IEL(J),J=1,NELI elements excavated number, adjacent to NNYL(I)................(10I5)

   2) horizontal load definition NXL sets of two lines similar to the vertical load definition.

c. load transfer

The program allows for the transfer of

horizontal loads from a node to two others by beam effect. This feature accomodate the existence of sheet piles transferring their loads to points of contact with the structure.(figure A.1) when the deformation of the wall is required.

1) NLD number of nodes which will transfer the horizontal. If NLD equals to zero no more load transfer input are required.

2) a) NA upper node carryimg the transferred load.

   b) NB lower node........................(2I5)

3) NU number of the node which will have its load transferred to NA and NB. NLD lines to be supplied...................................(I5)

d. element material redefinition

1) NELCA number of elements excavated..........(I5)

2) INEL element excavated. After this phase this element will be of type number 8. NELCA lines to be supplied.................................(I5)

3) NELCC number of elements changed to material number 8. After this phase this element will be of type number 8...........................(I5)

4) INEL element number. NELCC lines to be supplied. (I5)

5) NELCG number of elements changed to material number 10. If this material is under tension in any phase it will have a small value assigned to the modulus of defcrmation.................(I5)

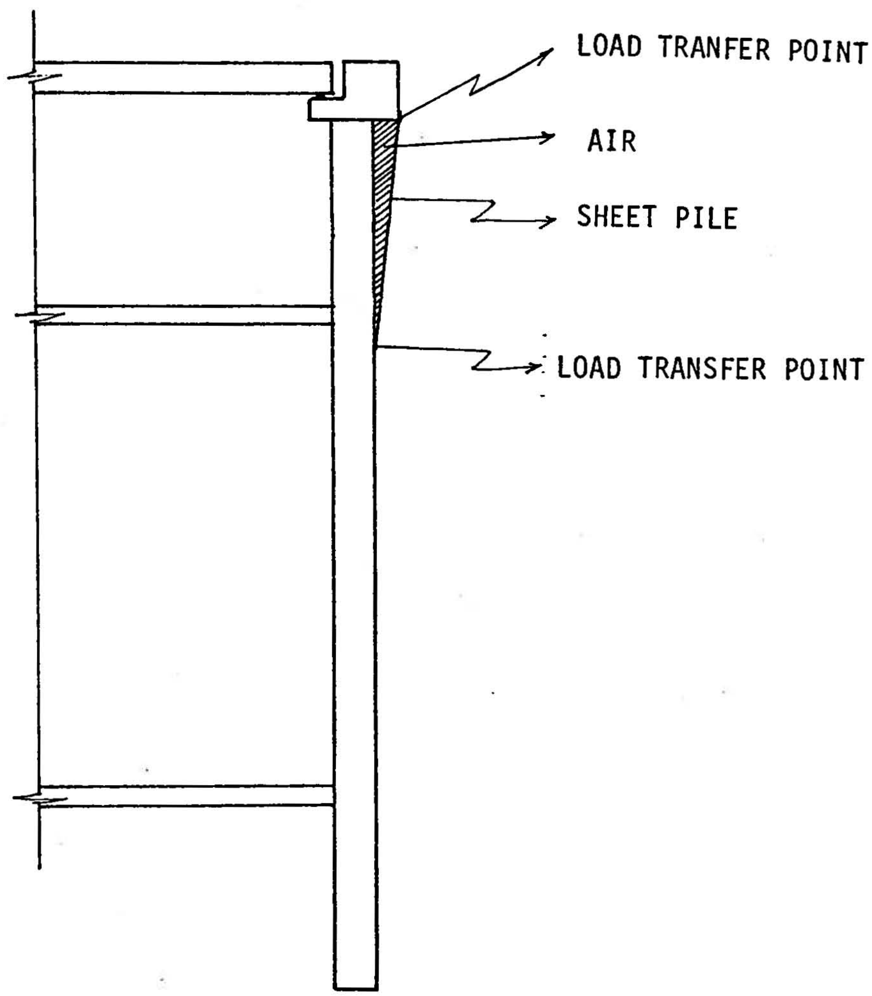

FIGURE A.1 LOAD TRANFER

6) INEL element number. NELCG lines to be supplied. (I5)

e. nodal stress redefinition

This set of data defines the nodes which will have the stresses zeroed. They represent the nodes which are inside elements changed into concrete , grout or have been excavated.

1) NNC number of nodes........................(I5)

2) J node number. NNC lines to be supplied.....(I5)

Sample Program

An input sample is listed below. For the load application figure A.2 illustrates the procedure.

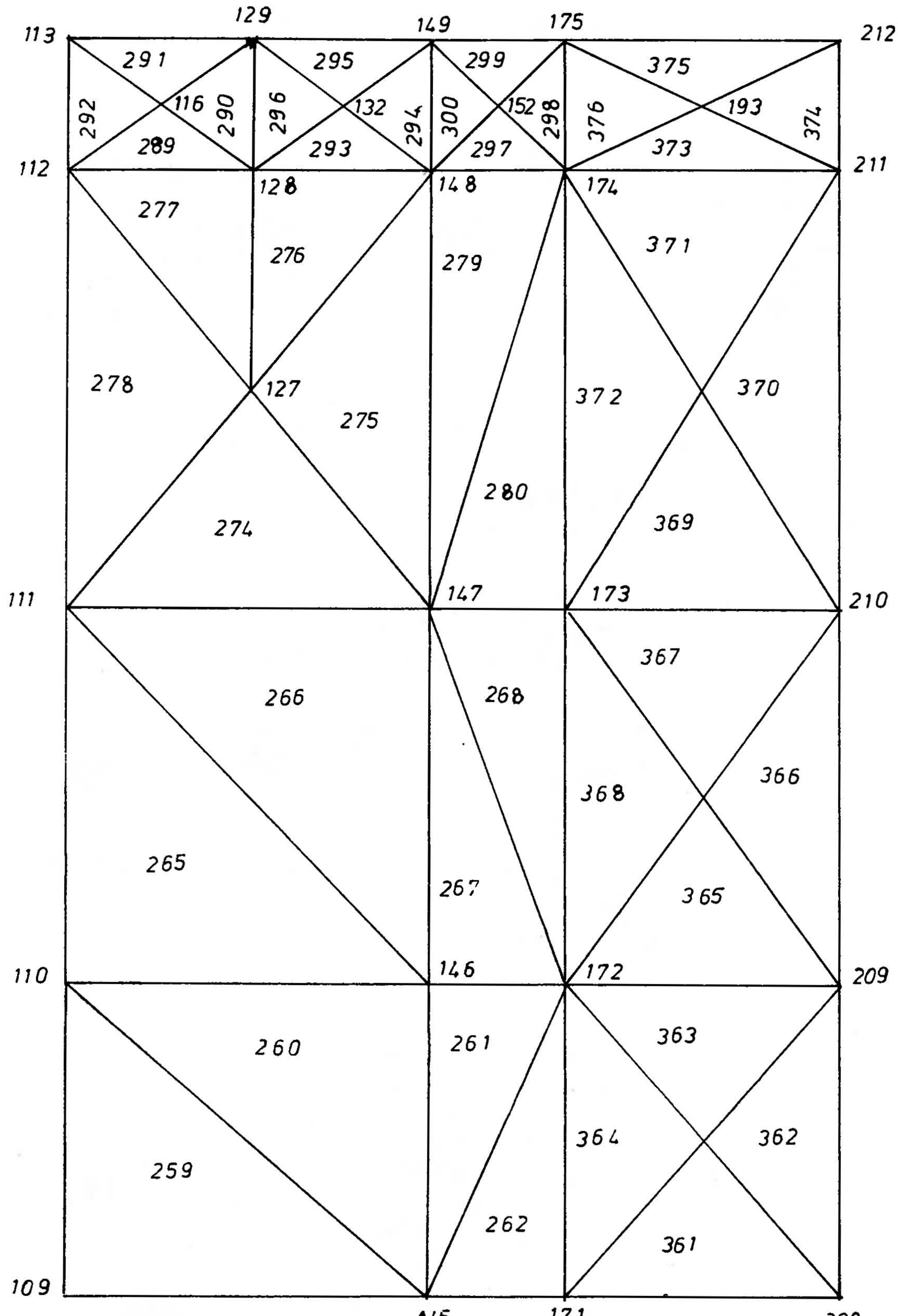

FIGURE A.2 BLOWUP OF THE MESH CLOSE TO THE WALL

```
   0     0     0     0
RAPID TRANSIT STRESS PATH SIMULATION SECOND MESH SHORT PILE
  326   596    10
    1    11        0.0        0.0         0.0        0.0   9
    2    10        0.0      700.0         0.0        0.0   9
    3    10        0.0     1060.0         0.0        0.0   7
    4    10        0.0     1270.0         0.0        0.0   7
    5    10        0.0     1322.0         0.0        0.0   7
    6    10        0.0     1500.0         0.0        0.0   7
    7    10        0.0     1700.0         0.0        0.0   7
    8    10        0.0     1900.0         0.0        0.0   7
    9    10        0.0     2070.0         0.0        0.0   7
   10    10        0.0     2100.0         0.0        0.0   7
   11    10        0.0     2400.0         0.0        0.0   7
   12    10        0.0     2500.0         0.0        0.0   7
   13    10        0.0     2620.0         0.0        0.0   7
   14    10        0.0     2745.0         0.0        0.0   7
   15    10        0.0     2800.0         0.0        0.0   7
   16     0       50.0     1296.0         0.0        0.0   7
   17     0       50.0     2085.0         0.0        0.0   7
   18     0       50.0     2772.5         0.0        0.0   7
   19     0      100.0     1165.0         0.0        0.0   7
   20     0      100.0     1270.0         0.0        0.0   7
   21     0      100.0     1322.0         0.0        0.0   7
   22     0      100.0     1411.0         0.0        0.0   7
   23     0      100.0     1985.0         0.0        0.0   7
   24     0      100.0     2070.0         0.0        0.0   7
   25     0      100.0     2100.0         0.0        0.0   7
   26     0      100.0     2250.0         0.0        0.0   7
   27     0      100.0     2680.0         0.0        0.0   7
   28     0      100.0     2745.0         0.0        0.0   7
   29     0      100.0     2800.0         0.0        0.0   7
   30     0      150.0     1296.0         0.0        0.0   7
   31     0      150.0     2085.0         0.0        0.0   7
   32     0      150.0     2772.5         0.0        0.0   7
   33     0      200.0      900.0         0.0        0.0   9
   34     0      200.0     1060.0         0.0        0.0   7
   35     0      200.0     1270.0         0.0        0.0   7
   36     0      200.0     1322.0         0.0        0.0   7
   37     0      200.0     1500.0         0.0        0.0   7
   38     0      200.0     1700.0         0.0        0.0   7
   39     0      200.0     1900.0         0.0        0.0   7
   40     0      200.0     2070.0         0.0        0.0   7
   41     0      200.0     2100.0         0.0        0.0   7
   42     0      200.0     2400.0         0.0        0.0   7
   43     0      200.0     2500.0         0.0        0.0   7
   44     0      200.0     2620.0         0.0        0.0   7
   45     0      200.0     2745.0         0.0        0.0   7
   46     0      200.0     2800.0         0.0        0.0   7
   47     0      250.0     1296.0         0.0        0.0   7
   48     0      250.0     2085.0         0.0        0.0   7
   49     0      250.0     2772.5         0.0        0.0   7
   50     0      300.0     1165.0         0.0        0.0   7
   51     0      300.0     1270.0         0.0        0.0   7
   52     0      300.0     1322.0         0.0        0.0   7
   53     0      300.0     1411.0         0.0        0.0   7
   54     0      300.0     1985.0         0.0        0.0   7
```

58	55	0	300.0	2070.0	0.0	0.0	7
59	56	0	300.0	2100.0	0.0	0.0	7
60	57	0	300.0	2250.0	0.0	0.0	7
61	58	0	300.0	2680.0	0.0	0.0	7
62	59	0	300.0	2745.0	0.0	0.0	7
63	60	0	300.0	2800.0	0.0	0.0	7
64	61	0	350.0	1296.0	0.0	0.0	7
65	62	0	350.0	2085.0	0.0	0.0	7
66	63	0	350.0	2772.5	0.0	0.0	7
67	64	11	400.0	0.0	0.0	0.0	9
68	65	0	400.0	700.0	0.0	0.0	9
69	66	0	400.0	900.0	0.0	0.0	9
70	67	0	400.0	1060.0	0.0	0.0	7
71	68	0	400.0	1270.0	0.0	0.0	7
72	69	0	400.0	1322.0	0.0	0.0	7
73	70	0	400.0	1500.0	0.0	0.0	7
74	71	0	400.0	1700.0	0.0	0.0	7
75	72	0	400.0	1900.0	0.0	0.0	7
76	73	0	400.0	2070.0	0.0	0.0	7
77	74	0	400.0	2100.0	0.0	0.0	7
78	75	0	400.0	2400.0	0.0	0.0	7
79	76	0	400.0	2500.0	0.0	0.0	7
80	77	0	400.0	2620.0	0.0	0.0	7
81	78	0	400.0	2745.0	0.0	0.0	7
82	79	0	400.0	2800.0	0.0	0.0	7
83	80	0	450.0	1296.0	0.0	0.0	7
84	81	0	450.0	2085.0	0.0	0.0	7
85	82	0	450.0	2772.5	0.0	0.0	7
86	83	0	500.0	1165.0	0.0	0.0	7
87	84	0	500.0	1270.0	0.0	0.0	7
88	85	0	500.0	1322.0	0.0	0.0	7
89	86	0	500.0	1411.0	0.0	0.0	7
90	87	0	500.0	1985.0	0.0	0.0	7
91	88	0	500.0	2070.0	0.0	0.0	7
92	89	0	500.0	2100.0	0.0	0.0	7
93	90	0	500.0	2250.0	0.0	0.0	7
94	91	0	500.0	2680.0	0.0	0.0	7
95	92	0	500.0	2745.0	0.0	0.0	7
96	93	0	500.0	2800.0	0.0	0.0	7
97	94	0	550.0	1296.0	0.0	0.0	7
98	95	0	550.0	2085.0	0.0	0.0	7
99	96	0	550.0	2772.5	0.0	0.0	7
100	97	11	600.0	0.0	0.0	0.0	9
101	98	0	600.0	350.0	0.0	0.0	9
102	99	0	600.0	700.0	0.0	0.0	9
103	100	0	600.0	900.0	0.0	0.0	9
104	101	0	600.0	1060.0	0.0	0.0	7
105	102	0	600.0	1270.0	0.0	0.0	7
106	103	0	600.0	1322.0	0.0	0.0	7
107	104	0	600.0	1500.0	0.0	0.0	7
108	105	0	600.0	1700.0	0.0	0.0	7
109	106	0	600.0	1900.0	0.0	0.0	7
110	107	0	600.0	2070.0	0.0	0.0	7
111	108	0	600.0	2100.0	0.0	0.0	7
112	109	0	600.0	2400.0	0.0	0.0	7
113	110	0	600.0	2500.0	0.0	0.0	7
114	111	0	600.0	2620.0	0.0	0.0	7
115	112	0	600.0	2745.0	0.0	0.0	7
116	113	0	600.0	2800.0	0.0	0.0	7
117	114	0	650.0	1296.0	0.0	0.0	7

118	115	0	650.0	2085.0	0.0	0.0	7
119	116	0	650.0	2772.5	0.0	0.0	7
120	117	0	700.0	1165.0	0.0	0.0	7
121	118	0	700.0	1270.0	0.0	0.0	7
122	119	0	700.0	1322.0	0.0	0.0	7
123	120	0	700.0	1411.0	0.0	0.0	7
124	121	0	700.0	1600.0	0.0	0.0	7
125	122	0	700.0	1800.0	0.0	0.0	7
126	123	0	700.0	1985.0	0.0	0.0	7
127	124	0	700.0	2070.0	0.0	0.0	7
128	125	0	700.0	2100.0	0.0	0.0	7
129	126	0	700.0	2250.0	0.0	0.0	7
130	127	0	700.0	2680.0	0.0	0.0	7
131	128	0	700.0	2745.0	0.0	0.0	7
132	129	0	700.0	2900.0	0.0	0.0	7
133	130	0	750.0	1296.0	0.0	0.0	7
134	131	0	750.0	2085.0	0.0	0.0	7
135	132	0	750.0	2780.0	0.0	0.0	7
136	133	0	800.0	1270.0	0.0	0.0	7
137	134	0	800.0	1322.0	0.0	0.0	7
138	135	0	800.0	1411.0	0.0	0.0	7
139	136	0	800.0	1500.0	0.0	0.0	7
140	137	0	800.0	1600.0	0.0	0.0	7
141	138	0	800.0	1700.0	0.0	0.0	7
142	139	0	800.0	1800.0	0.0	0.0	7
143	140	0	800.0	1900.0	0.0	0.0	7
144	141	0	800.0	1985.0	0.0	0.0	7
145	142	0	800.0	2070.0	0.0	0.0	7
146	143	0	800.0	2100.0	0.0	0.0	7
147	144	0	800.0	2250.0	0.0	0.0	7
148	145	0	800.0	2400.0	0.0	0.0	7
149	146	0	800.0	2500.0	0.0	0.0	7
150	147	0	800.0	2620.0	0.0	0.0	7
151	148	0	800.0	2780.0	0.0	0.0	7
152	149	0	800.0	2800.0	0.0	0.0	7
153	150	0	835.0	1296.0	0.0	0.0	7
154	151	0	835.0	2085.0	0.0	0.0	7
155	152	0	835.0	2790.0	0.0	0.0	7
156	153	11	870.0	0.0	0.0	0.0	9
157	154	0	870.0	350.0	0.0	0.0	9
158	155	0	870.0	700.0	0.0	0.0	9
159	156	0	870.0	900.0	0.0	0.0	9
160	157	0	870.0	1060.0	0.0	0.0	7
161	158	0	870.0	1165.0	0.0	0.0	7
162	159	0	870.0	1270.0	0.0	0.0	7
163	160	0	870.0	1322.0	0.0	0.0	7
164	161	0	870.0	1411.0	0.0	0.0	7
165	162	0	870.0	1500.0	0.0	0.0	7
166	163	0	870.0	1600.0	0.0	0.0	7
167	164	0	870.0	1700.0	0.0	0.0	7
168	165	0	870.0	1800.0	0.0	0.0	7
169	166	0	870.0	1900.0	0.0	0.0	7
170	167	0	870.0	1985.0	0.0	0.0	7
171	168	0	870.0	2070.0	0.0	0.0	7
172	169	0	870.0	2100.0	0.0	0.0	7
173	170	0	870.0	2250.0	0.0	0.0	7
174	171	0	870.0	2400.0	0.0	0.0	7
175	172	0	870.0	2500.0	0.0	0.0	7
176	173	0	870.0	2620.0	0.0	0.0	7
177	174	0	870.0	2780.0	0.0	0.0	7

178	175	0	870.0	2800.0	0.0	0.0	7
179	176	0	910.0	175.0	0.0	0.0	9
180	177	0	910.0	525.0	0.0	0.0	9
181	178	0	910.0	800.0	0.0	0.0	9
182	179	0	910.0	980.0	0.0	0.0	9
183	180	1	910.0	1165.0	0.0	0.0	4
184	181	1	910.0	1296.0	0.0	0.0	4
185	182	1	910.0	1411.0	0.0	0.0	4
186	183	1	910.0	1600.0	0.0	0.0	4
187	184	1	910.0	1800.0	0.0	0.0	4
188	185	1	910.0	1940.0	0.0	0.0	4
189	186	1	910.0	2028.0	0.0	0.0	4
190	187	1	910.0	2085.0	0.0	0.0	4
191	188	0	910.0	2175.0	0.0	0.0	4
192	189	0	910.0	2325.0	0.0	0.0	4
193	190	0	910.0	2450.0	0.0	0.0	4
194	191	0	910.0	2560.0	0.0	0.0	4
195	192	0	910.0	2680.0	0.0	0.0	4
196	193	0	910.0	2780.0	0.0	0.0	4
197	194	11	945.0	0.0	0.0	0.0	9
198	195	0	945.0	350.0	0.0	0.0	9
199	196	0	945.0	700.0	0.0	0.0	9
200	197	0	945.0	900.0	0.0	0.0	9
201	198	0	945.0	1060.0	0.0	0.0	7
202	199	0	945.0	1270.0	0.0	0.0	7
203	200	0	945.0	1322.0	0.0	0.0	7
204	201	0	945.0	1500.0	0.0	0.0	7
205	202	0	945.0	1700.0	0.0	0.0	7
206	203	0	945.0	1900.0	0.0	0.0	7
207	204	0	945.0	1985.0	0.0	0.0	7
208	205	0	945.0	2070.0	0.0	0.0	7
209	206	0	945.0	2100.0	0.0	0.0	7
210	207	0	945.0	2250.0	0.0	0.0	7
211	208	0	945.0	2400.0	0.0	0.0	7
212	209	0	945.0	2500.0	0.0	0.0	7
213	210	0	945.0	2620.0	0.0	0.0	7
214	211	0	945.0	2745.0	0.0	0.0	7
215	212	0	945.0	2800.0	0.0	0.0	7
216	213	0	1010.0	1165.0	0.0	0.0	7
217	214	0	1010.0	1296.0	0.0	0.0	7
218	215	0	1010.0	1411.0	0.0	0.0	7
219	216	0	1010.0	1600.0	0.0	0.0	7
220	217	0	1010.0	1800.0	0.0	0.0	7
221	218	0	1010.0	1940.0	0.0	0.0	7
222	219	0	1010.0	2028.0	0.0	0.0	7
223	220	0	985.0	2085.0	0.0	0.0	7
224	221	0	985.0	2175.0	0.0	0.0	7
225	222	0	985.0	2325.0	0.0	0.0	7
226	223	0	985.0	2450.0	0.0	0.0	7
227	224	0	985.0	2560.0	0.0	0.0	7
228	225	0	985.0	2680.0	0.0	0.0	7
229	226	0	985.0	2772.5	0.0	0.0	7
230	227	0	1060.0	980.0	0.0	0.0	9
231	228	0	1060.0	1060.0	0.0	0.0	7
232	229	0	1060.0	1270.0	0.0	0.0	7
233	230	0	1060.0	1322.0	0.0	0.0	7
234	231	0	1060.0	1500.0	0.0	0.0	7
235	232	0	1060.0	1700.0	0.0	0.0	7
236	233	0	1060.0	1900.0	0.0	0.0	7
237	234	0	1060.0	1985.0	0.0	0.0	7

238	235	0	1025.0	2070.0	0.0	0.0	7
239	236	0	1025.0	2100.0	0.0	0.0	7
240	237	0	1025.0	2250.0	0.0	0.0	7
241	238	0	1025.0	2400.0	0.0	0.0	7
242	239	0	1025.0	2500.0	0.0	0.0	7
243	240	0	1025.0	2620.0	0.0	0.0	7
244	241	0	1025.0	2745.0	0.0	0.0	7
245	242	0	1025.0	2800.0	0.0	0.0	7
246	243	11	1200.0	0.0	0.0	0.0	9
247	244	0	1200.0	350.0	0.0	0.0	9
248	245	0	1200.0	700.0	0.0	0.0	9
249	246	0	1200.0	900.0	0.0	0.0	9
250	247	0	1200.0	1060.0	0.0	0.0	7
251	248	0	1150.0	1215.0	0.0	0.0	7
252	249	0	1280.0	1300.0	0.0	0.0	7
253	250	0	1120.0	1300.0	0.0	0.0	7
254	251	0	1150.0	1370.0	0.0	0.0	7
255	252	0	1200.0	1500.0	0.0	0.0	7
256	253	0	1200.0	1900.0	0.0	0.0	7
257	254	0	1120.0	2085.0	0.0	0.0	7
258	255	0	1200.0	2400.0	0.0	0.0	7
259	256	0	1200.0	2620.0	0.0	0.0	7
260	257	0	1200.0	2800.0	0.0	0.0	7
261	258	0	1400.0	350.0	0.0	0.0	9
262	259	0	1400.0	900.0	0.0	0.0	9
263	260	0	1400.0	1700.0	0.0	0.0	7
264	261	0	1300.0	2030.0	0.0	0.0	7
265	262	0	1380.0	2110.0	0.0	0.0	7
266	263	0	1300.0	2210.0	0.0	0.0	7
267	264	11	1600.0	0.0	0.0	0.0	9
268	265	0	1600.0	700.0	0.0	0.0	9
269	266	0	1600.0	1060.0	0.0	0.0	7
270	267	0	1600.0	1500.0	0.0	0.0	7
271	268	0	1600.0	1900.0	0.0	0.0	7
272	269	0	1600.0	2400.0	0.0	0.0	7
273	270	0	1600.0	2620.0	0.0	0.0	7
274	271	0	1600.0	2800.0	0.0	0.0	7
275	272	0	1900.0	350.0	0.0	0.0	9
276	273	0	1900.0	880.0	0.0	0.0	9
277	274	0	1900.0	1280.0	0.0	0.0	7
278	275	0	1900.0	1700.0	0.0	0.0	7
279	276	0	1900.0	2150.0	0.0	0.0	7
280	277	0	1900.0	2620.0	0.0	0.0	7
281	278	0	1900.0	2800.0	0.0	0.0	7
282	279	11	2200.0	0.0	0.0	0.0	9
283	280	0	2200.0	700.0	0.0	0.0	9
284	281	0	2200.0	1060.0	0.0	0.0	7
285	282	0	2200.0	1500.0	0.0	0.0	7
286	283	0	2200.0	1900.0	0.0	0.0	7
287	284	0	2200.0	2400.0	0.0	0.0	7
288	285	0	2200.0	2800.0	0.0	0.0	7
289	286	0	2500.0	350.0	0.0	0.0	9
290	287	0	2500.0	990.0	0.0	0.0	9
291	288	0	2500.0	1280.0	0.0	0.0	7
292	289	0	2500.0	1700.0	0.0	0.0	7
293	290	0	2500.0	2150.0	0.0	0.0	7
294	291	0	2500.0	2620.0	0.0	0.0	7
295	292	0	2500.0	2800.0	0.0	0.0	7
296	293	11	2800.0	0.0	0.0	0.0	9
297	294	0	2800.0	700.0	0.0	0.0	9

298	295	0	2800.0	1060.0	0.0	0.0	7
299	296	0	2800.0	1500.0	0.0	0.0	7
300	297	0	2800.0	1900.0	0.0	0.0	7
301	298	0	2800.0	2400.0	0.0	0.0	7
302	299	0	2800.0	2800.0	0.0	0.0	7
303	300	0	3100.0	2620.0	0.0	0.0	7
304	301	0	3100.0	2800.0	0.0	0.0	7
305	302	11	3400.0	0.0	0.0	0.0	9
306	303	0	3400.0	700.0	0.0	0.0	9
307	304	0	3400.0	1060.0	0.0	0.0	7
308	305	0	3400.0	1500.0	0.0	0.0	7
309	306	0	3400.0	1900.0	0.0	0.0	7
310	307	0	3400.0	2400.0	0.0	0.0	7
311	308	0	3400.0	2800.0	0.0	0.0	7
312	309	0	3700.0	2620.0	0.0	0.0	7
313	310	0	3700.0	2800.0	0.0	0.0	7
314	311	11	4000.0	0.0	0.0	0.0	9
315	312	0	4000.0	700.0	0.0	0.0	9
316	313	0	4000.0	1060.0	0.0	0.0	7
317	314	0	4000.0	1500.0	0.0	0.0	7
318	315	0	4000.0	1900.0	0.0	0.0	7
319	316	0	4000.0	2400.0	0.0	0.0	7
320	317	0	4000.0	2800.0	0.0	0.0	7
321	318	0	4300.0	2620.0	0.0	0.0	7
322	319	0	4300.0	2800.0	0.0	0.0	7
323	320	11	4600.0	0.0	0.0	0.0	9
324	321	10	4600.0	700.0	0.0	0.0	9
325	322	10	4600.0	1060.0	0.0	0.0	9
326	323	10	4600.0	1500.0	0.0	0.0	9
327	324	10	4600.0	1900.0	0.0	0.0	9
328	325	10	4600.0	2400.0	0.0	0.0	9
329	326	10	4600.0	2800.0	0.0	0.0	9
330	1	1	64	65	2	1.00	
331	2	1	65	2	2	1.0	
332	3	2	65	33	2	1.0	
333	4	65	66	33	2	1.0	
334	5	66	67	33	2	1.0	
335	6	67	34	33	2	1.0	
336	7	34	3	33	2	1.0	
337	8	3	2	33	2	1.0	
338	9	34	19	3	5	1.0	
339	10	34	35	19	5	1.0	
340	11	35	20	19	5	1.0	
341	12	20	4	19	5	1.0	
342	13	4	3	19	5	1.0	
343	14	34	67	50	5	1.0	
344	15	67	68	50	5	1.0	
345	16	68	51	50	5	1.0	
346	17	51	35	50	5	1.0	
347	19	35	34	50	5	1.0	
348	19	4	20	16	5	1.0	
349	20	20	21	16	5	1.0	
350	21	21	5	16	5	1.0	
351	22	5	4	16	5	1.0	
352	23	20	35	30	5	1.0	
353	24	35	36	30	5	1.0	
354	25	36	21	30	5	1.0	
355	26	21	20	30	5	1.0	
356	27	35	51	47	5	1.0	
357	28	51	52	47	5	1.0	

358	29	52	36	47	5	1.0
359	30	36	35	47	5	1.0
360	31	51	68	61	5	1.0
361	32	68	69	61	5	1.0
362	33	69	52	61	5	1.0
363	34	52	51	61	5	1.0
364	35	5	21	22	5	1.0
365	36	21	36	22	5	1.0
366	37	36	37	22	5	1.0
367	38	37	6	22	5	1.0
368	39	6	5	22	5	1.0
369	40	36	52	53	5	1.0
370	41	52	69	53	5	1.0
371	42	69	70	53	5	1.0
372	43	70	37	53	5	1.0
373	44	37	36	53	5	1.0
374	45	6	38	7	5	1.0
375	46	6	37	38	5	1.0
376	47	37	70	38	5	1.0
377	48	70	71	38	5	1.0
378	49	7	39	8	5	1.0
379	50	7	38	39	5	1.0
390	51	38	71	39	5	1.0
381	52	71	72	39	5	1.0
382	53	39	23	8	5	1.0
383	54	39	40	23	5	1.0
384	55	40	24	23	5	1.0
385	56	24	9	23	5	1.0
386	57	9	8	23	5	1.0
387	58	39	72	54	5	1.0
388	59	72	73	54	5	1.0
389	60	73	55	54	5	1.0
390	61	55	40	54	5	1.0
391	62	40	39	54	5	1.0
392	63	9	24	17	5	1.0
393	64	24	25	17	5	1.0
394	65	25	10	17	5	1.0
395	66	10	9	17	5	1.0
396	67	24	40	31	5	1.0
397	68	40	41	31	5	1.0
398	69	41	25	31	5	1.0
399	70	25	24	31	5	1.0
400	71	40	55	48	5	1.0
401	72	55	56	48	5	1.0
402	73	56	41	48	5	1.0
403	74	41	40	48	5	1.0
404	75	55	73	62	5	1.0
405	76	73	74	62	5	1.0
406	77	74	56	62	5	1.0
407	78	56	55	62	5	1.0
409	79	10	25	26	5	1.0
409	80	25	41	26	5	1.0
410	81	41	42	26	5	1.0
411	82	42	11	26	5	1.0
412	83	11	10	26	5	1.0
413	84	41	56	57	5	1.0
414	85	56	74	57	5	1.0
415	86	74	75	57	5	1.0
416	87	75	42	57	5	1.0
417	88	42	41	57	5	1.0

418	89	11	43	12	6	1.0
419	90	11	42	43	6	1.0
420	91	43	42	75	6	1.0
421	92	43	75	76	6	1.0
422	93	12	44	13	6	1.0
423	94	12	43	44	6	1.0
424	95	43	76	44	6	1.0
425	96	76	77	44	6	1.0
426	97	13	44	27	6	1.0
427	98	44	45	27	6	1.0
428	99	27	45	28	6	1.0
429	100	28	14	27	6	1.0
430	101	14	13	27	6	1.0
431	102	44	77	58	6	1.0
432	103	77	78	58	6	1.0
433	104	78	59	58	6	1.0
434	105	59	45	58	6	1.0
435	106	45	44	58	6	1.0
436	107	14	28	18	6	1.0
437	108	28	29	18	6	1.0
438	109	29	15	18	6	1.0
439	110	15	14	18	6	1.0
440	111	28	45	32	6	1.0
441	112	45	46	32	6	1.0
442	113	46	29	32	6	1.0
443	114	29	28	32	6	1.0
444	115	45	59	49	6	1.0
445	116	59	60	49	6	1.0
446	117	60	46	49	6	1.0
447	118	46	45	49	6	1.0
448	119	59	78	63	6	1.0
449	120	78	79	63	6	1.0
450	121	79	60	63	6	1.0
451	122	60	59	63	6	1.0
452	123	64	97	98	2	1.0
453	124	97	153	98	2	1.0
454	125	153	154	98	2	1.0
455	126	154	155	98	2	1.0
456	127	155	99	98	2	1.0
457	128	99	65	98	2	1.0
458	129	65	64	98	2	1.0
459	130	100	66	65	2	1.0
460	131	65	99	100	2	1.0
461	132	99	155	100	2	1.0
462	133	156	100	155	2	1.0
463	134	66	101	67	2	1.0
464	135	66	100	101	2	1.0
465	136	157	101	100	2	1.0
466	137	100	156	157	2	1.0
467	138	67	101	83	5	1.0
468	139	101	102	83	5	1.0
469	140	102	84	83	5	1.0
470	141	84	68	83	5	1.0
471	142	68	67	83	5	1.0
472	143	102	101	117	5	1.0
473	144	101	157	117	5	1.0
474	145	157	158	117	5	1.0
475	146	158	133	117	5	1.0
476	147	158	159	133	5	1.0
477	148	133	118	117	5	1.0

478	149	118	102	117	5	1.0
479	150	68	84	80	5	1.0
480	151	84	85	80	5	1.0
481	152	85	69	80	5	1.0
482	153	69	68	80	5	1.0
483	154	84	102	94	5	1.0
484	155	102	103	94	5	1.0
485	156	103	85	94	5	1.0
486	157	85	84	94	5	1.0
487	158	102	118	114	5	1.0
488	159	118	119	114	5	1.0
489	160	119	103	114	5	1.0
490	161	103	102	114	5	1.0
491	162	118	133	130	5	1.0
492	163	133	134	130	5	1.0
493	164	134	119	130	5	1.0
494	165	119	118	130	5	1.0
495	166	133	159	150	5	1.0
496	167	159	160	150	5	1.0
497	168	160	134	150	5	1.0
498	169	134	133	150	5	1.0
499	170	85	103	86	5	1.0
500	171	103	104	86	5	1.0
501	172	104	70	86	5	1.0
502	173	70	69	86	5	1.0
503	174	69	85	86	5	1.0
504	175	119	134	120	5	1.0
505	176	134	135	120	5	1.0
506	177	135	136	120	5	1.0
507	178	136	104	120	5	1.0
508	179	104	103	120	5	1.0
509	180	103	119	120	5	1.0
510	181	134	160	161	5	1.0
511	182	161	135	134	5	1.0
512	183	136	135	161	5	1.0
513	184	162	136	161	5	1.0
514	185	71	70	105	5	1.0
515	186	70	104	105	5	1.0
516	187	104	136	121	5	1.0
517	188	135	137	121	5	1.0
518	189	137	138	121	5	1.0
519	190	138	105	121	5	1.0
520	191	105	104	121	5	1.0
521	192	136	162	163	5	1.0
522	193	163	137	136	5	1.0
523	194	163	138	137	5	1.0
524	195	163	164	138	5	1.0
525	196	71	106	72	5	1.0
526	197	71	105	106	5	1.0
527	198	105	138	122	5	1.0
528	199	138	139	122	5	1.0
529	200	139	140	122	5	1.0
530	201	140	106	122	5	1.0
531	202	106	105	122	5	1.0
532	203	138	164	165	5	1.0
533	204	165	139	138	5	1.0
534	205	165	140	139	5	1.0
535	206	165	166	140	5	1.0
536	207	72	106	87	5	1.0
537	208	106	107	87	5	1.0

538	209	107	88	87	5	1.0
539	210	88	73	87	5	1.0
540	211	73	72	87	5	1.0
541	212	106	140	123	5	1.0
542	213	140	141	123	5	1.0
543	214	141	142	123	5	1.0
544	215	142	124	123	5	1.0
545	216	124	107	123	5	1.0
546	217	107	106	123	5	1.0
547	218	140	166	167	5	1.0
548	219	140	167	141	5	1.0
549	220	167	142	141	5	1.0
550	221	167	168	142	5	1.0
551	222	73	88	81	5	1.0
552	223	88	89	81	5	1.0
553	224	89	74	81	5	1.0
554	225	74	73	81	5	1.0
555	226	88	107	95	5	1.0
556	227	107	108	95	5	1.0
557	228	108	89	95	5	1.0
558	229	89	88	95	5	1.0
559	230	107	124	115	5	1.0
560	231	124	125	115	5	1.0
561	232	125	108	115	5	1.0
562	233	108	107	115	5	1.0
563	234	124	142	131	5	1.0
564	235	142	143	131	5	1.0
565	236	143	125	131	5	1.0
566	237	125	124	131	5	1.0
567	238	142	168	151	5	1.0
568	239	168	169	151	5	1.0
569	240	169	143	151	5	1.0
570	241	143	142	151	5	1.0
571	242	89	108	90	5	1.0
572	243	108	109	90	5	1.0
573	244	109	75	90	5	1.0
574	245	75	74	90	5	1.0
575	246	74	89	90	5	1.0
576	247	125	143	126	5	1.0
577	248	143	144	126	5	1.0
578	249	144	145	126	5	1.0
579	250	145	109	126	5	1.0
580	251	109	108	126	5	1.0
581	252	108	125	126	5	1.0
582	253	143	169	170	5	1.0
583	254	170	144	143	5	1.0
584	255	170	145	144	5	1.0
585	256	170	171	145	5	1.0
586	257	75	110	76	6	1.0
587	258	75	109	110	6	1.0
588	259	109	145	110	6	1.0
589	260	145	146	110	6	1.0
590	261	145	172	146	6	1.0
591	262	145	171	172	6	1.0
592	263	76	111	77	6	1.0
593	264	76	110	111	6	1.0
594	265	110	146	111	6	1.0
595	266	146	147	111	6	1.0
596	267	147	146	172	6	1.0
597	268	173	147	172	6	1.0

598	269	77	111	91	6	1.0
599	270	111	112	91	6	1.0
600	271	91	112	92	6	1.0
601	272	92	78	91	6	1.0
602	273	77	91	78	6	1.0
603	274	111	147	127	6	1.0
604	275	147	148	127	6	1.0
605	276	148	128	127	6	1.0
606	277	128	112	127	6	1.0
607	278	112	111	127	6	1.0
608	279	174	148	147	6	1.0
609	280	147	173	174	6	1.0
610	281	78	92	82	6	1.0
611	282	92	93	82	6	1.0
612	283	93	79	82	6	1.0
613	284	79	78	82	6	1.0
614	285	92	112	96	6	1.0
615	286	112	113	96	6	1.0
616	287	113	93	96	6	1.0
617	288	93	92	96	6	1.0
618	289	112	128	116	6	1.0
619	290	128	129	116	6	1.0
620	291	129	113	116	6	1.0
621	292	113	112	116	6	1.0
622	293	128	148	132	6	1.0
623	294	148	149	132	6	1.0
624	295	149	129	132	6	1.0
625	296	129	128	132	6	1.0
626	297	148	174	152	6	1.0
627	298	174	175	152	6	1.0
628	299	175	149	152	6	1.0
629	300	149	148	152	6	1.0
630	301	153	194	176	2	1.0
631	302	194	195	176	2	1.0
632	303	195	154	176	2	1.0
633	304	154	153	176	2	1.0
634	305	154	195	177	2	1.0
635	306	195	196	177	2	1.0
636	307	196	155	177	2	1.0
637	308	155	154	177	2	1.0
638	309	155	196	178	2	1.0
639	310	196	197	178	2	1.0
640	311	197	156	178	2	1.0
641	312	156	155	178	2	1.0
642	313	156	197	179	2	1.0
643	314	197	198	179	2	1.0
644	315	198	157	179	2	1.0
645	316	157	156	179	2	1.0
646	317	157	198	180	4	.35
647	318	198	199	180	4	.35
648	319	199	159	180	4	.35
649	320	159	158	180	4	.35
650	321	158	157	180	4	.35
651	322	159	199	181	4	.35
652	323	199	200	181	4	.35
653	324	200	160	181	4	.35
654	325	160	159	181	4	.35
655	326	160	200	182	4	.35
656	327	200	201	182	4	.35
657	328	201	162	182	4	.35

658	329	162	161	182	4	.35
659	330	161	160	182	4	.35
660	331	162	201	183	4	.35
661	332	201	202	183	4	.35
662	333	202	164	183	4	.35
663	334	164	163	183	4	.35
664	335	163	162	183	4	.35
665	336	164	202	184	4	.35
666	337	202	203	164	4	.35
667	338	203	166	184	4	.35
668	339	166	165	184	4	.35
669	340	165	164	184	4	.35
670	341	166	203	185	4	.35
671	342	203	204	185	4	.35
672	343	204	167	185	4	.35
673	344	167	166	185	4	.35
674	345	167	204	186	4	.35
675	346	204	205	186	4	.35
676	347	205	168	186	4	.35
677	348	168	167	186	4	.35
678	349	168	205	187	4	.35
679	350	205	206	187	4	.35
680	351	206	169	187	4	.35
681	352	169	168	187	4	.35
682	353	169	206	188	4	.035
683	354	206	207	188	4	.035
684	355	207	170	188	4	.035
685	356	170	169	188	4	.035
686	357	170	207	189	4	.035
687	358	207	208	189	4	.035
688	359	208	171	189	4	.035
689	360	171	170	189	4	.035
690	361	171	208	190	4	.035
691	362	208	209	190	4	.035
692	363	209	172	190	4	.035
693	364	172	171	190	4	.035
694	365	172	209	191	4	.035
695	366	209	210	191	4	.035
696	367	210	173	191	4	.035
697	368	173	172	191	4	.035
698	369	173	210	192	4	.035
699	370	210	211	192	4	.035
700	371	211	174	192	4	.035
701	372	174	173	192	4	.035
702	373	174	211	193	4	.035
703	374	211	212	193	4	.035
704	375	212	175	193	4	.035
705	376	175	174	193	4	.035
706	377	194	243	195	2	1.0
707	378	243	244	195	2	1.0
708	379	244	245	195	2	1.0
709	380	195	245	196	2	1.0
710	381	243	264	258	2	1.0
711	382	264	265	258	2	1.0
712	383	265	245	258	2	1.0
713	384	245	244	258	2	1.0
714	385	258	244	243	2	1.0
715	386	197	196	245	2	1.0
716	387	246	197	245	2	1.0
717	388	259	246	245	2	1.0

718	389	259	245	265	2	1.0
719	390	266	259	265	3	1.0
720	391	266	247	259	3	1.0
721	392	247	246	259	2	1.0
722	393	227	197	246	2	1.0
723	394	247	227	246	2	1.0
724	395	247	228	227	2	1.0
725	396	228	198	227	2	1.0
726	397	227	198	197	2	1.0
727	358	228	213	198	5	1.0
728	399	229	213	228	5	1.0
729	400	229	199	213	5	1.0
730	401	213	199	198	5	1.0
731	402	229	214	199	5	1.0
732	403	229	230	214	5	1.0
733	404	230	200	214	5	1.0
734	405	214	200	199	5	1.0
735	406	248	229	228	5	1.0
736	407	248	228	247	5	1.0
737	408	249	248	247	5	1.0
738	409	249	247	266	5	1.0
739	410	267	249	266	5	1.0
740	411	267	252	249	5	1.0
741	412	250	229	248	5	1.0
742	413	249	250	248	5	1.0
743	414	251	250	249	5	1.0
744	415	252	251	249	5	1.0
745	416	250	230	229	5	1.0
746	417	251	230	250	5	1.0
747	418	231	230	251	5	1.0
748	419	252	231	251	5	1.0
749	420	215	200	230	5	1.0
750	421	231	215	230	5	1.0
751	422	231	201	215	5	1.0
752	423	215	201	200	5	1.0
753	424	216	201	231	5	1.0
754	425	232	216	231	5	1.0
755	426	232	202	216	5	1.0
756	427	216	202	201	5	1.0
757	428	232	231	252	5	1.0
758	429	260	232	252	5	1.0
759	430	260	252	267	5	1.0
760	431	268	260	267	5	1.0
761	432	268	253	260	5	1.0
762	433	253	232	260	5	1.0
763	434	253	233	232	5	1.0
764	435	217	202	232	5	1.0
765	436	233	217	232	5	1.0
766	437	233	203	217	5	1.0
767	439	203	202	217	5	1.0
768	439	233	218	203	5	1.0
769	440	234	218	233	5	1.0
770	441	234	204	218	5	1.0
771	442	218	204	203	5	1.0
772	443	219	204	234	5	1.0
773	444	235	219	234	5	1.0
774	445	235	205	219	5	1.0
775	446	204	219	205	5	1.0
776	447	235	220	205	5	1.0
777	448	236	220	235	5	1.0

778	449	236	206	220	5	1.0
779	450	220	206	205	5	1.0
780	451	236	221	206	5	1.0
781	452	237	221	236	5	1.0
782	453	237	207	221	5	1.0
783	454	221	207	206	5	1.0
784	455	207	237	222	5	1.0
785	456	237	238	222	5	1.0
786	457	238	208	222	5	1.0
787	458	208	207	222	5	1.0
738	459	233	253	234	5	1.0
789	460	253	254	234	5	1.0
790	461	234	254	235	5	1.0
791	462	253	261	254	5	1.0
792	463	253	268	261	5	1.0
793	464	261	268	262	5	1.0
794	465	268	269	262	5	1.0
795	466	254	236	235	5	1.0
796	467	261	263	254	5	1.0
797	468	262	263	261	5	1.0
798	469	262	269	263	5	1.0
799	470	236	254	237	5	1.0
800	471	237	255	238	5	1.0
801	472	254	255	237	5	1.0
802	473	254	263	255	5	1.0
803	474	263	269	255	5	1.0
804	475	208	238	223	6	1.0
805	476	238	239	223	6	1.0
806	477	239	209	223	6	1.0
807	478	209	208	223	6	1.0
809	479	209	239	224	6	1.0
609	480	239	240	224	6	1.0
810	481	240	210	224	6	1.0
811	482	210	209	224	6	1.0
812	483	210	240	225	6	1.0
813	484	240	241	225	6	1.0
814	485	241	211	225	6	1.0
815	486	211	210	225	6	1.0
816	487	211	241	226	6	1.0
817	488	241	242	226	6	1.0
818	489	242	212	226	6	1.0
819	490	212	211	226	6	1.0
820	491	239	238	255	6	1.0
821	492	256	239	255	6	1.0
872	493	256	240	239	6	1.0
823	494	270	256	255	6	1.0
824	495	270	255	269	6	1.0
825	496	271	256	270	6	1.0
826	497	271	257	256	6	1.0
827	498	241	240	256	6	1.0
828	439	257	241	256	6	1.0
829	500	257	242	241	6	1.0
830	501	264	279	272	2	1.0
831	502	279	280	272	3	1.0
832	503	280	265	272	3	1.0
833	504	265	264	272	2	1.0
834	505	265	280	273	3	1.0
835	506	280	281	273	3	1.0
836	507	281	266	273	3	1.0
837	508	266	265	273	3	1.0

838	509	266	281	274	5	1.0
839	510	281	282	274	5	1.0
840	511	282	267	274	5	1.0
841	512	267	266	274	5	1.0
842	513	267	282	275	5	1.0
843	514	282	283	275	5	1.0
844	515	283	268	275	5	1.0
845	516	268	267	275	5	1.0
846	517	268	283	276	5	1.0
847	518	283	284	276	5	1.0
848	519	284	269	276	5	1.0
849	520	269	258	276	5	1.0
850	521	269	284	277	6	1.0
851	522	284	285	277	6	1.0
852	523	285	278	277	6	1.0
853	524	278	271	277	6	1.0
854	525	271	270	277	6	1.0
855	526	270	269	277	6	1.0
856	527	279	293	286	3	1.0
857	528	293	294	286	3	1.0
858	529	294	280	286	3	1.0
859	530	280	279	286	3	1.0
860	531	280	294	287	3	1.0
861	532	294	295	287	3	1.0
862	533	295	281	287	3	1.0
863	534	281	280	287	3	1.0
864	535	281	295	288	5	1.0
865	536	295	296	288	5	1.0
866	537	296	282	288	5	1.0
867	538	282	281	288	5	1.0
868	539	282	296	289	5	1.0
869	540	296	297	289	5	1.0
870	541	297	283	289	5	1.0
871	542	283	292	289	5	1.0
872	543	283	297	290	5	1.0
873	544	297	298	290	5	1.0
874	545	298	284	290	5	1.0
975	546	284	283	290	5	1.0
876	547	284	298	291	6	1.0
877	548	298	299	291	6	1.0
878	549	299	292	291	6	1.0
879	550	292	285	291	6	1.0
880	551	285	284	291	6	1.0
881	552	294	293	302	3	1.0
882	553	302	303	294	3	1.0
883	554	294	303	295	3	1.0
984	555	303	304	295	3	1.0
885	556	296	295	304	5	1.0
886	557	304	305	296	5	1.0
887	558	297	296	305	5	1.0
888	559	305	306	297	5	1.0
889	560	298	297	306	5	1.0
890	561	306	307	298	5	1.0
891	562	298	307	300	6	1.0
892	563	307	308	300	6	1.0
893	564	308	301	300	6	1.0
894	565	301	299	300	6	1.0
895	566	299	298	300	6	1.0
896	567	302	311	312	3	1.0
897	568	312	303	302	3	1.0

```
569   303   312   313     3   1.0
570   313   304   303     3   1.0
571   304   313   314     5   1.0
572   314   305   304     5   1.0
573   305   314   315     5   1.0
574   315   306   305     5   1.0
575   306   315   316     5   1.0
576   316   307   306     5   1.0
577   307   316   309     6   1.0
578   316   317   309     6   1.0
579   317   310   309     6   1.0
580   310   308   309     6   1.0
581   308   307   309     6   1.0
582   312   311   320     3   1.0
583   320   321   312     3   1.0
584   313   312   321     3   1.0
585   321   322   313     3   1.0
586   314   313   322     5   1.0
587   322   323   314     5   1.0
588   315   314   323     5   1.0
589   323   324   315     5   1.0
590   316   315   324     5   1.0
591   324   325   316     5   1.0
592   316   325   318     6   1.0
593   325   326   318     6   1.0
594   326   319   318     6   1.0
595   319   317   318     6   1.0
596   317   316   318     6   1.0
 63     7
 19    33    34    50    65    67    98   100   101   176
177   178   179   230   231   232   233   254   238   240
244   245   246   249   260   262   269   270   271   272
273   274   275   276   277   278   286   287   288   289
290   291   292   303   304   305   306   307   308    66
 99   154   155   156   265   266   267   268   280   281
282   283   284
DISPLACEMENT DISTRIBUTION
 27
212   326   320     1    15   212   194   153   159     4
  5   160   168     9    10   169   174   148   128    14
 15   326   325   208   198   322     3
  1
    0.42      0.85
    2.10      0.09285    0.50573
    2.45      0.04601    0.44903
    2.90      0.03656    0.37339
  2
    0.40      0.36
   1.733      0.03379    0.17235
   1.969      0.02690    0.17297
   2.205      0.02155    0.16458
  3
    0.40      0.36
   5046.      0.01980    2.63
  4
    0.25      1.0
 140000.
  5
    0.42      0.85
   1.726      0.08000    0.2483
```

```
          2.205   0.06355    0.2287
       6
          0.40       1.00
        100.0
       7
          0.42       0.85
          1.54    0.22912    0.1190
          2.765   0.1737     0.0847
          3.36    0.07391    0.1013
     0.698,282.,1.5,
       8
         0.000        1.
           0.1
       9
          0.40       0.36
          3.85    0.05406    0.0520
      10
          0.15       1.0
        3500.
     0.00212     2800.
       1     6      4
       2    12
      89    94
       4    43
      89    92     94   95
       4    76
      92    95    257  264
       4   110
     257   260    264  265
       4   146
     260   261    265  267
       2   172
     261   267
       2   172
     261   267
       2   173
     268   280
       1   174
     297
       1   175
     299
       0
      68
      93
      94
      95
      96
      97
      98
      99
     100
     101
     102
     103
     104
     105
     106
     107
     108
     109
```

1018	110			
1019	111			
1020	112			
1021	113			
1022	114			
1023	115			
1024	116			
1025	117			
1026	118			
1027	119			
1028	120			
1029	121			
1030	122			
1031	263			
1032	264			
1033	265			
1034	266			
1035	267			
1036	268			
1037	269			
1038	270			
1039	271			
1040	272			
1041	273			
1042	274			
1043	275			
1044	276			
1045	277			
1046	278			
1047	279			
1048	280			
1049	281			
1050	282			
1051	283			
1052	284			
1053	285			
1054	286			
1055	287			
1056	288			
1057	289			
1058	290			
1059	291			
1060	292			
1061	293			
1062	294			
1063	295			
1064	296			
1065	297			
1066	298			
1067	299			
1068	300			
1069	0			
1070	0			
1071	2	6	2	
1072	2	11		
1073	82	90		
1074	4	42		
1075	82	87	90	91
1076	4	75		
1077	87	91	244	258

1078	4	109		
1079	244	250	258	259
1080	2	145		
1081	250	259		
1082	2	171		
1083	261	262		
1084	2	171		
1085	256	262		
1086	1	172		
1087	262			
1088	0			
1089	10			
1090	89			
1091	90			
1092	91			
1093	92			
1094	257			
1095	258			
1096	259			
1097	260			
1098	261			
1099	262			
1100	32			
1101	107			
1102	108			
1103	109			
1104	110			
1105	111			
1106	112			
1107	113			
1108	114			
1109	115			
1110	116			
1111	117			
1112	118			
1113	119			
1114	120			
1115	121			
1116	122			
1117	281			
1118	282			
1119	283			
1120	284			
1121	285			
1122	286			
1123	287			
1124	288			
1125	289			
1126	290			
1127	291			
1128	292			
1129	293			
1130	294			
1131	295			
1132	296			
1133	4			
1134	297			
1135	298			
1136	299			
1137	300			

1138	27
1139	14
1140	15
1141	18
1142	28
1143	29
1144	32
1145	45
1146	46
1147	49
1148	59
1149	60
1150	63
1151	78
1152	79
1153	82
1154	92
1155	93
1156	96
1157	112
1158	113
1159	116
1160	128
1161	129
1162	132
1163	148
1164	149
1165	152

A.5 Listing of the program

```
      COMMON E(10),PR(10),KO(10),X(350),Y(350),U(350),V(350),TH(600),
     1STIF(700,140),AP(700),ESTIF(6,6),ECM(3,3),FBM(3,6),FSM(3,6),AF
      COMMON NUMNP,NUMEL,NUMAT,KODE(350),NP(3,600),MAT(600),MBAND,
     1 NEQ,M,LM(6)
      COMMON KODE1(350)
      COMMON SIGC(10,4),AA(10,4),BB(10,4),KO(10),ZSFC
      COMMON DSIGEL(600,3),SIGIEL(600,3),DSIGA(350,3),SIGIA(350,3)
      COMMON TSIGEL(600,3),TSIGA(350,3),TB(700)
      COMMON UN(350),VN(350),NNYL(25),NNXL(25)
      COMMON EB(600),PRT(600),TSIGEP(600,2)
      COMMON PHI,XK,YEP
      COMMON DI(700)
      DIMENSION XP(80,8),YP(80,8),NTP(80),NG(30),
     1TITLE(20),XG(80),YG(80),XPF(10),YPF(10)
      REAL KO
      READ(5,200)IPRINT,NIPRIN,IPLOT,NIPRIF
  200 FORMAT(4I5)
      CALL READGE
      READ(5,450) NNTP,NPH
  450 FORMAT(2I5)
      WRITE(6,451)NNTP
  451 FORMAT(///,'      NUMBER OF NODES TO BE PLOTTED',I5,
     1//,10X,'NODES NO')
      READ(5,452) (NTP(I),I=1,NNTP)
  452 FORMAT(10I5)
      WRITE(6,452) (NTP(I),I=1,NNTP)
      READ(5,457) (TITLE(I),I=1,20)
  457 FORMAT(20A4)
      READ(5,450)NNG
      READ(5,452) (NG(I),I=1,NNG)
      DO 456 I=1,NNG
      NNN=NG(I)
      XG(I)=X(NNN)
  456 YG(I)=Y(NNN)
      DO 453 I=1,NNTP
      J=NTP(I)
      XP(I,1)=X(J)
  453 YP(I,1)=Y(J)
      DO 80 L=1,NEQ
   80 TB(L)=0.
      CALL SST
C
C   CALL INITIAL STRESSES
C
      CALL INIT
      DO 59 M=1,NUMNP
      TSIGA(M,1)=SIGIA(M,1)
      TSIGA(M,2)=SIGIA(M,2)
   59 TSIGA(M,3)=0.
      DO 50 M=1,NUMEL
      TSIGEL(M,1)=SIGIEL(M,1)
      TSIGEL(M,2)=SIGIEL(M,2)
   50 TSIGEL(M,3)=0.
C
C   CALL NEW LOAD
C
   90 CALL NLOAD(NPHASE,NIPRIN)
      IF(NPHASE.EQ.0) GO TO 91
   41 FORMAT(///,10X,19H NODAL POINT OUTPUT,///
     11H ,59H NODE  KODE     X COORD      Y COORD     X FORCE      Y FORCE
```

```
     2//)
  40  FORMAT( 5X, 'OUTPUT OF COMPLETE NODAL DATA  ')
  43  FORMAT(I4,I6,F13.3,3F12.3,I5)
  46  FORMAT(///,10X, 13H ELEMENT DATA ///,
     1 40H ELEM     I     J     K    MAT  THICKNESS //)
C
C   CALCULATE PRINCIPAL STRESSES
C
      DO 51 M=1,NUMEL
      SIGM=(TSIGEL(M,1)+TSIGEL(M,2))/2.
      SIGD2=(TSIGEL(M,1)-TSIGEL(M,2))/2.
      RAD=SQRT(SIGD2**2+TSIGEL(M,3)**2)
      TSIGEP(M,1)=SIGM+RAD
   51 TSIGEP(M,2)=SIGM-RAD
   60 FORMAT(1H1,5X,'TOTAL PRINCIPAL STRESSES',/,5X,
     1'   EL     SIGX       SIGY       SIGXY      SIG1       SIG3')
   61 FORMAT(5X,I5,5F10.4)
C
C   DIVIDE THE LOAD IN STEPS
C
      DO 62 I=1,NUMNP
      U(I)=UN(I)/4.
   62 V(I)=VN(I)/4.
      DO 70 IJ=1,4
C
C   COMPUTE E BEFORE EACH STEP
C
      CALL DET3(NIPRIE,NPHASE,IJ)
   64 FORMAT(1H1,10X,11HSTEP NUMBER,I5,
     1/,11X,16('*'),///)
      IF(IPRINT.NE.1)GO TO 201
      WRITE(6,64) IJ
      WRITE(6,40)
      WRITE(6,41)
      WRITE(6,43) (N,KODE(N),X(N),Y(N),U(N),V(N),KODE1(N),
     1N=1,NUMNP)
      WRITE(6,46)
      WRITE(6,65) (M,(NP(J,M),J=1,3),MAT(M),TH(M),EE(M),M=1,NUMEL)
   65 FORMAT(I4,4I6,E11.4,F14.3)
  201 CONTINUE
C
C
C   UPDATE STRESSES AND DISPLACEMENTS
C   AFTER EACH STEP
C   TSIGA = TOTAL NODAL STRESSES
C   TSIGEL = TOTAL ELEMENT STRESSES
C   TSIGEP = TOTAL PRINCIPAL STRESSES
C   TB = TOTAL NODAL DISPLACEMENTS
C   DI = DISPLACEMENT FOR EACH INCREMENT
C
C
      CALL CST
      DO 63 I=1,NUMNP
      DO 67 J=1,3
   67 TSIGA(I,J)=TSIGA(I,J)+DSIGA(I,J)
   63 CONTINUE
      DO 66 I=1,NUMEL
      DO 68 J=1,3
   68 TSIGEL(I,J)=TSIGEL(I,J)+DSIGEL(I,J)
   66 CONTINUE
```

```
      DO 69 I=1,NEQ
   69 TB(I)=TB(I)+DI(I)
C
C   CALCULATE PRINCIPAL STRESSES
C
      DO 71 M=1,NUMEL
      SIGM=(TSIGEL(M,1)+TSIGEL(M,2))/2.
      SIGD2=(TSIGEL(M,1)-TSIGEL(M,2))/2.
      RAD=SQRT(SIGD2**2+TSIGEL(M,3)**2)
      TSIGEP(M,1)=SIGM+RAD
   71 TSIGEP(M,2)=SIGM-RAD
   70 CONTINUE
      IF(NIPRIE.EQ.1)GO TO 300
      IF(NPHASE.NE.NPH)GO TO 660
  300 WRITE(6,60)
      WRITE(6,61)(M,TSIGEL(M,1),TSIGEL(M,2),TSIGEL(M,3),
     1TSIGEP(M,1),TSIGEP(M,2),M=1,NUMEL)
      WRITE(6,72)
   72 FORMAT(///,'  TOTAL NODAL DISPLACEMENT')
      WRITE(6,76)
   76 FORMAT(///,'  NODE NO',10X,'U',14X,'V')
      DO 75 I=1,NUMNP
      IY=I*2
      IX=IY-1
   75 WRITE(6,77)I,TB(IX),TB(IY)
   77 FORMAT(I10,2F15.6)
  660 K=NPHASE+1
      DO 454 I=1,NNTP
      J=NTP(I)
      IY=J*2
      IX=IY-1
      DX=TB(IX)*50.
      DY=TB(IY)*50.
      XP(I,K)=X(J)+DX
  454 YP(I,K)=Y(J)+DY
  600 FORMAT(3I5,4F15.5)
C
C   IF ALL THE STEPS HAVE BEEN PERFORMED
C   PROCEED TO THE NEXT PHASE
C
      GO TO 90
   91 WRITE(6,92)
   92 FORMAT(//////////,'  UNREAL EVERYTHING WORKED !')
      IF(IPLOT.NE.1)GO TO 455
      CALL CGPL(XG,YG,YG,NNG,1,1,1,4,1,-200.,200.,24.,
     1-200.,200.,16.,TITLE,6)
      DO 470 KL=1,NNTP
      XPF(1)=XP(KL,1)
      YPF(1)=YP(KL,1)
      CALL CGPL(XPF,YPF,XPF,1,4,1,1,1,1,-200.,200.,24.,
     1-200.,200.,16.,TITLE,6)
  470 CONTINUE
      NPH=NPH+1
      DO 458 I=1,NNTP
      DO 459 K=1,NPH
      XPF(K)=XP(I,K)
  459 YPF(K)=YP(I,K)
  458 CALL CGPL(XPF,YPF,XPF,NPH,130,1,1,4,1,-200.,200.,24.,
     1-200.,200.,16.,TITLE,6)
      CALL CGPL(XPF,YPF,XPF,NPH,0,1,1,4,1,-200.,200.,24.,
```

```
     1-200.,200.,16.,TITLE,6)
 455  CONTINUE
      STOP
      END
      SUBROUTINE CST
      COMMON E(10),PR(10),RO(10),X(350),Y(350),U(350),V(350),TH(600),
     1STIF(700,140),AP(700),ESTIF(6,6),ECM(3,3),EBM(3,6),ESM(3,6),WT
      COMMON NUMNP,NUMEL,NUMAT,KODE(350),NP(3,600),MAT(600),MBAND,
     1 NEQ,M,LM(6)
      COMMON KODE1(350)
      COMMON SIGC(10,4),AA(10,4),BB(10,4),KO(10),ZSFC
      COMMON DSIGEL(600,3),SIGIEL(600,3),DSIGA(350,3),SIGIA(350,3)
      COMMON TSIGEL(600,3),TSIGA(350,3),TB(700)
      COMMON UN(350),VN(350),NNYL(25),NNXL(25)
      COMMON EE(600),PRT(600),TSIGEP(600,2)
      COMMON PHI,XK,XEP
      COMMON DI(700)
      REAL KO
C
C
      CALL ASTIF
C
      CALL BAND1
C
      CALL STRESS
      RETURN
      END
      SUBROUTINE ASTIF
C
C     THIS SUBROUTINE TAKES EACH ELEMENT IN TURN AND FORMS THE ELEMENT STIFF
C     MATRIX (BY CALLING ELSTIF).IT ASSEMBLES THE ELEMENT STIFFNESSES INTO
C     KSTIF , ASSEMBLES THE APPLIED LOAD VECTOR (AP), AND MODIFIES THE
C     ASSEMBLAGES FOR DISPLACEMENT BOUNDARY CONDITIONS (BY CALLING MODIFY)
C
      COMMON E(10),PR(10),RO(10),X(350),Y(350),U(350),V(350),TH(600),
     1STIF(700,140),AP(700),ESTIF(6,6),ECM(3,3),EBM(3,6),ESM(3,6),WT
      COMMON NUMNP,NUMEL,NUMAT,KODE(350),NP(3,600),MAT(600),MBAND,
     1 NEQ,M,LM(6)
      COMMON KODE1(350)
      COMMON SIGC(10,4),AA(10,4),BB(10,4),KO(10),ZSFC
      COMMON DSIGEL(600,3),SIGIEL(600,3),DSIGA(350,3),SIGIA(350,3)
      COMMON TSIGEL(600,3),TSIGA(350,3),TB(700)
      COMMON UN(350),VN(350),NNYL(25),NNXL(25)
      COMMON EE(600),PRT(600),TSIGEP(600,2)
      COMMON PHI,XK,XEP
      COMMON DI(700)
      REAL KO
C
C   INITIALIZE APPLIED LOAD VECTOR AND MASTER STIFFNESS MATRIX AND ECM
C
      DO 10 I=1,NEQ
      AP(I)=0.0
      DO 10 J=1,MBAND
 10    STIF(I,J)=0.0
      DO 20 I=1,3
      DO 20 J=1,3
 20   ECM(I,J)=0.0
C   FORM ELEMENT CONSTITUTIVE MATRIX (ECM) IF NUMAT=1)
C
      IF(NUMAT.NE.1) GO TO 30
```

```
      EPR=PR(1)
      COM=E(1)/((1.+EPR)*(1.-2.*EPR))
      COM1=COM*(1.-EPR)
      COM2=COM*EPR
      ECM(1,1)=COM1
      ECM(2,2)=COM1
      ECM(1,2)=COM2
      ECM(2,1)=COM2
      ECM(3,3)=E(1)/(2.*(1.+EPR))
C
   30 DO 45 M=1,NUMEL
C
      CALL ELSTIF(1)
C
C   ASSEMBLE ELSTIF INTO MASTER STIFFNESS MATRIX
C
      DO 35 I=1,3
      I2=2*I
      LM(I2)=2*NP(I,M)
   35 LM(I2-1)=LM(I2)-1
C
C
      DO 40 I=1,6
      II=LM(I)
      DO 40 J=1,6
      JJ=LM(J)-II+1
      IF (JJ.LE.0) GO TO 40
       STIF(II,JJ)= STIF(II,JJ)+ESTIF(I,J)
   40 CONTINUE
C
C   ADD GRAVITY LOADS INTO AP VECTOR
C
      DO 45 I=2,6,2
      II=LM(I)
      AP(II)=AP(II)-WT
   45 CONTINUE
C
C   ADD NODAL LOADS INTO AP VECTOR
C
      DO 50 N=1,NUMNP
      N2=2*N
      AP(N2)=AP(N2)+V(N)
   50 AP(N2-1)=AP(N2-1)+U(N)
C
C   MODIFY STIFFNESS AND LOAD VECTOR FOR DISPLACEMENT BOUNDARY CONDITIONS.
C
      DO 100 N=1,NUMNP
      N2=2*N
      IF (KODE(N)-10) 80,70,60
   60 II=N2-1
      CALL MODIFY(II,N)
      CALL MODIFY(N2,N)
      GO TO 100
   70 II=N2-1
      CALL MODIFY(II,N)
      GO TO 100
   80 IF(KODE(N).EQ.0)  GO TO 100
      CALL MODIFY(N2,N)
  100 CONTINUE
C
```

```
      RETURN
      END
      SUBROUTINE ELSTIF(KOP)
C  THIS SUBROUTINE FORMS THE ELEMENT STIFFNESS MATRIX (ESTIF) OR
C  ELEMENT STRESS MATRIX (ESM) FOR THE CONSTANT STRAIN TRIANGLE
C
      COMMON E(10),PR(10),RO(10),X(350),Y(350),U(350),V(350),TH(600),
     1STIF(700,140),AP(700),ESTIF(6,6),ECM(3,3),EBM(3,6),ESM(3,6),WT
      COMMON NUMNP,NUMEL,NUMAT,KODE(350),NP(3,600),MAT(600),MBAND,
     1 NEQ,M,LM(6)
      COMMON KODE1(350)
      COMMON SIGC(10,4),AA(10,4),BB(10,4),KO(10),ZSFC
      COMMON DSIGEL(600,3),SIGIEL(600,3),DSIGA(350,3),SIGIA(350,3)
      COMMON TSIGEL(600,3),TSIGA(350,3),TB(700)
      COMMON UN(350),VN(350),NNYL(25),NNXL(25)
      COMMON EE(600),PRT(600),TSIGEP(600,2)
      COMMON PHI,XK,XEP
      COMMON DI(700)
      REAL KO
C
      DIMENSION AV(3),BV(3)
C
      DO 10 I=1,3
      DO 10 J=1,6
10    EBM(I,J)=0.0
      I=NP(1,M)
      J=NP(2,M)
      K=NP(3,M)
C
C   FORM ELEMENT DIMENSIONS
C
      AV(1)=X(K)-X(J)
      AV(2)=X(I)-X(K)
      AV(3)=X(J)-X(I)
      BV(1)=Y(J)-Y(K)
      BV(2)=Y(K)-Y(I)
      BV(3)=Y(I)-Y(J)
      AREA2=AV(3)*BV(2)-AV(2)*BV(3)
      IF (TH(M).EQ.0.) TH(M)=1.
      VOL=TH(M)*AREA2/2.
      IF (VOL.LE.0.) GO TO 75
C   FORM CONSTITUTIVE MATRIX
C
      IF (NUMAT.EQ.1) GO TO 30
      NM=MAT(M)
      EPR=PRT(M)
      COM=EE(M)/((1.+EPR)*(1.-2.*EPR))
      COM1=COM*(1.-EPR)
      COM2=COM*EPR
      ECM(1,1)=COM1
      ECM(2,2)=COM1
      ECM(1,2)=COM2
      ECM(2,1)=COM2
      ECM(3,3)=EE(M)/(2.*(1.+EPR))
C
C   FORM ELEMENT B MATRIX (EBM)
C
30    DO 40 I=1,3
      I2=2*I
      I2M=2*I-1
```

```
      EBM(1,I2M)=BV(I)/AREA2
      EBM(2,I2)=AV(I)/AREA2
      EBM(3,I2M)=EBM(2,I2)
 40   EBM(3,I2)=EBM(1,I2M)
C
C   FORM ELEMENT STRESS MATRIX (ESM)
C
      DO 50 I=1,3
      DO 50 J=1,6
      ESM(I,J)=0.0
      DO 50 K=1,3
   50 ESM(I,J)=ESM(I,J)+ECM(I,K)*EBM(K,J)
C
      IF(KOP.EQ.2) GO TO 80
      IF(NUMAT.EQ.1)  NM=1
      WT=VOL*RO(NM)/3.
C
C     FORM ELEMENT STIFFNESS MATRIX (ESTIF)
C
      DO 70 I=1,6
      DO 70 J=1,6
      ESTIF(I,J)=0.0
      DO 60 K=1,3
 60   ESTIF(I,J)=ESTIF(I,J)+EBM(K,I)*ESM(K,J)
 70   ESTIF(I,J)=ESTIF(I,J)*VOL
      GO TO 80
 75   WRITE(6,1000) M
      CALL EXIT
 80   RETURN
C
C
 1000 FORMAT (1H1, 18H VOLUME OF ELEMENT ,I4, 18H IS LESS THAN ZERO)
C
      END
      SUBROUTINE MODIFY (I,N)
C
C  THIS SUBROUTINE MODIFIES KSTIF AND AP IF A DISPLACEMENT BOUNDARY CONDITIO
C  IS IMPOSED IN EQUATION I ASSOCIATED WITH NODAL POINT N
C
      COMMON E(10),PR(10),RO(10),X(350),Y(350),U(350),V(350),TH(600),
     1STIF(700,140),AP(700),ESTIF(6,6),ECM(3,3),EBM(3,6),ESM(3,6),WT
      COMMON NUMNP,NUMEL,NUMAT,KODE(350),NP(3,600),MAT(600),MBAND,
     1 NEQ,M,LM(6)
      COMMON KODE1(350)
      COMMON SIGC(10,4),AA(10,4),BB(10,4),KO(10),ZSFC
      COMMON DSIGEL(600,3),SIGIEL(600,3),DSIGA(350,3),SIGIA(350,3)
      COMMON TSIGEL(600,3),TSIGA(350,3),TB(700)
      COMMON UN(350),VN(350),NNYL(25),NNXL(25)
      COMMON EE(600),PRI(600),TSIGEP(600,2)
      COMMON PHI,XK,XEP
      COMMON DI(700)
      REAL KO
C
      DISP=U(N)
      IF((I-2*N).EQ.0)  DISP=V(N)
C
      DO 50 J=2,MBAND
      IL=I+J-1
      IU=I-J+1
      IF(IU.LE.0) GO TO 10
```

```
      AP(IU)=AP(IU) - STIF(IU,J)*DISP
       STIF(IU ,J)=0.0
10    IF(IL.GT.NEQ) GO TO 50
      AP(IL)= AP(IL)- STIF(I,J)*DISP
       STIF(I,J)=0.0
50    CONTINUE
      AP(I)=DISP
       STIF(I,1)=1.0
      RETURN
      END
      SUBROUTINE BAND1
C
C  THIS SUBROUTINE SOLVES FOR DISPLACEMENTS USING A GAUSSIAN ELIMINATION
C  TECHNIQUE FOR SYMMETRIC BANDED MATRICES STORED IN CORE
C
      COMMON E(10),PR(10),RO(10),X(350),Y(350),U(350),V(350),TH(600),
     1 A(700,140), B(700),ESTIF(6,6),ECM(3,3),EBM(3,6),ESM(3,6),WT
      COMMON NUMNP,NUMEL,NUMAT,KODE(350),NP(3,600),MAT(600),MM,
     1  NN ,M,LM(6)
      COMMON KODE1(350)
      COMMON SIGC(10,4),AA(10,4),BB(10,4),KO(10),ZSPC
      COMMON DSIGEL(600,3),SIGIEL(600,3),DSIGA(350,3),SIGIA(350,3)
      COMMON TSIGEL(600,3),TSIGA(350,3),TB(700)
      COMMON UN(350),VN(350),NNYL(25),NNXL(25)
      COMMON EE(600),PRT(600),TSIGEP(600,2)
      COMMON PHI,XK,XEP
      COMMON DI(700)
      REAL KO
C
C TRIANGULARIZE AND REDUCE RIGHT HAND SIDE
      NL=NN-MM+1
      NM=NN-1
      MR=MM
C
      DO 100 N=1,NM
      IF (A(N,1).LE.0.) GO TO 700
      BN=B(N)
      B(N)=BN/A(N,1)
      IF (N.GT.NL) MR=NN-N+1
C
      DO 100 L=2,MR
      IF (A(N,L).EQ.0.)GO TO 100
      C= A(N,L)/A(N,1)
      I= N+L-1
      J= 0
      DO 50 K=L,MR
      J=J+1
50    A(I,J)= A(I,J)-C*A(N,K)
      B(I)=B(I)-C*BN
      A(N,L)=C
100   CONTINUE
C
C   BACK SUBSTITUTE
C
      I=NN
C
      B(NN)=B(NN)/A(NN,1)
      DO 600 N=1,NM
      I=I-1
      IF (N.LT.MM)      MR= N+1
```

```
      DO 600 J=2,MR
      K=I+J-1
600   B(I) =B(I)- A(I,J)*B(K)
      DO 30 I=1,NN
  30  DI(I)=B(I)
      RETURN
700   WRITE (6,2000) N
      CALL EXIT
2000  FORMAT(1H0, 81H ZERO OR NEGATIVE ELEMENT ON  MAIN DIAGONAL OF TRIA
     1NGULARIZED MATRIX FOR EQUATION  ,I5)
C
      END
      SUBROUTINE STRESS
C
C   THIS SUBROUTINE FORMS THE ELEMENT STRESS MATRIX (ESM),MULTIPLIES BY
C   THE ELEMENT DISPLACEMENT VECTOR (ELDISP)AND RECORDS THE STRESSES IN
C   SIGEL. IT THEN COMPUTES THE PRINCIPAL STRESSES AND DIRECTIONS(SIGP)
C
      COMMON E(10),PR(10),RO(10),X(350),Y(350),U(350),V(350),TH(600),
     1STIF(700,140),AP(700),ESTIF(6,6),ECM(3,3),EBM(3,6),ESM(3,6),WT
      COMMON NUMNP,NUMEL,NUMAT,KODE(350),NP(3,600),MAT(600),MBAND,
     1 NEQ,M,LM(6)
      COMMON KODE1(350)
      COMMON SIGC(10,4),AA(10,4),BB(10,4),KO(10),ZSPC
      COMMON DSIGEL(600,3),SIGIEL(600,3),DSIGA(350,3),SIGIA(350,3)
      COMMON TSIGEL(600,3),TSIGA(350,3),TB(700)
      COMMON UN(350),VN(350),NNYL(25),NNXL(25)
      COMMON EE(600),PRT(600),TSIGEP(600,2)
      COMMON PHI,XK,XEP
      COMMON DI(700)
      REAL KO
C
      DIMENSION SIGEL(600,3),SIGP(600,4),ELDISP(6),SIGA(350,3),
     1  KOUNT(350)
      EQUIVALENCE ( STIF(1,1),SIGEL(1,1)),( STIF(1,4),SIGP(1,1)),
     1  (STIF(1,8),SIGA(1,1))
C
      DO 5 N=1,NUMNP
      KOUNT(N)=0
      DO 5 J=1,3
5     SIGA(N,J)=0.0
C
      DO 100 M=1,NUMEL
C   COMPUTE ELEMENT DISPLACEMENTS
C
      DO 10 I=1,3
      I2=2*I
      LMI2  =2*NP(I,M)
      ELDISP(I2)=AP(LMI2)
10    ELDISP(I2-1)=AP(LMI2-1)
C
C  COMPUTE  ELEMENT STRESSES
C
      CALL ELSTIF(2)
C
      DO 20 I=1,3
      SIGEL(M,I)=0.0
      DO 20 J=1,6
20    SIGEL(M,I)=SIGEL(M,I)+ESM(I,J)*ELDISP(J)
C
```

```
C  ACCUMULATE FOR NODAL STRESSES
C
      DO 30 K=1,3
      N=NP(K,M)
      KOUNT(N)=KOUNT(N)+1
      DO 30 I=1,3
30    SIGA(N,I)=SIGA(N,I) + SIGEL(M,I)
C
C  COMPUTE ELEMENT PRINCIPAL STRESSES  AND DIRECTIONS
C
      SIGM=(SIGEL(M,1)+SIGEL(M,2))/2.
      SIGD2=(SIGEL(M,1)-SIGEL(M,2))/2.
      RAD =SQRT(SIGD2**2 +SIGEL(M,3)**2)
      SIGP(M,1)=SIGM+RAD
      SIGP(M,2)= SIGM-RAD
      SIGP(M,3)= RAD
      IF(SIGP(M,3).LT.0.01.AND.SIGP(M,3).GT.-0.01)GO TO 700
      SIGP(M,4)= 0.5*57.29578*ATAN2(SIGEL(M,3),SIGD2)
      GO TO 100
  700 SIGP(M,4)=0.
100   CONTINUE
C
C  FIND AVERAGE NODAL STRESSES
C
      DO 110 N=1,NUMNP
      RK=KOUNT(N)
      DO 110 I=1,3
110   SIGA(N,I)= SIGA(N,I)/RK
      DO 47 M=1,NUMEL
      DO 47 I=1,3
   47 DSIGEL(M,I)=-SIGEL(M,I)
      DO 48 N=1,NUMNP
      DO 48 I=1,3
   48 DSIGA(N,I)=-SIGA(N,I)
      END
C
C
C
C   SUBROUTINE DETE
C
C
C
      SUBROUTINE DETE(NIPRIE,NPHASE,IJ)
C
C
C
C   THIS SUBROUTINE DETERMINES E FOR EACH ELEMENT
C
C
C
       COMMON E(10),PR(10),RO(10),X(350),Y(350),U(350),V(350),TH(600),
      1STIF(700,140),AP(700),ESTIF(6,6),FCM(3,3),EBM(3,6),ESM(3,6),WT
       COMMON NUMNP,NUMEL,NUMAT,KODE(350),NP(3,600),MAT(600),MBAND,
      1 NEQ,M,LM(6)
       COMMON KODE1(350)
       COMMON SIGC(10,4),AA(10,4),BB(10,4),KO(10),ZSFC
       COMMON DSIGEL(600,3),SIGIEL(600,3),DSIGA(350,3),SIGIA(350,3)
       COMMON TSIGEL(600,3),TSIGA(350,3),TB(700)
       COMMON UN(350),VN(350),NNYL(25),NNXL(25)
       COMMON PE(600),PET(600),TSIGEP(600,2)
```

```
      COMMON PHI,XK,XEP
      COMMON DI(700)
      REAL KO
      EP1(SIG3,SIG1,AA,BB)=AA*(SIG1-SIG3)/(1.-(SIG1-SIG3)*BB)
      E1(AA,BB,FEP1,PR)=2.*PR*AA*100./(AA+BB*FEP1)**2
      EP2(SIG3,SIG1,SIG3I,SIG1I,AA,BB)=AA*((SIG3-SIG1)-
     1(SIG3I-SIG1I))/(1.-((SIG3-SIG1)-(SIG3I-SIG1I))*BB)
      E2(AA,BB,FEP2)=AA*100./(AA+BB*FEP2)**2
      EP5(SIG3,SIG1,SIG3I,SIG1I,AA,BB)=AA*((SIG1-SIG3)-
     1(SIG1I-SIG3I))/(1.-((SIG1-SIG3)-(SIG1I-SIG3I))*BB)
      E5(AA,BB,FEP5,P)=(AA*100./(AA+BB*FEP5)**2)*P*(1.+P)
      EP7(SIG3,SIG1,AA,BB)=AA*(SIG1-SIG3)/(1.-(SIG1-SIG3)*BB)
      E7(AA,BB,FEP7)=AA*100./(AA+BB*FEP7)**2
      IF(NIPRIE.EQ.1)GO TO 450
      IF(NPHASE.NE.7) GO TO 451
      IF(IJ.NE.4)GO TO 451
  450 WRITE(6,105)
  105 FORMAT(1H1,5X,'NEW STRESS STRAIN PARAMETERS',//,1X,
     1'   EL  MAT    SIGX IN    SIGY IN        SIG1        SIG3',
     26X,'SIGX        SIGY        ETANGENT')
  451 CONTINUE
      DO 999 M=1,NUMEL
C
C   PRINCIPAL STRESSES
C
      S2=TSIGEP(M,2)
      S1=TSIGEP(M,1)
      S3=S1-S2
      T1=SIGIEL(M,1)
      T2=SIGIEL(M,2)
C
C   MATERIAL NUMBER 1
C
      IF(MAT(M).NE.1) GO TO 1
      PRT(M)=PR(1)
      V1=SIGC(1,1)/KO(1)
      V2=SIGC(1,2)/KO(1)
      V3=SIGC(1,3)/KO(1)
C
C   CHECKING WHERE SIGMA3 INITIAL STANDS
C
      IF(SIGIEL(M,1).LT.SIGC(1,1))GO TO 83
      IF(SIGIEL(M,1).GT.SIGC(1,3)) GO TO 81
      IF(SIGIEL(M,1).GT.SIGC(1,2)) GO TO 82
C
C   SU ALWAYS IS A VALUE OF DEVIATOR STRESS ABOVE
C   WHICH IT IS TOO CLOSE TO FAILURE.
C   IF THAT HAPPENS E VALUE IS ASSUMED A VERY SMALL
C   VALUE TO AVOID PROBLEMS WHEN CALCULATING EPSILON1
C
      SU=0.95/BB(1,1)
      AS=SIGC(1,1)
      AB=SIGC(1,2)
      IF(S3.GT.SU) GO TO 41
      XS=EP1(S2,S1,AA(1,1),BB(1,1))
      ES=E1(AA(1,1),BB(1,1),XS,PR(1))
  100 FORMAT(5F15.5)
      GO TO 42
   41 ES=20.
   42 SU=0.95/BB(1,2)
```

```
      IF(S3.GT.SU) GO TO 43
      XB=EP1(S2,S1,AA(1,2),BB(1,2))
      EB=E1(AA(1,2),BB(1,2),XB,PR(1))
      GO TO 99
   43 EB=20.
C
C
C   INTERPOLATING E VALUE
C   IF SIGMA3 INITIAL SMALLER THAN THE ANY OF THE TESTS
C   USE STRESS STRAIN CURVE WHERE A=A(1,1)
C   B FUNCTION OF PHI AND SIGMA VERTICAL
C   FOR THIS PARTICULAR CASE SIN(PHI)=.642
C   IF SIGMA3 INITIAL GREATER THAN ANY OF THE TESTS
C   USE STRESS STRAIN CURVE FOR THE GREATEST SIGMA3
C
C
   99 EE(M)=(EB*(SIGIEL(M,1)-AS)+ES*(AB-SIGIEL(M,1)))/(AB-AS)
      GO TO 10
   82 SU=0.95/BB(1,2)
      AS=SIGC(1,2)
      AB=SIGC(1,3)
      IF(S3.GT.SU) GO TO 44
      XS=EP1(S2,S1,AA(1,2),BB(1,2))
      ES=E1(AA(1,2),BB(1,2),XS,PR(1))
      GO TO 45
   44 ES=20.
   45 SU=0.95/BB(1,3)
      IF(S3.GT.SU) GO TO 46
      XB=EP1(S2,S1,AA(1,3),BB(1,3))
      EB=E1(AA(1,3),BB(1,3),XB,PR(1))
      GO TO 99
   46 EB=20.
      GO TO 99
   81 SU=0.95/BB(1,3)
      IF(S3.GT.SU) GO TO 40
      XX=EP1(S2,S1,AA(1,3),BB(1,3))
      EE(M)=E1(AA(1,3),BB(1,3),XX,PR(1))
      GO TO 10
   83 BE=(1.+.642)/(2.*.642*T2)
      SU=.95/BE
      IF(S3.GT.SU) GO TO 40
      XX=EP1(S2,S1,AA(1,1),BE)
      EE(M)=E1(AA(1,1),BE,XX,PR(1))
      GO TO 10
   40 EE(M)=20.
      GO TO 10
C
C   MATERIAL NUMBER 2
C
    1 IF(MAT(M).NE.2)GO TO 2
      PRT(M)=PR(2)
      S3=-S3
      IF(TSIGEL(M,2).GT.TSIGEL(M,1)) GO TO 101
      TEMP=S2
      S2=S1
      S1=TEMP
      S3=-S3
  101 V1=SIGC(2,1)/KO(2)
      V2=SIGC(2,2)/KO(2)
      V3=SIGC(2,3)/KO(2)
```

```
C
C   CHECKING WHERE SIGMA3 INITIAL STANDS
C
      IF(SIGIEL(M,1).LT.SIGC(2,1))GO TO 13
      IF(SIGIEL(M,1).GT.SIGC(2,3))GO TO 11
      IF(SIGIEL(M,1).GT.SIGC(2,2)) GO TO 12
C
C   SIGMA3 IN BETWEEN TESTS 1 AND 2
C
      SU=0.95*((T1-T2)+1./BB(2,1))
      AS=SIGC(2,1)
      AB=SIGC(2,2)
      IF(S3.GT.SU) GO TO 48
      XS=EP2(S2,S1,T1,T2,AA(2,1),BB(2,1))
      IF(XS)321,321,322
 321  XS=0.
 322  ES=E2(AA(2,1),BB(2,1),XS)
      GO TO 47
   48 ES=20.
   47 SU=0.95*((T1-T2)+1./BB(2,2))
      IF(S3.GT.SU) GO TO 58
      XB=EP2(S2,S1,T1,T2,AA(2,2),BB(2,2))
      IF(XB) 323,323,324
 323  XB=0.
 324  EB=E2(AA(2,2),BB(2,2),XB)
      GO  TO 99
   58 EB=20.
      GO TO 99
C
C   SIGMA3 IN BETWEEN TESTS 2 AND 3
C
   12 SU=0.95*((T1-T2)+1./BB(2,2))
      AS=SIGC(2,2)
      AB=SIGC(2,3)
      IF(S3.GT.SU) GO TO 55
      XS=EP2(S2,S1,T1,T2,AA(2,2),BB(2,2))
      IF(XS) 325,325,326
 325  XS=0.
 326  ES=E2(AA(2,2),BB(2,2),XS)
      GO TO 56
   55 ES=20.
   56 SU=0.95*((T1-T2)+1./BB(2,3))
      IF(S3.GT.SU) GO TO 57
      XB=EP2(S2,S1,T1,T2,AA(2,3),BB(2,3))
      IF(XB)327,327,328
 327  XB=0.
 328  EB=E2(AA(2,3),BB(2,3),XB)
      GO TO 99
   57 EB=20.
      GO TO 99
C
C   SIGMA3 GREATER THAN TEST 3
C
   11 SU=0.95*((T1-T2)+1./BB(2,3))
      IF(S3.GT.SU) GO TO 40
      XX=EP2(S2,S1,T1,T2,AA(2,3),BB(2,3))
      IF(XX) 329,329,330
 329  XX=0.
 330  EB(M)=E2(AA(2,3),BB(2,3),XX)
      GO TO 10
```

```
C
C   SIGMA3 SMALLER THAN TEST 1
C
   13 SU=0.95*((T1-T2)+1./BB(2,1))
      IF(S3.GT.SU) GO TO 40
      XX=EP2(S2,S1,T1,T2,AA(2,1),BB(2,1))
      IF(XX)331,331,332
  331 XX=0.
  332 EE(M)=E2(AA(2,1),BB(2,1),XX)
      GO TO 10
C
C   MATERIAL NUMBER 3
C
    2 IF(MAT(M).NE.3) GO TO 3
      V1=SIGIEL(M,2)
      PRT(M)=PR(3)
      T3=(T2-T2)*0.95
      IF(S3.LT.T3) GO TO 31
C
C   IF DEVIATOR STRESS GREATER THAN INITIAL DEVIATOR STRESS
C   USE STRESS STRAIN CURVE DISPLACED BY INITIAL DEVIATOR STRESS
C
      SU=1.00*((T2-T1)+1./BB(3,1))
      IF(S3.GT.SU) GO TO 61
      XX=EP2(S1,S2,T2,T1,AA(3,1),BB(3,1))
      EE(M)=E1(AA(3,1),BB(3,1),XX,PR(3))
      GO TO 10
   61 EE(M)=20.
      GO TO 10
C
C   IF DEVIATOR STRESS LESS THAN INITIAL DEVIATOR STRESS
C   USE E FOR LOADING UNLOADING ACCORDING TO THIS STRESS PATH
C
   31 EE(M)=E(3)
      GO TO 10
C
C   MATERIAL NUMBER 4
C
    3 IF(MAT(M).NE.4) GO TO 4
      EE(M)=E(4)
      PRT(M)=PR(4)
      GO TO 10
C
C   MATERIAL NUMBER 5
C
    4 IF(MAT(M).NE.5) GO TO 5
      PRT(M)=PR(5)
      V1=SIGC(5,1)/KO(5)
      V2=SIGC(5,2)/KO(5)
      IF(SIGIEL(M,1).LT.SIGC(5,1)) GO TO 51
      IF(SIGIEL(M,1).GT.SIGC(5,2)) GO TO 51
C
C   INTERPOLATION OF E
C
      SU=0.95*((T2-T1)+1./BB(5,1))
      AS=SIGC(5,1)
      AB=SIGC(5,2)
      IF(S3.GT.2.) GO TO 63
      IF(S2.LT.0.) GO TO 63
      XS=EP5(S2,S1,T1,T2,AA(5,1),BB(5,1))
```

```
      IF(XS)400,400,401
  400 XS=0.
  401 ES=E5(AA(5,1),BB(5,1),XS,PR(5))
      GO TO 64
   63 ES=20.
   64 SU=0.95*((T2-T1)+1./BB(5,2))
      IF(S3.GT.2.5)GO TO 65
      IF(S2.LE.0.)GO TO 65
      XB=EP5(S2,S1,T1,T2,AA(5,2),BB(5,2))
      IF(XB)402,402,403
  402 XB=0.
  403 EB=E5(AA(5,2),BB(5,2),XB,PR(5))
      GO TO99
   65 EB=20.
      GO TO 99
C
C
C   IF SIGMA3 GREATER THAN THE GREATEST OF SIGMA3 IN THE
C   TESTS ASSUME THE SAME STRESS STRAIN CURVE SHIFTED
C   BY INITIAL DEVIATOR STRESS
C
C
   61 IF(S2.LT.0.)GO TO 62
      SU=T2
      IF(S3.GT.SU)GO TO 62
      EYOI=7.696*(T1/1.033)**0.9436
      AE=1./EYOI
      BE=(0.25+AE*(T2-T1-T2))/(.25*(T2-(T2-T1)))
      XX=EP5(S2,S1,T1,T2,AE,BE)
      IF(XX)404,404,405
  404 XX=0.
  405 EE(M)=E5(AE,BE,XX,PR(5))
      GO TO 10
   62 EE(M)=20.
      GO TO 10
C
C   MATERIAL NUMBER 6
C
    5 IF(MAT(M).NE.6) GO TO 6
      EE(M)=E(6)
      PRT(M)=PR(6)
      GOTO 10
C
C   MATERIAL NUMBER 7
C
    6 IF(MAT(M).NE.7) GO TO 7
      PRT(M)=PR(7)
C
C   CHECKING WHERE SIGMA3 STANDS
C
      IF(S2.LT.SIGC(7,1)) GO TO 73
      IF(S2.GT.SIGC(7,3)) GO TO 71
      IF(S2.GT.SIGC(7,2)) GO TO 72
C
C   IF SIGMA3 IS IN BETWEEN TETS 1 AND 2
C
      SU=0.95/BB(7,1)
      AS=SIGC(7,1)
      AB=SIGC(7,2)
      IF(S3.GT.SU) GO TO 66
```

```
      XS=EP7(S2,S1,AA(7,1),BB(7,1))
      IF(XS) 301,301,302
301   XS=0.
302   ES=E7(AA(7,1),BB(7,1),XS)
      GO TO 67
   66 ES=20.
   67 SU=0.95/BB(7,2)
      IF(S3.GT.SU) GO TO 68
      XB=EP7(S2,S1,AA(7,2),BB(7,2))
      IF(XB)303,303,304
303   XB=0.
304   EB=E7(AA(7,2),BB(7,2),XB)
      GO TO 89
   68 EB=20.
      GO TO 89
C
C   IF SIGMA3 STANDS IN BETWEEN TESTS 2 AND 3
C
   72 SU=0.95/BB(7,2)
      AS=SIGC(7,2)
      AB=SIGC(7,3)
      IF(S3.GT.SU) GO TO 84
      XS=EP7(S2,S1,AA(7,2),BB(7,2))
      IF(XS) 305,305,306
305   XS=0.
306   ES=E7(AA(7,2),BB(7,2),XS)
      GO TO 85
   84 ES=20.
   85 SU=0.95/BB(7,3)
      IF(S3.GT.SU) GO TO 86
      XB=EP7(S2,S1,AA(7,3),BB(7,3))
      IF(XB)307,307,308
307   XB=0.
308   EB=E7(AA(7,3),BB(7,3),XB)
      GO TO 89
   86 EB=20.
      GO TO 89
C
C   IF SIGMA3 GREATER THAN IN TEST 3
C
   71 SU=0.95/BB(7,3)
      IF(S3.GT.SU) GO TO 95
      XX=EP7(S2,S1,AA(7,3),BB(7,3))
      IF(XX) 309,309,310
309   XX=0.
310   EE(M)=E7(AA(7,3),BB(7,3),XX)
      GO TO 10
C
C   IF SIGMA3 SMALLER THAN IN TEST 1
C   USE STRESS STRAIN CURVE WHERE
C   B FUNCTION OF PHI AND SIGMA HORIZONTAL
C   A FUNCTION OF SIGMA3 , XK AND XEP
C
   73 IF(S2.LT.0.5) GO TO 95
      AE=1./(XK*1.033*(S2/1.033)**XEP)
      BE=(1.-SIN(PHI))/(2.*S2*SIN(PHI))
       SU=0.95/BE
      IF(S3.GT.SU) GO TO 95
      XX=EP7(S2,S1,AE,BE)
      IF(XX)311,311,312
```

```
  311   XX=0.
  312   EE(M)=(E7(AE,BE,XX))/100.
        GO TO 10
   95 EE(M)=20.
        GO TO 10
   60 EE(M)=(EB*(TSIGEP(M,2)-AS)+ES*(AB-TSIGEP(M,2)))
      1/(AB-AS)
        GO TO 10
C
C   MATERIAL NUMBER 8
C
    7   IF(MAT(M).NE.8) GO TO 8
        PRT(M)=PR(8)
        EE(M)=E(8)
         GO TO 10
C
C   MATERIAL NUMBER 9
C
    8   IF(MAT(M).NE.9) GO TO 200
        IF(S2.LT.0.2) GO TO 103
        PRT(M)=PR(9)
        BE=(1.-1.143*SIN(PHI))/(2.*S2*1.143*SIN(PHI))
        SU=0.75/BE
        IF(S3.GT.SU) GO TO 103
        XX=EP7(S2,S1,AA(9,1),BE)
        EE(M)=E7(AA(9,1),BE,XX)
        GO TO 10
  103 EE(M)=20.
        GO TO 10
  200   PRT(M)=PR(10)
        EE(M)=E(10)
        IF(TSIGEL(M,1).LT.0.) EE(M)=10.
   10   IF(NIPRIE.EQ.1) GO TO 998
        IF(NPHASE.NE.7) GO TO 999
        IF(IJ.NE.4) GO TO 999
  998   WRITE(6,93) M,MAT(M),SIGIEL(M,1),SIGIFL(M,2),TSIGEP(M,1),
       1TSIGEP(M,2),TSIGEL(M,1),TSIGEL(M,2),EE(M)
   93 FORMAT(1X,2I5,6F10.3,F14.3)
  999 CONTINUE
        RETURN
        END
C
C
C
C   SUBROUTINE INIT
C
C
C
        SUBROUTINE INIT
C
C
C THIS SUBROUTINE CALCULATES THE INITIAL STRESSES
C AT THE NODES AND ELEMENTS
C
C
        COMMON E(10),PR(10),RO(10),X(350),Y(350),U(350),V(350),TH(600),
       1STIF(700,140),AF(700),ESTIF(6,6),ECM(3,3),EBM(3,6),ESM(3,6),WT
        COMMON NUMNP,NUMEL,NUMAT,KODE(350),NP(3,600),MAT(600),MBAND,
       1 NFC,M,L1(6)
        COMMON KODE1(350)
```

```
      COMMON SIGC(10,4),AA(10,4),BB(10,4),KO(10),ZSFC
      COMMON DSIGEL(600,3),SIGIEL(600,3),DSIGA(350,3),SIGIA(350,3)
      COMMON TSIGEL(600,3),TSIGA(350,3),TB(700)
      COMMON UN(350),VN(350),NNYL(25),NNXL(25)
      COMMON EE(600),PRT(600),TSIGEP(600,2)
      COMMON PHI,XK,XEP
      COMMON DI(700)
      REAL KO
C
C   READ SPECIFIC WEIGHT AND ELEVATION OF THE GROUND SURFACE
C
      READ(5,13)GAMA,ZSFC
      WRITE(6,10) GAMA,ZSFC
   10 FORMAT(//,5X,'SPECIFIC WEIGHT ',F10.5,/,5X,'HEIGHT',F10.3)
   13 FORMAT(2F10.3)
C
C   IF THE MATERIAL ELEMENT IS CONCRETE
C   SET INITIAL STRESSES = 0
C
      DO 1 M=1,NUMEL
      IF(MAT(M).NE.4) GO TO 2
      SIGIEL(M,1)=0.
      SIGIEL(M,2)=0.
      SIGIEL(M,3)=0.
      GO TO 1
C
C   INITIAL ELEMENT STRESSES
C
    2 I=NP(1,M)
      J=NP(2,M)
      K=NP(3,M)
      YEL=(Y(I)+Y(J)+Y(K))/3.
      DEPTH=ZSFC-YEL
      SIGIEL(M,2)=GAMA*DEPTH
      MATN=MAT(M)
      SIGIEL(M,1)=SIGIEL(M,2)*KO(MATN)
      SIGIEL(M,3)=0.
    1 CONTINUE
C
C   INITIAL NODE STRESSES
C
      DO 3 M=1,NUMNP
      IF(KODE1(M).NE.4) GO TO 4
      SIGIA(M,1)=0.
      SIGIA(M,2)=0.
      SIGIA(M,3)=0.
      GO TO 3
    4 DEPTH=ZSFC-Y(M)
      SIGIA(M,2)=GAMA*DEPTH
      MATN=KODE1(M)
      SIGIA(M,1)=SIGIA(M,2)*KO(MATN)
      SIGIA(M,3)=SIGIA(M,2)-SIGIA(M,1)
    3 CONTINUE
      RETURN
      END
C
C
C
C   SUBROUTINE NLOAD
C
```

```
C
C
      SUBROUTINE NLOAD(NPHASE,NIPRIN)
      COMMON E(10),PR(10),RO(10),X(350),Y(350),U(350),V(350),TH(600),
     1STIF(700,140),AP(700),ESTIF(6,6),ECM(3,3),EBM(3,6),ESM(3,6),WT
      COMMON NUMNP,NUMEL,NUMAT,KODE(350),NP(3,600),MAT(600),MBAND,
     1 NEQ,M,LM(6)
      COMMON KODE1(350)
      COMMON SIGC(10,4),AA(10,4),BB(10,4),KO(10),ZSFC
      COMMON DSIGEL(600,3),SIGIEL(600,3),DSIGA(350,3),SIGIA(350,3)
      COMMON TSIGEL(600,3),TSIGA(350,3),TB(700)
      COMMON UN(350),VN(350),NNYL(25),NNXL(25)
      COMMON EE(600),PRT(600),TSIGEP(600,2)
      COMMON PHI,XK,XEP
      COMMON DI(700)
      DIMENSION SIGNR(350,2),IEL(20)
C
C
C
C   THIS SUBROUTINE DETERMINES THE NEW LOADS DUE TO ANOTHER
C   CONSTRUCTION PHASE.IT CHANGES THE MATERIAL PROPERTIES FOR
C   THE MATERIAL WHICH HAS BEEN REMOVED OR CONCRETE WHICH
C   HAS BEEN POURED
C
C
C
      DO 35 I=1,NUMNP
      SIGNR(I,1)=0.
      SIGNR(I,2)=0.
      UN(I)=0.
   35 VN(I)=0.
      READ(5,1)NPHASE,NYL,NXL
      IF(NPHASE.EQ.0) RETURN
      WRITE(6,2)NPHASE
    2 FORMAT(1H1,/,5(1X,60('*'),/),2(1X,20('*'),20X,20('*'),/),
     11X,20('*'),'    PHASE NUMBER',I3,2X,20('*'),/,2(1X,
     220('*'),20X,20('*'),/),5(1X,60('*'),/),//////)
C
C   NYL NUMBER OF NODES LOADED VERTICALLY
C   NNYL NODE NUMBER WHICH WILL BE LOADED
C   NELI NUMBER OF ELEMENTS INVOLVED IN THIS NODE
C
      DO 40 I=1,NYL
      READ(5,1)NELI,NNYL(I)
      READ(5,1)(IEL(J),J=1,NELI)
      NN=NNYL(I)
      DO 41 K=1,NELI
   41 SIGNR(NN,2)=SIGNR(NN,2)+TSIGEL(IEL(K),2)
      XN=NELI
      SIGNR(NN,2)=SIGNR(NN,2)/XN
      WRITE(6,42)NN,SIGNR(NN,2)
   42 FORMAT(//,'  NODE NO ',I5,'  SIGY REMOVED',F10.5)
      WRITE(6,60)
   60 FORMAT(/,'    ELEMENTS INVOLVED')
      WRITE(6,3)(IEL(J),J=1,NELI)
   40 CONTINUE
C
C   NXL NUMBER OF NODES LOADED HORIZONTALLY
C   NNXL NODE NUMBER WHICH WILL BE LOADED
C   NELI NUMBER OF ELEMENTS INVOLVED IN THIS NODE
```

```
C
      DO 50 I=1,NXL
      READ(5,1) NELI,NNXL(I)
      READ(5,1) (IEL(J),J=1,NELI)
      NN=NNXL(I)
      DO 51 K=1,NELI
   51 SIGNR(NN,1)=SIGNR(NN,1)+TSIGEL(IEL(K),1)
      XN=NELI
      SIGNR(NN,1)=SIGNR(NN,1)/XN
      WRITE(6,52) NN,SIGNR(NN,1)
   52 FORMAT(//,'  NODE NO ',I5,'  SIGX REMOVED',F10.5)
      WRITE(6,60)
      WRITE(6,3) (IEL(J),J=1,NELI)
   50 CONTINUE
    1 FORMAT(10I5)
      WRITE(6,80)
   80 FORMAT(/,5X,'NODES LOADED HORIZ')
      WRITE(6,3) (NNXL(I),I=1,NXL)
    3 FORMAT(/,5X,5I7)
      WRITE(6,4)
    4 FORMAT(/,5X,'NODES LOADED VERT')
      WRITE(6,3) (NNYL(I),I=1,NYL)
      DO 5 I=1,NUMNP
C
C   LOADS IN THE X DIRECTION
C
      DO 6 J=1,NXL
      XLOAD=0.
      IF(I.EQ.NNXL(J))GO TO 7
      GO TO 6
C
C   CHECK IF IT IS THE LAST NODE AFFECTED
C
    7  IF(J.EQ.NXL) GO TO 9
C
      K=NNXL(J+1)
      DL=Y(K)-Y(I)
C
C   CHECK IF THE ADJACENT NODE HAS HIGHER STRESSES
C
      IF(SIGNR(K,1).GT.SIGNR(I,1)) GO TO 10
      XB=SIGNR(I,1)
      XS=SIGNR(K,1)
      XLOAD=XS*DL/2.+2./3.*0.5*(XB-XS)*DL
      XLOAD=XLOAD*TH(1)
      GO TO 9
   10 XB=SIGNR(K,1)
       XS=SIGNR(I,1)
      XLOAD=XS*DL/2.+1./3.*0.5*(XB-XS)*DL
      XLOAD=XLOAD*TH(1)
C
C   CHECK IF IT IS THE FIRST NODE AFFECTED
C
    9  IF(J.EQ.1) GO TO 12
      K=NNXL(J-1)
      DL=Y(I)-Y(K)
C
C   CHECK IF THE ADJACENT NODE HAS HIGHER STRESSES
C
      IF(SIGNR(K,1).GT.SIGNR(I,1)) GO TO 11
```

```
      XB=SIGNR(I,1)
      XS=SIGNR(K,1)
      XLOAD=XLOAD+(XS*DL/2.+2./3.*0.5*(XB-XS)*DL)*TH(1)
      GO TO 12
   11 XB=SIGNR(K,1)
      XS=SIGNR(I,1)
      XLOAD=XLOAD+(XS*DL/2.+1./3.*.5*(XB-XS)*DL)*TH(1)
   12 UN(I)=-XLOAD*1.1
    o CONTINUE
C
C   LOADS IN THE Y DIRECTION
C
      DO 13 J=1,NYL
      YLOAD=0.
      IF(I.EQ.NNYL(J)) GO TO 14
C
C   CHECK IF IT IS THE LAST NODE AFFECTED
C
      GO TO 13
   14 IF(J.EQ.NYL) GO TO 17
      K=NNYL(J+1)
      DL=X(K)-X(I)
C
C   CHECK IF THE ADJACENT NODE HAS HIGHER STRESSES
C
      IF(SIGNR(K,2).GT.SIGNR(I,2)) GO TO 16
      YB=SIGNR(I,2)
      YS=SIGNR(K,2)
      YLOAD=YS*DL/2.+2./3.*0.5*(YB-YS)*DL
      YLOAD=YLOAD*TH(1)
      GO TO 17
   16 YB=SIGNR(K,2)
      YS=SIGNR(I,2)
      YLOAD=YS*DL/2.+1./3.*0.5*(YB-YS)*DL
      YLOAD=YLOAD*TH(1)
   17 IF(J.EQ.1) GO TO 18
      K=NNYL(J-1)
      DL=X(I)-X(K)
C
C   CHECK IF THE ADJACENT NODE HAS HIGHER STRESSES
C
      IF(SIGNR(K,2).GT.SIGNR(I,2)) GO TO 19
      YB=SIGNR(I,2)
      YS=SIGNR(K,2)
      YLOAD=YLOAD+(YS*DL/2.+2./3.*0.5*(YB-YS)*DL)*TH(1)
      GO TO 18
   19 YB=SIGNR(K,2)
      YS=SIGNR(I,2)
      YLOAD=YLOAD+(YS*DL/2.+1./3.*0.5*(YB-YS)*DL)*TH(1)
   18 VN(I)=YLOAD
   13 CONTINUE
    5 CONTINUE
C
C
C   IF THERE IS ANY TRANSFER OF NODAL LOADS
C   DUE TO GEOMETRICAL CONFIGURATION ENTER NLD
C   NUMBER OF NODES WHICH WILL HAVE THE LOAD
C   TRANSFERRED OTHERWISE
C
C
```

```
      READ(5,1)NLD
      WRITE(6,501)NLD
  501 FORMAT(//,5X,'NUMBER OF NODES WHICH WILL HAVE ',
     1'THE LOAD TRANSFERRED',I5)
      IF(NLD.EQ.0)GO TO 502
      READ(5,1)NA,NB
      WRITE(6,503)NA,NB
  503 FORMAT(//,5X,'NODES CARRYING THE LOAD',2I10)
      DO 504 I=1,NLD
      READ(5,1)NU
      WRITE(6,505)NU
  505 FORMAT(//,5X,'NODE UNLOADED',I5)
C
C
C   TRANSFER THE LOAD OF NODE NU TO NODES NA NB
C   Y(NA) HAS TO BE GREATER THAN Y(NB)
C
C
      XXA=Y(NA)-Y(NU)
      XXL=Y(NA)-Y(NB)
      RB=UN(NU)*XXA/XXL
      RA=UN(NU)-RB
      UN(NU)=0.
      UN(NA)=UN(NA)+RA
  504 UN(NB)=UN(NB)+RB
  506 FORMAT(4F10.5)
      WRITE(6,21) (I,UN(I),VN(I),I=1,NUMNP)
  502 IF(NIPPIN.NE.1)GO TO 666
      WRITE(6,20)NPHASE
   20 FORMAT(//,5X,'NODAL LOAD FOR PHASE NUMBER',I5,
     1///,5X,'NODE HORIZONTAL  VERTICAL')
      WRITE(6,21) (I,UN(I),VN(I),I=1,NUMNP)
   21 FORMAT(5X,I5,2F10.5)
C
C
C  ELEMENTS TO BE CHANGED
C
C
  600 READ(5,22)NELCA
      WRITE(6,26)
   26 FORMAT(/,5X,'ELEMENTS WHICH WILL BE REMOVED')
   22 FORMAT(I5)
      IF(NELCA.EQ.0) GO TO 27
      DO 23 I=1,NELCA
      READ(5,22)INEL
      WRITE(6,22)INEL
      TSIGEL(INEL,1)=0.
      TSIGEL(INEL,2)=0.
      TSIGEL(INEL,3)=0.
   23 MAT(INEL)=8
   27 READ(5,22)NELCC
      WRITE(6,28)
   28 FORMAT(/,5X,'ELEMENTS WHICH WILL BE CHANGED TO CONCRETE')
      IF(NELCC.EQ.0)GO TO 31
      DO 24 I=1,NELCC
      READ(5,22)INEL
      WRITE(6,22)INEL
      MAT(INEL)=4
      TSIGEL(INEL,1)=0.
      TSIGEL(INEL,2)=0.
```

```
   24 TSIGEL(INEL,3)=0.
      READ(5,22)NELCG
      WRITE(6,70)
   70 FORMAT(/,5X,'ELEMENTS WHICH WILL BE GROUTED')
      IF(NELCG.EQ.0) GO TO 31
      DO 71 I=1,NELCG
      READ(5,22)INEL
      TSIGEL(INEL,1)=0.
      TSIGEL(INEL,2)=0.
      TSIGEL(INEL,3)=0.
      WRITE(6,22)INEL
   71 MAT(INEL)=10
C
C
C  NODES WHICH WILL HAVE THE STRESSES ZEROED
C  CONCRETE JUST POURED OR CONCRETE SOIL REMOVED INTERFACE NODES
C
C
   31 WRITE(6,29)
   29 FORMAT(/,5X,'NODES WHICH WILL HAVE THE STRESSES ZEROED')
      READ(5,22)NNC
      IF(NNC.EQ.0)GO TO 32
      DO 25 I=1,NNC
      READ(5,22)J
      WRITE(6,22)J
      TSIGA(J,1)=0.
      TSIGA(J,2)=0.
   25 TSIGA(J,3)=0.
   32 RETURN
      END
C
      SUBROUTINE SST
C
C  THIS SUBROUTINE READS STRESS STRAIN PARAMETERS
C
      COMMON E(10),PR(10),RO(10),X(350),Y(350),U(350),V(350),TH(600),
     1STIF(700,140),AP(700),ESTIF(6,6),ECM(3,3),EBM(3,6),ESM(3,6),WT
      COMMON NUMNP,NUMEL,NUMAT,KODE(350),NP(3,600),MAT(600),MBAND,
     1 NEQ,M,LM(6)
      COMMON KODE1(350)
      COMMON SIGC(10,4),AA(10,4),BB(10,4),KO(10),ZSPC
      COMMON DSIGEL(600,3),SIGIEL(600,3),DSIGA(350,3),SIGIA(350,3)
      COMMON TSIGEL(600,3),TSIGA(350,3),TB(700)
      COMMON UN(350),VN(350),NNYL(25),NNXL(25)
      COMMON EE(600),PRE(600),TSIGEP(600,2)
      COMMON PHI,XK,XEP
      COMMON DI(700)
      REAL KO
C
C READ AND WRITE STRESS STRAIN PARAMETERS
C
      WRITE(6,48)
   48 FORMAT(1H1)
   10 READ(5,1)MM
    1 FORMAT(I5)
C
C  POISSONS RATIO AND KO
C
      READ(5,4)PR(MM),KO(MM)
    4 FORMAT(2F10.5)
```

```
      IF(MM-1) 13,13,3
C
C   MATERIAL NUMBER 1
C   3 TESTS TRIAXIAL STRESS PATH  COMP ACTIVE
C
   13 DO 5 J=1,3
    5 READ(5,6)SIGC(MM,J),AA(MM,J),BB(MM,J)
      WRITE(6,7)MM,PR(MM),KO(MM)
    7 FORMAT(///,5X,'MATERIAL NUMBER',I5,//,5X,'POISSONS RATIO ',
     1F10.2,/,5X,'KO= ',F10.2)
      WRITE(6,9)
    9 FORMAT(5X,'CONF STR          A          B')
      WRITE(6,8) (SIGC(MM,J),AA(MM,J),BB(MM,J),J=1,3)
    8 FORMAT(5X,3F10.6)
      GO TO 10
    3 IF(MM-2)11,11,12
C
C   MATERIAL NUMBER 2
C   3 TESTS TRIAXIAL STRESS PATH EXTENSION ACTIVE
C
   11 READ(5,6) (SIGC(MM,J),AA(MM,J),BB(MM,J),J=1,3)
      WRITE(6,7) (MM,PR(MM),KO(MM))
      WRITE(6,9)
      WRITE(6,8) (SIGC(MM,J),AA(MM,J),BB(MM,J),J=1,3)
      GO TO 10
   12 IF(MM-3)16,16,17
C
C   MATERIAL NUMBER 3
C   1 TEST TRIAXIAL STRESS PATH KO-COMP ACTIVE
C
   16 READ(5,6)E(MM),AA(MM,1),BB(MM,1)
      WRITE(6,15)MM,PR(MM),E(MM),AA(MM,1),BB(MM,1),KO(MM)
   15 FORMAT(///,5X,'MATERIAL NUMBER',I5,//,5X,'POISSONS RATIO ',
     1F10.2,/,5X,'E UNLOAD-RELOADING ',F10.3,//,5X,'A  ',F10.6,
     2/,5X,'B  ',F10.6,/,5X,'KO'  ,F10.2)
    6 FORMAT(3F10.6)
      GO TO 10
   17 IF(MM-4)18,18,19
C
C   MATERIAL NUMBER 4
C   1 TEST CONCRETE
C
   18 READ(5,6)E(MM)
      WRITE(6,21)MM,E(MM),PR(MM),KO(MM)
   21 FORMAT(///,5X,'MATERIAL NUMBER ',I5,/,5X,'E ',F15.5,/,
     15X,'POISSONS RATIO ',F10.5,/,5X,'KO', F10.2)
      GO TO 10
   19 IF(MM-5) 22,22,23
C
C   MATERIAL NUMBER 5
C   2 TESTS PLANE STRAIN COMP. ACTVE
C
   22 DO 24 J=1,2
   24 READ(5,6)SIGC(MM,J),AA(MM,J),BB(MM,J)
      WRITE(6,7)MM,PR(MM),KO(MM)
      WRITE(6,9)
      WRITE(6,8)(SIGC(MM,J),AA(MM,J),BB(MM,J),J=1,2)
      GO TO 10
   23 IF(MM-6) 25,25,26
C
```

```
C   MATERIAL NUMBER 6
C    1 TEST CONVENTIONAL TRIAXIAL FOR FILL
C
   25  READ(5,4) E(MM)
       WRITE(6,7) MM,PR(MM),KO(MM)
       WRITE(6,28) E(MM)
   28 FORMAT(5X,'E',F15.5)
       GO TO 10
  26   IF(MM-7) 36,36,27
C
C   MATERIAL NUMBER 7
C    3 TESTS TRIAXIAL CONVENTIONAL TRIAXIAL
C
   36 DO 30 J=1,3
  30   READ(5,6) SIGC(MM,J),AA(MM,J),BB(MM,J)
       WRITE(6,7) MM,PR(MM),KO(MM)
       WRITE(6,9)
       WRITE(6,8) (SIGC(MM,J),AA(MM,J),BB(MM,J),J=1,3)
       READ(5,6) PHI,XK,XEP
       WRITE(6,49) PHI,XK,XEP
   49 FORMAT(5X,'PHI=',F10.3,/,5X,'K=',F10.2,/,5X,'N=',F10.2)
       GO TO 10
  27   IF(MM-8) 37,37,38
C
C   MATERIAL NUMBER 8
C   AIR
C
  37   READ(5,6) E(MM)
       WRITE(6,34) MM,E(MM),PR(MM),KO(MM)
  34   FORMAT(///,5X,'MATERIAL NUMBER',I5,/,5X,'E',F10.2,
      1/,5X,'PR',F10.3,/,5X,'KO',F10.2)
       GO TO 10
   38 IF(MM-9) 52,52,53
C
C   MATERIAL NUMBER 9
C    1 TEST CONVENTIONAL TRIAXIAL
C
   52 READ(5,6) SIGC(MM,1),AA(MM,1),BB(MM,1)
       WRITE(6,7) MM,PR(MM),KO(MM)
       WRITE(6,9)
       WRITE(6,8) SIGC(MM,1),AA(MM,1),BB(MM,1)
       GO TO 10
  53   IF(MM-10) 250,250,251
  250  READ(5,6) E(MM)
       WRITE(6,21) MM,E(MM),PR(MM),KO(MM)
       RETURN
  251   WRITE(6,31)
  31   FORMAT(//,5X,'ERROR TOO MANY MATERIALS')
       RETURN
       END
C
C
C
C   SUBROUTINE READGE
C
C
C
        SUBROUTINE READGE
C
C THIS SUBROUTINE READS AND PRINTS MATERIAL DATA, NODAL DATA, ELEMENT DATA.
```

```
C  IT GENERATES COORDINATES OF INTERMEDIATE NODAL POINTS AND CALCULATES
C  THE BAND WIDTH AND NUMBER OF EQUATIONS
C
C
C
      COMMON E(10),PR(10),RO(10),X(350),Y(350),U(350),V(350),TH(600),
     1STIF(700,140),AP(700),ESTIF(6,6),ECM(3,3),EBM(3,6),ESM(3,6),WT
      COMMON NUMNP,NUMEL,NUMAT,KODE(350),NP(3,600),MAT(600),MBAND,
     1 NEQ,M,LM(6)
      COMMON KODE1(350)
      COMMON SIGC(10,4),AA(10,4),BB(10,4),KO(10),ZSFC
      COMMON DSIGEL(600,3),SIGIEL(600,3),DSIGA(350,3),SIGIA(350,3)
      COMMON TSIGEL(600,3),TSIGA(350,3),TB(700)
      COMMON UN(350),VN(350),NNYL(25),NNXL(25)
      COMMON EE(600),PRT(600),TSIGEP(600,2)
      COMMON PHI,XK,XEP
      COMMON DI(700)
      REAL KO
C
      DIMENSION HED(20)
C  READ PRELIMINARY INFORMATION
      READ(5,1000) HED,NUMNP,NUMEL,NUMAT
      WRITE(6,2000) HED,NUMNP,NUMEL,NUMAT
C
C  READ AND WRITE NODAL DATA AND GENERATE INTERMEDIATE NODAL DATA
C
      L=1
      READ(5,1020) N,KODE(N),X(N),Y(N),U(N),V(N),KODE1(N)
      GO TO 40
C
20    READ(5,1020) N,KODE(N),X(N),Y(N),U(N),V(N),KODE1(N)
      DN = N-L
      DX =(X(N)-X(L))/DN
      DY =(Y(N)-Y(L))/DN
25    L=L+1
C
      IF(N-L) 50,40,30
30    X(L) = X(L-1)+DX
      Y(L) = Y(L-1)+DY
      KODE1(L)=KODE1(L-1)
      KODE(L)= 0
      U(L) = 0
      V(L)= 0
      GO TO 25
C
40    CONTINUE
      IF(NUMNP-N) 50,60,20
C
50    WRITE (6,2025) N
      CALL EXIT
C
60    WRITE(6,2016)
      WRITE(6,2015)
      WRITE (6,2020)  (N,KODE(N),X(N),Y(N),U(N),V(N),KODE1(N),N=1,NUMNP)
C
C  READ AND WRITE ELEMENT DATA
C
      ML=0
51    IF (ML.GE.NUMEL)  GO TO 70
      READ(5,1035)  M,NP(1,M),NP(2,M),NP(3,M),MAT(M),TH(M)
```

```
      MM=ML+1
      IF (MM.EQ.M)  GO TO 65
C
   55 ML1=ML+1
      IF(ML1.EQ.M)  GO TO 65
      ML2=ML+2
      MLM1=ML-1
      IF(MLM1.LE.0) GO TO 85
      DO 62  I=1,3
      NP(I,ML2)=NP(I,ML)+1
   62 NP(I,ML1)=NP(I,MLM1)+1
      MAT(ML2)=MAT(ML)
      MAT(ML1)=MAT(MLM1)
      TH(ML2)=TH(ML)
      TH(ML1)=TH(MLM1)
      ML=ML2
      GO TO 55
C
65    ML=M
      GO TO 51
70    CONTINUE
      WRITE(6,2032)
      WRITE(6,2030)
      WRITE (6,2035) (M,(NP(J,M),J=1,3),MAT(M),TH(M),M=1,NUMEL)
C
C     DETERMINE BAND WIDTH AND NUMBER OF EQUATIONS
C
      L=0
      DO 80 M=1,NUMEL
      DO 80 I=1,2
      II=I+1
      DO 80 J=II,3
      K= IABS(NP(I,M)-NP(J,M))
      IF (K.GT.L)    L=K
80    CONTINUE
C
      MBAND = 2*(L+1)
      NEQ= 2*NUMNP
C
      WRITE(6,2040) MBAND,NEQ
       IF(MBAND.LE. 140.AND.NEQ.LE.700)  GO TO 90
      WRITE(6,2050)
      CALL EXIT
85    WRITE(6,2060)
      CALL EXIT
C
90    WRITE(6,3000)
3000  FORMAT( '  READIN COMPLETED ' ///)
      RETURN
C
C  FORMAT STATEMENTS
1000  FORMAT(20A4/ 3I6)
2000  FORMAT(/,10X,20A4,////
     1 1H ,    26H NUMBER OF NODAL POINTS = ,I6/
     2 1H ,    26H NUMBER OF ELEMENTS     = ,I6/
     3 1H ,    26H NUMBER OF MATERIALS    = ,I6)
1010  FORMAT(5X,F12.0,2F6.0)
2010  FORMAT(1H ,I5,F17.0,F15.3,F17.1)
2014  FORMAT( /,  5X, 'OUTPUT OF INPUT NODAL DATA ')
2015  FORMAT(///,10X,19H NODAL POINT OUTPUT,///
```

```
          11H ,59H NODE  NODE    X COORD     Y COORD     X FORCE     Y FORCE
          2//)
     2010 FORMAT('1',  5X,  'OUTPUT OF COMPLETE NODAL DATA  ')
     1020 FORMAT(2I6,4F12.0,I5)
     2020 FORMAT(I4,I6,F13.3,3F12.3,I5)
     2025 FORMAT(1H0,28H ERROR IN NODAL DATA,NODE = ,I4)
     2030 FORMAT(///,10X, 13H ELEMENT DATA ///,
          1 40H ELEM     I       J       K     MAT  THICKNESS //)
     2031 FORMAT('1',5X, 'OUTPUT OF INPUT ELEMENT DATA' )
     2032 FORMAT( '1', 5X, 'OUTPUT OF COMPLETE ELEMENT DATA  ' )
     1035 FORMAT (5I6,F6.0)
     2035 FORMAT ( I4, 4I6,F11.4).
     2040 FORMAT (///10X, 22H BAND WIDTH           = ,I6/
          1                10X, 22H NUMBER OF EQUATIONS = ,I6)
     2050 FORMAT(///10X, 33H PROBLEM EXCEEDS SPECIFIED LIMITS )
     2055 FORMAT(  'MLM1 IS LESS THAN OR EQUAL TO ZERO ')
C
          END
END OF FILE
```

APPENDIX B PLANE STRAIN APPARATUS

Descrition of the apparatus

The design of this plane strain apparatus was inspired by similar equipments described by Duncan and Seed (1966) and Campanella and Vaid (1972).

The sample dimensions are 2.5 cm wide, 5 cm high and 10 cm long. The plane strain condition is guaranteed by two fixed smooth plates which restrain movement lengthwise (figure B.1) . A load cell is housed in one of the end plates to measure the intermediate principal stress (Figure B.2). The lateral principal stress is applied by a pair of flexible, air filled, rubber membranes (figure B.3) fixed to the lateral support plate (figure B.4). The vertical principal stress is applied by a rigid loading cap. There is a load cell at the base pedestal to monitor the amount of vertical load being absorbed by friction between the sample membrane and the side plates and membrane sealing plates. (figure B.5) . There is a clearance of 0.06 cm between the top cap and membrane sealing plates. The top cap and base pedestal are sectioned horizontally to seal a membrane which encloses the sample between both halves. One of the halves accomodates a "O" ring to prevent leakage between the the sample membrane and one of the halves of the top cap or base pedestal. The same precaution was taken with respect to the lateral membrane.

The dimensions of all the parts are shown in figures B.6 to B.11.

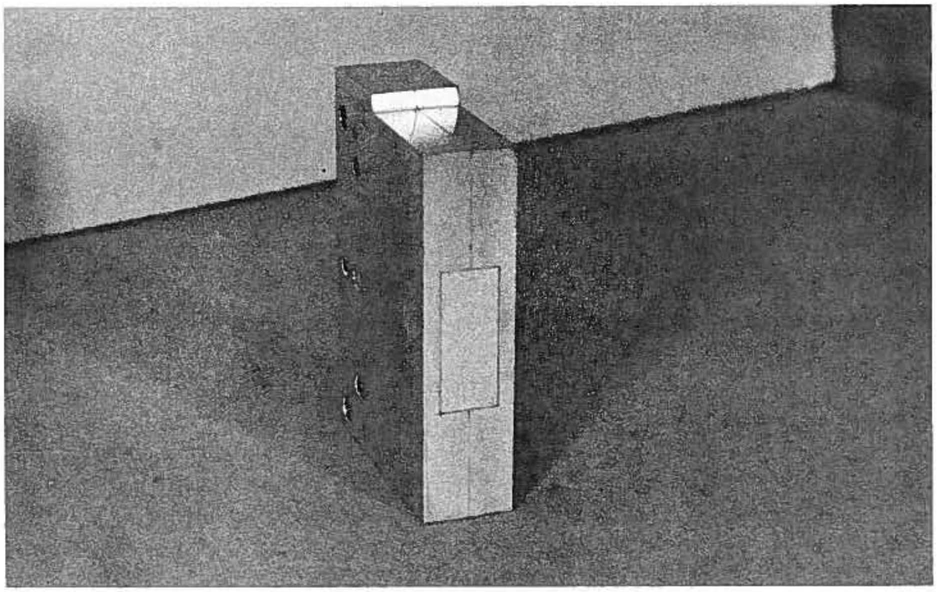

FIGURE B.1 FRICTIONLESS END PLATE

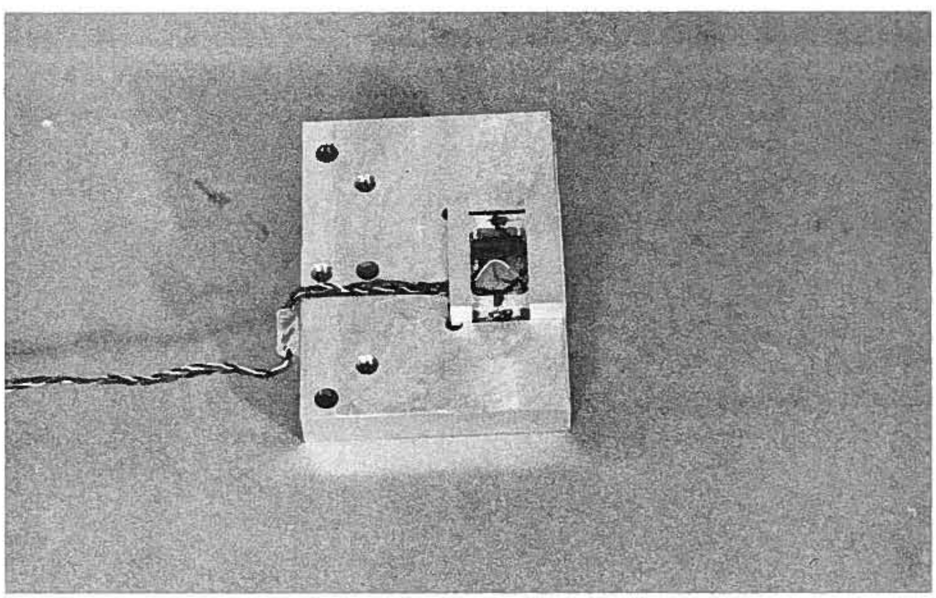

FIGURE B.2 LATERAL LOAD CELL

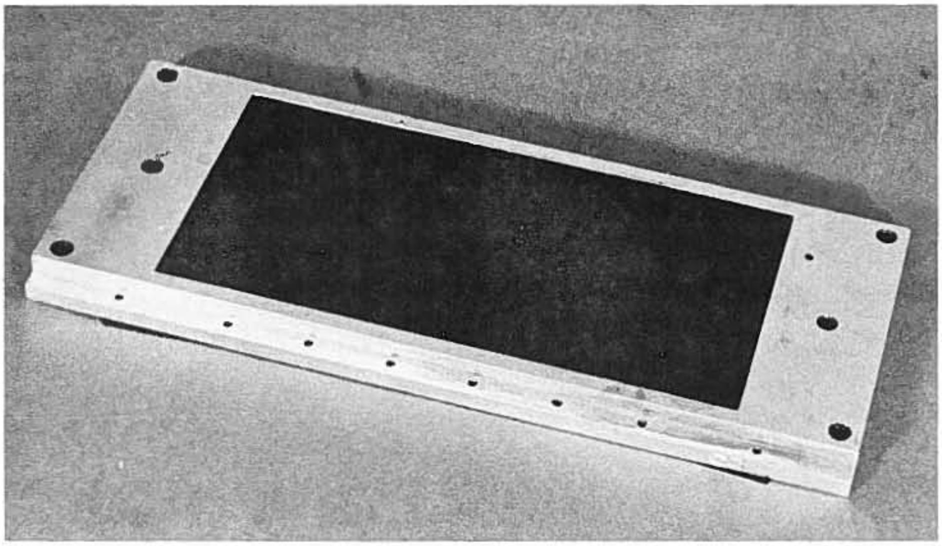

FIGURE B.3 SEALING PLATE WITH MEMBRANE

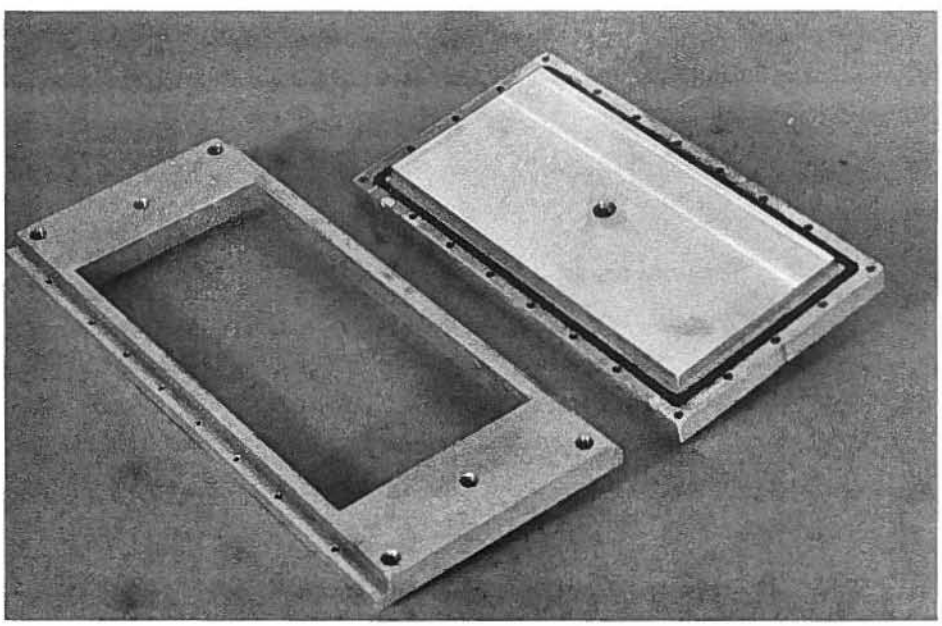

FIGURE B.4 LATERAL SUPPORT AND MEMBRANE SEALING PLATES

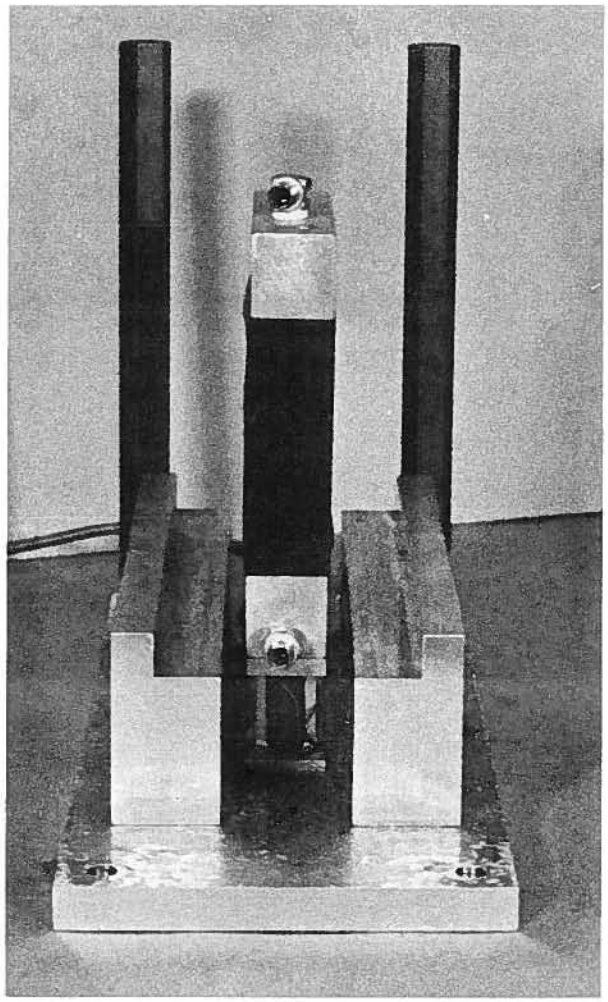

FIGURE B.5 LOAD CELL AT THE BASE PEDESTAL

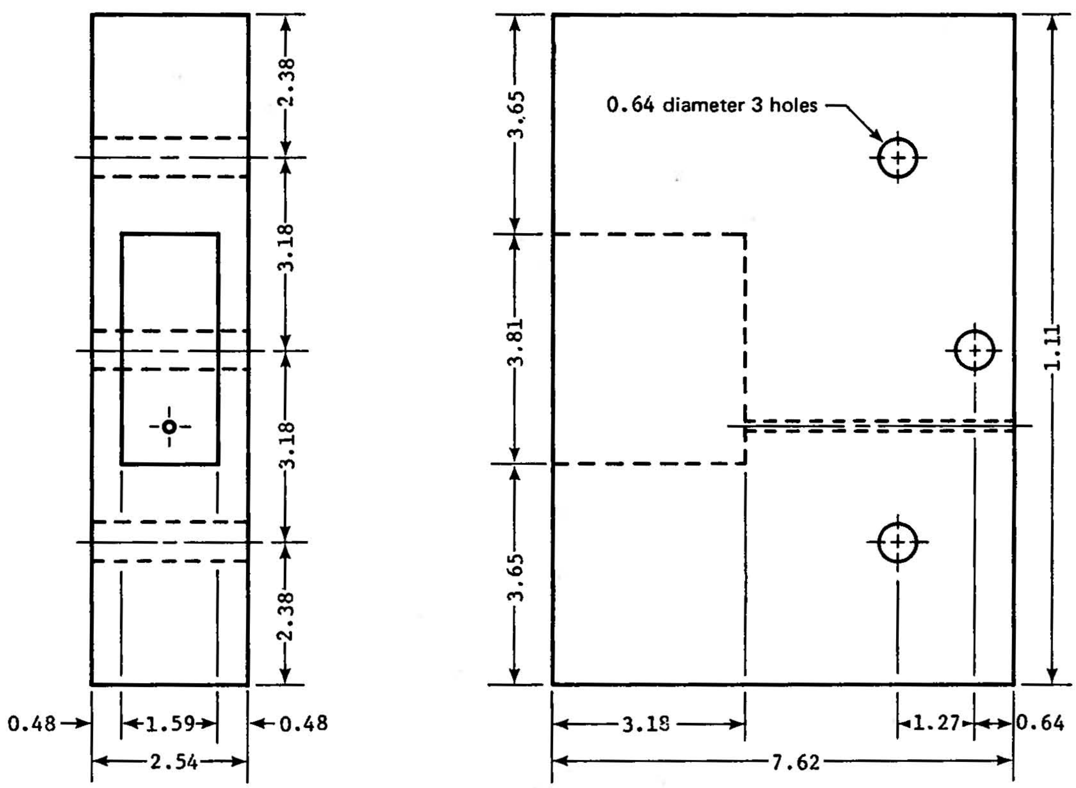

note: all dimensions in cm

FIGURE B.6 END PLATE

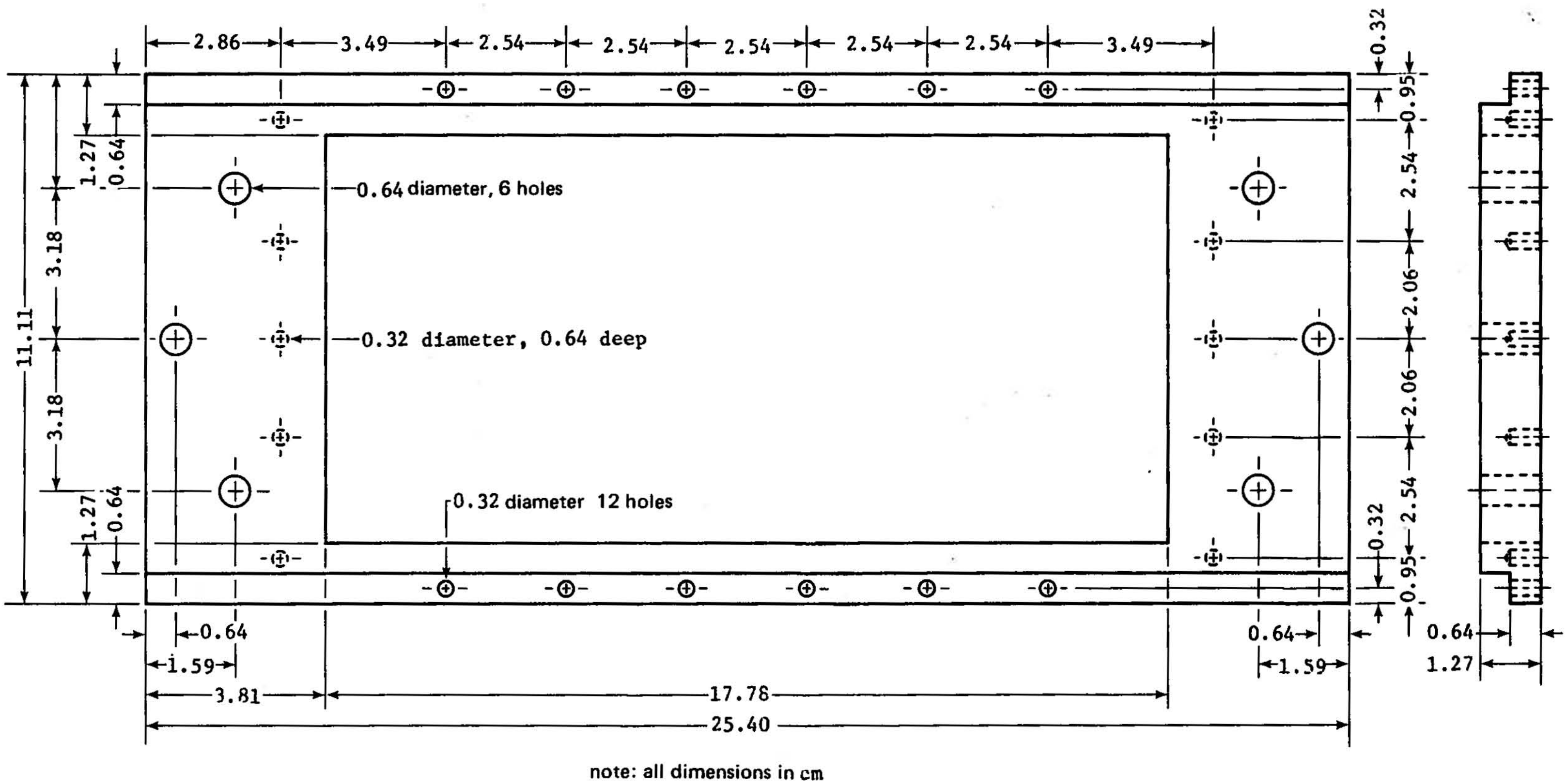

FIGURE B.7 LATERAL MEMBRANE SEALING PLATE

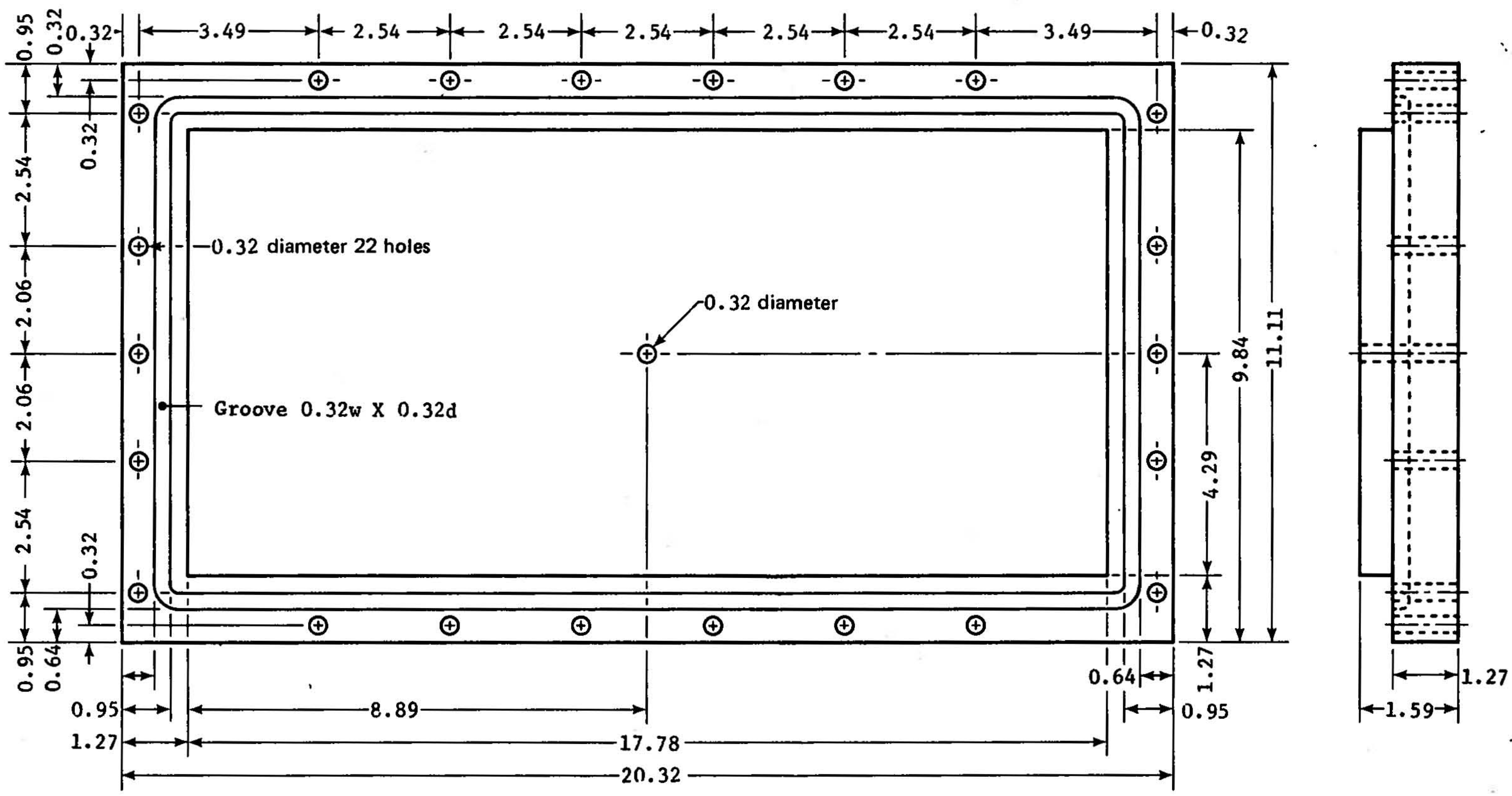

note: all dimensions in cm

FIGURE B.8 LATERAL MEMBRANE SUPPORT PLATE

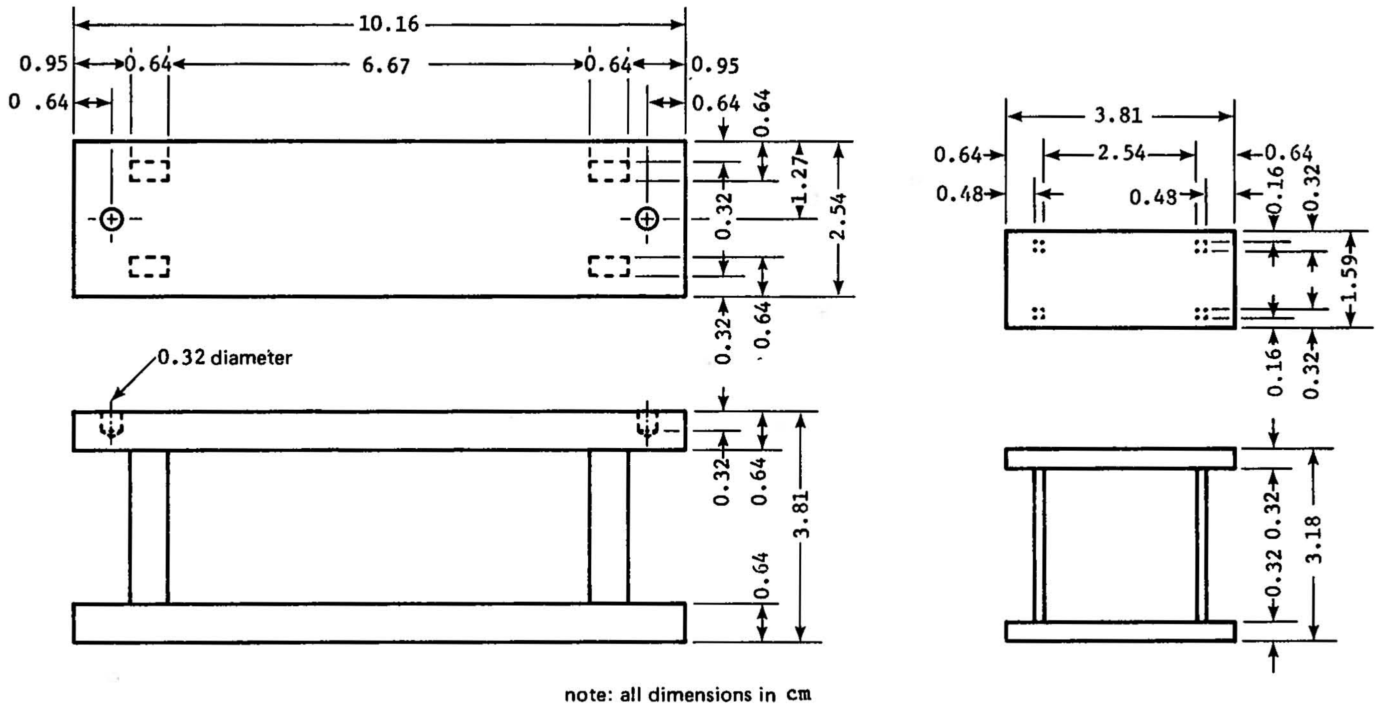

FIGURE B.9 LATERAL AND BOTTOM LOAD CELLS

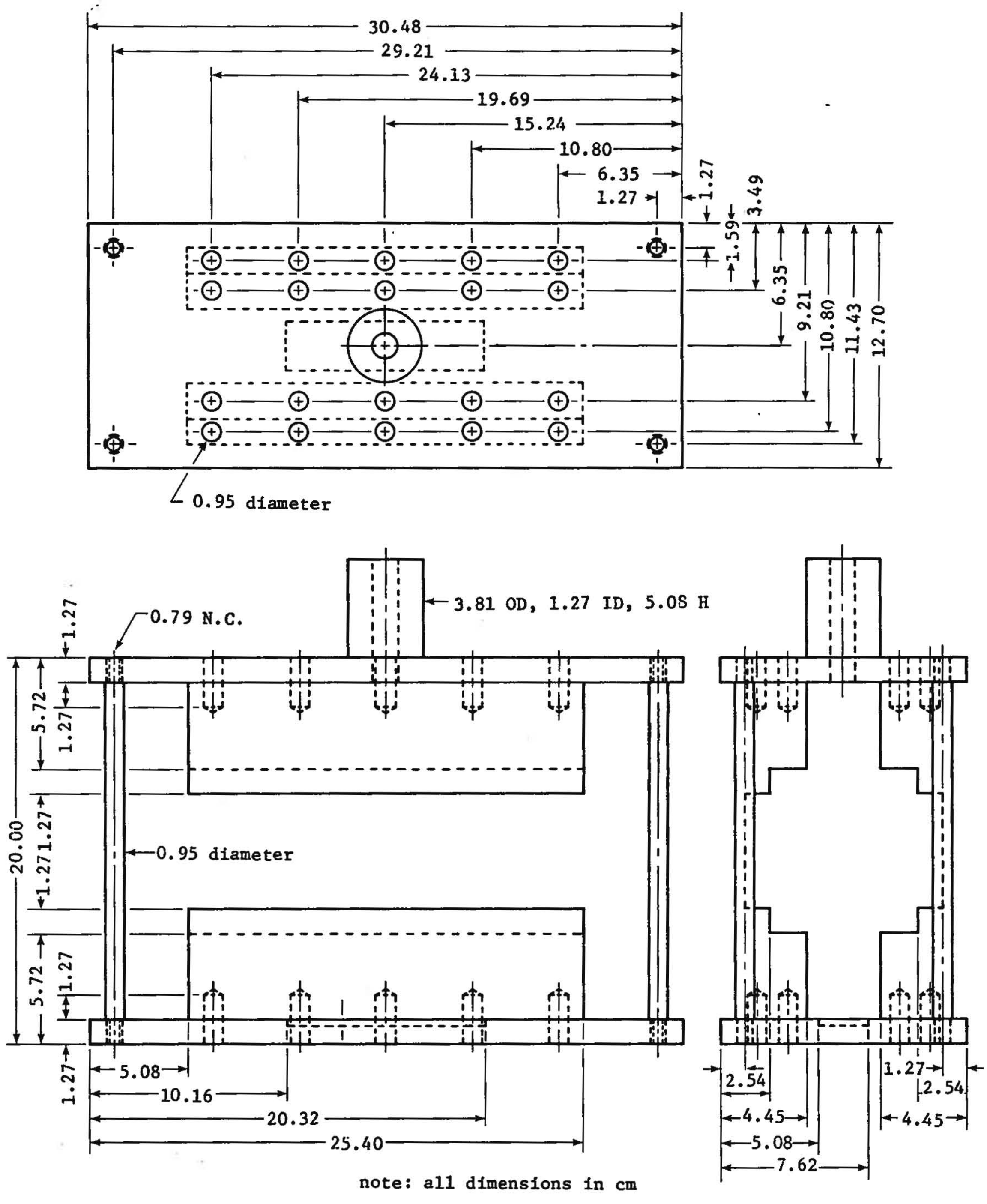

FIGURE B.10 LOADING FRAME

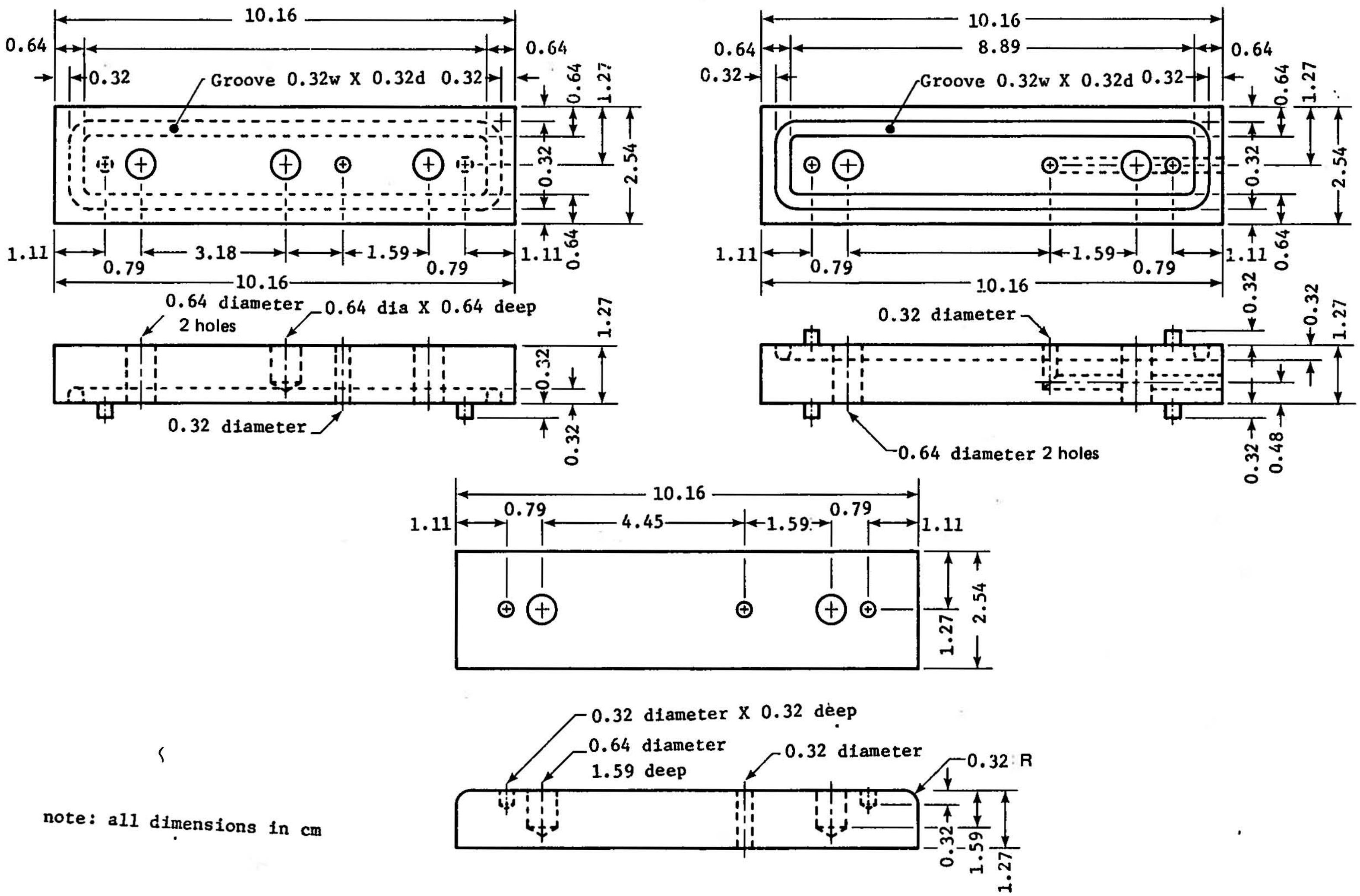

note: all dimensions in cm

FIGURE B.11 LOAD CAP AND PEDESTAL

APPENDIX C. CALCULATION OF MEZZANINE LOAD

The straight line in figure 3.10 was determined by least minimum square which indicates there will be tension at the lower part until a point at a distance 22.7 cm from the bottom.

Figure C.1.a represents the cross section of the mezzanine while C.1.b is the transformed section. The moment of inertia is:

$$I = 4947834.\ cm4$$

and the cross sectional area

$$A = 5685\ cm2.$$

The normal stress at the top is 50.26 kg/cm2 therefore

$$50.26 = P/A + 53.35\ M/I$$

and at the bottom is -13.58 kg/cm2 therefore

$$-13.58 = P/A - 53.35\ M/I$$

where P is the normal load and M the bending moment in the section, which solving for P and M yields P = 208533 kg per 533.4 cm. which is the horizontal distance between long piles (figure 2.9) resulting in a load of 39,095 kg/m

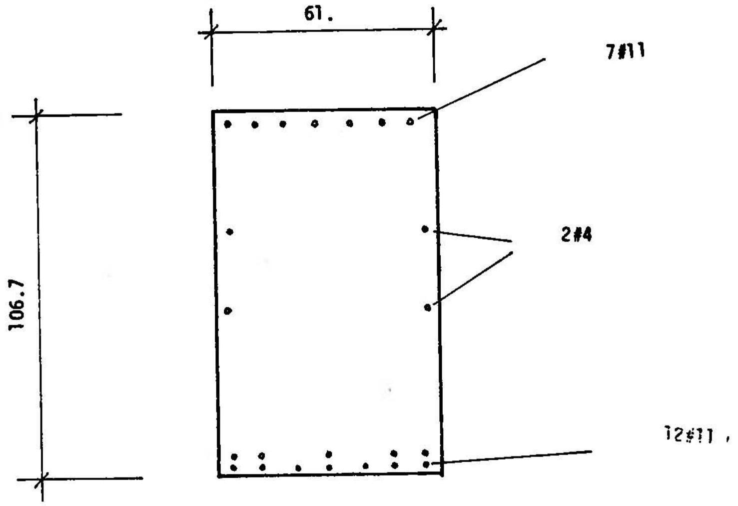

C.1.a TRUE CROSS SECTION

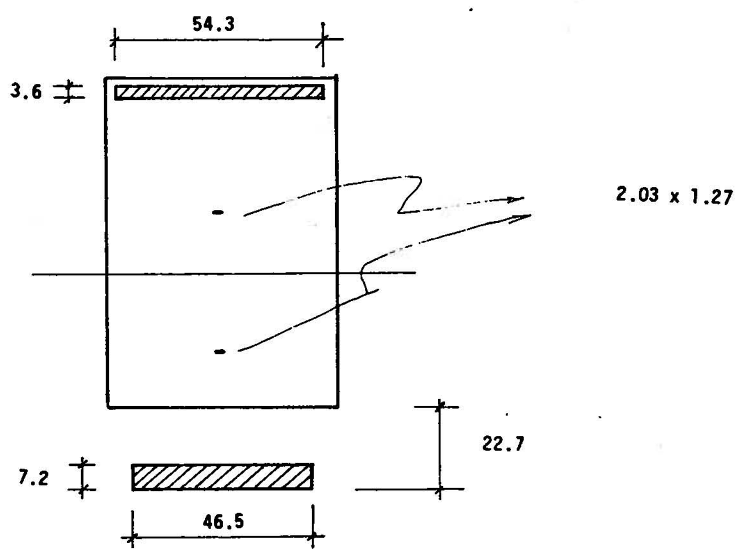

C.1.b TRANSFORMED CROSS SECTION

FIGURE C.1 COMPOSITE CROSS SECTION OF THE MEZZANINE

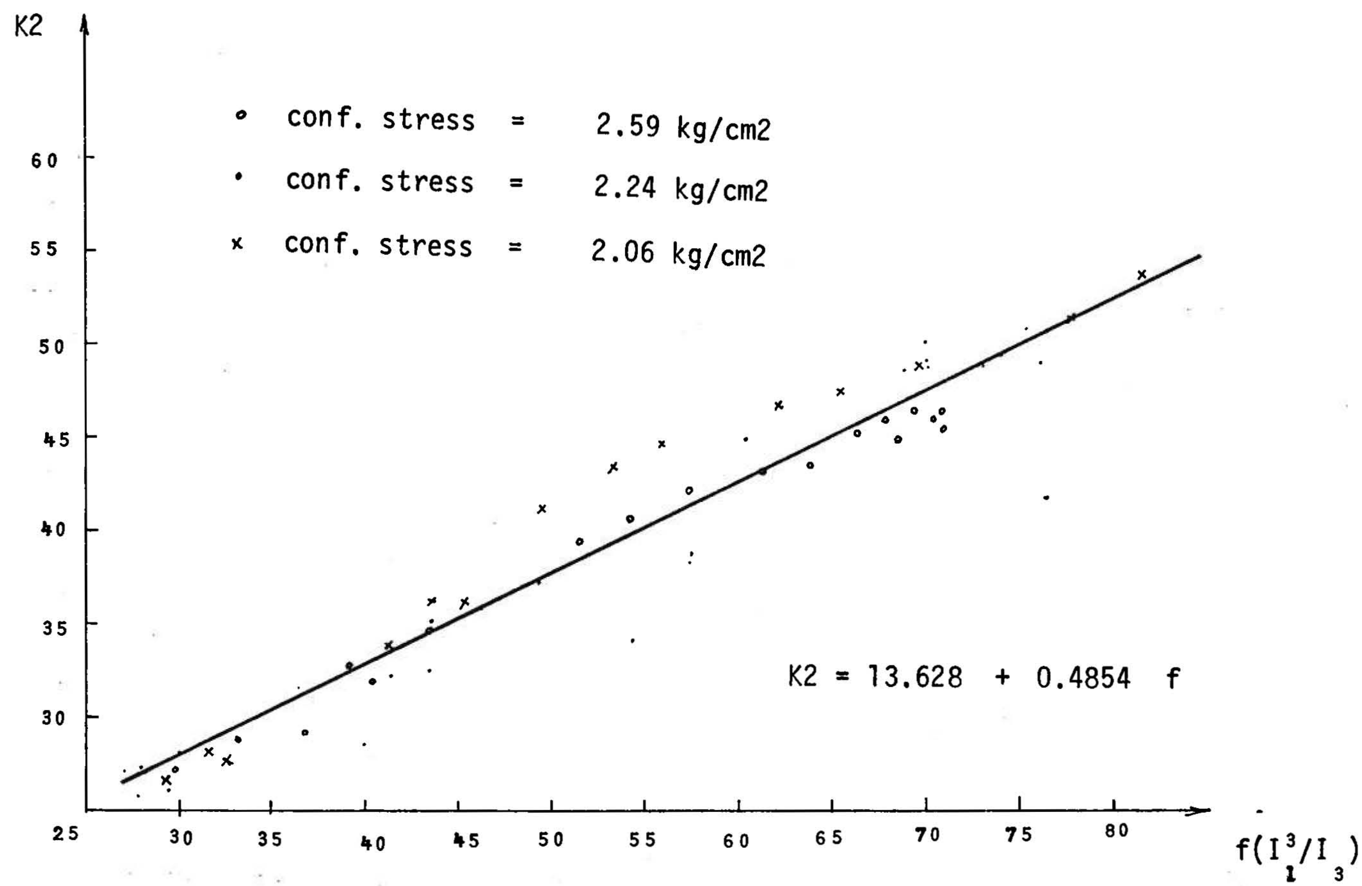

FIGURE 5.1 VARIATION OF K2 WITH STRESS LEVEL EDMONTON TILL

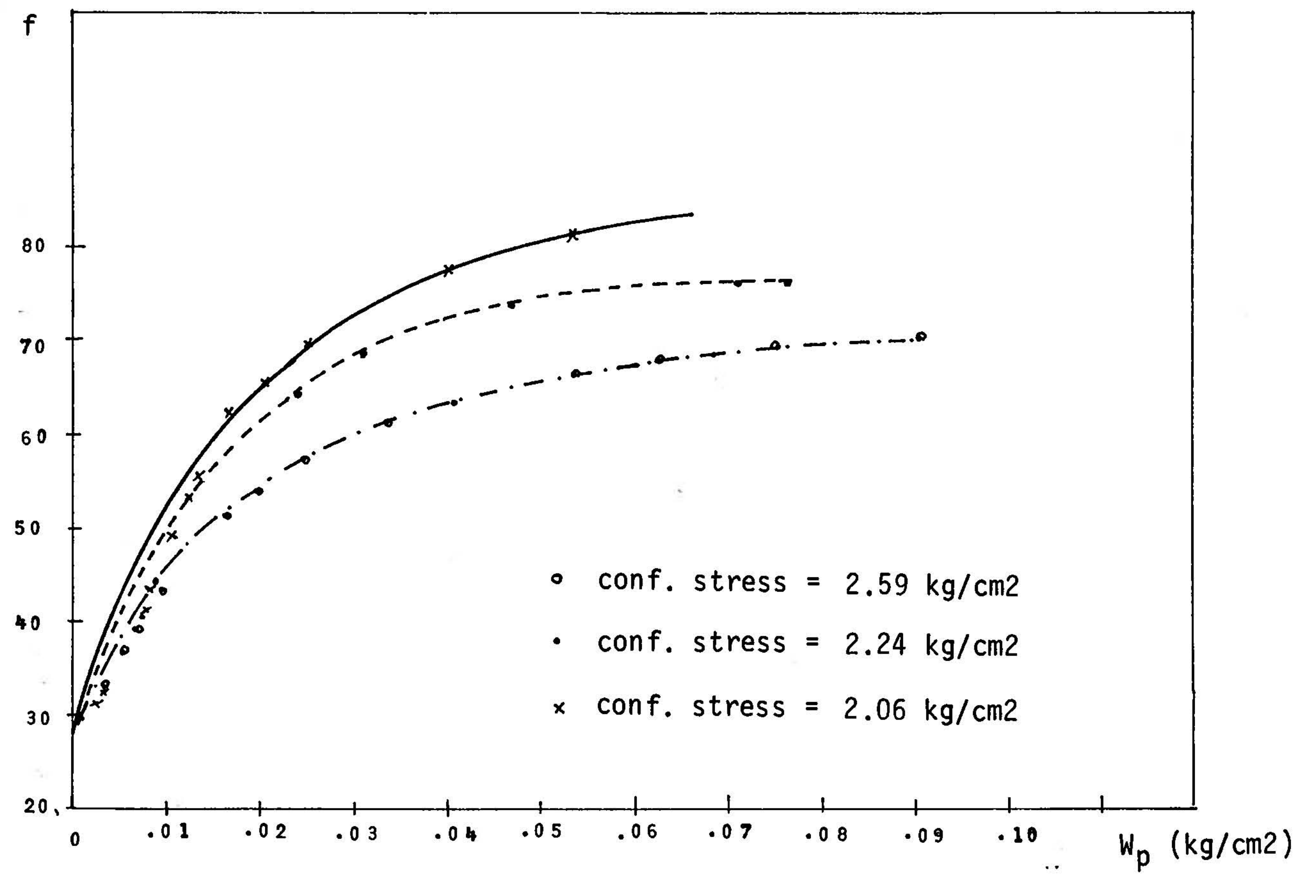

FIGURE 5.2 RELATION BETWEEN PLASTIC WORK AND STRESS LEVEL EDMONTON TILL

occur. A redefinition of stress level which includes the first stress invariant seems to be more appropriate. A latter modification of the theory by Lade (1975) defined the stress level as :

$$f_p = \left(\frac{I_1^3}{I_3}\right)\left(\frac{I_1}{pa}\right)^m \qquad \ldots.(5.15)$$

where $\underline{m}$ is a material property.

Values of $\underline{m}$ smaller than 1 were encountered for sand (Lade 1975) and clay (Lade and Musante 1976). The same trend occurred for the Edmonton till where higher values of $\underline{f}$ were reached for smaller values of the confining stress (figure 5.2). The yield surfaces (equation 5.3) in Rendulic stress space represent a cone (figure 5.3) while a redefinition of the stress level as in equation 5.15 with values of $\underline{m}$ less than unity makes it concave towards the hydrostatic axes. A average value for the limiting value of the stress level was taken to perform the calculations, yielding :

$$(f - f_t)_{ult} = \frac{1}{b} = 55$$

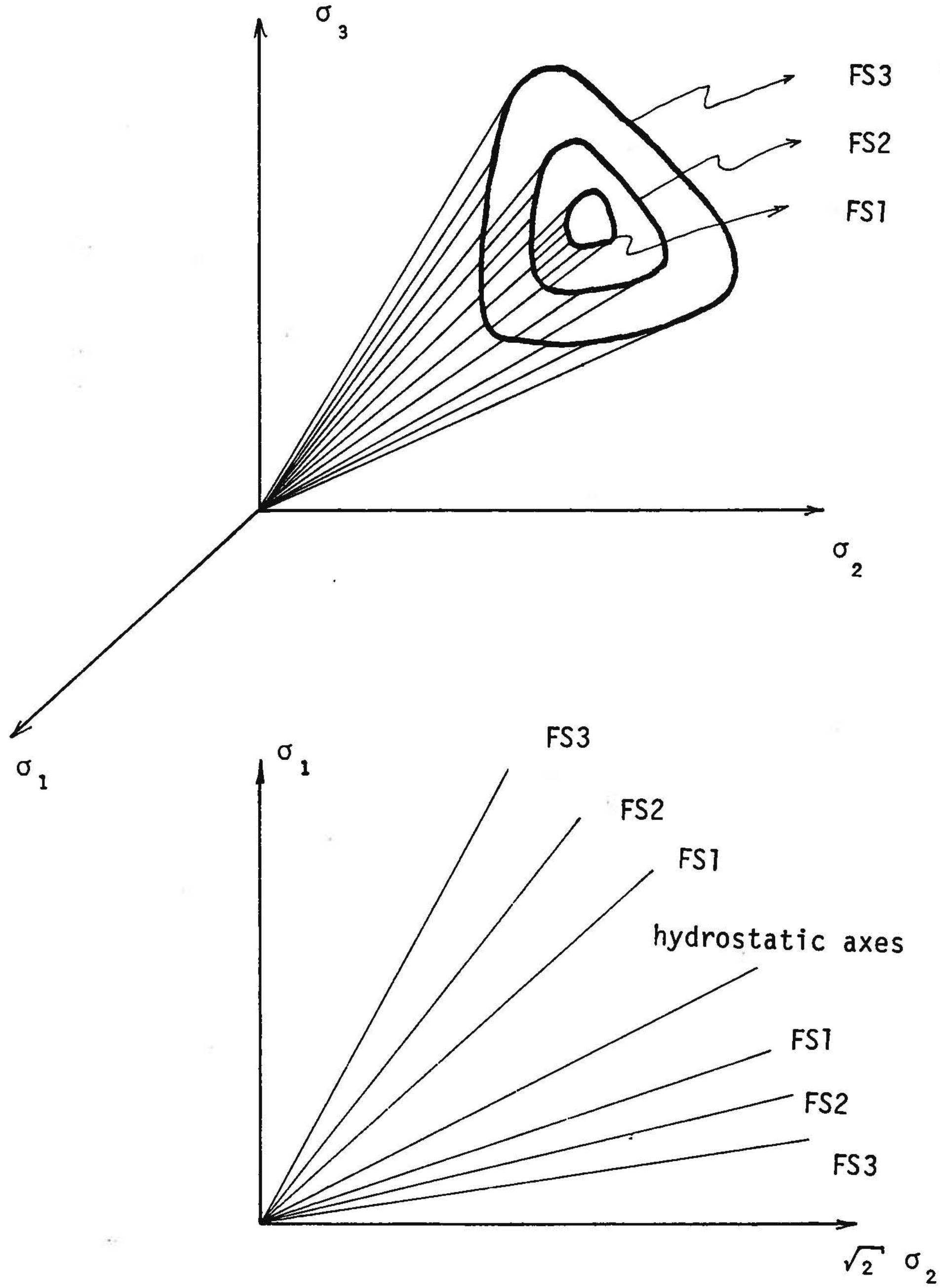

FIGURE 5.3 REPRESENTATION OF THE YIELD SURFACES

Values of a and l for the equation 5.13 obtained from figure 5.4 are 0.00012 and 1.099 respectively.

5.4 Analysis

Based on the parameters just obtained, predictions from triaxial compression active tests, described in chapter 4 , were performed (figure 5.5 to 5.9) . These tests were selected among others to investigate the applicability of the model since plane strain tests have already been predicted in sands successfully and the active compression tests depart the most from the conventional triaxial test.Although the parameters were obtained from tests which exhibited failure at values of 2% for the vertical strain, the model predicted satisfactorily vertical strains in tests failing at strain values as low as .5 %. Test 18-23 with an initial confining stress of 2.275 kg/cm2 was not accurately predicted but its behaviour does not seem to be representative when compared with tests 18-25 and 18-27 with initial confining stresses of 2.10 kg/cm2 and 2.45 kg/cm2 respectively. Despite the averaging of the value of (f-ft)ult, failure was predicted accurately. The samples were initially isotropically stressed, therefore f initial=27 and taken to failure which was assumed to occur at f=82. Plastic strains of the same magnitude of the elastic ones were observed at values of f=27.8, doubled the elastic strains at f=30. and quadrupled at f=40. The material exhibits a significant portion of plastic strain at

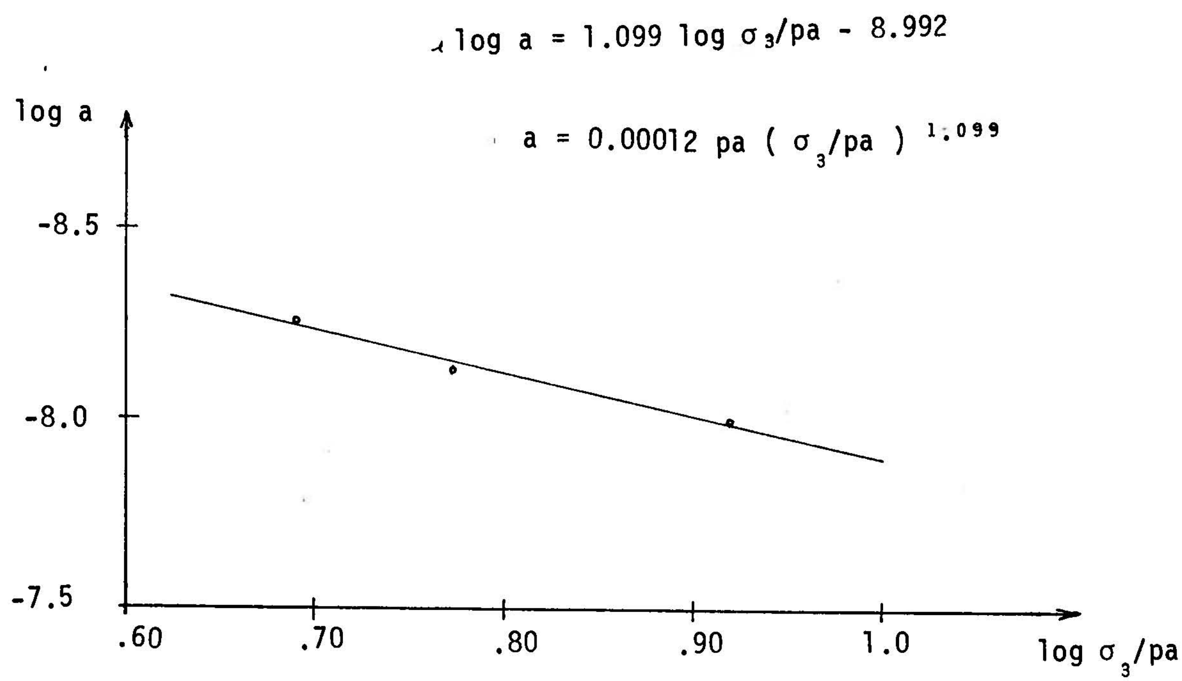

FIGURE 5.4 VARIATION OF PARAMETER <u>a</u> WITH CONFINING STRESS EDMONTON TILL

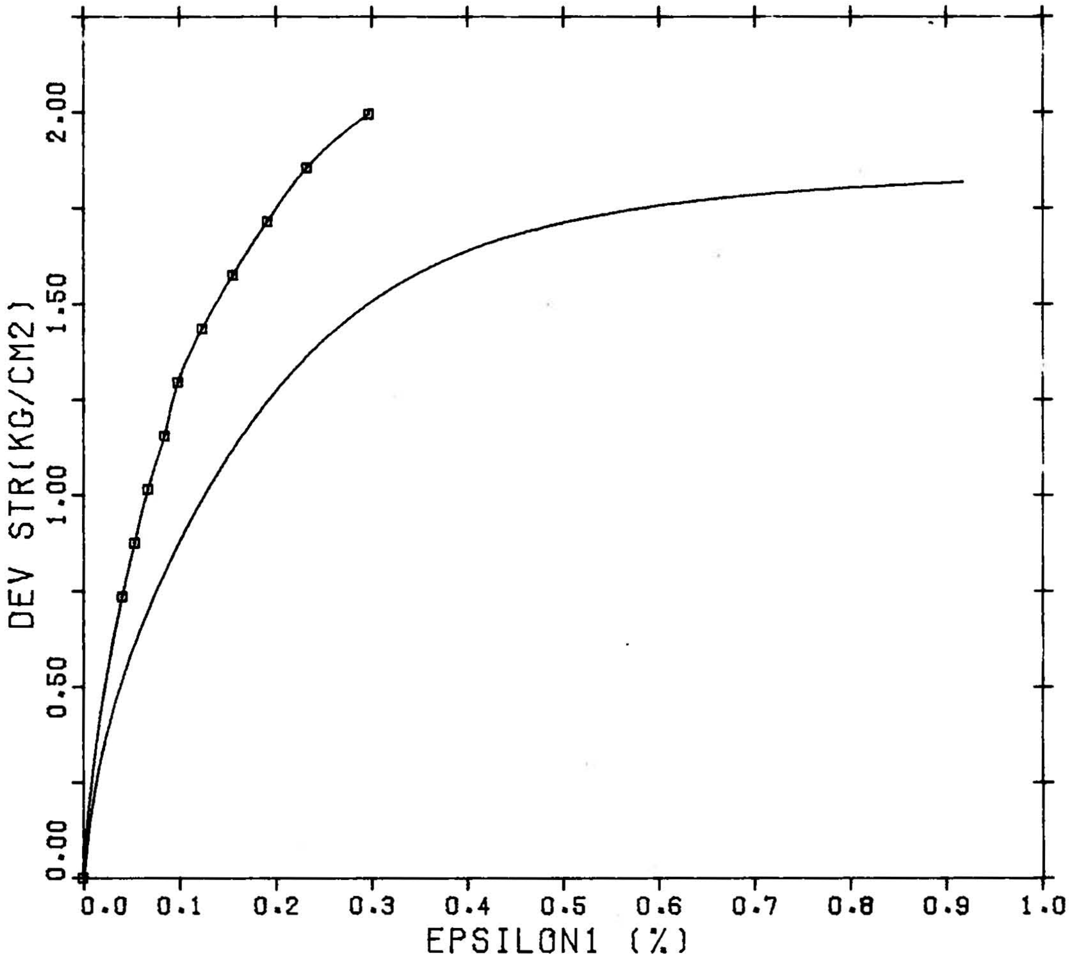

TEST 18-23 SIGMA3 2.275

FIGURE 5.5 ELASTOPLASTIC MODEL PREDICTION

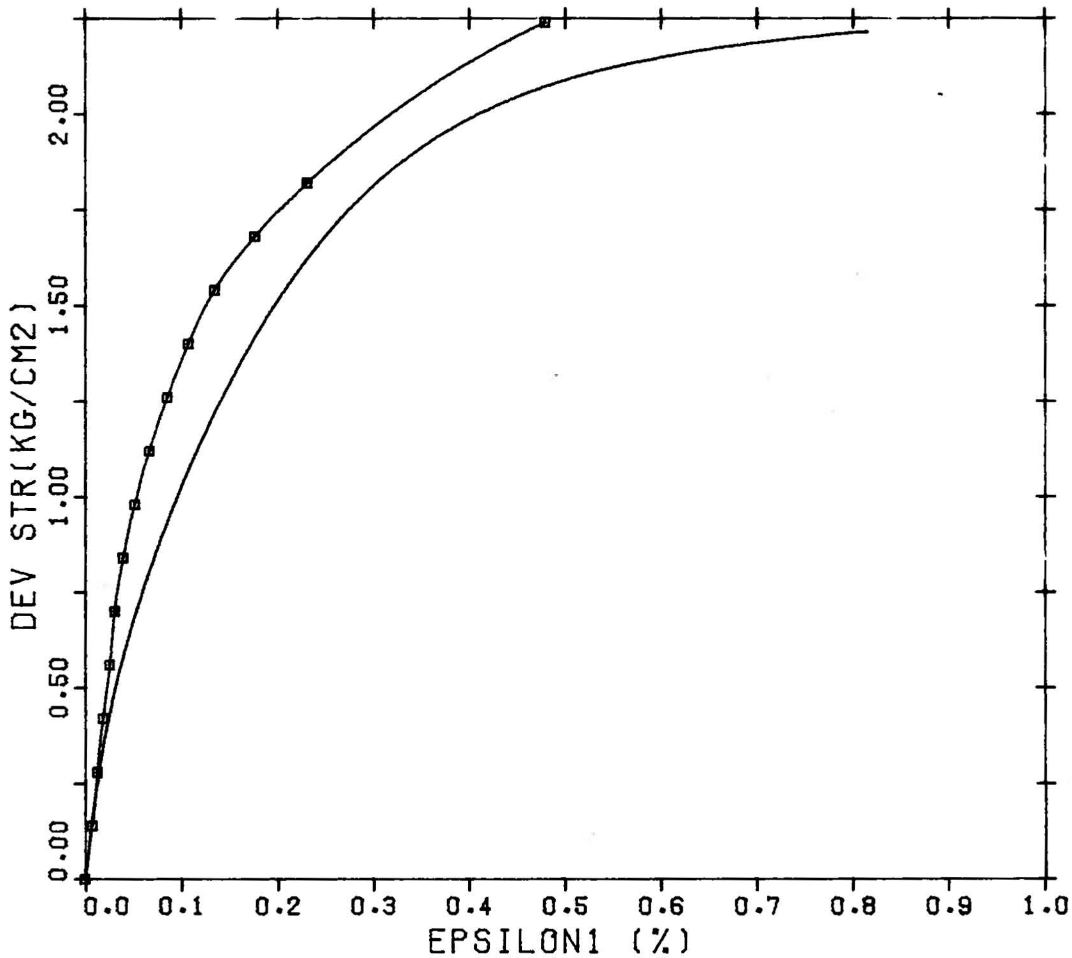

TEST 18-24 SIGMA3 2.80

FIGURE 5.6 ELASTOPLASTIC MODEL PREDICTION

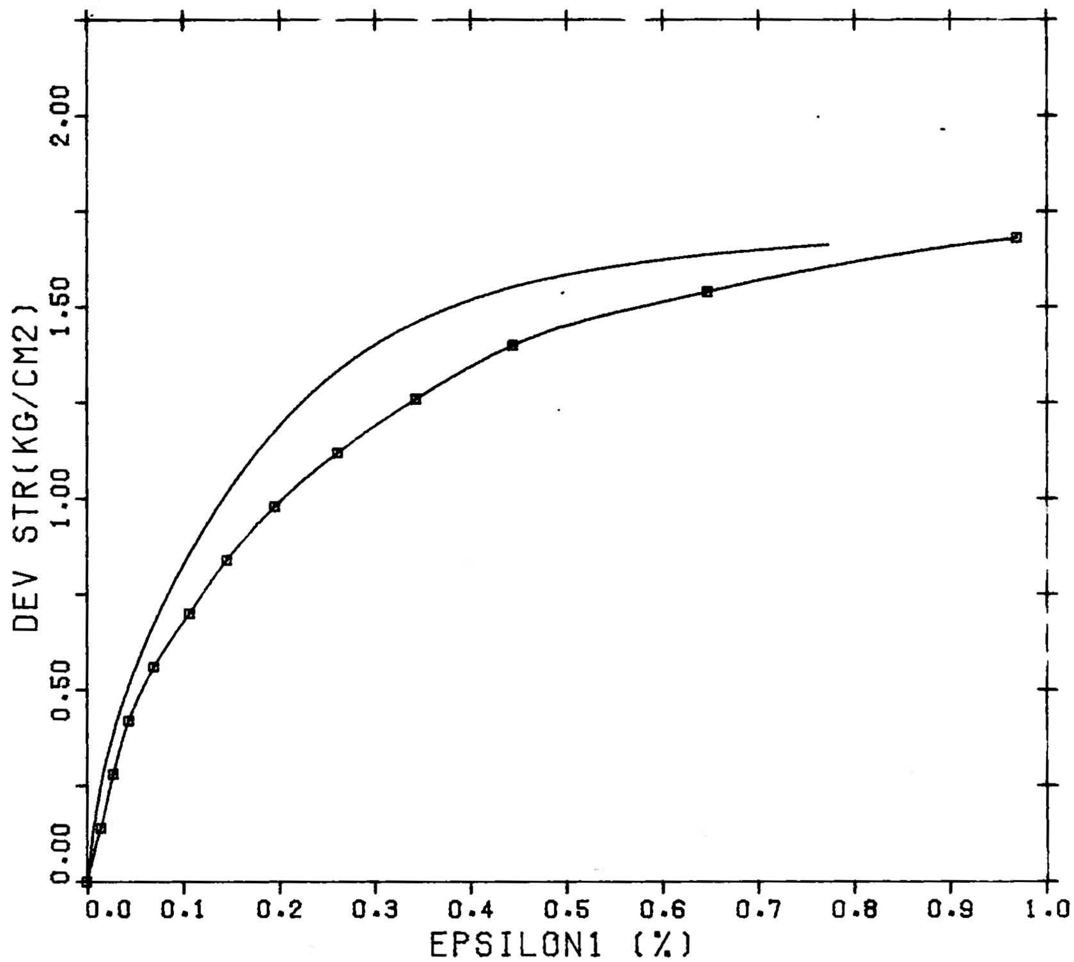

TEST 18-25 SIGMA3 2.10

FIGURE 5.7 ELASTOPLASTIC MODEL PREDICTION

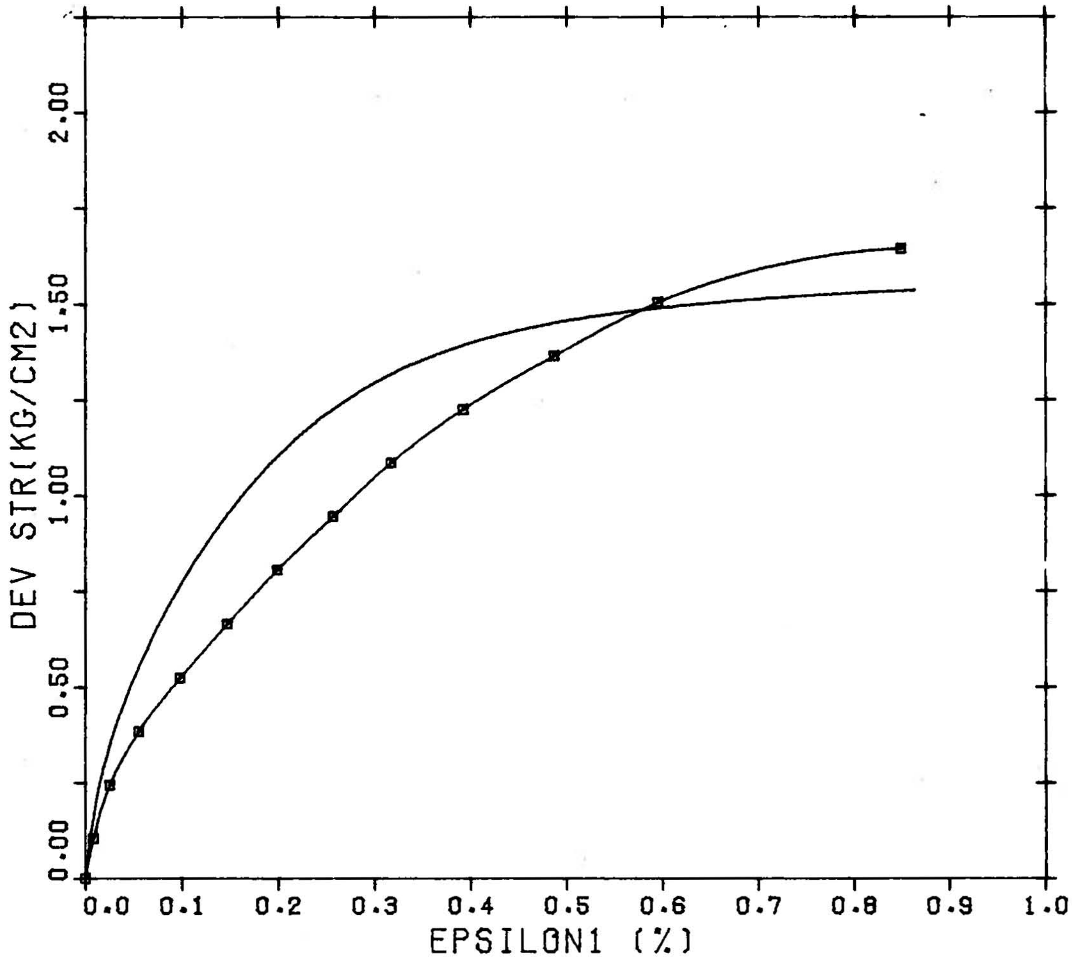

TEST 18-26 SIGMA3 1.925

FIGURE 5.8 ELASTOPLASTIC MODEL PREDICTION

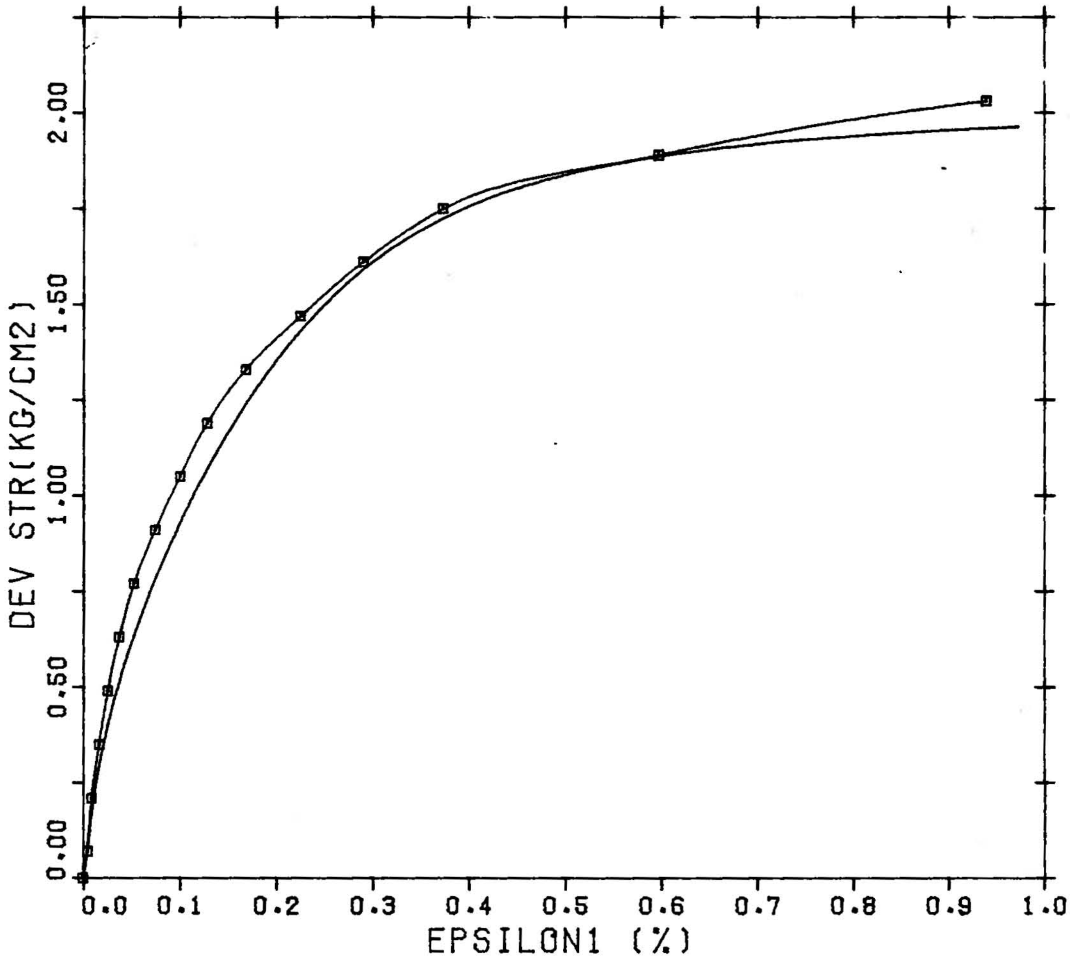

TEST 18-27 SIGMA3 2.45

FIGURE 5.9 ELASTOPLASTIC MODEL PREDICTION

early stages of loading.

Predictions of strains in compression active tests using Lade's stress strain theory compared very favorably with the laboratory measurements. It seems promising to pursue the subject further to investigate the possibility of using the model for other types of stress paths. For situations involving primary loading with predominant increase on the isotropic stress (figure 5.10) , the inclusion of a cap at the open end of the yield surface as suggested by Drucker, Gibson and Henkel (1957) and employed by Roscoe and Poorooshasb (1963) and Lade (1975), makes it it necessary to account for the plastic strain contribution of the isotropic stress

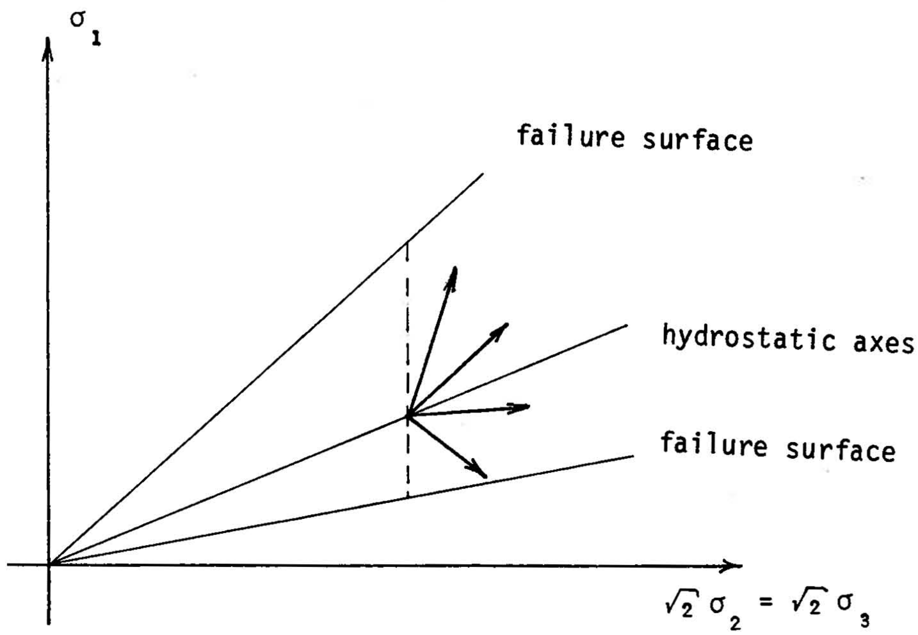

FIGURE 5.10 STRESS PATHS WITH PREDOMINANT INCREASE IN ISOTROPIC STRESS COMPONENT

6. NUMERICAL SOLUTION

6.1 Introduction

The finite element method, as a result of its ability to simulate complicated boundary conditions, construction sequences and to deal with different constitutive models, has been widely used for complicated Geotechnical Engineering problems. The method has been used extensively to analyse the behaviour of retaining walls and excavations (Duncan and Dunlop 1969, Clough and Duncan 1969, Chang and Duncan 1970, Clough, Weber and Lamont 1972, Clough and Mana 1976, Izumi, Kamemura and Sato 1976, Stroh and Breth 1976) and results have compared very favorably with field measurements. A finite element program was written to simulate various phases of the construction procedure in connection to the stress strain behaviour exhibited during the laboratory testing.

6.2 General description of the solution

In this section the overall logic of the solution will be presented while the techniques employed will be explained in subsequent sections.

Due to the rapid response of the slope indicator and the monuments to the excavation , and because of the very short time required to consolidate the laboratory samples, the treatment will be entirely in terms of effective stresses.

The initial vertical stresses are equal to the overburden stress while the horizontal stresses are calculated using the equation :

$$\sigma_h = K_o \sigma_v \qquad \text{.....(6.1)}$$

where KO is the at rest coefficient of earth pressure. The elastic constants are then obtained from these initial conditions. In order to represent different construction phases and the constitutive model adopted, the problem is solved in stages. The first operation which involves the excavation of some material is represented by the application of surface tension at the boundary, equal and opposite to the stress distribution on that surface. The finite element method requires the surface tension to be imposed by means of nodal loads. Consequentely the element stresses are to be reduced to nodal loads. The new boundary is now stress free. The elements removed have their elastic constants reduced to very small values to represent the air and have their stresses zeroed. The load just obtained is divided into a number of steps and applied incrementally. The first increment is applied and the finite element calculations are performed. The stresses and strains obtained are accumulated and the resultant stresses are used to obtain another set of elastic constants for the next increment. After all the load increments have been applied, another construction phase will take place. If it involves the placement of any structural elements, such as struts, the elements correspondent to them have their elastic constants assigned new values to represent the structural material. The material properties from now on will remain constant throughout the analysis. Figure 6.1 illustrates the logic just explained.

6.3 Load determination

In excavation problems where the boundary conditions are specified as a change in load, without modification in the boundary shape with the surrounding ground being linear elastic and time independent, it can be proven that the solution is unique (Ishihara, 1970). Under these circumstances there is no need to treat the problem incrementally. In the field however, it is very difficult to satisfy all of these requirements. The introduction of struts and tiebacks represents a modification in the boundary shape. Even if the material is linearly elastic and stress path independent, for one final state there is not a unique solution. The soil stress strain properties for the case history under investigation has proven its dependency on the stress path. There is therefore ample evidence that for a realistic analysis of an excavation in stiff soils every phase of construction must be simulated as closely as possible. This requirement is not unique to excavation

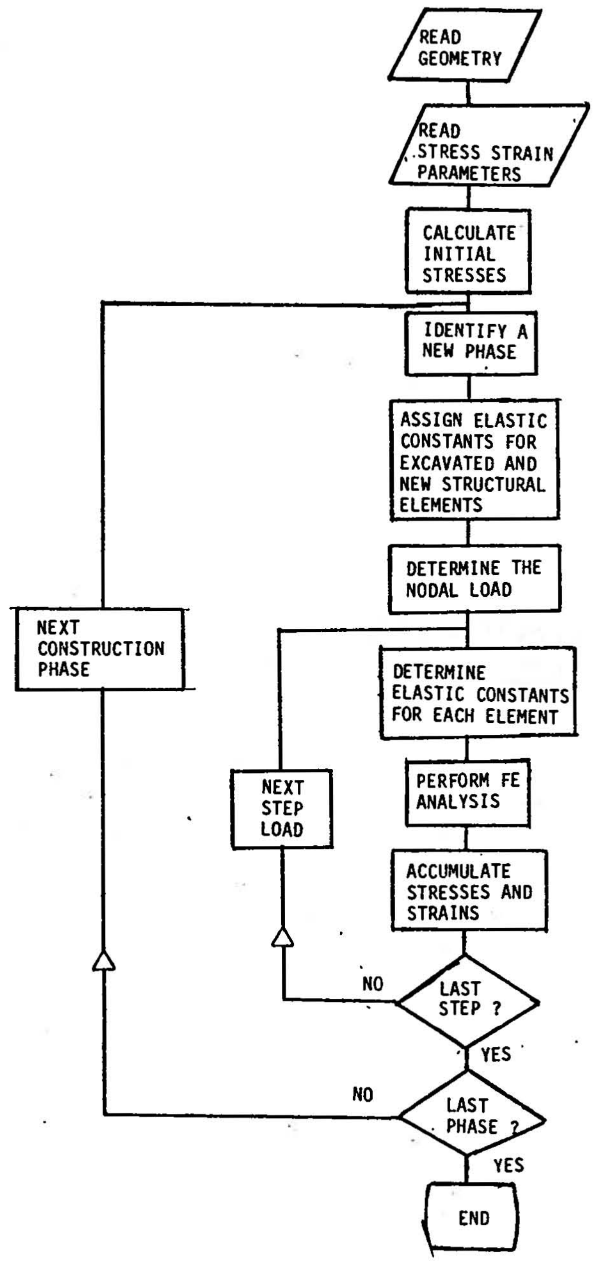

FIGURE 6.1 FLOWCHART

problems; previous experience with the analysis of embankments indicates a remarkable difference in strains between one step and an incremental analysis (Clough and Woodward 1967). The stresses were also affected but to a much smaller extent.

One of the first approaches to this type of problem is the so called gravity turn on analysis. It consists basically of two steps: the first involves the application of gravity forces to a finite element mesh prior to the excavation, and the second involves the application of the gravity forces to a finite element mesh with the opening. The difference between both analysis represent the change in stress and the displacements caused by the excavation (Kulhawy 1974). This type of analysis is very attractive due to its simplicity, but has some deficiencies which prevent a broader use of the technique. The analysis has a built-in at rest coefficient of earth pressure (KO= PR /(1- PR), PR is the Poisson's ratio) which cannot be changed. The surrounding ground has one set of elastic constants throughout the analysis, therefore it is not possible to analyse materials with non-linear stress-strain relationship. A final drawback is the impossibility of modelling construction procedure. The incremental approach can easily overcome these difficulties; the initial state of stress can accommodate any at rest coefficient of earth pressure and the excavation is then simulated by reducing the elastic constants of the excavated material to a very small value. The nodal load applied to the boundary points is obtained from the accumulated stresses of the elements adjacent to the boundary at the previous step. The stresses determined by the finite element method are representative of points inside the element, while the incremental load is to be determined from stresses at the excavation boundary. There is therefore a gradient of stresses between these two points which will be discussed here. For the bottom of the excavation Dunlop, Duncan and Seed (1968) proposed to obtain the nodal loads by averaging the stresses between pairs of elements situated above and below the boundary. This method has been proved accurate provided the elements on both sides of the excavation are rectangles of the same size. Chang (1969) calculated the boundary stresses from the element directly above and assumed a gravity stress gradient. Clough and Duncan (1969) developed interpolation formulas to express the relationship between the known stresses at the element centers and the unknown stresses at the nodes of the excavation boundary. Christian and Wong (1973) used extrapolation formulas from elements in a horizontal row to obtain the load caused by the excavation. Chandrasekaran and King (1974) overcame this drawback by a completely different approach.It consists of imposing a boundary displacement equal to the one observed in the previous step which, when multiplied by the stiffness matrix of the structure below this line, will determine the nodal load due to that increment. Clough and Mana (1976) calculated the nodal loads by obtaining the resultant of the forces from values at Gauss points.

During the development of the program for this project the mesh was designed to provide small elements beside the vertical wall to initially reduce the distance between the boundary nodes and the centers of the adjacent elements. A qualitative horizontal stress distribution of the shape of figure 6.2 was observed. Higher stress gradients in a horizontal line for points closer to the wall, as mentioned by Christian and Wong (1972), were detected, although much reduced due to the presence of the wall. In this project the nodal loads were obtained from averaging the stresses of the elements to be excavated adjacent to the wall. These results were analysed for a wall without embedment, for which case the resultant of the final lateral stress should correspond to the strut loads. The results indicated consistently a difference of 10% between both loads towards the lateral stress distribution. To account for this difference the nodal load in each phase was increased by 10%, after the averaging. The final result exhibited besides the equalization of the loads a coincidence of the point of application of both resultants. For the load at the bottom of the excavation the average was taken between pairs of elements above and below the nodal points. The exacavation was incremented in layers of no more than 2.5 meters thick, which is considered small when compared with layers of 6 meters used by Clough and Duncan (1969). The elements were

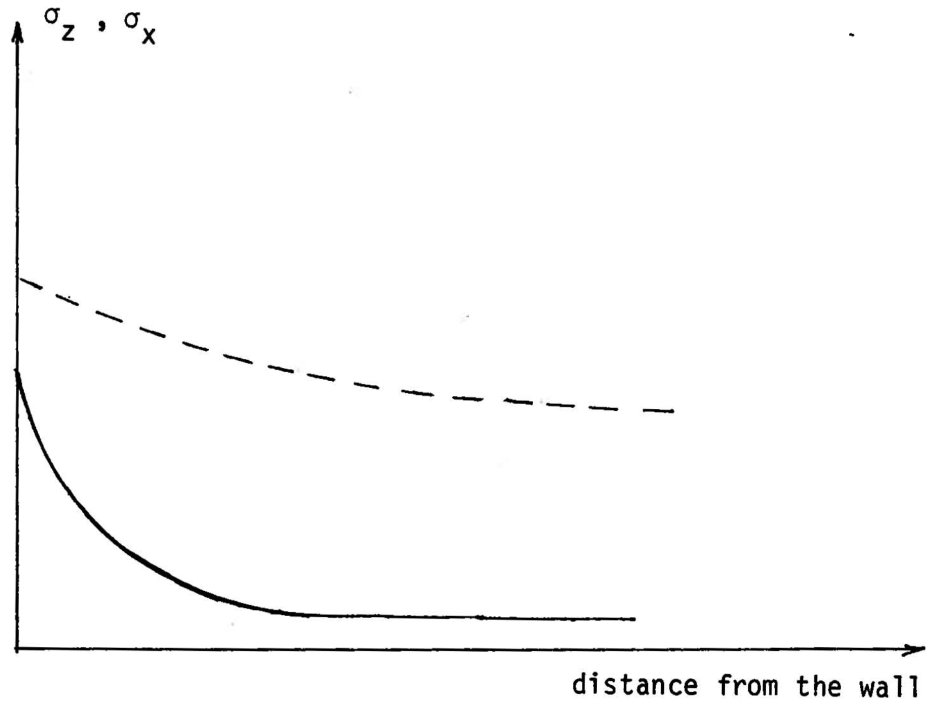

——————— horizontal line immediately below the bottom of the excavation

\- - - - - - - - - - horizontal line at some distance from the bottom of the excavation

FIGURE 6.2 STRESS DISTRIBUTION BELOW THE BOTTOM OF THE EXCAVATION therefore smaller which decreases the distance between the point where the stress is known and the boundary point.

6.4 Stress strain relationship

The stress strain curves obtained in the laboratory indicated that the nonlinearity can not be ignored. The incremental procedure can accommodate this behaviour quite easily. After each load increment is performed the stresses are evaluated to determine the new set of elastic constants to be used for the next increment. This procedure has been called by Clough and Duncan (1969) the "past stress solution" , because the analysis is performed using elastic constants which are a result of a previous increment. An alternate method consists in determining the elastic constants also for stresses at the end of the increment, average them, and perform another set of calculations, this time with the averaged stress strain parameters. This method has been used by Kulhawy, Duncan and Seed (1969), Clough and Duncan (1969) and Gopalakrishnayya (1973), where it reduced the number of iterations to obtain the same precision. The modified Newton-Raphson method or initial stress method (Zienkiewicz, Valliappan and King 1969) also reduces the number of iterations since the stiffness matrix does not have to be inverted for each increment. The analysis was performed with a different number of increments to evaluate the necessity of using the average stress solution. No significant difference was encountered for subdivisions beyond 4 increments. Since average stress solution requires fewer than half of the increments of the past stress solution, the latter is adequate for this problem. Each time the change in configuration occurs in the mesh, another stiffness matrix is generated, therefore the benefit of a constant stiffness matrix, as it occurs in the initial stress method cannot be exercised. It was considered for the present circumstances the past stress method to be the most suitable.

In order to fit the stress strain data points in a smooth curve the following relationships were tried:

$$\sigma_1 - \sigma_3 = a\,\epsilon^{b} \qquad \text{.....(6.2)}$$

$$\sigma_1 - \sigma_3 = a\,\epsilon^{2} + b\,\epsilon \qquad \text{.....(6.3)}$$

$$\sigma_1 - \sigma_3 = a\,e^{b\epsilon}\,\epsilon^{c} \qquad \text{.....(6.4)}$$

$$\sigma_1 - \sigma_3 = \frac{\epsilon}{a + b\,\epsilon} \quad \text{.....(6.5)}$$

Curves of the type of equation 6.5 , which represent a hyperbola (Kondner 1963) , exhibited the best approximation for the data points. For stress level beyond failure there is some degree of departure due to the fact the asymptotic value of the deviator stress is larger than the failure value. The inverse of b represents this asymptotic value, and Duncan and Chang (1970) proposed a correction factor Rf applied on it to correct this ill behaviour :

$$b = \frac{(\sigma_1 - \sigma_3)_f}{R_f} \quad \text{.....(6.6)}$$

where

- $(\sigma_1 - \sigma_3)_f$ is deviator stress at failure
- R_f is the correction factor, which has been found to vary between 0.75 and 1

The use of Rf different than one caused excessive deviation of the hyperbolae from the data points at the early stages of the stress strain curve. Equation 6.5 was hence left in its original form. Whenever the magnitude of the deviator stress would reach failure, a small modulus of deformation would be assigned to that element simulating failure. For each stress path the elastic contants were determined in the following way :

1. Passive compression tests: with a set of stress strain curves obtained from the laboratory (figure 6.3.a) the magnitude of the modulus of deformation was obtained by interpolating linearly between values from two adjacent curves with confining stresses below and above the one being searched. For points falling beyond the limits of the tests, an additional assumption was made with respect to the relationship between the initial modulus and the confining stress of the form:

$$E_i = K\ pa \left(\frac{\sigma_3}{pa} \right)^n \qquad .(6.7)$$

A hyperbola for these points is obtained, where a =1/Ei and b expressed in terms of Mohr-Coulomb failure criteria as :

$$b = \frac{1 - \sin\phi}{2\sigma_3 \sin\phi} \qquad .(6.8)$$

2. Active extension tests: they are determined in the same

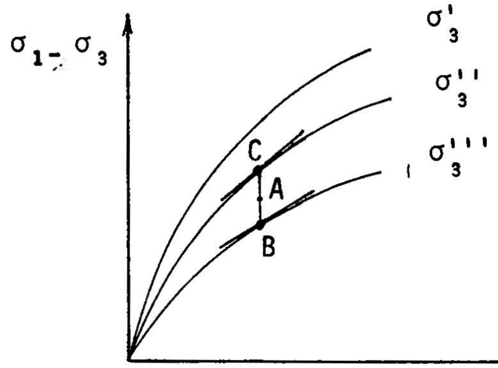

6.3.a Passive compression triaxial

$$E_A = \frac{E_B + E_C}{2}$$

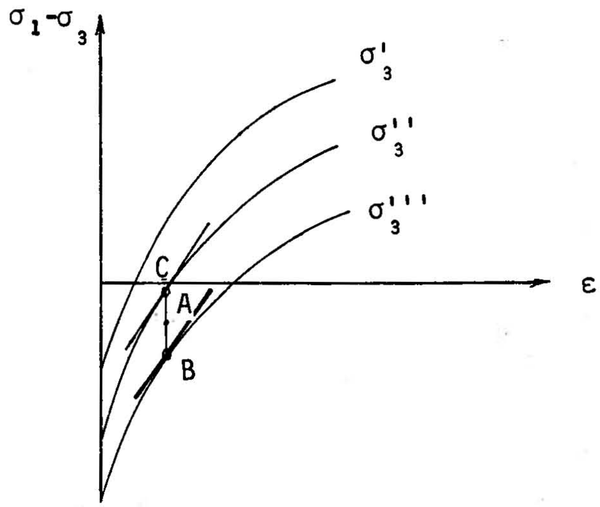

6.3.b Active extension triaxial

$$E_A = \frac{E_B + E_C}{2}$$

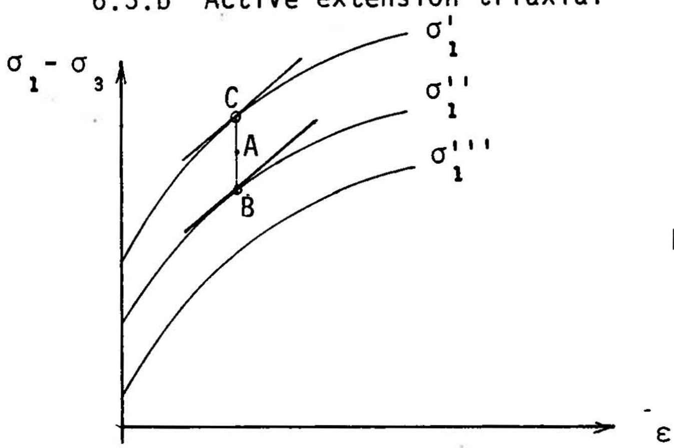

$$E_A = \frac{E_B + E_C}{2}$$

6.3.c Active compression plane strain

FIGURE 6.3 DETERMINATION OF THE MODULUS OF DEFORMATION way as the passive compression tests with the only difference being the hyperbola has its origin displaced by a certain amount as the result of anisotropic consolidation (figure 6.3.b). The equation now becomes:

$$\sigma_{dev} = \frac{\epsilon}{a + b\epsilon} - (\sigma_1^i - \sigma_3^i) \qquad .(6.9)$$

or

$$\sigma_{dev} = \frac{\epsilon}{a + b\epsilon} - \sigma_1^i \,(1 - K_o) \qquad ..(6.10)$$

3. Active compression tests: the only difference between these types of test and the passive compression tests lies in the fact each stress strain curve refers to a value of the major principal stress which remains constant during the test (figure 6.3.c). The expression 6.7 did not hold for these tests, but due to the range of the performed tests, the few points falling beyond the limits were close enough to allow the use of a obtained from the rearest stress strain curve and the value of b expressed in terms of the Mohr-Coulomb failure criterium as:

$$b = \frac{1 + \sin\phi}{2\,\sigma_1 \sin\phi} \tag{6.11}$$

4. Proportional loading active tests: it was observed during the test with this type of stress path very little difference in the modulus of deformation for deviator stresses below the initial value and a curve of the shape of a hyperbolae from there on. A constant value of the modulus was therefore assumed for deviator stresses below the initial and a hyperbolae afterwards, similar to the procedure adopted in active compression tests.

Duncan and Dunlop (1969) approaching the problem of slopes in stiff fissured clays using the finite element method, observed no significant difference in stresses and strains for values of Poisson's ratio from 0.2 to 0.475. The value of 0.42 encountered by back analysis in the Edmonton area (Eisenstein and Morrison, 1972) was used for this case history.

The modulus of deformation for the different stress paths were obtained from the general equations:

$$\Delta\epsilon_x = \frac{1}{E}[\Delta\sigma_x - \nu(\Delta\sigma_y + \Delta\sigma_z)]$$

$$\Delta\epsilon_y = \frac{1}{E}[\Delta\sigma_y - \nu(\Delta\sigma_x + \Delta\sigma_z)]$$

$$\Delta\epsilon_z = \frac{1}{E}[\Delta\sigma_z - \nu(\Delta\sigma_x + \Delta\sigma_y)] \qquad \text{....(6.12)}$$

For triaxial compression passive and triaxial extension active cases the modulus is readily obtained as:

$$E = \frac{\Delta\sigma_z}{\Delta\epsilon_z} \qquad \text{....(6.13)}$$

For triaxial compression active tests:

$$E = -2\nu\frac{\Delta\sigma_x}{\Delta\epsilon_z} \qquad \text{....(6.14)}$$

For plane strain compression passive:

$$E = \frac{\Delta\sigma_z}{\Delta\epsilon_z}\left(1 - \nu^2\right) \qquad \text{....(6.15)}$$

and finally for plane strain compression active:

$$E = -(1 + \nu)\nu\frac{\Delta\sigma_x}{\Delta\epsilon_z} \qquad \text{....(6.16)}$$

The ratio between stresses and strains required in equations 6.13 to 6.16 is obtained from corresponding hyperbolae.

The last stress strain relationship left to determine, regards the interface between the vertical wall and the surrounding ground. Goodman, Taylor and Brekke (1968) developed an uridimensional element capable of modeling the behaviour cf jointed rock. The same element has been used (Clough and Duncan 1969 and 1971) to simulate a soil structure interface. The element accounts for the relative movement between the structure and the ground. The readings of the vertical movement exhibited no relative displacement between both (chapter 3), therefore the program developed in this chapter does not accommodate such elements.

7. RESULTS OF ANALYSIS AND CONCLUSIONS

7.1 Introduction

Certain characteristics of the particular case history which was analyzed that deserved special treatment before the finite element program developed in chapter 6 could be utilized are going to be described. The cross section of the girders and mezzanine are discontinuous along the axis of the excavation. As both of these structural elements work under axial load, they were reduced to a continuous section with the same cross sectional area. To represent the sheet pile wall covering the vertical distance between the girders and the mezzanine floor, an extremely large number of elements would be required because of their reduced thickness. The stress distribution inside these elements is not being investigated here, therefore they will be replaced by a continuous wall with equivalent stiffness and thickness comparable to the tangent pile wall. As opposed to the struts, the sheet pile wall basically works in bending. It was replaced by a vertical wall with the same flexural rigidity EI (E = modulus of elasticity and I = moment of inertia). This approximation has been used successfully to substitute composite walls of soldier piles and lagging by a continuous planar wall (Tsui and Clough 1974 and Murphy, Clough and Woolworth 1975).

The retaining wall is primarily subjected to bending moment having a very reduced axial load. The stress at any point along its cross section can be determined with the use of the equation:

$$\sigma = \frac{M y}{I} \qquad .....(7.1)$$

where

- M -bending moment at the section
- y distance from the neutral axis
- I moment of inertia with respect to the neutral axis

Equation 7.1 indicates, for the present circumstances an accentuated gradient of stress along the cross section. The finite element provides only an approximate solution since the structure can only deform into specified shapes. The approximate solution therefore stiffens the true structure. The finite element program developed in chapter 6 made use of constant strain triangles, which implies a constant stress inside each element. This additional restraint has a large influence on the modeling of the behaviour of the retaining wall where the gradient of stress is significant. A sufficient increase in the number of elements to overcome the problem satisfactorily, would produce a significant expansion in computing time and memory requirements.Consequently the part of the mesh representing the pile was taken separately , fixed at one end and a concentrated load perpendicular to its axis was applied on the other end. The resultant displacements should be smaller than those of the actual structure would undergo, which are provided by the governing differential equation for deflection of elastic beams. The element stiffness in the finite element method is:

$$\left[K\right] = \left[B\right]^T \left[D\right] \left[B\right] t\ A \qquad .....(7.2)$$

where

- t element thickness
- A element area
- D constitutive matrix. It expresses the stress strain relationship.
- B matrix transformation. It expresses the strain displacement relationship. For isotropic material in plane strain :

$$\begin{bmatrix} \sigma_x \\ \sigma_y \\ \tau_{xy} \end{bmatrix} = \frac{E}{(1+\nu)(1-2\nu)} \begin{bmatrix} 1-\nu & \nu & 0 \\ \nu & 1-\nu & 0 \\ 0 & 0 & \frac{1-2\nu}{2} \end{bmatrix} \begin{bmatrix} \epsilon_x \\ \epsilon_y \\ \gamma_{xy} \end{bmatrix}$$

The stiffness of the element can be reduced by decreasing E or t which are constant factors. In order to obtain the results from the closed form solution a factor of 0.35 was employedin all the elements to reduce their stiffness.

The mcst representative section of the overall behaviour does not include the long piles. Their presence much beyond the bottom of the excavation (Figure 7.1 - shaded area) prevents ground movement below the short piles. The analysis of soil displacement , lateral stress and strut load was consequently performed in a section where only the short piles were present. Fcr the analysis of the slope indicator movement inside the long piles this section would indicate excessive movements since the points in the shaded area of figure 7.1 would be free to move, which does not represent the field condition. Alternatively the elements in this area could be assigned concrete elastic properties. This assumption is equivalent to saying there is a continuous wall from the surface to the shale which will cause excessively high lateral stress during excavation, since the soil cannot flow around it, which in turn will produce unrealistic pile movement in that area.

The finite element mesh employed (figure 7.2) contained 326 nodes and 596 elements. The average CPU time to execute all the construction phases, using the

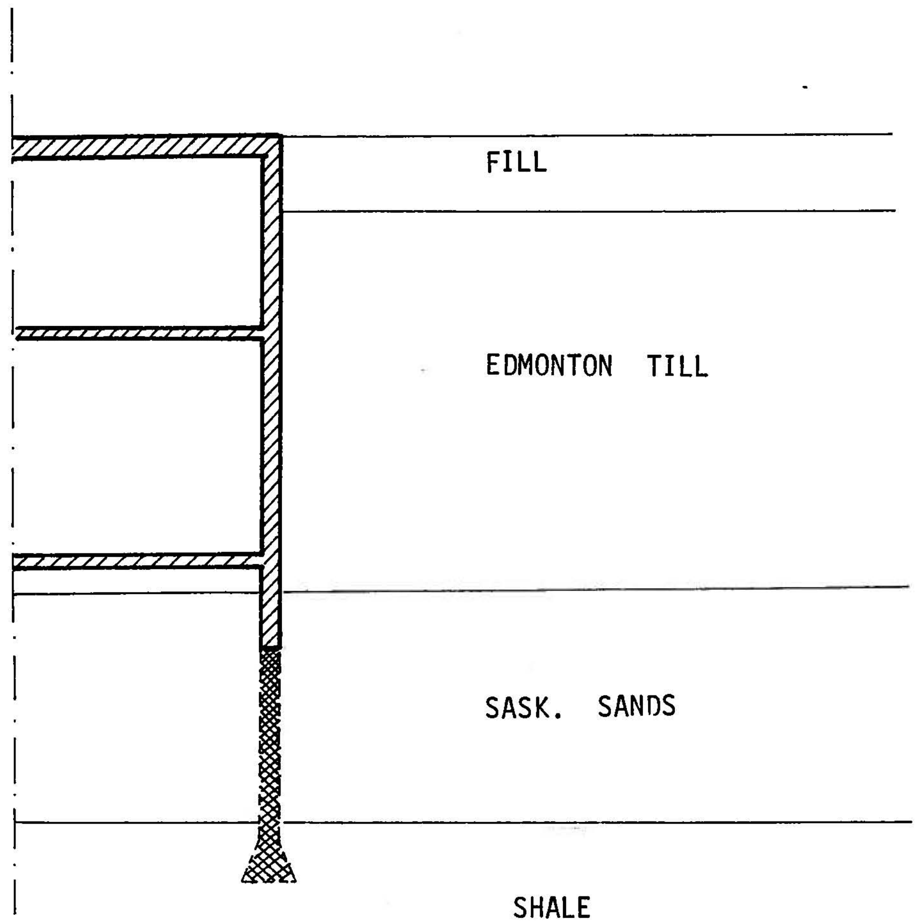

FIGURE 7.1 CROSS SECTION IDEALIZATION

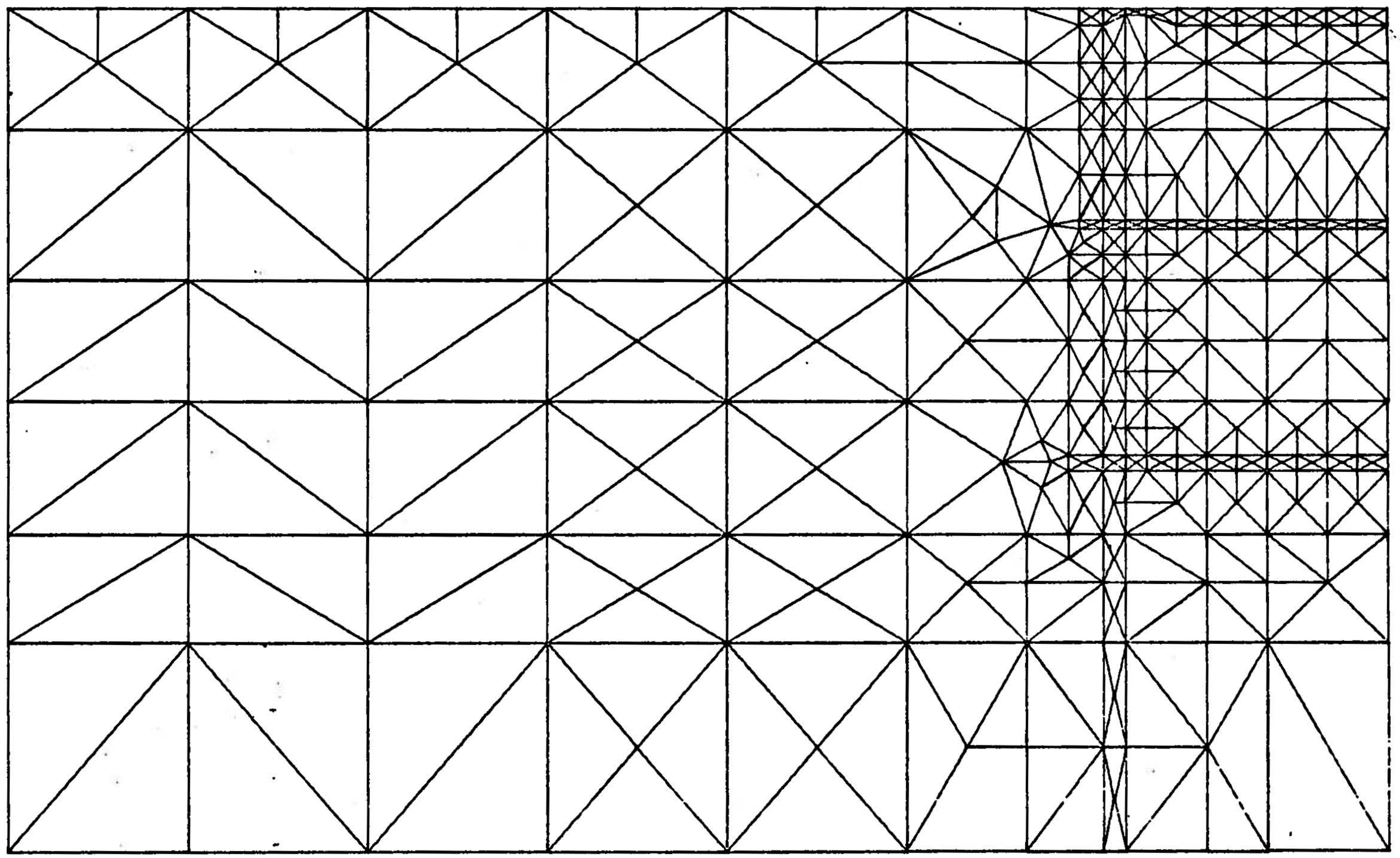

FIGURE 7.2 FINITE ELEMENT MESH

University of Alberta computer(Amdahl 470v6), was 275 seconds with a CPU storage of virtual memory integral (VMI) of 770 page-min, each page containing 4096 bytes. The band width for this mesh was 130.

The analysis was performed under different assumptions with regard to the stress-strain relationship in order to evaluate the most appropriate one to represent the actual field condition. The assumptions employed as follows:

- Linear elasticity

The ground was assumed to behave as a linearly elastic material throughout the analysis. The modulus of elasticity employed was obtained from pressuremeter results.

- Non linear elasticity

The stress-strain relationships for both Edmonton till and Saskatchewan Sands were obtained from passive compression tests in triaxial equipment.

- Triaxial active compression

The stress-strain relationship for the Edmonton Till was obtained from results of active compression test in conventional triaxial equipment and for the Saskatchewan Sands from active extension and proportional-active tests in conventional triaxial equipment

- Plane strain active compression

The stress-strain relationship for the Edmonton

Till was obtained from active compression tests in a plane strain apparatus, while the Saskatchewan Sands from active extension and proportional-active tests in conventional triaxial equipment.

The construction was simulated in 7 different phases as follows (figure 7.3) :

1. Excavation of the first 3 meters of soil. The tangent piles already in place.
2. Excavation of an extra meter of soil (4 meters deep) and placement of the first level of struts (girders)
3. Excavation of another 2.5 meters of soil (6.5 meters deep).
4. Excavation of another 2.5 meters of soil (9 meters deep) and placement of the second level of struts (mezzanine).
5. Excavation of another 2 meters of soil (11 meters deep).
6. Excavation of another 2 meters of soil (13 meters deep).
7. Excavation of the last 2.3 meters of soil (15.3 meters deep).

7.2 Pile movement

The results of initial analysis performed indicated extremely small lateral movement at the top of the pile. If the amount of movement observed in the field had been absorbed by contraction of the girder due to axial load, it would amount to a value much beyond the load capacity of the

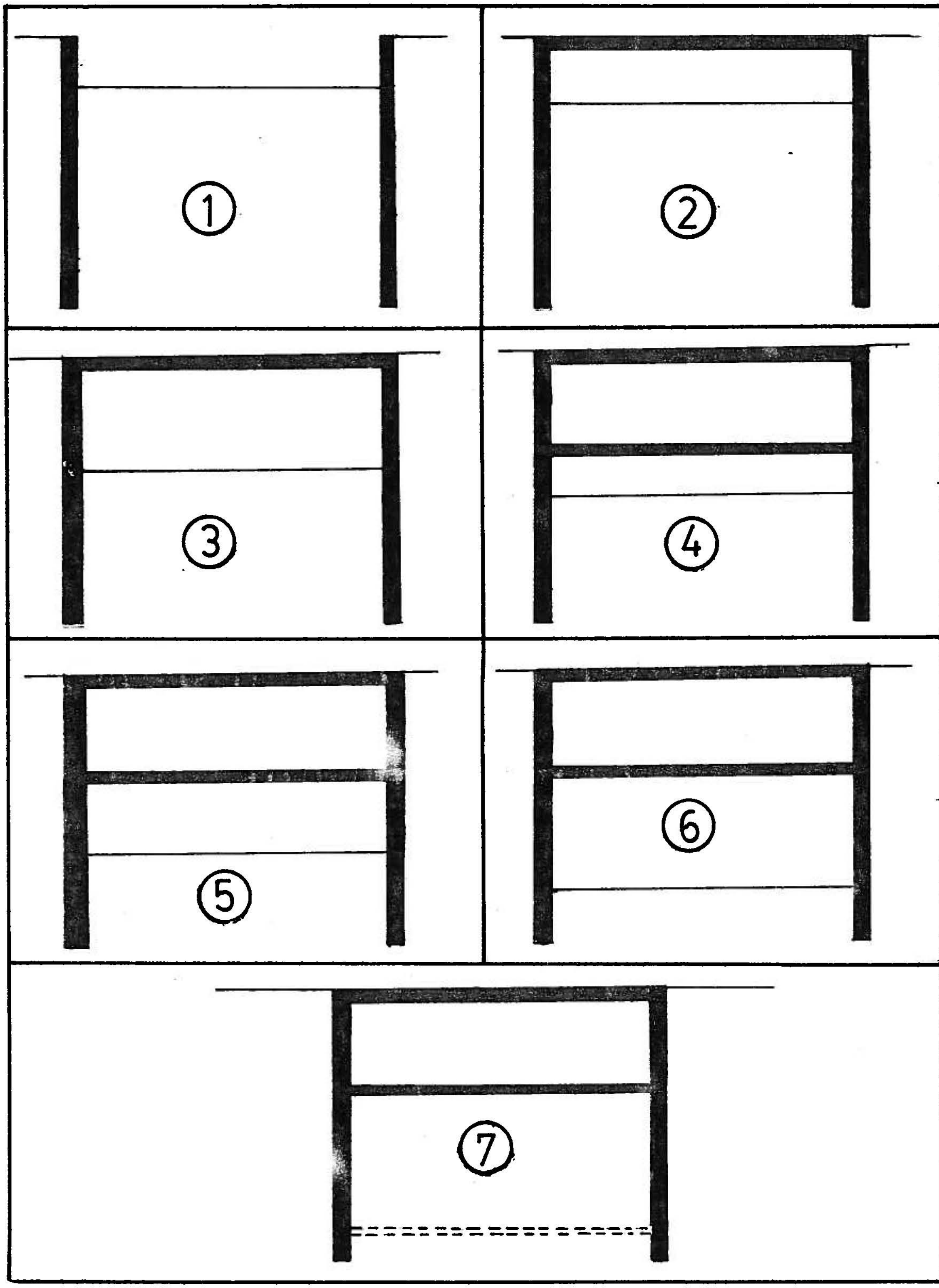

FIGURE 7.3 SIMULATION OF THE CONSTRUCTION PHASES

girder. As was pointed out in chapter 2 (figure 2.7), there is a gap of 7.6 cm between the girders and the "L" shaped beam, which is filled with cement grout. The large horizontal movement at the top of the pile is attributed to a low value of the modulus of deformation of the grout. Initially the grout was assigned the same modulus of the girders and the concrete wall (140,000 kg/cm2), but to reach movements compatible with the field observations it had to be reduced by a factor of 40.

The resultant pile movements employing different assumptions regarding the stress strain relationship are in figure 7.4 . The use of a linear elastic material (E=1050 kg/cm2) assumption results in reduced displacements which is caused by a constant value of the modulus of deformation even for elements with high values of stress level. Results from a a non-linear elastic material assumption based on results from conventional triaxial tests exhibit displacements significantly higher than field measurements. The values of moduli of deformation encountered in the laboratory resulted in excessive displacement predictions. There is not a significant difference between results from active compression predictions from triaxial and plane strain, which indicate a better agreement with the field data. A good opportunity to evaluate the assumptions made along the line, rests in the field data provided by slope indicator SI2. It indicated the girder was not activated. The analysis was performed with exactly the same input data

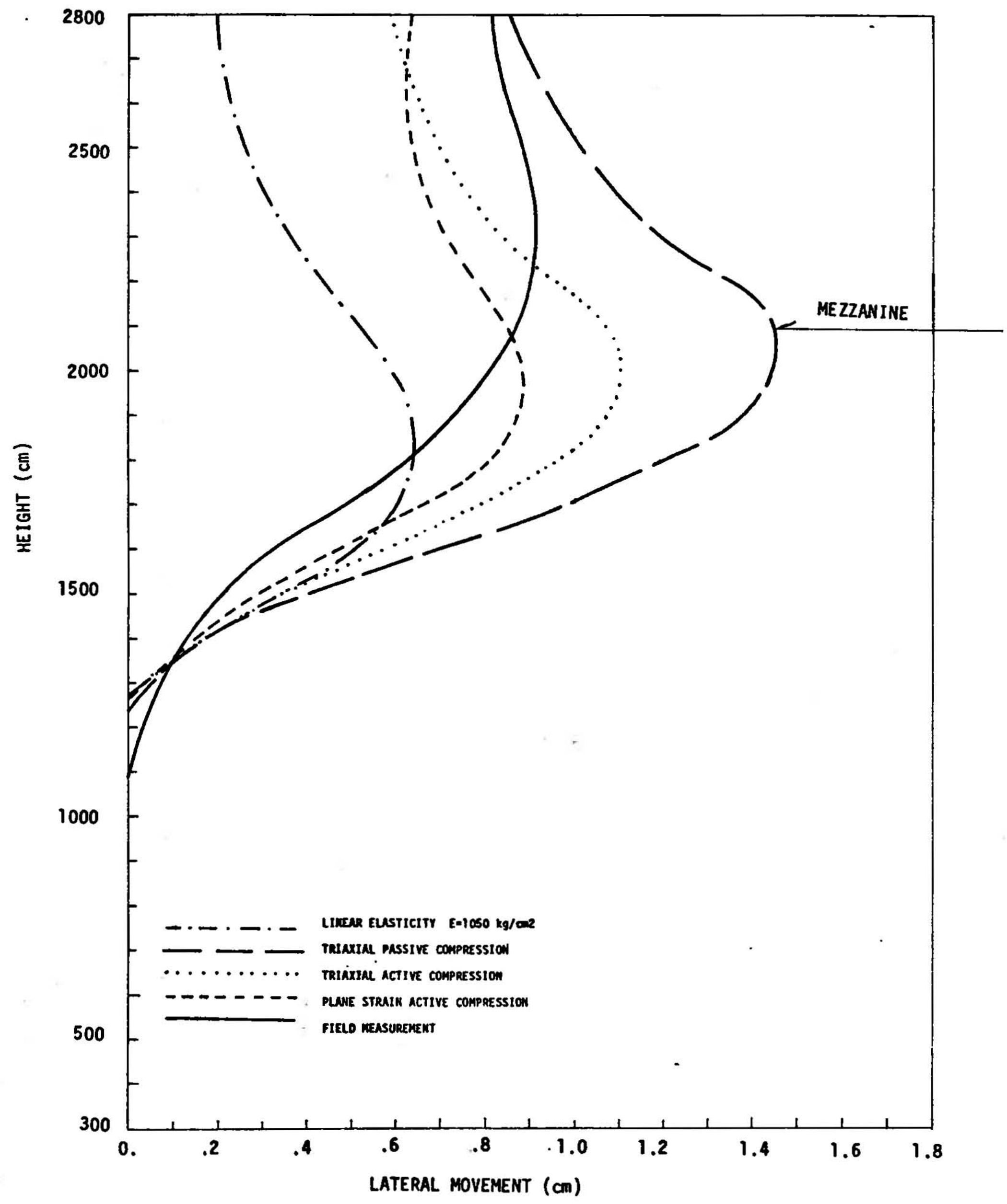

FIGURE 7.4 COMPARISON OF FIELD MEASUREMENT OF SLOPE INDICATOR SI2 AND FINITE ELEMENT PREDICTIONS

for SI3, with the cnly difference being an extremely low value of the modulus of deformation (E=10 kg/cm2) was assigned for the elements representing the grout. Figure 7.5 supports the view the grout properties are responsible for a poor use of the girders to carry horizontal load.

7.3 Vertical movement

The results obtained for the different stress-strain assumptions are indicated in figure 7.6 . The displacements obtained from conventional triaxial tests again reflect the reduced modulus of deformation obtained thereby. Maximum displacement of 1.23 cm was predicted whereas the highest value encountered was 0.67 cm. Results obtained from an assumption of linear elasticity were in good agreement with the actual measurements. Smaller movements were indicated in the vicinity of the wall. Elements next to the wall remained with the same modulus, however due to the flexibility of the wall, there should have been a reduction in the modulus which was not properly represented. This assumption also tends to enlarge the zone of influence of the movements due to the excavation. If one extrapolates the field curve for points beyond 16 meters from the wall a significant difference is observed. The higher stiffness inherent from this assumption broadens the displacement pattern. The predictions based on active compression tests in triaxial test depart considerably from the field curve for points close to the wall. The conclusion that the modulus of

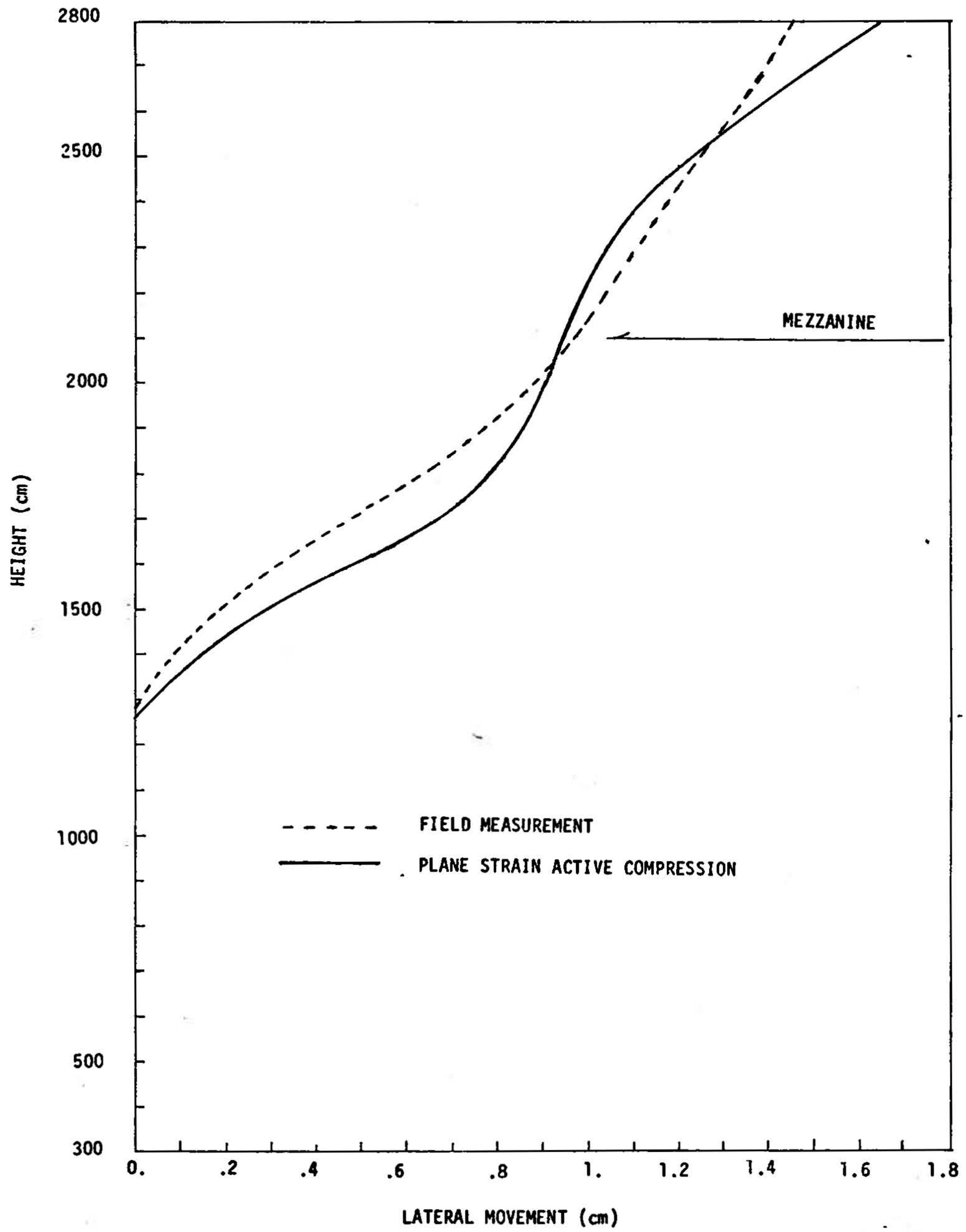

FIGURE 7.5 COMPARISON OF FIELD MEASUREMENT OF SLOPE INDICATOR SI3 AND FINITE ELEMENT PREDICTIONS

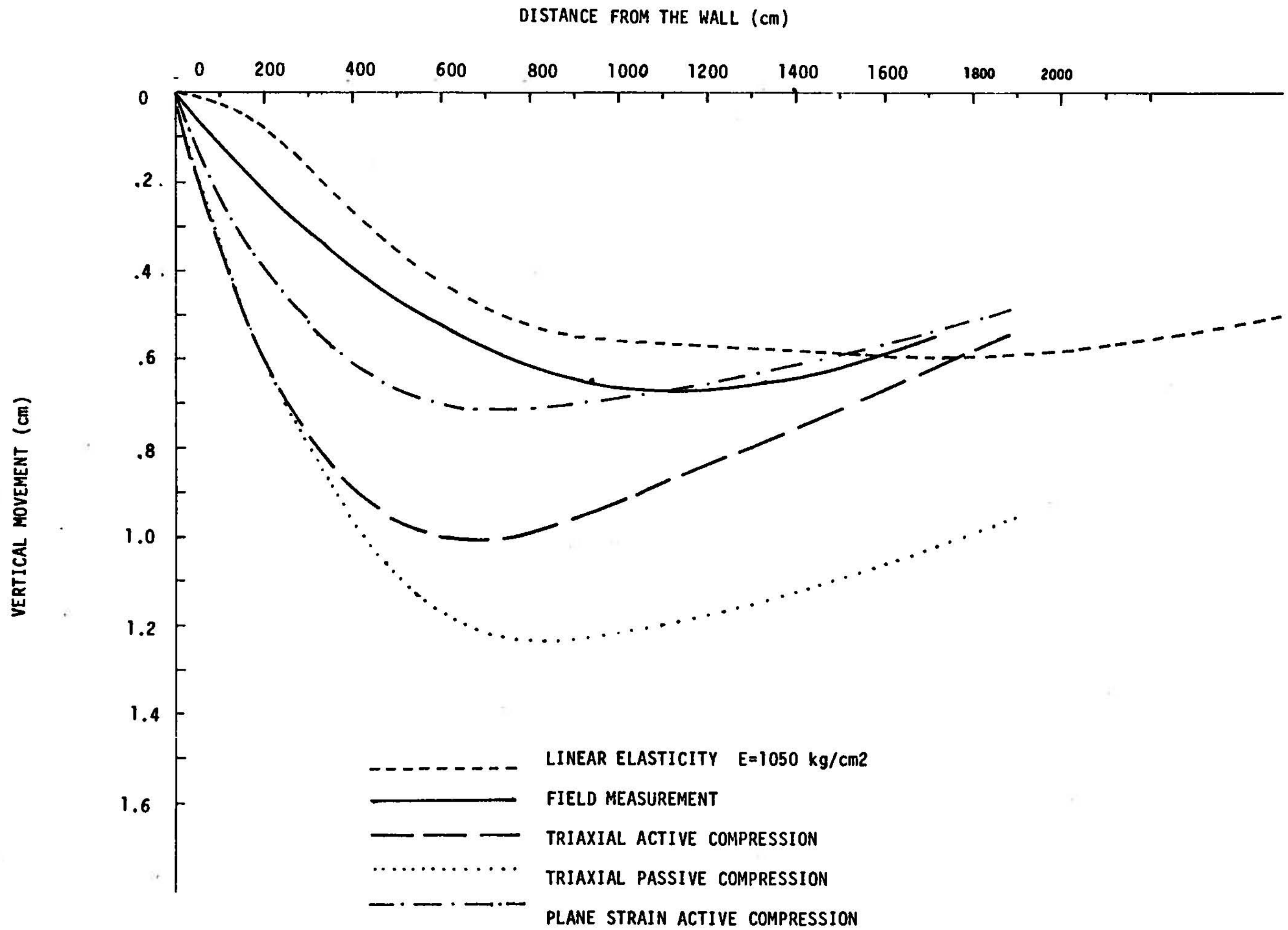

FIGURE 7.6 COMPARISON OF GROUND MOVEMENT AND FINITE ELEMENT PREDICTIONS

deformation from triaxial tests with a passive compression stress path can not be used to obtain the strains in a plane strain condition (Chapter 4) , can be extended to active compression tests. The results from active compression tests in plane strain predicted a maximum displacement of 0.71 cm when it was observed to be 0.68 cm. This assumption exaggerated the displacements for points close to the wall but predicted accurately the extension of the zone of influence of the excavation.

7.4 Lateral load and stress

Due to the change in the original project for the addition of a pedestrian exit it was not possible to monitor the strut loads beyond 10 meters of excavation. The only field measurement available for comparison refers to the mezzanine load for these 10 meters of excavation. Table 7.1 presents the normal stress for the different analytic assumptions. The results indicate the magnitude of the predicted load is not as much affected by the assumed stress-strain relationship as are the displacements. The only analysis falling outside the acceptable range refers to the assumption that the material behaves linearly elastic.

The lateral stress distribution encountered for each of the stress strain assumptions are represented in figure 7.7, where Peck's lateral stress distribution for lateral stress is also indicated. Apart from the assumption of linear elasticity, which indicates an unreasonable distribution,

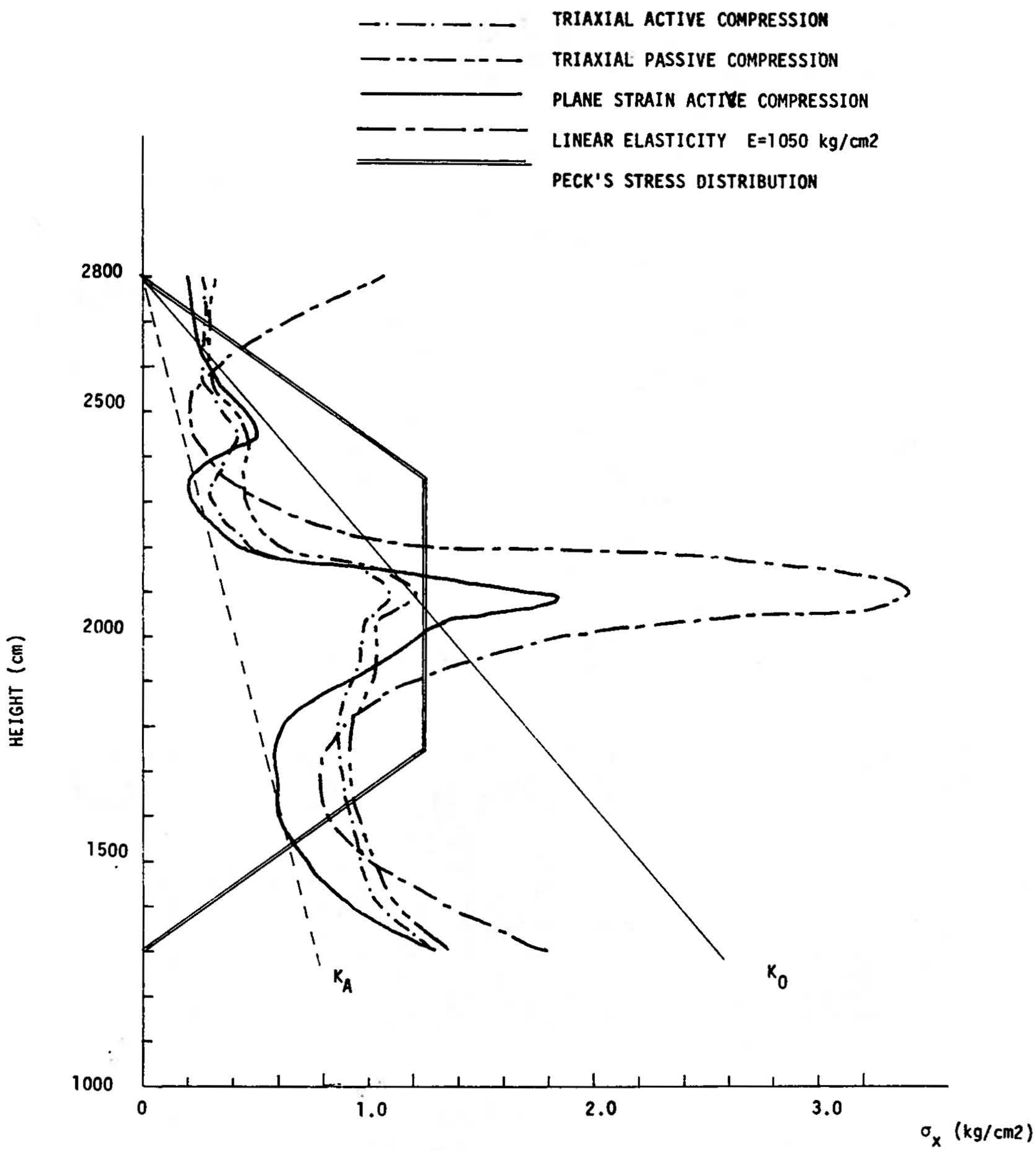

FIGURE 7.7 LATERAL STRESS DISTRIBUTION

ALONG THE WALL

there is a reduction of the lateral stress in zones where the retaining structure yields and an increase on the supporting points, which agrees with results in model tests in sands by Bros (1972). Below the bottom of the excavation the stresses increase very rapidly in the direction of the at rest state of stress. The stress distribution can be approximated by a linear increase of the lateral stress with depth, exhibiting peaks in the presence of struts.

TABLE 7.1

Normal stress in the mezzanine.

condition	normal stress (kg/cm2)
field measurement	13.03
linear elasticity E=1050 kg/cm2	19.5
ncn-linear elasticity	13.6
stress path triaxial	12.13
stress path plane strain	12.6

7.5 Influence of the thickness of the wall

As the cost of the walls for the underground stations represented 10% of the total cost of the project , whereas the price of both tunnels joining both stations accounted for only 3.3% of the total cost, an evaluation of the influence of the stiffness of the wall will be of economical interest, particularly for future similar projects.

Clearly, a reduction in the stiffness of the retaining structure decreases the lateral load. Figure 7.8 illustrates the comparison of the lateral stress distribution when the sheet pile portion of the wall is replaced by a tangent pile wall of the same stiffness as the rest of the wall. The stresses in the upper part approach the K0 line , while with the sheet pile wall there is a stress release due to the reduction in stiffness with a transfer of some of the load to the non-yielding part.

A change in thickness of the entire wall has a much more significant effect (figure 7.9). Walls 2 meters thick bring the stress distribution closer to the at rest state of stress and reduce the stress concentrations at the support levels as a result of their large bending resistance. Figure 7.10 indicates the influence of the wall thickness on the total and strut load. A flexible wall does not give the opportunity for the embedment to carry some of the load. A 2 meters thick wall enables the ground to carry as much as 20% of the total load. Even with such a stiff strutted wall the

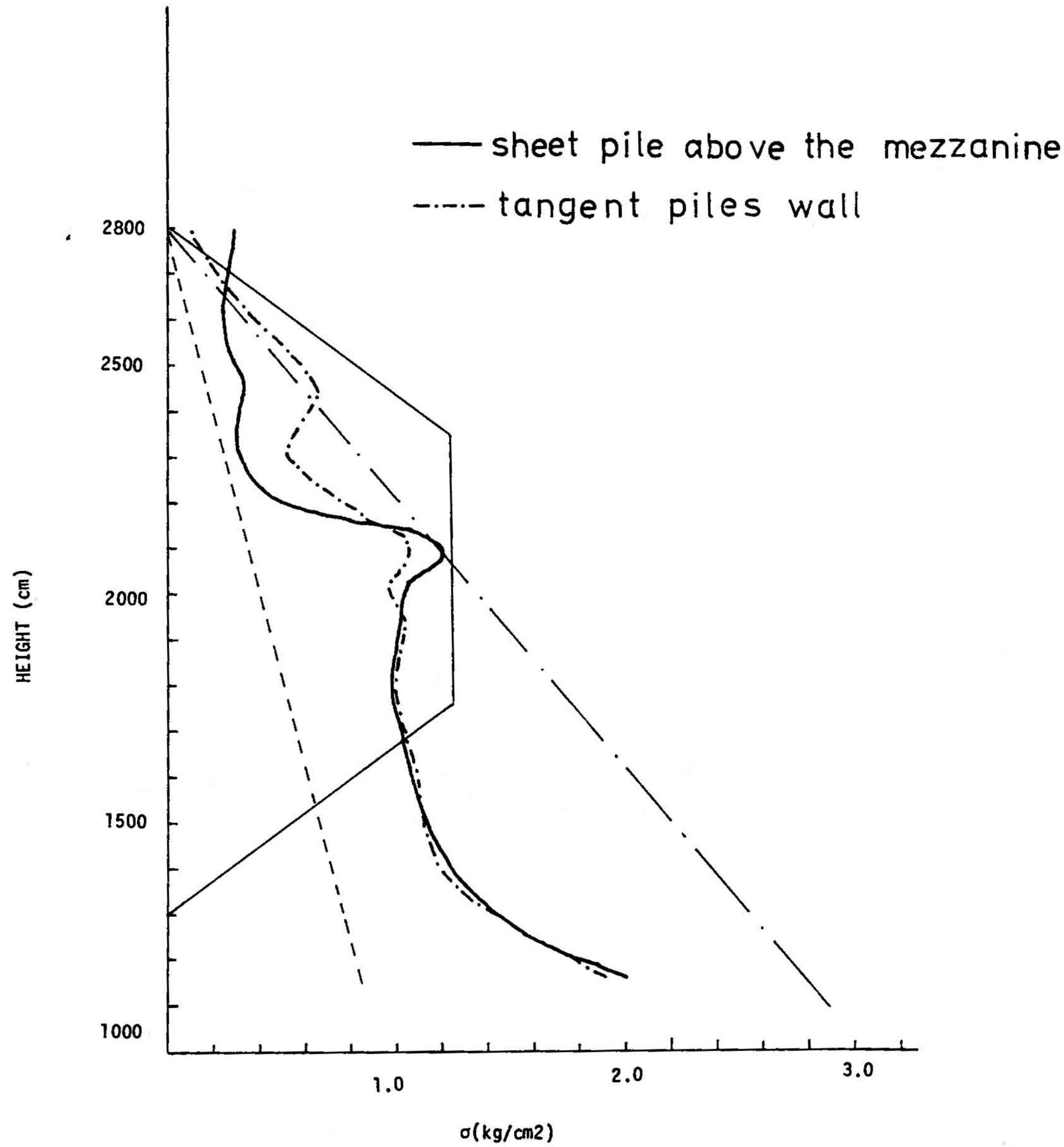

FIGURE 7.8 COMPARISON OF LATERAL STRESS DISTRIBUTION BETWEEN CONCRETE TANGENT PILES AND SHEET PILE WALL ABOVE THE MEZZANINE

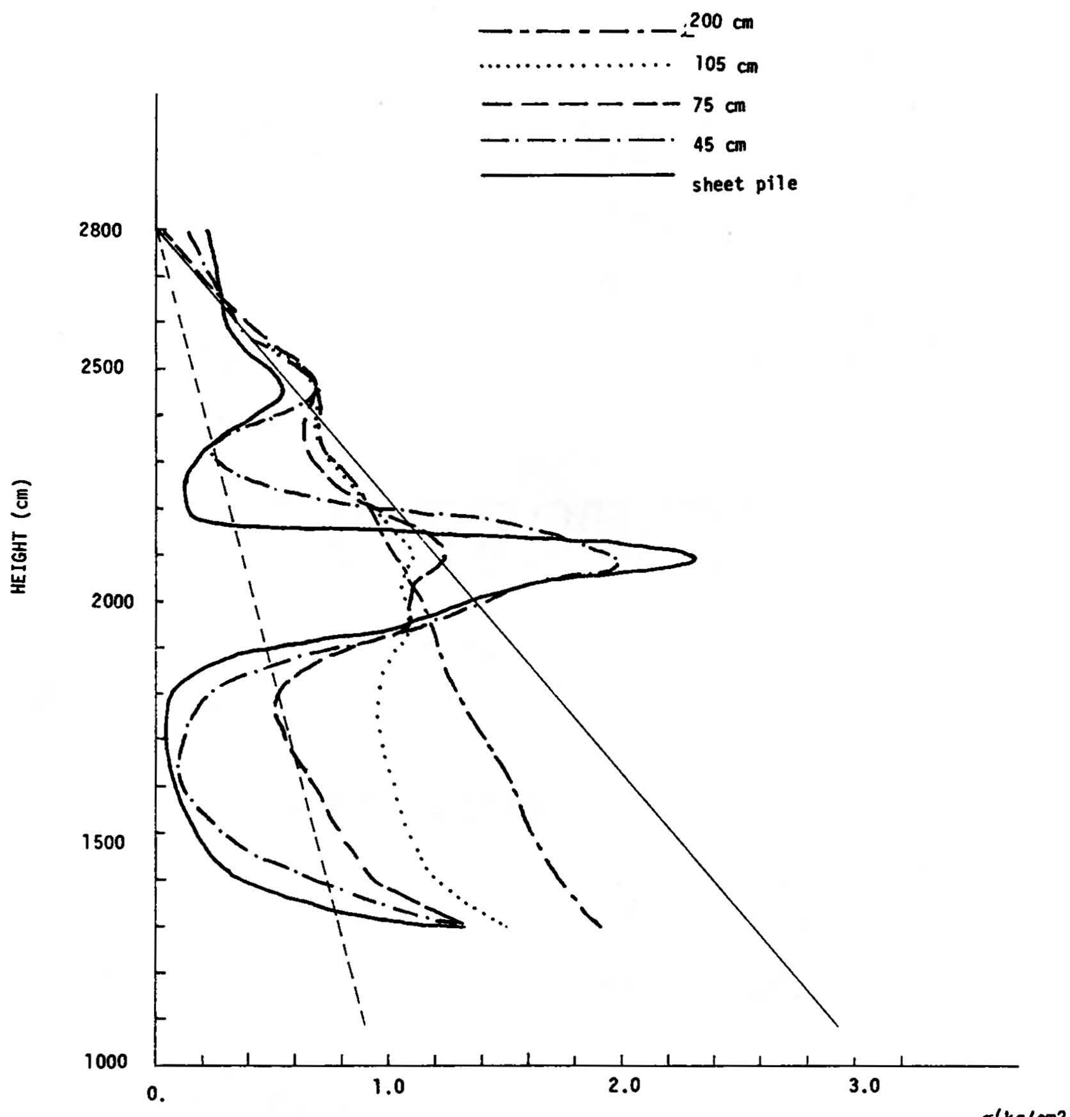

FIGURE 7.9 INFLUENCE OF WALL THICKNESS ON THE LATERAL STRESS DISTRIBUTION

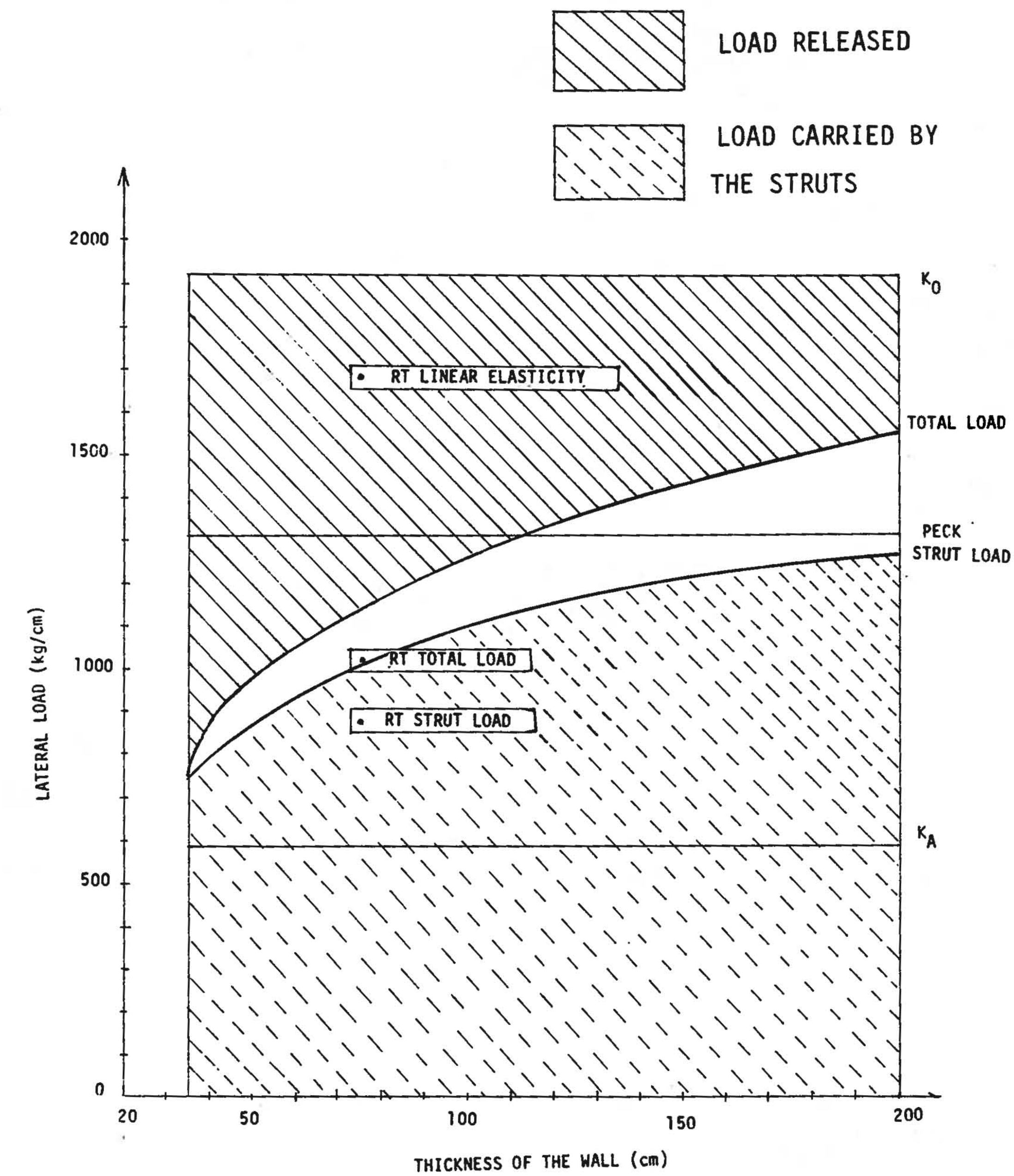

FIGURE 7.10 INFLUENCE OF THE WALL THICKNESS ON THE LATERAL LOAD

initial lateral pressure is reduced in 20%.

The reduction of load is done at the expense of some ground movement (Figure 7.11) and expansion of the zone affected by the excavation. A stiff wall reduces the maximum displacement but the improvement becomes less effective at greater thicknesses. An increase in thickness from 40 cm to 80 cm reduces the maximum displacement from 0.75 cm to 0.55 cm while an increase in thickness from 160 cm to 200 cm reduces the maximum displacement from 0.40 cm to 0.38 cm. Figure 7.10 and 7.11 indicate the minimum possible displacement tends to a value of .36 cm and the load to a value of 1650 kg/cm.

7.6 Summary

During the present research a field case of a deep excavation in stiff clay was documented with the purpose of measuring the earth pressure distribution imposed on the retaining structure and the ground movement associated with it. As frequently occurs, a fragmented set of data was collected. With the use of laboratory tests following the appropriate stress path for excavations, a numerical solution was employed aiming to reproduce the field measurements. Some information with respect to the lateral load was obtained but not enough by itself to consider its reproduction by an analytical solution to be satisfactory. In addition to lateral load, movement of the retaining wall and the ground were also obtained. The results of

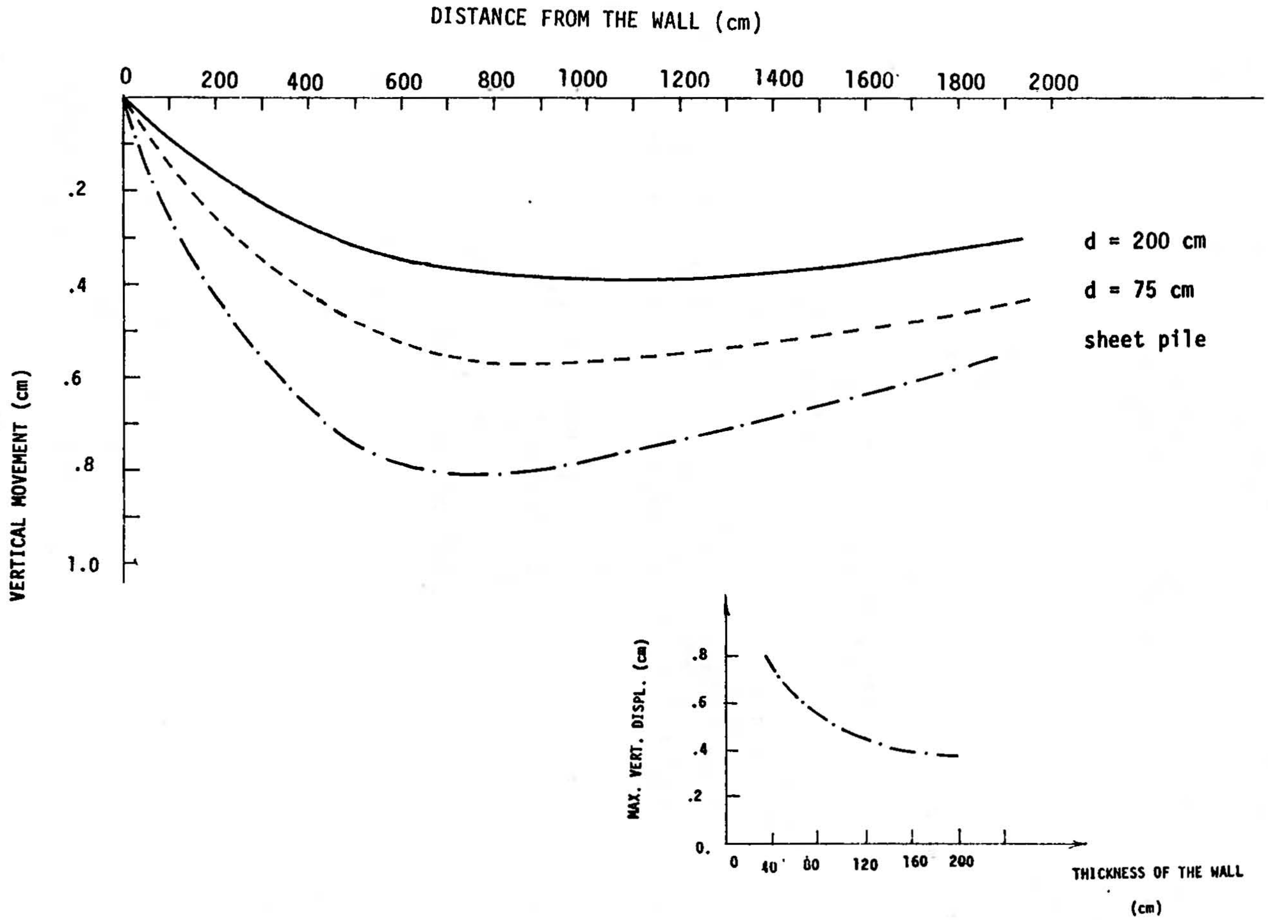

FIGURE 7.11 INFLUENCE OF THE WALL THICKNESS ON THE GROUND MOVEMENT

deformation obtained by the analytical solution were in very good agreement with the field measurements. The evaluation of displacements in Geotechnical enginering are extremely sensitive to the modelling employed. It is therefore considered that a solution which provides good reproduction of the displacements in problems of such kind, is bound to give even better results with respect to the lateral stress which in stiff clays are extremely difficult to measure in the field. In the case history analysed the scarce field data of the strut load was also reproduced accurately.

7.7 Conclusions and suggestions for further research

An integrated approach involving field observation, laboratory testing and the use of a numerical analysis followed by an evaluation of its results proved to be of great value to understand the behaviour of deep excavations supported by semirigid structures. Even with the usual limitations existing in the field and the laboratory testing and the simplifications necessary to secure a relatively simple analytical solution, loads and deformations for the case history investigated were reproduced within reasonable accuracy which indicates this approach as viable to obtain engineering solutions for this type of problem. The outcome of this research managed to give a significantly better perspective of the lateral stress distribution to expect during the construction of retaining walls in stiff soils and the most important factors involved in this type of problem.

Field measurements indicated that for stiff soils a reduced zone of influence of displacements is caused by the excavation when one uses semirigid structures. No vertical or horizontal movement was observed for points at a horizontal distance equal to twice the depth of the excavation.

Direct measurements of lateral stress in stiff clays are extremely difficult to obtain. Very small values of lateral strain are enough to release a significant portion of the lateral stress thereby preventing reliable measurements. The appearance of gravel in glacial tills also presents an obstacle to good performance of the measuring device. The monitoring of lateral load by means of load cells and strain gauges in the struts offers an alternative approach to the measurement of lateral load imposed on the structure.

To guarantee an efficient usage of struts, if they are not cast in place, special care must be taken with respect to the connection between the wall and the struts. The degree of importance increases very rapidly the stiffer the soil. A poor contact, in soils which require very little movement to mobilize their shear strength, causes a remarkable reduction in the strut load, resulting in overdesigning of the struts and undesirable soil movement.

Stiff clays when tested under active compression stress paths indicated a remarkable reduction in the strain to failure and consequently a significant increase in the modulus of deformation when compared with passive compression tests. A reduction in the isotropic stress component causes a expansion in all directions . The total vertical strain will be the resultant of this expansion and the contraction due to an increase in the deviator stress.

Active extension tests in dense sands also reduce the isotropic stress component therefore causing an increase in the modulus of deformation. Due to the fact these two stress paths are dominantly present in excavations and they depart substantially from conventional triaxial testing, it is of paramount importance to obtain the stress-strain parameters from tests following the appropriate stress path. In these cases the soil is being loaded by the decrease of one of the principal stresses. For situations involving loading with increase in the principal stresses not so much difference should be expected.

Passive compression tests in triaxial and plane strainloading led to significantly different values of the modulus of deformation. The prediction of displacements based on results from plane strain and triaxial results in active compression indicated significantly higher values of ground displacements from triaxial results. Values of modulus of deformation from plane strain and triaxial do not lead to the same values . The theory of elasticity can not be used to simulate plane strain conditions from triaxial tests results, even for small values of the stress level.

Stiff clays are very highly stress path dependent materials.

The assumption that the stress-strain relationship can be represented by two constants, even if they are obtained by following appropriate stress path, leads to a gross overestimation of the lateral load. For a retaining wall or a construction procedure permitting considerable movement, a more pronounced departure is to be expected.

Stiff clays require such a small strain under active compression loading that the construction of an extremely thick wall will not prevent the soil from contributing with its shear strength to the carrying of the lateral load. The construction of a semirigid wall can reduce the lateral load 45% from the initial conditions.

Laboratory testing with lightly overconsolidated soils leads to appropriate estimation of the stress-strain relationship provided the field stress path is observed. The unloading caused by the sampling and the presence of fissures in highly overconsolidated soils lead to erroneous values of the modulus of deformation, but the lightly overconsolidated clay investigated here did not exhibit this behaviour. The stress path assumes such an overwhelming importance that the performance of large in-situ tests are not adequate to obtain the representative stress-strain parameters for excavations.

The stiffness of the wall plays an important role in the lateral stress distribution and ground movement. Maximum vertical displacement of the ground as well as the extension of the zone of influence by the excavation can be reduced by constructing a stiffer wall. The efficiency of the wall is reduced as the wall becomes thicker. The lateral stress distribution departs from a triangular shape as the rigidity of the wall is reduced, with concentration of stresses at strut levels. The ground movement in stiff soils is very reduced for any wall rigidity. It seems therefore , since the wall is able to sustain the resulting bending moment and failure of the surrounding ground does not occur , a flexible structure represents an economical and convenient solution.

An earth pressure distribution in the form of a diagram to guide the designers has to include the stiffness of the wall. Peck's empirical earth pressure distribution for permanent structuresis indicated to be on the conservative side for any wall stiffness for the case history investigated.

The flow of soil below the bottom of the excavation is responsible for a significant portion of the ground movement. The presence of a rigid base at the bottom of the excavation can therefore effectively reduce ground movements.

The conclusions being presented refer to an excavation with the ratio between depth and width of approximately 1. The evaluation of the importance of different factors, such as the width of the excavation and the depth of the embedment has not been studied here.However they will prove to change significantly the distribution of stresses and displacements.

Better information with respect to loads and displacements for future design in this type of material can be successfully obtained if the importance of including laboratory testing involving the stress paths is recognized and described with the use of the finite element methodwith the appropriate simulation of the stepwise construction procedure.

Since stiff clays are highly stress path dependent, the evaluation of loads and displacements, especially in excavations, require laborious tests involving stress paths which are significantly different from the conventional ones. By the use of an elastoplastic model which stress-strain parameters were obtained from passive compression tests , good predictions of active compression tests were achieved. Investigation in this area should be pursued to evaluate the applicability of the model for different stress paths and the possibility of its use in actual engineering structures The use of the model in overconsolidated soils can, in theory, also be performed since the volume change caused by shear stresses can be represented, but considerable more investigation is needed with respect to the definition of the yield surface. It is expected the fissures in this case will introduce considerable difficulty. An evaluation of the behaviour of stiff clays under different stress paths can also provide an new engineering insight for the design of structures in these soils.

BIBLIOGRAPHY

Armento, W.J., "Criteria for lateral pressures for braced cuts", Proceedings of the ASCE Specialty Conference on Performance of Earth and Earth Supported Structures, Vol.1 , Part 2, 1972, pp.1283-1302.

Arthur, J.R.F. and Menzies, B.K., Correspondence on: "A new soil testing apparatus' Geotechnique , Vol.15 no.2, 1968, pp.271-272.

Bayrock, L.A., and Hughes, G.M., "Surficial geology of Edmonton district, Alberta", Earth Science Report, 62-6, Alberta Research Council, 1962.

Bayrock, L.A., and Berg, T.E., " Geology of the City of Edmonton. Part 1: Central Edmonton", Earth Science Report, 66-1, Alberta Research Council, 1966.

Bell, J.M., Correspondence on: "A new soil testing apparatus", Geotechnique , Vol.18, no.2, 1968, pp.267-271.

Bishop ,A.W. "Test requirements for measuring the coefficient of earth pressure at rest", Brussels Conference on Earth Pressure, Vol.1, 1958 ,pp.2-14

Bishop, A.W., Webb, D.L., and Lewin, P.I., "Undisturbed samples of London clay from the Ashford Common shaft: strength-effective stress relationships", Geotechnique , Vol.15, no.1, 1965, pp.1-31.

Bjerrum, L., and Andersen, K.H., "In situ measurement of lateral pressures in clay", Proc. 5th European Conference on Soil Mechanics and Foundation Engineering, Vol.1, Madrid, 1972, pp.29-38.

Bjerrum, L., and Eide, O., "Stability of strutted excavations in clay", _Geotechnique_ , Vol.6, no.1, 1956, pp.32-47.

Bjerrum, L., Frimann Clausen, C.J., and Duncan, J.M.," Earth pressure on flexible structures", 5th European Conference on Soil Mechanics and Foundation Engineering, State of the Art Report, Madrid, 1972, pp.169-196.

Bjerrum, L., Kenney, T.C., and Kjaernsli, B., "Measuring instruments for strutted excavations", _Journal of the Soil Mechanics and Foundation Division_ ASCE, SM1, January 1965 , pp.111-140

Bjerrum, L., and Kirkedam, R., "Some notes on earth pressure in stiff fissured clay", Proceedings of Brussels Conference 1958 on earth Pressure Problems", 1958, vol.1, pp.15-27

Brooker, E.W., and Ireland, W.C., "Earth pressure at rest related to stress history", _Canadian Geotechnical Journal_ , Vol.2, no.1, 1965 pp.1-15.

Brown, C.B., and King, I.P., "Automatic embankment analysis: equilibrium and instability condition", _Geotechnique_ , Vol.16, no.3, 1966, pp.209-219

Bros ,B. "The influence of model retaining wall displacements on active and passive earth pressure in sand" Proceedings of the 5th European Conference on Soil Mechanics and Foundation Engineering, Madrid, vol.1, 1972, pp.241-249

Burland, J.B., "The yielding and dilation of clay", Correspondence *Geotechnique* , Vol.15, 1965, pp. 211-214.

Burland, J.B., "Some examples of the influence of field measurements on foundation design and construction", BRE , CP 11-77, 1977.

Burland, J.B., Moore, J.F.A., and Smith, P.D.K., "A simple and precise borehole extensometer", *Geotechnique* , Vol.22, pp. 174-177, also BRE , CP 11-72, 1972.

Burland, J.B., and Hancock, R.J.R., "Underground car park at the House of Commons, London: Geotechnical Aspects", *Structural Engineer* 55(2), pp.87-100,also BRE CP 13-77, 1977.

Burland, J.B., Longworth, T.I., and Moore, J.F.A., " A study of ground movement and progressive failure caused by a deep excavation in Oxford clay", *Geotechnique* , Vol. 27, no.4, 1977, pp.557-591.

Burland, J.B., and Moore, J.I.A., "The measurement of ground displacement around deep excavations",Symposium on Field Instrumentatin British Geotech. Society, London Butterworks, 1973, pp. 70-84.

Calladine, C.R., "A theoretical and experimental study on strains on triaxial test on normally consolidated clays", Correspondence *Geotechnique* , Vol.13, no.3, 1963, pp.250.

Campanella, R.G., and Vaid, Y.P., "Influence of stress path on the plane strain behavior of a sensitive clay", Dept. Civil Engineering, University of British Columbia, Vancouver, Soil Mechanics Series, no.19, 1972.

Chandrasekaran, V.S., and King, G.J.W., "Simulation of excavation using FEM", Journal of the Geotechnical Engineering Division , ASCE GT9, 1974, pp.1086-1089.

Chang, C.V. "Finite element analysis of soil movements caused by deep excavation and dewatering" Ph.D. Thesis, University of California, Berkeley, 1969

Chang, C.Y., and Duncan, J.M., "Analysis of soil movement around a deep excavation", Journal of the Soil Mechanics and Foundation Division , ASCE, Vol.96, SM5, 1970, pp.1655-1679.

Chapman, K.R., Cording, E.J., and Schnabel, J.R. "Performance of a braced excavation in granular and cohesive soils", Proc. Specialty Conference on Performance of Earth and Earth Supported Structures, ASCE, Vol.3, 1972, pp.271-293, Purdue University, Lafayette Indiana.

Christensen, N.H. and Hansen, B. "Shear strength properties of Skive Septarian Clay" Bulletin no. 7, Danish Geotechnical Institute, 1959

Christian, J.T., and Wong, I.H., "Errors in simulating excavation in elastic media by finite element", Soils and Foundation , Vol.13, no.1, 1973, pp.1-10.

Clough, G.W., and Duncan, J.M., "Finite element analysis of Port Allen and Old River locks", U.S. Army Engineers Waterways Experiment Station, Vicksburg, Mississipi, Contract Report, S 696, 1969.

Clough, G.W., and Duncan, J.M., "Finite element analysis of retaining wall behavior", Journal of the Soil Mechanics and Foundation Division , ASCE, Vol.97, SM12, 1971, pp.1657-1673.

Clough, G.W., and Mana, A., "Lessons learned in finite element analyses on temporary excavations in soft clay", 2nd International Conference in Numerical Methods in Geomechanics, ASCE, Vol.1, 1976, pp.496-510.

Clough, G.W., Weber, P.R., and Lamont, J., "Design and observation of a tied-back wall", Proceedings of ASCE Specialty Conference on Performance of Earth and Earth-Supported Structures, Vol.1, Part 2, 1972, pp.1367-1389.

Clough, R.W., and Woodward, R.J., "Analysis of embankment stresses and deformations", Journal of the Soil Mechanics and Foundation Division , ASCE, Vol.93, SM4, 1967, pp.529-550.

Cole, K.W., and Burland, J.B., "Observation of retaining wall movements associated with a large excavation", Proc. of 5th International Conference Soil Mechanics and Foundation Eng., Madrid, Vol. 1, pp.445-453, also BRE , CP 8-72, 1972.

Coulomb, C.A., "Essai sur une application des regles des maximis et minimis a quelques problemes de statique relatifs a l'architecture", 1776, Reprinted on "Coulomb's Memoir on Statics", (in french and english), Heyman, J., 1972.

De Jong, J., "Foundation displacement of multi-storey Structures", Ph.D Thesis, Dept. Civil Eng., University of Alberta, 1971.

De Jong, J., Morgenstern, N.R., "Heave and settlement of 2 tall building foundations in Edmonton, Alberta", Canadian Geotechnical Journal , vol.10, no.2, 1973, pp.261-281

De Josselin de Jong, G., " Lower bound collapse theorem and lack of normality of strain rate to yield surface for soils", Proc. IUTAM Symposium on Rheology and Soil Mechanics, Grenoble, 1964, pp.70-78

Desai, C.S., "Nonlinear analysis using spline functions", Journal of the Soil Mechanics and Foundation Division , ASCE, Vol.97, SM10, 1971, pp.1461-1480.

DiBiaggio, E., and Bjerrum, L., "Earth pressure measurements in a trench in stiff marine clay", Proc. 4th ICSMFE, London, Vol.2, 1957, pp.395-401.

DiMaggio, F.L., and Sandler, I.S., "Material model for granular soils", Journal of the Mechanical Enginering Division , ASCE, EM3, 1971, pp.935-949.

Drucker, D.C., "Some implication of work hardening and ideal plasticity", Quarterly of Applied Mathematics , Vol.7, 1950, pp.411-418.

Drucker ,D.C. "Soil mechanics and plastic analysis or limit design " Quarterly of Applied Mathematics , vol.X, no.2, 1952 , pp.157-165

Drucker, D.C., "A more fundamental approach to plastic stress strain relations", Proc. U.S. National Congress of Applied Mechanics, ASME, 1951, pp.487-491.

Drucker, D.C.,"A definition of stable inelastic material", Journal cf Applied Mechanics Trans., ASME, March 1959, pp.101-106.

Drucker, D.C., "On stress strain relations for soils and load carrying capacity", Proc. of the 1st International Conference on the Mechanics of Soil Vehicle Systems, Torino, Italy, 1961, pp.15-27.

Drucker, D.C., "Concept of path independence and material stability for soils", Proc. IUTAM Symposium on Rheology and Soil Mechanics, Grenoble ,1964, pp.23-46

Drucker, D.C., Gibson, R.E., and Henkel, D.J., "Soil mechanics and work hardening theories of plasticity", Transactions ASCE, 1957, pp.338-346.

Duncan, J.M., Discussion: Symposium on Plasticity and Soil Mechanics, Cambridge, 1973, pp.248-250

Duncan, J.M., and Seed, H.B., "Strength variation along failure surfaces in clay", Journal of the Soil Mechanics and Foundation Division , ASCE, Vol.92, SM6, 1966, pp.81-104

Duncan, J.M., and Dunlop, P., "Slopes in stiff fissured clays and shales", Journal of the Soil Mechanics and Foundation Division , ASCE, March 1969, pp.467-492.

Duncan, J.M., and Chang, C.Y., "Non linear analysis of stress and strain in soils", Journal of the Soil Mechanics and Foundation Division , ASCE, Vol.96, SM5, 1970, pp.1629-1653.

Dunlop, P., Duncan, J.M. and Seed, H.B. "Finite element analisis of slopes in soil" Report no. TE-68-1 University of California, Berkeley,

Dunlop, P., and Duncan, J.M., "Development of failure around excavated slopes", Journal of the Soil Mechanics and Foundation Division , ASCE, March 1970, pp.471-492.

EBA Eng. Consultants, Geotechnical Evaluation Report of North East Rail Rapid TransitLine Presented to B.W. Brooker Eng. Ltd from EBA Eng. Consultants, 1975.

Eisenstein, Z., "Application of finite element method to Analysis of Earth Dams", State of the Art Report, First Brazilian Seminar on Application of Finite Element Method in Soil Mechanics, 1974, pp.1-70.

Eisenstein, Z., Krishnayya, A.V.G., and Morgenstern, N.R., " An analysis of cracking of dams", Application of Finite Element Method in Geotechnical Engineering, U.S. Waterways Experimental Station, Vicksburg, Mississipi,1972, pp. 431- 455.

Eisenstein, Z., and Morrison, N.A., "Prediction of foundation deformation in Edmonton using an in situ pressure probe", Canadian Geotechnical Journal , Vol.10, 1972, pp.193-210.

Eisenstein, Z., and Thomson, S., "Geotechnical performance of a tunnel in till", Canadian Geotechnical Journal , Vol.15, no.3, 1978, pp.332-345.

Finn, W.D.L., "Boundary values problems of soil mechanics", _Journal of the Soil Mechanics and Foundation Division_ , ASCE, Vol.89, SM5, 1963, pp.39-72.

Flaate, K., "Stresses and movements in connection with braced cuts in sand and clay", Ph.D Thesis, University of Illinois, 1966.

Frydman ,B.E. and Zeitlen ,J.G. "Some pseudo elastic properties of granular media" Proc. 7th ICSMFE vol.1, 1969, pp.135-141

Frydman ,B.E. ,Zeitlen ,J.G. and Alpan ,I. "The yielding behaviour of a particulate media" _Canadian Geotechnical Journal_ , vol.10, no.4, 1973, pp.341-362.

Frydman, S., "The strain hardening behaviour of particulate media", _Canadian Geotechnical Journal_ , Vol.13, 1976, pp.311-323.

Gibson, R.E., "Experimental determination of the true cohesion and true angle of internal friction in clays", Third ICSMFE, Zurich, Vol.1, 1953, p.126.

Golapakrishnayya ,A.V. "Analysis of cracking of earth dams" Ph.D. thesis, The University of Alberta, 1973.

Golder, H.C., "Earth pressure against flexible vertical walls", Proc. 2nd ICSMFE, London, Vol.2, 1948, pp.76-81.

Golder, H.Q.,Gould, J.P.,Lambe ,T.W.,Tschebotarioff ,G.P. and Wilson ,S.D. "Predicted performance of braced excavation ", _Journal of the Soil Mechanics and Foundation Division_ ASCE vol.96, SM3, 1970, pp.801-815

Goodman ,L.E. and Brown ,C.B. "Dead load stresses and the instability of slopes" _Journal of the Soil Mechanics and_

Foundation Division ASCE vol 89, SM3, 1963, pp.103-134

Goodman ,R.E.,Taylor ,R.L. and Brekke ,T.L. "A model for the mechanism of jointed rock" Journal of the Soil Mechanics and Foundation Division ASCE vol 94, SM3, 1968, pp.637-659

Gould ,J.P. "Design of temporary earth retaining structures for the Washington Subway System" Proc, of Specialty Conference on Performance of Earth and Earth Supported Structures ASCE vol. III , 1972 ,Purdue University Lafayette , Indiana, pp.251-253

Green ,G.E. correspondence on : " A new soil testing apparatus" , Geotechnique vol 17, no 3, 1967, p.295

Green ,G.E. "Strength and deformation of sands measured in an independent stress control cell" , Stress-strain behaviour of soils, Proceedings of Roscoe Memorial Symposium , 1971, pp.285-323.

Green ,G.E. and Bishop ,A.W. " A note on the drained strength of sand under generalized strain conditions" , Geotechnique vol. 9 no 1 , 1969, pp. 144-149

Hambly ,E.C. " A new true triaxial apparatus" , Geotechnique , vol.9,no.2,1969,pp.397-309

Hanna ,T.H. and Adams ,J.I. "Comparisons of field and lab measurements of modulus of deformation of clay" Highway Research Record ,no.243,1968,pp.12-22

Henkel ,D.J. "The shear strength of saturated remolded clays" , Research Conference on the Shear Strength of Cohesive Soils ,ASCE, 1960,Boulder,Colorado, pp.533-554

Henkel ,D.J. "Geotechnical considerations of lateral stresses" , Proceedings ASCE Specialty Conference on Lateral Stresses Retaining Structures ,1970,Cornell University, pp. 1-49.

Henkel, D.J. Discussion on the panel of stability of flexible structures Proceedings of the 5th European Conf. on Soil Mechanics and Foundation Engineering, vol.2, Madrid, 1972, p.217.

Henkel ,D.J. and Skempton ,A.W. " A landslide at Jackfield , Shropshire in a heavily overconsolidated clay" Geotechnique , vol.5,no.1 ,1955,pp.131-137

Henkel ,D.J. and Wade ,N.H. "Plane strain tests on saturated remolded clay" Journal of the Soil Mechanics and Foundation Division ,ASCE,vol.96,SM6,1966, pp. 67-80.

Hoeg ,K. "Finite element analysis of strain softening clay" Journal of the Soil Mechanics and Foundation Division , ASCE, vol.97,SM1,1972, pp.43-58.

Iergatoulis ,B. ,Irons ,M. and Zienkiewicz O.C. "Curved isoparametric quadrilateral elements for finite element analysis" ,International Journal of Solid Structures ,vol.4, 1968 pp.33-41

Ishihara ,K. "Relations between process of cutting and uniqueness of solution" Soils and Foundation vol X,no.3,1970 pp. 50-65

Izumi ,H. ,Kamemura ,K. and Sato ,S. "Finite element analysis of stresses and movements in excavations" ,Proceedings of 2nd. International Conference in

Numerical Methods in Geomechanics, ASCE vol.II,1976, pp.701-712

Jaeger ,J.C. and Cook ,N.G.W. Fundamentals of Rock Mechanics 1969, published by Methuen and Co. Ltd.

Jones ,K. "Calculation of stress from strain in concrete" U.S.Dept. of Interior,Bureau of Reclamation, Eng. monograph 29, 1961

Kirkpatrick ,W.M. "The behaviour of sands under 3 dimensional stress systems", Ph.D. Thesis, University of Glasgow , 1954

Ko ,H.Y. and Scott ,R.F. "Deformation of sand in hydrostatic compression " , Journal of the Soil Mechanics and Foundation Division ,ASCE , vol.17, SM3, 1967 , pp.137-156

Ko ,H.Y. and Scott ,R.F. "Deformation of sand in shear", Journal of the Soil Mechanics and Foundation Division ,ASCE, sept.1967 ,SM5,pp.283-310

Ko ,H.Y. and Scott ,R.F. "A new soil testing apparatus", Geotechnique ,vol.17, 1967, pp.40-57.

Kondner ,R.L. "Hyperbolic stress strain response : cohesive soils" Journal of the Soil Mechanics and Foundation Division , ASCE , vol.89, SM1, 1963 , pp.115-143

Kulhawy ,F.H. "Finite element modeling criteria for underground openings in rock" International Journal of Rock Mech. , Min. Sci. and Geomech. vol.11 , 1974 , pp.465-472

Kulhawy, F.H., Duncan ,J.M. and Seed, H.B. "Finite element analysis of stresses and movements in embankments during construction" Report TE 69-4, University of California, Berkeley, 1969.

Ladd ,C.C. "Stress strain modulus of clay in undrained shear" Journal of the Soil Mechanics and Foundation Division , ASCE, vol.90, SM5, 1964 pp.103-132

Lade, P.V. "The stress strain and strength characteristics of cohesionless soils" Ph.D. thesis University of California, Berkeley , 1972

Lade ,P.V. "Elastoplastic stress strain theory for cohesionless soil with curved yield surfaces" Report UCLA-Eng-7594 ,School of Eng. and Applied Science, 1975

Lade ,P.V. and Duncan ,J.M. "Cubical triaxial tests on cohesionless soil", Journal of the Soil Mechanics and Foundation Division ,ASCE,vol.99,SM10, 1973, pp.793-812

Lade ,P.V. and Duncan ,J.M. "Stress path dependent behavior of cohesionless soil " , Journal of the Geotechnical Engineering Division ,ASCE,vol.102,GT1, 1976 , pp.1037-1053

Lade ,P.V. and Musante ,H.M. "3D behavior of normaly consolidated cohesive soil" Report UCLA-Eng-7626 , School of Eng. and Applied Sciences ,1976

Lambe ,T.W. "Up to date methods of investigating the strength and deformability of soils" , General report , 8th. ICSMFE vol.3, Moscow, 1973, pp.3-46.

Lambe ,T.W. "Stress path method" , Journal of the Soil Mechanics and Foundation Division , ASCE,vol.93,SM6, 1967 pp.309-331

Lambe ,T.W. "Braced excavations", Proc. ASCE Specialty Conference on Lateral Stresses Retaining Structures ,ASCE, Cornell University, 1970, pp.149-218

Lambe ,T.W. ,Wolfskill ,L.A. and Jaworsky ,W.E. " The performance of a subway excavation",Proceeding of ASCE Specialty Conference of Earth and Earth Supported Structures ,vol.1 part 2, 1972 , pp.1404-1424

Lambe ,T.W. ,Wolfskill ,L.A. and Wong ,I.H. "Measured performance of braced excavation", Journal of the Soil Mechanics and Foundation Division , ASCE,vol.96,SM3, 1970 pp.817-836

Lee ,K.L. "Comparison of plane strain and triaxial tests on sand" , Journal of the Soil Mechanics and Foundation Division ,ASCE,vol.96, SM3, 1970, pp.901-923

Lee ,K.L. and Seed ,H.B. "Drained characteristics of sands" , Journal of the Soil Mechanics and Foundation Division ,ASCE,vol.93,SM6, 1967, , pp.117-141

Linell K.A. and Shea ,H.F. "Strength and deformation characteristics of various glacial tills in New England", Research Conf. on the Shear Strength og Cohesive Soils, ASCE, Boulder,Colorado, 1960, pp. 275-314

Lo ,K.Y. "The operational strength of fissured clays" , Geotechnique ,vol.20,no.1, 1970 pp.57-74

Lo ,K.Y. ,Adams ,J.I. and Seychuk ,J.K, "The shear behavior of a stiff fissured clay" , Proc. ICSMFE , vol.I,

,Mexico City, 1969, pp.249-255.

Lo ,K.Y. ,Seychuk ,J.K. and Adams ,J.I. "A study of the deformation characteristics of a stiff fissured clay" , Sampling Soil and Rock, ASTM,STP 48, 1971 pp.60-76

Mansur ,C.I. and Alizadeh ,M. "Tiebacks in clay to support sheeted excavation", Journal of the Soil Mechanics and Foundation Division ,ASCE,vol.96,SM2, 1970 , pp.495-509

Marcal ,P.V. and King ,I.P. "Elasto-plastic analysis of 2D stress systems by finite element method" International Journal of Mechanical Science ,vol.9, 1967 , pp.143-155

Marcal ,P.V. "A stiffness method for elastic plastic poblems" International Journal of Mechanical Science vol.7, 1965 , pp.229-238

Marsland ,A. "The shear strength of fissured clays", Roscoe Memorial Symposium , 1971, also BRE CP 21/71

Marsland ,A. "Large in situ tests to measure the properties of stiff fissured clays " , 1rst. Australian-New Zealand Conference on Geomechanics , Melbourne, 1971, also BRE CP 1/73

Marsland ,A. "In situ plate tests in lined and unlined boreholes in highly fissured London clay ", Ground Engineering , vol.5,no.6, 1972 ,also BRE CP5/73

Marsland ,A. "Laboratory and in situ measurement of deformation moduli of London clay" , BRE CP 24/73 , 1973

Marsland ,A. "In-situ and laboratory tests on glacial clays at Redcar" ,Proc. of the Symposium on the Behaviour of Glacial Materials , Birmingham , 1975 ,also BRE CP 65/76

Marsland ,A. "The evaluation of the Engineering design parameters for glacial tills " , Quarterly journal on Engineering Geology , vol.10,no.1, 1977, pp.1-26, also BRE CP19/77

Marsland, A. and Butler, M.E. "Strength measurements in stiff fissured Barton Clay from Fawley, Hampshire" Proc. Geotechnical Conference, Oslo, vol I, 1967, pp.139-146

Marsland ,A. and Quarterman ,R. "Further development of multipoint magnectic extensometers for use in highly compressible ground" , Geotechnique vol.24, 1974 , pp.429-433

Marsland ,A. and Randolph ,M.F. "Comparisons of the results from pressuremeter tests and large in-situ plate tests in London clay " , Geotechnique ,vol.27,no.2,pp.217-243, 1977, also ,BRE CP 10/78

May ,R.W. and Thomson ,S. "The geology and geotechnical properties of till and related deposits in the Edmonton, Alberta, area" Canadian Geotechnical Journal vol.15, no.3, 1978, pp.362-370

Meen ,J.C. "The tracing of trenches and tunnels with practical formulas for earth pressure" Trans. ASCE vol LX, paper no. 1062, 1908

Mendelson ,A. "Plasticity:theory and application" Macmillan, 1970 , Macmillan

Mitchell ,R.J. "An apparatus for plane strain and true triaxial" , Canadian Geotechnical Journal , vol.10, 1973, pp.520-527

Morgenstern ,N.R. and Eisenstein ,Z. "Methods of estimating lateral loads and deformations" Proc. ASCE Specialty Conference on Lateral Stresses and Retaining Structures , 1970, Cornell University, pp. 51-102

Morgenstern ,N.R. and Thomson ,S. "Comparative observations on the use of the Pitcher sampler in stiff clay" Sampling of Soil and Rock ,ASTM, STP 43 , 1970, pp.180-191

Morgenstern ,N.R. "Shear strength of stiff clay" Proc. of the Geotechnical Conf. Oslo ,vol II, 1967, pp.59-69, and discussion pp.139-186

Moulton H.G. "Earth and rock pressures " Trans. American Institute of Mining and Metallurgical Engineers , feb. 1920, pp.327-369

Murphy ,D.J. ,Clough ,G.W. and Woolworth ,R.S. "Temporary excavation in varved clay" Journal of the Geotechnical Engineering Division ,ASCE ,vol.101, GT3, 1975, pp.279-295

NGI "Measurements at strutted excavation, Oslo subway, Vaterland", NGI Technical reports 6 to 8, 1962

Ozawa ,Y. and Duncan , J.M. "Elastoplastic finite element analysis of sand deformations" Proc. 2nd International Conference on Numerical Methods in Geomechanics , ASCE, vol I, 1976, pp.243-263

Palmer ,J.H.L. and Kenney ,T.C. "Analytical study of a braced excavation in weak clay" Canadian Geotechnical Journal , vol.9, 1972, pp 145-164

Peck ,R.B. "The measurement of earth pressure on the Chicago Subway " Bulletin ASTM ,august 1941

Peck ,R.B. "Earth pressure measurements in open cuts Chicago (Illinois) Subway" Trans. ASCE vol.108 ,1943, pp.1008-1036

Peck ,R.B. "Deep excavations and tunneling in soft ground" State of the art report 7th ICSMFE Mexico , 1969, pp.215-290.

Poorooshasb ,H.B. and Roscoe ,K.H. "The correlation of results of shear tests with varying degrees of dilation", Proc. 5th ICSMFE , vol.1, 1961, pp.297-304

Poorooshasb ,H.B. ,Holubec ,I. and Sherborne ,A.N. "Yielding and flow of sand in triaxial compression : part I " Canadian Geotechnical Journal vol.III ,no.4 , 1966 , pp.179-190

Poulos ,H.G. and Davis ,E.H. "Laboratory determination of in situ horizontal stresses in soli masses " Geotechnique ,vol. 22, 1972, pp.177-182

Ramsden, J. and Westgate, J.A. "Evidence of reorientation of a till fabric in the Edmonton area, Alberta" Till, A Symposium, Ohio State University, 1971, pp.335-344

Rankine, W.J.M. "on the stability of loose earth", Trans. Royal Soc. London, vol. 147, 1857

Resal, J. "La pousse des Terres", Paris, 1910

Rodriguez, J.M. and Flammand, C.L. "Strut loads recorded in a deep excavation", Proc. 7th ICSMFE, vol.2, 1969, pp.458-468.

Raymond ,G.P. and Soh ,K.K. discussion on : "Making rubber membranes" Canadian Geotechnical Journal vol.11, 1974, pp.661-662

Roscoe ,K.H. and Burland ,J.B. "On the generalized stress strain behaviour of wet clay ", Engineering Plasticity, edited by Heyman and Leckie, Cambridge University Press, 1968, pp.535-609

Roscoe ,K.H. and Poorooshasb ,H.B. " A theoretical and experimental study of strains in triaxial compression tests on normally consolidated clays", Geotechnique vol.13, no.1, 1963, pp.12-38

Roscoe ,K.H. ,Schofield ,A.N. and Thurairajah ,A. "Yielding of clays in states wetter than critical", Geotechnique , vol.13, 1963, pp.211-240

Roscoe ,K.H. ,Schofield ,A.N. and Thurairajah ,A. "Energy components during triaxial and direct shear tests", correspondence , Geotechnique , vol.15, 1965, pp.127-130

Roscoe ,K.H. Schofield ,A.N. and Wroth ,C.P. " On the yielding of soils", Geotechnique vol.8, no.1, 1958, pp.22-53

Roscoe ,K.H. ,Schofield ,A.N. and Wroth ,C.P. correspondence on : "The yielding of soils" , Geotechnique , vol.9, no.2, 1959, pp.72-83

Scott ,R.F. Principles of Soil Mechanics , Addison Wesley , 1963

Scott ,R. and Ko ,H.Y. "Stress deformation and strength characteristics" , State of the art report, 7th ICSMFE , 1969, pp.1-47

Sills ,G.C. ,Burland ,J.B. and Czechowski ,M.K. "Behaviour of an anchored diaphragm wall in stiff clay" Proc. 9th ICSMFE , Tokyo, vol.2, 1967, pp.147-154 also BRE CP 38/78

Simons ,N.E. and Som ,N.N. "The influence of lateral stresses on the stress deformation characteristics of London clay" ,Proc. 7th ICSMFE , Mexico City , vol.1, 1969, pp.369-377

Skempton ,A.W. "Study of the immediate triaxial test on cohesive solis" Proc. 2nd ICSMFE , vol. I, 1948,pp.192-196

Skempton ,A.W. "Earth pressure, retaining walls, tunnels and strutted excavations " Proc 3rd ICSMFE, vol. II, 1953, pp.353-361.

Skempton ,A.W. "Horizontal stresses in overconsolidated eocene clay " Proc. 5th ICSMFE , vol. I, 1961, pp. 351-357.

Skempton ,A.W. and Bishop ,A.W. Chapter X of Building Materials Their Elasticity and Inelasticity edited by Noth-Holland , 1954

Skempton ,A.W. Schuster ,R.L. and Petley ,D.J. "Joints and fissures in London clay at Wrasbury and Edgeware" <u>Geotechnique</u> ,vol.19, no.2, 1969 , pp.205-217

Skempton ,A.W. and Sowa ,V.A. "The behaviour of saturated samples during sampling and testing", <u>Geotechnique</u> vol.13, no.4, 1963, pp.269-290.

Skempton ,A.W. and Ward ,W.H. "Investigations concerning a deep cofferadm in the Thames estuary clay at Shellhaven", <u>Geotechnique</u> , vol.3, 1953, pp.119-139

Smith ,P.D.K. and Burland ,J.B. "Performance of a high precision multipoint borehole extensometer in soft rock" <u>Canadian Geotechnical Journal</u> , vol.13, no.2, 1976, pp.172-176 also BRE CP 41/76

Soderman ,L.G. Kim ,Y.D. and Milligan ,V. "Field and laboratory studies of modulus of elasticity of a clay till" Highway Research Record no. 243 , 1968 ,pp.1-11

Stroh ,D. and Breth ,H. "Deformation of deep excavations" Proc. 2nd International Conf. on Numerical Methods in Geomechanics ,vol.II, 1976, pp.686-700

Suhara ,J. and Fukuda J. "Automatic mesh generation for finite element analysis" Advances in Computational in Structural Mechanics and Design" 2nd U.S.-Japan Seminar Berkeley California , 1972, pp.607-624

Swatek ,E.P.Jr. ,Asrow ,S.P. and Seitz ,A.M. "Performance of bracing for deep Chicago excavation" Proc. of ASCE Specialty Conf. on Performance of Earth and Earth Supported Structures, vol.1, part 2, 1972, pp.1303-1322

Tavenas ,F.A. ,Blanchette ,G. ,Leroueil ,S. and LaRochelle ,P. "Difficulties in the in situ determination of K0 in soft sensitive clays" Proc. of Conf. on Insitu Measurement of Soil Properties , vol.1 ,Specialty Conf. ASCE, 1975, North Carolina State University Raleigh, pp.450-476

Terzaghi ,K. Theoretical Soil Mechanics, John Wiley and Sons , 1943

Terzaghi ,K. "Distribution of the lateral pressure of sand on the timbering of cuts " Proc. 1rst ICSMFE , Cambridge, Massachussets , 1936,a

Terzaghi ,K. "A fundamental fallacy in earth pressure calculations" Journal of the Boston Society of Civil Engineers ,april 1936,b, pp.277-294.

Terzaghi, K. "General wedge theory of earth pressure" Trans. ASCE , 1941, pp.68-80 and pp.89-97

Terzaghi, K. and Peck, R.B. "Soil Mechanics in Engineering Practice ", Jonh Wiley and Sons, first edition, 1948, second edition 1967.

Tschebotarioff ,G. Soil Mechanics ,Foundations and Earth Structures MacGraw-Hill , 1951

Tsui ,Y. and Clough ,G.W. "Plane strain approximations in finite element analysis of temporary walls" Proc. of the Conf. on Analysis and Design in Geotechnical Engineering Specialty Conf. ASCE University of Texas vol.2, 1974, pp.173-198.

TTC "Lateral earth pressure studies on strutted excavations of the Toronto Subway System" , 1967

Vaid ,Y.P and Campanella ,R.G. "Making rubber membranes" note: Canadian Geotechnical Journal , vol.10 ,1973 , pp.643-644

Vaid ,Y.P. and Campanella ,R.G. "Triaxial and plane strain behaviour of natural clay" Journal of the Geotechnical

Engineering Division ASCE , vol.100, GT3, 1974, pp.207-224

Ward ,W.H "Some field techniques for improving site investigation and Engineering design" Roscoe Memorial Symposium ,1971 , pp. 676-682, also BRE CP 30/71

Ward ,W.H. and Burland ,J.B. "The use of ground strain measurements in Civil Engineering" BRE CP 13/73 , 1973

Ward ,W.H. ,Marsland ,A. and Samuels ,S.G. "Properties of the London clay at the Ashford common shaft: insitu and undrained strength tests " Geotechnique vol.15, 1965, pp.321-344

Ward ,W.H. ,Samuels ,S.G. and Butler, M.E., "Further studies of the properties of London clay" Geotechnique vol.10 , no.2 , 1959, pp.33-58

Westgate ,J.A. "The quaternary geology of the Edmonton area, Alberta" Proc. of the Symposium on Pedology and Quaternary Research , 1969, University of Alberta Press , Edmonton , pp.129-151

Wilson ,E.L. "Finite element analysis of 2-D structures" University of California - Berkeley Structures and Materials Research Dept. Civil Eng. report no. CE 63-2 , 1963

Wroth ,C.P. "Some aspects of the elastic behaviour of overconsolidated clay" Proc. Roscoe Memorial Symposium ,1971, pp.347-361.

Wroth ,C.P. "In-situ measurement of initial stresses and deformation characteristics" Proc of Conf. on Insitu